Synthesis and Chemistry of Agrochemicals VII

ACS SYMPOSIUM SERIES **948**

Synthesis and Chemistry of Agrochemicals VII

John W. Lyga, Editor
FMC Corporation

George Theodoridis, Editor
FMC Corporation

Sponsored by the
ACS Division of Agrochemicals

American Chemical Society, Washington, DC

The paper used in this publication meets the minimum requirements of American National Standard for Information Sciences—Permanence of Paper for Printed Library Materials, ANSI Z39.48–1984.

PRINTED IN THE UNITED STATES OF AMERICA

Foreword

The ACS Symposium Series was first published in 1974 to provide a mechanism for publishing symposia quickly in book form. The purpose of the series is to publish timely, comprehensive books developed from ACS sponsored symposia based on current scientific research. Occasionally, books are developed from symposia sponsored by other organizations when the topic is of keen interest to the chemistry audience.

Before agreeing to publish a book, the proposed table of contents is reviewed for appropriate and comprehensive coverage and for interest to the audience. Some papers may be excluded to better focus the book; others may be added to provide comprehensiveness. When appropriate, overview or introductory chapters are added. Drafts of chapters are peer-reviewed prior to final acceptance or rejection, and manuscripts are prepared in camera-ready format.

As a rule, only original research papers and original review papers are included in the volumes. Verbatim reproductions of previously published papers are not accepted.

ACS Books Department

Preface

The American Chemical Society (ACS) Agrochemical Division sponsored the symposia, *Synthesis and Chemistry of Agrochemicals*, at its National meetings since 1984 to provide the agrochemical community with a forum in which to present work in the field. The emphasis of the presentations at these symposia, published in Volumes I–VI, was primarily research that led to the successful discovery of a new active ingredient, with a focus on chemists presenting the synthesis and chemistry of their discoveries. In a slight departure from this, we wanted to broaden the scope and encourage all agricultural scientists to share their successes and failures in the quest to discover new agrochemicals. The symposia *Translation of Pesticidal Activity from Lab to Greenhouse to Field* and *Good Ideas That Never Made It to Products* conducted at the Fall ACS National meetings in Philadelphia in 2004 and Washington, D.C. in 2005, provided the venue.

Successful translation of biological activity from lab to field is a key factor in our industry. Of the many thousands of compounds screened for biological activity each year, only a small percentage survive to advanced laboratory biological testing, and eventually to field testing. Only the precious few go into more extensive field, toxicology and environmental fate studies. More often than not, a compound that is biologically active under laboratory or greenhouse conditions will not survive the numerous barriers and harsh conditions that Nature inflicts. The symposium presentations included in this volume dealt not only with factors contributing to the success of a given project, but also with factors that played a role in the inability of some of these compounds to advance, from screens to lab to field.

This book opens with an overview of innovation and challenges in the agrochemical industry followed by a discussion of the physical properties of agrochemicals, as well as early-stage assessment of meta-

bolic stability. The book is then divided into four sections, each section addressing a different stage in the development of an agrochemical product. Chapters in each section address the technical difficulties commonly encountered at each stage. Topics include the synthesis, biological activity, structure–activity relationships, mode of action, and experimental design of the various chemistries. Chapters in each of the four sections present examples of agrochemicals in the areas of herbicides, fungicides, and insecticides.

We express our deepest appreciation to all of those who contributed papers and presented their work at both symposia. Our special thanks go to the authors for their efforts in preparing the chapters that makeup this book. We are also indebted to Barbara Collura at FMC for her administrative help in producing this book.

John W. Lyga
Agricultural Products Group
FMC Corporation
P.O. Box 8
Princeton, NJ 08543

George Theodoridis
Agricultural Products Group
FMC Corporation
P.O. Box 8
Princeton, NJ 08543

Synthesis and Chemistry of Agrochemicals VII

Chapter 1

Innovation Opportunities in the Crop Protection Industry

Ann Orth, George Theodoridis, and John W. Lyga

Discovery Research and Development Department, Agricultural Products Group, FMC Corporation, P.O. Box 8, Princeton, NJ 08543

"Be sure to take change by the hand before it takes you by the throat"
                                                    Sir Winston Churchill

The crop protection industry has gone through remarkable change over the past ten years. There has been unprecedented merger and acquisition activity, with more than half of the top agricultural chemical companies from the mid-1990's no longer independently active. The company with the highest level of sales growth over the past decade was Nufarm; however, their success was based not on internal discovery of new active ingredients, but through acquisition of companies and products *(1)*. During this same period, however, we also have experienced unprecedented innovation, most notably the introduction of genetically altered crops. As of last year, nearly 240 million acres of genetically modified (GM) crops were planted worldwide, taking a continually increasing market share from the more traditional chemical pesticides *(2)*.

We live in an ever-changing global marketplace. The agricultural chemicals industry was at its lowest in sales in 2003 after years of decline, but 2004 brought an upturn with 5.5% real growth *(3)*. Overall trends show a positive forecast for South America and Eastern Europe, but the rest of the world is experiencing stagnant or declining profits. There are several key factors which

1

are influencing this trend. We continue to experience an overall rising cost of R&D, including discovery, development, label expansion and defense (pre- and post-launch). Increased regulatory hurdles and consumer scrutiny have led to re-registration requirements for older products and higher costs for toxicology, environmental studies, risk assessments, and other supporting research. One outcome of increasing regulatory requirements is the declining proportion of large and medium products and the rise in the number of small products introduced over time, which now represent over 70% of all launches since 1990 *(3)*.

Synthesis and screening costs have also escalated significantly due to more sophisticated tools and shift to target R&D. There is a greater need to investigate more complex molecules to improve both efficacy and safety, and to test products in more markets segments and applications so that the projected payback justifies the investment. Expanding regional markets dictate conducting more field trials, which also adds to registration costs. Many companies have invested in technology tools such as genomics, combinatorial chemistry, and high through-put screening which are both necessary and costly. The multiplicity of discovery approaches, each of which has different investment, time and risk profiles, requires firms to make choices about which tools to utilize. Perhaps most importantly, though, a robust generic pesticide industry is gaining strength, offering farmers a choice between the known, lower cost inputs of off-patent products and the premium price of new innovation.

Especially for smaller agricultural chemical companies, there is a need to stay focused on those areas in which we can compete on a global scale. The 'tool-kit' for survival is a mixed group of strategies. We must apply innovative solutions to product life cycle management, manage costs, *and* maintain Discovery productivity. Internal and external innovation is key, including establishing effective alliances and partnerships, as is the discriminate use of costly Discovery technology. We need to maintain a lean, flexible, focused organization and goals. The ultimate key to success is active pipeline management, closely aligned with Development and business goals, and a strong emphasis on enabling creative people to fully utilize their talents.

Despite the challenges of our business, there are a number of clear opportunities in the agrochemical industry today. Global population will continue to grow dramatically, increasing the demand for food and energy. This is compounded by decreasing arable acreage and fresh water supplies, which ensure the need for innovative solutions to enhance agricultural productivity. Resistance will continue to generate new opportunities for herbicides, insecticides and fungicides. Pest spectrum shifts will continue, especially if we increase our reliance on older chemistries. Regulatory pressure on older compounds opens new opportunities for newer products. Non-crop markets will continue to expand. 'Discontinuities' such as the soybean rust epidemic are

always possible, presenting outbreaks of pests or diseases requiring new, effective solutions. To meet these demands, new chemistries will continue to be a necessary asset to the grower.

One measure of the innovation and productivity of agrochemical discovery is the number of new chemical entries reported in the Annual Ag Chem New Compound Review *(4)*. These new compound reports have continued to be in the range of 50-100 per year over the past six years with only a slight downward trend, which is impressive considering all the factors described above that are pressing on the industry. Since the publication of the last volume in this ACS Symposium Series in 2002 (*Synthesis and Chemistry of Agrochemicals VI*) *(5)*, we have seen a number of new innovations in chemical crop protection, many of which are captured in the present volume. Of note is the introduction of two new insecticides by Nihon-Bayer and DuPont acting at the ryanodine receptor. Also included in this symposium are reports on continued innovation in the herbicide and fungicide area with new chemistry and new modes of action described. As an industry, we have developed techniques and strategies to enable earlier decision making along the path of chemical optimization; as examples, two papers are included in this volume on the importance of understanding physical properties and on early stage assessment of metabolic stability. Innovation has continued in more familiar territory as well, such as the neonicotinoids, as presented in papers from Bayer and Syngenta, and in looking for new chemistries acting at known target sites.

It is clear that to sustain the demands of a growing population amid the increased regulation by governmental organizations and activism by environmental groups, we must continue to innovate. The rich expertise and talent of creative individuals in our R&D organizations are certainly up to this challenge.

"He that will not apply new remedies must expect new evils; for time is the great innovator."

-Francis Bacon

References

1. AgriFutura Newsletter April 2005, PhillipsMcDougall Agriservice, Edinburgh UK
2. James, C. 2005. Global Status of Commercialized Biotech/GM Crops: 2005. ISAAA Briefs No. 34. ISAAA: Ithaca, NY
3. Agrochemical Services, September 2005 Outlook, Cropnosis Limited, Agrochemical Industry Consultants, Edinburg, EH3 6AA, UK

4. Rob Bryant, Marie Bite, Ag Chem New Compound Review, Agranova, Kent UK, vol 18 – 23; 2000 – 2005 (www.agranova.com)
5. Baker, D. R, Fenyes, J. G.,Lahm, G. P., Selby, T. P., Stevenson, T. M., Synthesis and Chemistry of Agrochemicals VI, American Chemical Society, Oxford University Press, 2002.

Chapter 2

Physical Property Requirements of Agrochemicals

Stephen F. Donovan

Discovery Research Department, Agricultural Products Group,
FMC Corporation, P.O. Box 8, Princeton, NJ 08543–0008

Violation of the physical property requirements of an agrochemical will lead to poor translation from laboratory to field conditions. The optimum physical property requirements for an agrochemical will differ widely depending on their specific application. How an agrochemical is applied, where it is applied and where it needs to translocate to the ultimate site of action will dictate the physical property constraints. We will list some of the physical property relationships that that have been published and how these principles can then be applied to the end use. These relationships can be applied to fungicidal, herbicidal and insecticidal applications.

The specific use of an agrochemical will determine the physical property requirements. The failure of Agrochemicals in the translation from the laboratory to the field can often be traced to some barrier that needed to be traversed, that was not. We are going to ignore problems in the lack of translation due to such effects as photolysis, hydrolysis and oxidation. The optimum physical property requirements for compounds differ widely depending on their application. There has been proposed an "agricultural rule of five"*(1)* for commercial insecticides and post-emergent herbicides as a modification to the "Lipinski rule of five" for

7

orally active pharmaceuticals.*(2)* Since its publication in 1997, the Lipinski rule of five has been a critical filter for drug development programs. In general, an orally active drug has: not more than 5 hydrogen bond donors, not more than 10 hydrogen bond acceptors, not more than 10 rotatable bonds, a molecular weight less than 500, and a logP less than 5. The agrochemical rule of five (with a slightly lower number of hydrogen-bond donors) may be a good start for screening compounds that may have biological activity for agricultural use, but the rules need to be specifically tailored to meet the physical property requirements of a particular application. These rules for the end use are so disparate that an encompassing general rule for agricultural chemicals is unlikely to ever be written. When an active compound is found in an enzyme screening assay, the only physical properties requirement may be sufficient solubility. As the process goes from the screening assays to the laboratory assays, to the green house assays, to the mini-plot assays to full fledged field trials, the failures due to incompatible physical properties will often be seen. We will discuss some of the various relationships described in the literature and how these principles can be applied to the end use.

The first task is to decide on the end use in order to determine the optimum physical property requirements that will apply. It is not sufficient to say "I want to use it as a fungicide, or as an herbicide, or even as a foliar applied insecticide." You also need to specify how you are going to apply the compound (*i.e.*, a seed treatment, in furrow application, pre-application to the soil, post-application to the foliage, *etc.*). In the case of insecticidal use, the particular insect pest needs to be carefully considered. In particular, the feeding behavior of the insect is of utmost importance. The difference in feeding between a Lepidoptera that will eat the whole leaf, to a rasping insect such as a mite, or for a piecing-sucking insect such as an aphid that feeds on phloem requires quite different physical property optima in order to deliver the active material consistent with the feeding behavior. In the case of soil applied compounds, careful thought has to be given to where the compound is being applied and where it needs to go, and how much movement is desirable within the context of regulating agencies. Since all of this attention is ultimately directed at the plant itself and systemic movement is either often required or desired, we will start of with a discussion of the different types of systemicity.

There are four basic types of systemicity. These are listed in an increasing degree of systemicity; first is adsorption to the leaf surface and penetration into the leaf, second is translaminar systemicity, third is xylem systemicity (also known as apoplastic, acropetal, or meristemic movement, where the movement is upwards towards the growing point of the plant) and finally phloem mobility (also known as basostemic, basipetal or symplastic movement, where the movement is downwards from the shoots to the roots *via* the phloem). As the logP (the log of the octanol/water partition ratio) of non-volatile lipophilic

compounds is lowered, first movement into the leaf is seen, then translaminar systemicity, then xylem systemicity, and finally phloem systemicity.

Penetration into the Leaf

Penetration of the leaf surface is often not necessarily important to control insects that chew, such as Lepidoptera, but penetration is needed for insects that feed inside the leave such as a leafminer (*Liriomyzra trifolii*) and the tomato pinworm (*Keiferia lycopersicella*). Penetration is also needed for compounds that have limited photo-stability such as imidacloprid. Once compounds have penetrated the tissue of the leaf, if they have the appropriate physical properties, can move into xylem and/or phloem systems, otherwise they will remain located at their application site.

Simple penetration of a compound into the leaf surface is more complex than it might first appear, because some compounds can accumulate in the cuticular waxes, and yet others can also go deeper into the tissues of the leaves. Some compounds such as spinosad (literature logP at a pH of 7 for spinosad A is 4.0, and for spinosad D the logP is 4.5)*(3)* can move across and around the leaf surface by being soluble in the cuticular wax. Compounds like abamectin (logP 4.4) will penetrate the leaf and control the above mentioned leafminer and pinworm.

Other compounds such as trifloxystrobin are termed mesostemic.*(4)* Trifloxystrobin is absorbed by the waxy cuticle and penetrates into the leaf. It shows translaminar activity, as well as some local redistribution within the plant canopy. The effect of some local redistribution within the plant canopy is obviously dependant on sufficient vapor pressure. The literature vapor pressure for trifloxystrobin is 2.6×10^{-8} mm Hg (25˚C) is relatively non-volatile, therefore it might seem surprising to see such an effect. This caused us to measure the vapor pressure with our GC based technique*(5)* vapor pressure and found the vapor pressure to be 2.4×10^{-7} (corrected for a m.p. of 72.9 ˚C). If the GC-vapor pressure measurement more accurately reflects the true vapor pressure, this observed vapor pressure driven redistribution is then not so surprising. This moderate vapor pressure of trifloxystrobin may also play a major role in mobility within the plant as well, since it is also moderately lipophilic with a logP of 4.5 it should have limited movement. This measurement of lipophilicity (a biphasic index) was in good agreement with our HPLC-logP (hydrophobicity as a chromatographic index) method*(6)* with values of 4.24 (pH 2), 4.25 (pH 7), and 4.24 (pH 11). We have noticed similar vapor pressure effects for other lipophilic compounds that are moderately volatile, such as the insecticide bifenthrin that has an HPLC-logP value of 5.55 (pH 7) that has a GC vapor pressure of 2.4×10^{-7} mm Hg (25˚C) (uncorrected), 9.1×10^{-8} mm

Hg (25˚C) (corrected for a m.p. of 68 ˚C) and a literature vapor pressure of 1.8 X 10^{-7} mm Hg (25˚C). In order for the mesostemic effect to be seen, a minimum vapor pressure is essential as well as the compound needing to be a least moderately lipophilic. As such, it should accumulate on the surface of a hydrophilic layer and be readily available for vapor phase movement much like the vaporization off of a water surface is enhanced by lipophilic compounds as observed in measurements of the Henry constant.

Translaminar Systemicity

Translaminar movement is often critical for both fungicidal and insecticidal applications. Often the spray effectively reaches just the dorsal surface of the leaf, but fungus and insects (such as aphids) also reside on the ventral surface of the leaves. Compounds that have "mesostemic systemicity" can also show translaminar effects. We have also observed that translaminar systemicity can be seen when there is either a sufficiently low logP or sufficiently high vapor pressure, or a favorable combination of both properties. An example of such translaminar systemicity has been seen with compounds like carbosulfan and fipronil:

Table 1. Physical Properties of Translaminar Compounds.

	Literature logP	HPLC-logP[6] (pH 7)	Literature Vapor Pressure mm Hg (25˚C)	GC-Vapor Pressure(5) mm Hg (25˚C) (corrected for m.p.)
Carbosulfan	5.4	4.96	3.1 X 10^{-7}	2.7 X 10^{-7}
Fipronil	4.0	3.89	2.3 X 10^{-8}	1.3 X 10^{-7}

Xylem Systemicity

Xylem systemicity has been well studied and clear correlations with logP have been seen. Please see the seminal work of Briggs, Bromilow and Evans(7) as well as additional studies investigating root absorption followed by xylem transport.(8) To discern the correlation of xylem systemicity with logP from these studies one must first understand the correlation of root absorption with logP. It should be noted that these were carried out without soil; this point will be addressed later. The root concentration factor (RCF) is the concentration in

the root tissues divided by the concentration in the external solution. For barley, the RCF is fairly insensitive to logP values that are less than 1. Above a logP of 1, it logarithmically increases with increasing logP.*(7)*

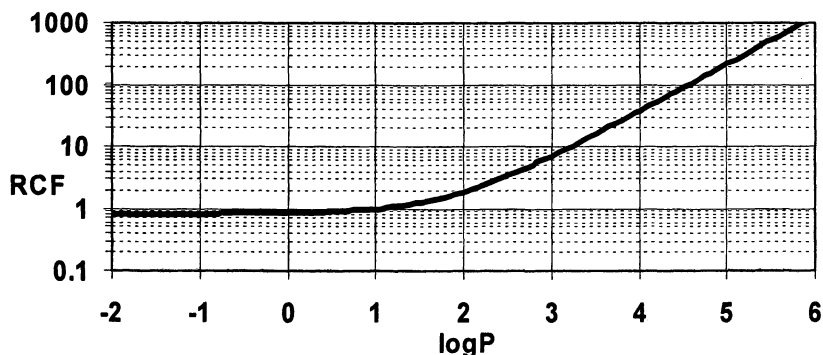$$RCF = 0.82 + 10^{[(0.77 \times logP) - 1.52]}$$

Equation 1

Figure 1. Root Concentration Factor (RCF) of Hydroponic Barley

Briggs, Bromilow and Evans subsequently examined the transportation stream concentration factor (TSFC) which is the concentration in the xylem divided by the concentration in the external solution. They developed Equation 2 for barley.

$$TSFC = 0.784 \exp - [(logP - 1.78)^2 / 2.44]$$

Equation 2

After comparing the two figures of RCF and TSCF, one can see the relation of xylem mobility to logP occurs when the logP falls below a value of 5, resulting in increasing xylem mobility. There is a decrease in the TSCF below a logP of 2 because of a marked decrease in the concentration in the roots. There is an additional factor for compounds having logP values below 2.5, namely phloem mobility. This type of graph is helpful to understand the movement and

usefulness of herbicides, fungicides and insecticides. For example, if a fungicide is too polar it will translocate to the peripheral edges of the leaf, leaving the center unprotected. If a fungicide was too lipophilic it would not translocate sufficiently resulting in leaving unsprayed portions of the leaf unprotected. Likewise, for an insect that feeds on the leaf where the compound is too xylem mobile it will translocate to the edges of the leaf, leaving the central portion relatively unprotected. Therefore, there is an optima for such considerations and is apt to fall somewhere in the region of a logP of 3-4. These same considerations of xylem mobility apply, can be applied to herbicides as well. The effects of xylem mobility has been observed on the redistribution of strobilurins.*(9)(10)*
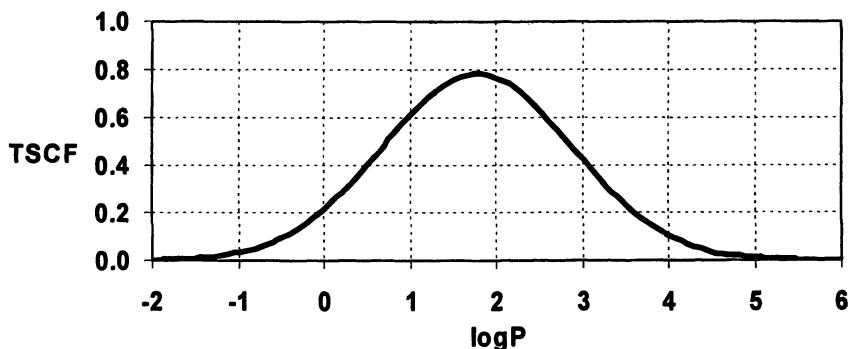
Figure 2. Transportation Stream Concentration Factor (TSCF) of Hydroponic Barley

Table 2 summarizes the redistribution properties of strobilurins from the two references and our experimental HPLC-logP*(6)* and gas chromatography vapor pressure*(5)* data for some of the referenced compounds. Literature values for the logP and vapor pressure were taken from the 13th Edition of the Pesticide Manual. The calculations of RCF and TSCF were calculated according to Equations 1 and 2. The phloem mobility was calculated for a 15 cm potato plant, according to the equation developed by Daniel Kleier and co-workers.*(11)*

Table 2. Redistribution Properties of Strobilurins Arranged in Order of Increasing LogP

	Metomino-strobin	Azoxy-strobin	Fluoxa-strobin	Kresoxim-methyl	Picoxy-strobin	Pyraclo-strobin	Trifloxy-strobin
Movement into leaf	high	Low	Yes	low	medium	v. low	v. low
Vapor active	no	No	no	yes	yes	no	yes
Trans-laminar systemic	yes	yes	yes	low	yes	low	low
Xylem systemic	yes	yes	yes	no	yes	no	no
Phloem systemic	no	No	no	no	no	no	no
Lit. logP	2.32	2.5	2.86	3.4	3.6	3.99	4.5
HPLC-logP[4]	NA	2.99	NA	3.63	NA	4.19	4.24
Lit. Vapor Pressure mm Hg (25°C)	1.4e-7	8.3e-13	5e-12	1.7e-9	4.1e-8	2.0e-10	2.6e-8
GC-Vapor Pressure[3] mm Hg (25°C)	NA	5.4E-10	NA	4.0E-7	NA	4.8E-9	2.3e-7
Calc. RCF[5] (Barley)	2.7	3.4	5.6	13	19	36	89
Calc.TSCF[5] (Barley)	0.70	0.63	0.49	0.27	0.20	0.11	0.04
Phloem log C_f	-4.3	-5.0	-6.8	-11	-12	-17	-25
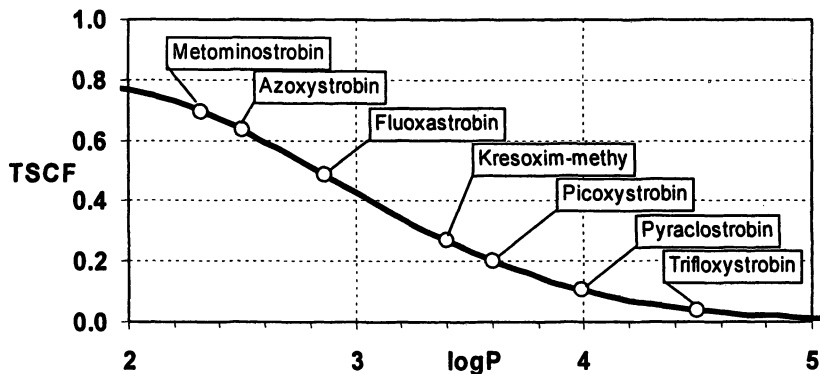
Figure 3. Calculated Transportation Stream Concentration Factor (TSCF) for Selected Strobilurins in Barley

There are a number of correlations that are apparent in Table 2. The first observation is that the movement into the leaf decreases with increasing logP. The second observation is the translaminar movement decreases with increasing logP. This translaminar movement is slightly confounded when there are vapor pressure effects. This is seen most clearly with trifloxystrobin which is moderately lipophilic, but since it has vapor activity, it shows some translaminar movement. As mentioned previously, the observed vapor activity of trifloxystrobin is consistent with the GC-vapor pressure [2.3 X 10^{-7} mm Hg (25°C)]. The third observation is that xylem systemicity falls off with increasing logP and tracks the TSCF.

Phloem Systemicity

Phloem systemicity is required when the application of a compound is to one leaf and translocation is needed to another leaf, unless the compound is volatile. This movement is important if one needs to protect new growth following treatment. Adequate accumulation of compounds in the phloem is also needed to control phloem feeding insects, such as aphids. Insects like aphids and whiteflies can be controlled by compounds that are not phloem mobile as long as there is sufficient vapor pressure to accomplish the redistribution. Kleier and coworkers have developed a phloem mobility model that predicts the log of the concentration factor (logC$_f$) using the logP (in the neutral form) and acidic

pK_a as input parameters, throughout this paper all calculations of $logC_f$ were carried out using a 15 cm potato plant as a model.*(11)(12)* A $logC_f$ greater than -4 is regarded as phloem mobile. It is important not to confuse post-activity for phloem feeding insects to mean there is necessarily phloem mobility. For example, this effect can be observed in cases such as bifenthrin that has an HPLC-logP of 5.6, therefore a $logC_f$ of -59, and therefore absolutely no phloem mobility, yet it has good aphid post-activity. We have measured the GC-vapor pressure of bifenthrin and found it to be $9.1X10^{-8}$ mm Hg (25°C, corrected for m.p. of 68°C) thus, a vapor pressure effect can be expected. The observed vapor activity of bifenthrin on an insect like an aphid is better described as contact activity, rather than true oral activity.

All of the compounds in Table 2 are too lipophilic to be phloem mobile with the possible exception of metominostrobin. When the log of the phloem concentration factor is greater than -4, it is considered to be phloem mobile. We have often seen that when the HPLC-logP is less than about 2.5 that phloem mobility occurs. This is in agreement with Kleier's phloem mobility model when solved for the phloem mobility of a neutral compound, as seen in Figure 4.
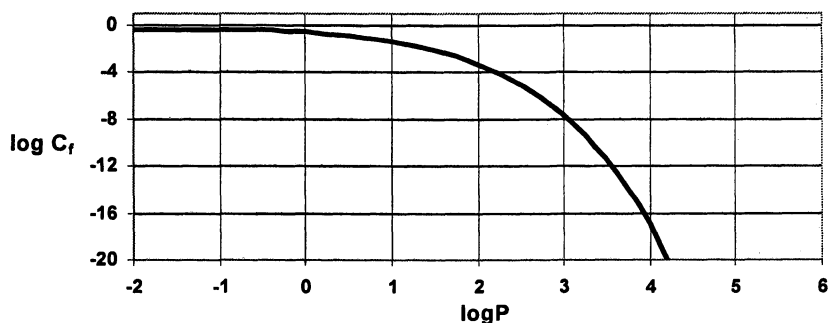
Figure 4. Calculated Log of the Phloem Concentration Factor for a 15 cm Tall Potato for Neutral Compounds.

If the logP of metominostrobin is truly represented by a logP of 2.32, then it might be expected to exhibit limited phloem mobility. If the logP is better represented by a higher logP, then one is apt to see little phloem activity because the log of the concentration factor falls very quickly when the logP exceeds 2.5.

An important contribution made by Kleier's phloem mobility model is the ability to predict the mobility of weak acids. Since the phloem vessel (apoplast or sieve tube) is more basic than the surrounding xylem vessel (symplast), weak acids are drawn into and sequestered in the phloem. This process has been

called the ion trapping mechanism. The corollary to the ion trapping mechanism is that basic compounds should be expelled from the phloem. It should be mentioned that basic compounds can have xylem systemicity. A study of two basic lipophilic fungicides, dodemorph and tridemorph, showed root to shoot translocation, believed to be through xylem systems. *(13)* An examination of a 3D plot of the relationship of logP, pK_a and the $logC_f$ (Figure 5) shows that if a compound is both lipophilic and non-acidic there is no phloem mobility. If partial ionization of a lipophilic weak acid occurs, then phloem mobility is predicted. It is hard to appreciate the 3D graph when printed in two dimensions. Therefore, the 3D graph shown in Figure 5 is followed by two slices of this graph, one in the logP axis and the other in the pK_a axis. Figure 6, shows the effect on $logC_f$ by a weak acid with a pK_a of 5, 7, 8, 9, and 14. Figure 7, shows the effect on $logC_f$ of a compound with a logP of 4 as a function of the pK_a.

After inspection of Figure 6 and Figure 7, one can appreciate the impact of the weak acid to convert a lipophilic compound with no phloem mobility into a very phloem mobile compound. This enhancement of phloem mobility can also be realized through the use of acid pro-groups. One often sees the use of a lipophilic ester in herbicide applications, which penetrates the leaf, with no phloem mobility that subsequently hydrolyses to the acid and becoming phloem mobile. The strategy of using a weak acid as a pro-group can also be used.(12)
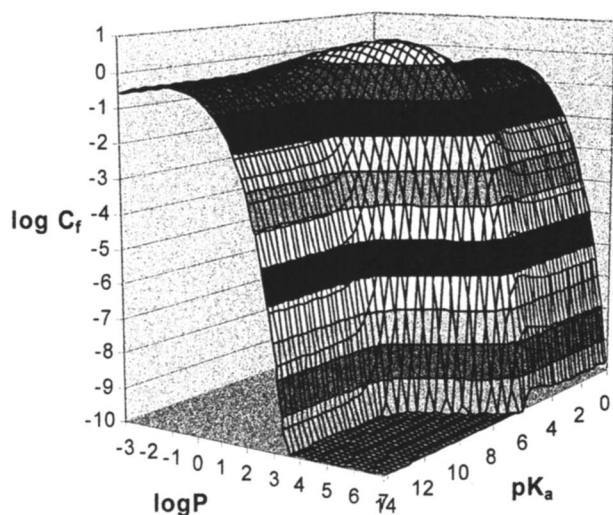
Figure 5.   Calculated Log of the Phloem Concentration Factor for a 15 cm Potato Plant for Acidic Compounds.
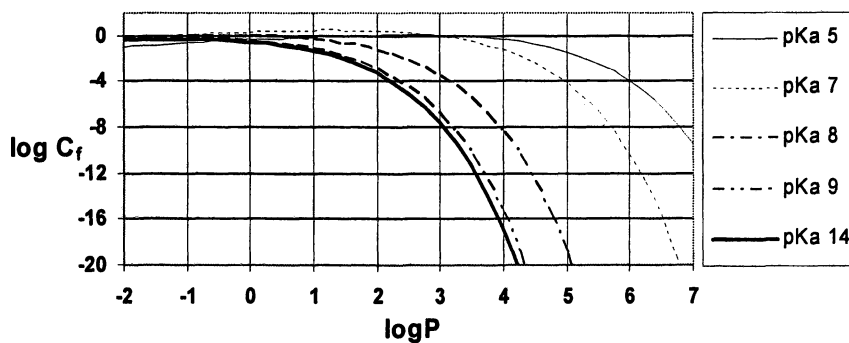
Figure 6. Calculated Log of the Phloem Concentration Factor for a 15 cm Tall Potato for Acids with a pK_a of 5, 7, 8, 9, and 14
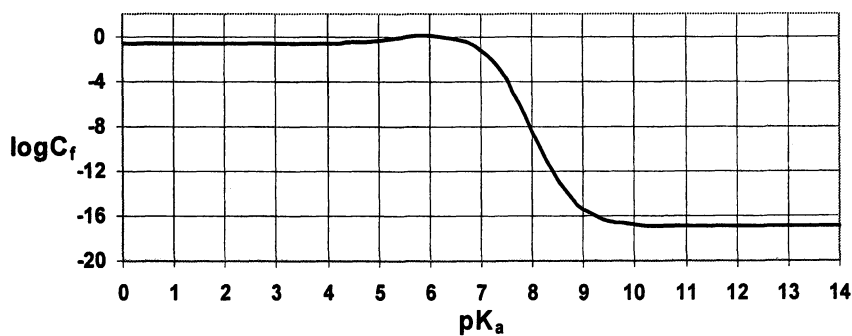
Figure 7. Calculated Log of the Phloem Concentration Factor for a 15 cm Tall Potato Plant for Compound with a LogP of 4 as a Function of the Acidic pK_a

Soil Effects

We briefly discussed the root concentration factor and the transpiration stream concentration factor in the section on xylem systemicity. It should be pointed out that those studies were done without soil. The use of hydroponic plants is often an experimental method used in the preliminary testing of Agrochemicals. We often experience translation problems moving from a hydroponic plant to a plant in soil study. For example, we often encounter problems going from one soil type to another, especially as it relates to the amount of organic material. For example, an herbicide may work fine in a soil containing 1% organic and show no damage to the beneficial plants. If the same plants are planted in a sandy soil, the beneficial plants often have an unacceptable amount of phytotoxicity. Another exemplification is a root systemic insecticide optimized in a hydroponic test. When the carried out in soil, there was no uptake by the roots and consequently no insecticidal protection. This discrepancy can often be traced to the organic in the soil competing for the agrochemical, hence dropping the effective concentration. We usually see this dichotomy of behavior for moderately lipophilic compounds (logP 2-4). Highly lipophilic compounds would have failed earlier in the screening process because of their lack of aqueous solubility, as well as being even more tightly bound to organic material in the soil.

A transpiration stream concentration factor study was carried out in soybeans (Figure 8) where a similar relationship to the one seen in Figure 2 was found.(13) Figure 8 shows the effect of having soil with no organic material (hydroponic), soil with 1% organic material, and soil with 5% organic material. Their TSCF equation, when expressed in the same form as Briggs,(7) is seen in Equation 3:

$$TSFC = 0.7 \exp - [(\log P - 3.07)^2 / 2.78]$$

Equation 3

The interpretation of Figure 8 is that when the TSCF is corrected for absorption to organic material (OM) in soil will cause the TSCF to drop in a direct response to the amount of OM, and lipophilic compounds will be most adversely affected. This effect also shifts in the optima from a logP of 3 in hydroponic situation to a logP of 1-2 when soil is used. The consequence of this effect resulting in translocation failures is great. If laboratory studies in a hydroponic system are used to optimize a series of analogs, one would gravitate to compounds having a logP of 3-4. In studies using soil, the actual amount of
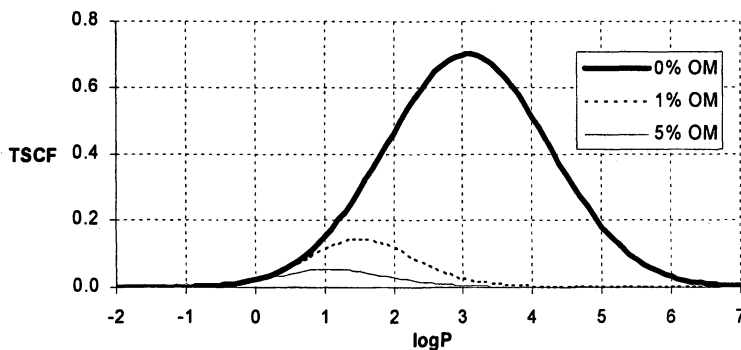
Figure 8. Calculated transpiration stream concentration factor for soybeans for soil with 0% organic material (hydroponic), 1% organic material, and 5% organic material.

compound absorbed by the plants through the roots would be drastically reduced. Another problem that is commonly seen is that a candidate agrochemical works fine using greenhouse soil. During field trials the candidate agrochemical may initially work fine as well. However, during larger scale field trials it may then be found that in sandy soils (low in organic material) there is an unacceptable amount of phytotoxicity to beneficial plants. The variability of performance of candidate Agrochemicals with different soil types is often directly tied to this effect. The effect of vapor pressure can sometimes help to overcome a difficulty if a compound is too lipophilic. Also, the use of compounds that are weak acids will often moderate the performance variability in different soil types.

A number of studies have examined the role of various factors such as volatility and solubility on the efficacy of soil insecticides.(14) While the soil itself affects the efficacy of soil insecticides, the major determinate of biological activity is the amount of organic material in the soil.(15) Simmons, Lew, Silverman and Ali studied the effect of pyrethroids and some commercial insecticides on 3rd instar southern corn rootworm larva (Diabrotica undecimpunctata howardii).(16) They found that a combination of calculated lipophilicity and calculated volatility could predict soil pLC_{50} based on the topical pLD_{50}. The volatility was expressed as the log of the vapor pressure in mm Hg. We re-plotted the difference of the topical pLD_{50} - soil pLC_{50} with the calculated logP and calculated log volatility in a 3D graph shown in Figure 9. It can be seen as the compounds become more volatile ($logV_p < 5$) that is a marked increase in soil toxicity. As the compounds become less lipophilic (more hydrophilic), they also become more toxic in the soil.
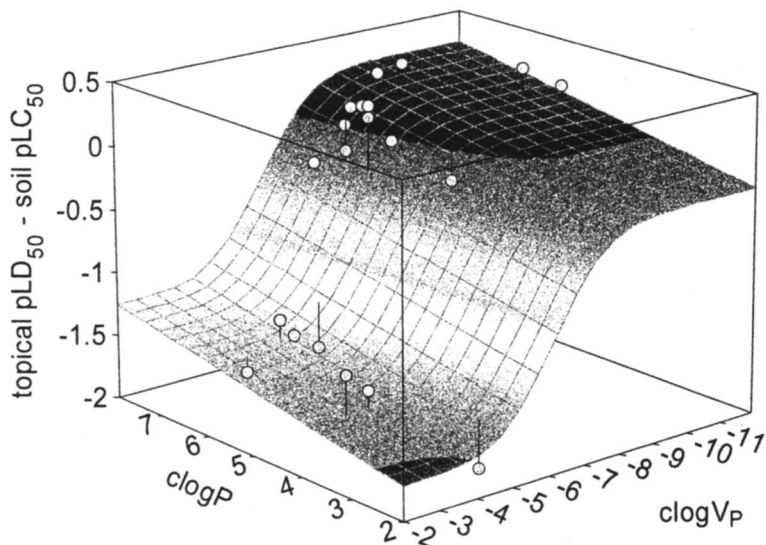
Figure 9. The difference in the topical pLD$_{50}$ and the soil pLC$_{50}$ plotted with calculated logP and calculated log volatility on 3rd instar southern corn rootworm larva (Diabrotica undecimpunctata howardi)

Concluding Recommendations

To try to avoid translation failure as one proceeds from the laboratory to the field one must have a clear understanding how the agrochemical will be to be applied as well as the physical property requirements required to satisfy its route to its final site of action. The three most important physical properties to monitor are the logP, the vapor pressure, and whether it is neutral, acidic or basic. One critical issue is how to get reliable physical property values that can be trusted? For example, knowing if a compound had a logP of 2.0 or 3.0 will determine if it can or cannot be phloem mobile. Calculated logP methods often fail to accurately predict the correct value when not properly parameterized for the specific chemical in question. We have come to rely on the HPLC-logP method(6) to provide lipophilicity values that are rapid, reliable and quite reproducible. In addition, when the HPLC-logP experiment is carried out at pH

values of 2, 7 and 11; it then also provides clear insight to the acidic and basic properties of the agrochemical. When the value of the vapor pressure is critical, there is a similar problem. It is common to see literature values to differ by an order of magnitude, and if the compound is in early stage of development, the expense and value of carrying out a formal vapor pressure measurement is highly questionable. We have also come to rely of the gas chromatography vapor pressure method(5) to provide volatility values that have been very useful for physical property QSAR studies, and also gaining a better understanding the behavior of commercial compounds.

References

1. Colin M. Tice, *Pest Management Science*, (2001) **57**, 3-16

2. Christopher A. Lipinski, *Adv. Drug Del. Rev.* (1997) **23**, 3

3. Unless otherwise mentioned, all literature logP and vapor pressure values were taken from the 13th Edition of the Pesticide Manual, BCPC, 7 Omni Business center, Omega Park, Alton, Hamshire, GU34 2QD, United Kingdom.

4. Tally, A., D. Laird, P. Margot and B. Weiss; *Phytopathology* (1998) 88:S88.

5. Stephen F. Donovan; *Journal of Chromatography, A* (1996), **749**(1+2), 123-129

6. Stephen F. Donovan and Mark Pescatore, *Journal of Chromatography A*, (2002) **952**, 47-61

7. Geoffrey G. Briggs, Richard H. Bromilow, and Avis A. Evans, *Pesticide Science*, (1982) **13**, 495-504; Geoffrey G. Briggs, Richard H. Bromilow, Avis A. Evans and M. Williams, *Pesticide Science*, (1983) **14**, 492-500

8. Scott D. Cunningham, Todd A. Anderson, A. Paul Schwab and Francis C. Hsu; *Advances in Agronomy*; (1996); **56**, 74-82 and Francis C. Hsu, Ronald L. Marxmiller, and Alex Y.S. Yang; *Plant Physiol.*, (1990) **93**, 1573-1578

9. I. Häuser-Hahn, P. Baur and W. Schmitt, *Pflanzenschutz-Nachrichten Bayer* (2004), **57**, 3, 437-450

10. Dave W. Bartlett, John M. Clough, Chris R. A. Godfrey, Jeremy R. Godwin, Alison A. Hall, Steve P. Heaney and Steve J. Maund, *Pesticide Outlook* , August (2001), 143-148

11. Francis C. Hsu, Kingmo Sun, Daniel Kleier, and Max Fielding; *Pestic. Sci.* (1995) 44, 9-19; Francis C. Hsu, Daniel A. Kleier, and Wayne Melander; *Plant Physiol.* (1988) **86**, 811-816

12. Francis C. Hsu and Daniel A. Kleier; *J. Exp. Bot.*; (1996) **47**, 1265-1271

13. Kieth Chamberlain, Shilpa Patel and Richard H. Bromilow; *Pestic. Sci.*; (1998) **54**, 1-7

14. Francis C. Hsu, Ronald L. Marxmiller, and Alex Y.S. Yang; *Plant Physiol.*, (1990) **93**, 1573-1578

15. C.A. Edwards; *Residue Rev.;* (1966) **13**, 83-132;   C.R. Harris; *Annu. Rev. Entomol.;* (1972) **17**, 177; G.G. Briggs; *BCPC Monograph* 27; British Crop Protection Council; Bracknell, U.K., (1984) 35-47; Kirk A. Simmons, *et.al.; J. Agric. Food Chem.*, (1992) **40**, 306-311.; C.R. Harris, B.T. Bowman; *J. Econ. Entomol.*; (1981) **74**, 210

16. A. S. Felsot, Albert C. Lew; *J. Econ. Entomol.*; (1989) **82**, 389

17. Kirk A. Simmons, Albert C. Lew, I. Robert Silverman, and Syed F. Ali; *J. Agric. Food Chem.*, (1992) **40**, 1432-1436

Chapter 3

Early Stage Assessment of Metabolic Stability *In Planta*

Roobina I. Baloch, Carla N. Yerkes, Gerrit J. Deboer, and Jeffrey R. Gilbert

Dow AgroSciences LLC, 9330 Zionsville Road, Indianapolis, IN 46268

Metabolic stability is a major factor impacting the translation of many agrochemical molecules from the *in vitro* to *in planta* bioactivity. Thus, assessment of metabolic stability can be highly beneficial when optimizing molecules in early stages of Discovery. This chapter introduces a medium throughput cell culture assay which successfully increased throughput by >20 fold, leading to efficient use of space and resources by miniaturizing the process. The use of more sensitive analytical techniques such as LC-MS has allowed this assay to provide reliable data with non-radiolabeled compounds, enabling the assessment of metabolism much earlier in the Discovery process. This chapter describes the development and validation of the assay using commercial fungicides and demonstrates the ability of this cell culture assay to identify many of the metabolites found in whole plants.

23

In planta metabolic stability of agrochemicals is a critical factor for successful activity translation. If the molecules in question are readily metabolized by the plant they may not provide robust and residual activity in the greenhouse or in the field, and therefore will not be suitable candidates for commercial products. Thus, metabolic stability of molecules in plants becomes a critical factor in early stage Discovery. However, determining metabolic stability in plants at such an early stage has its challenges. Radiolabeled molecules of interest are often not available, so metabolic information must be obtained from a complex matrix, such as a plant, without the benefit of radiochemical detection. The data also need to be generated in a timely fashion to be useful in making advancement decisions. Often at this stage there are a larger number of compounds to be analyzed than if the experiment were to be done later in the Discovery process. In addition to these challenging requirements, the data must be of high quality, be reproducible and be representative of what is found in whole plants. This is especially true for the primary metabolites formed early in the metabolic pathway.

The requirement for producing metabolism information without the use of radiolabel makes it very attractive to use a relatively clean system such as cell culture so that any metabolites formed can be more readily observed. Cell cultures have been used for many years to study metabolism of xenobiotics in plants. A number of studies have compared the metabolism observed in whole plants with the metabolites found in cell culture *(1-3)*. These studies have generally found that the metabolites observed were qualitatively very similar, although quantitatively there may be differences. However, at an early stage in Discovery where it is most important to find the primary sites of metabolism, plant cell cultures can provide a suitable model. In addition, the compounds can be added directly to the cell cultures, thus allowing the cells to be bathed in the media containing the compound of interest. The rate of metabolism in cell cultures is also often faster than that in whole plants. This allows metabolism information to be obtained with an incubation duration of 48 hours, whereas in the whole plant it may require a week or more to obtain the same level of metabolism. A number of excellent reviews have been published describing the benefits of using plant cell cultures to study metabolism in plants *(4-6)*. The capabilities of cell cultures to rapidly produce metabolites, often to high levels, with less purification of extracts required prior to analysis makes them the preferred system for studying plant metabolism at early stages in the Discovery process. The plant metabolism assay described in this chapter uses wheat cell cultures, but cell cultures have been produced from a large number other plant species. Examples from the literature include, corn and wheat *(7)*, carrot, soybean, thorn apple, wheat and purple foxglove *(8)*.

Prior to the development of the medium-throughput system described here, cell culture experiments were normally conducted in 250 mL Erlenmeyer flasks containing a 50 - 100 mL culture volume including the compound of interest. If media-only controls were included, an incubator equipped with an orbital shaker

with 40 spaces would allow only 20 compounds to be tested at one time. This shows that even with the use of cell cultures, laboratory space can be a limitation to the size of study and number of compounds that can be analyzed at one time. If more than 20 compounds were to be tested, a significant amount of shaker space was required. With the development of analytical systems which are more sensitive, such as the modern liquid chromatography/mass spectrometry (LC/MS) instruments, analysis of ng quantities of compounds is very possible. Thus, it is no longer necessary to extract milliliters of cell culture per time point for metabolism analysis. The same quality of data can now be obtained with sub-milliliter quantities of cell culture. With these advances in mind, a medium-throughput metabolism assay was developed utilizing wheat cells.

Medium-Throughput Cell Culture Assay

Cell Culture Volume

The minimum volume of cell culture which would provide sufficient aeration for good cell growth while still maintaining a reasonable extraction volume was determined over a range from 50 mL in the Erlenmeyer flasks down to one mL in a 96-well plate. The final volume which gave the correct balance between having sufficient aeration and amount of cell culture for metabolism was 7 mL of cell culture in a 6-well culture plate.

Cell Density Standardization

When optimizing cell density testing conditions for the assay, three factors were considered: (i) the cell density must be high enough to provide sufficient metabolism of the compound of interest, (ii) over a 48-hour period the cells must not over-grow and cause aeration issues and (iii) that the cells do not reach stationary phase before the end of the incubation period. Six different densities were evaluated, and a cell density of 30 mg/mL was chosen which met all three of the above criteria.

The cell density was obtained by measuring the fresh weight of an aliquot of cells removed from the parent culture. The medium was removed by vacuum filtration using a Buchner funnel and cells were collected on Whatman No. 1 filter paper. Cells were weighed immediately and fresh weight density was calculated. Once the cell density in the parent culture was determined, an aliquot was diluted with fresh media to produce a 30 mg/mL cell culture which was used in the assay.

Composition of the Media used in the Assay

MS2D medium (MS salts and vitamins *(9)* with 30 g/L sucrose, 100 mg/L myo-inositol, 100 mg/L casein hydrolysate, and 2 mg/L 2,4-D at pH 5.8) was utilized in the routine maintenance of the wheat cell culture, as well as for conducting metabolism and media stability testing.

Assay Set up

Seven mL of the cell culture adjusted to 30 mg/mL with media was aliquoted into each well of the 6-well plates. Care was taken to keep the cell culture well mixed as each 7 mL aliquot was removed. Each test compound was solubilized in DMSO and 14 µL of the stock solution added to each 7-mL sample of cell culture resulting in a final concentration of 20 ppm and DMSO concentration of 0.2% (v/v). At concentrations of approximately 10-20 ppm, the test compound concentrations were high enough to analyze by high-performance liquid chromatography (HPLC). However, when test compounds were not water-soluble at these concentrations, DMSO concentration could be increased as high as 1% (v/v) without negatively impacting the cell cultures. Alternatively, sample compounds could be tested at lower concentrations, down to 1 ppm. In these cases, the analysis was conducted by LC/MS.

A second culture plate was prepared with media alone (i.e., no cells were added) to assess the degree to which the compounds under test behave in simple hydrolytic conditions. This important control was added to assess abiotic hydrolytic breakdown that could be errantly attributed to metabolism in the plant. The media only control also gave information of the solubility of the compound under the test conditions as illustrated later in the chapter. Using this format, 6 compounds could be tested in 2 plates. Up to six 6-well plates could be stacked one on top the other without the stack becoming unstable on an orbital shaker. The surface area of one orbital shaker allowed for 12 stacks to be placed side by side. This meant that the capacity available on one shaker allowed for a potential total of 216 compounds to be tested at the same time.

Incubation and Sampling

The cell cultures were routinely maintained and the metabolism assays were incubated at 27°C on an orbital shaker set at 120 rpm. A time course with 4 time points was generally utilized. Aliquots of 0.5 mL were taken from the samples containing the cell cultures and also from those with media. The aliquots were taken at time 0 (within a few minutes of when the compound is added), at 6 hours, 24 hours, and 48 hours. Each sample taken was transferred to an individual well of a 96-deep-well plate with 2 mL capacity per well. Two 5mm

diameter ball bearings were added to each well containing the cell culture (Figure 1). All samples taken were frozen at -20°C until the last time point was taken and then all the samples were homogenized and extracted at the same time.
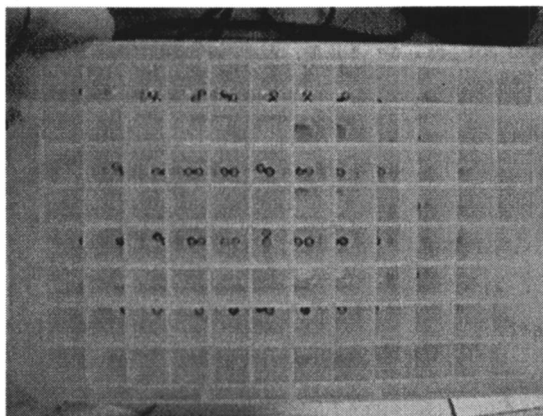
Figure 1. Showing Addition Location of Cell Culture and the Beads Ready for Homogenization

Extraction Procedure

A 0.5 mL aliquot of 100% acetonitrile was added to each of the deep wells. The 96-well plate was then covered and securely fastened onto the platform of a Geno Grinder (a homogenizer for small samples made by Spex CentiPrep Inc.). The samples were homogenized for 1 minute at 500 strokes per minute. After homogenization the plates containing the samples were centrifuged at 3,000 rpm (RCF 2000 g) for 10 minutes and the supernatant taken for HPLC analysis. If HPLC analysis was conducted using a 96-well plate autosampler, the transfer of supernatant was made into fresh 96-well plates using a liquid handler which greatly decreased the preparation time for the HPLC samples.

Cell Viability

Cell viability was assessed in all cell cultures remaining after the 48 hour time point was taken. Fluorescein diacetate was used to detect cell viability. Floreceine diacetate was added to the cell culture at a final concentration of 0.5% (w/v). Florescein diacetate is an ester which, as it enters a living cell, is

deesterified resulting in a fluorescent product *(10)*. The cells were observed under normal light (Figure 2 in the back ground) and an estimate of the number of cells was made. The same cells were then observed under fluorescent light (Figure 2 foreground) and an estimate of the number of living cells made. In this fashion the % viability of the cells at the end of the incubation period was estimated. Based on 18 months' experience with this system, the cell viability should be no lower than 50% if the results of the metabolism are to be accepted with confidence.
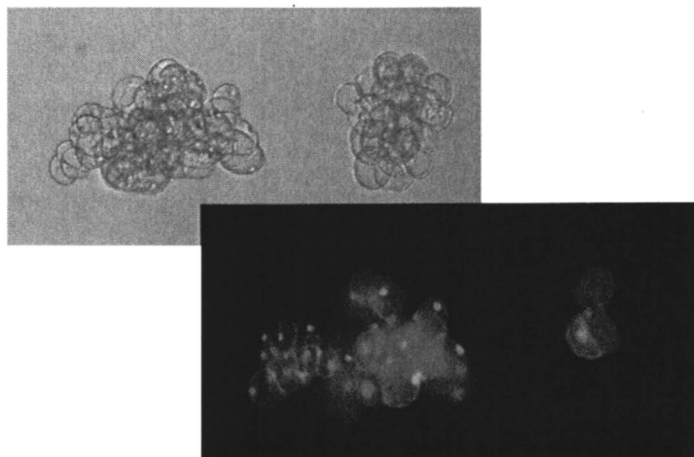
*Figure 2.   Use of Fluorescein Diacetate to Estimate Cell Viability
(See page 1 in color inserts.)*

The Commercial Standard Used to Evaluate Metabolism Assay

For this validation six commercial fungicides were selected; three strobilurins and three azoles. The fungicides were selected because their metabolism in whole plants is documented, and although they cover only 2 classes of fungicides they do vary in their physical/chemical properties, the rates of metabolism and the metabolites which are formed. The compounds tested are listed below.

- Azoxystrobin - Negative Standard
- Pyraclostrobin
- Trifloxystrobin

- Epoxiconazole
- Fenbuconazole
- Tebuconazole
- Florasulam - Positive Standard

Florasulam *(11)* is a triazolopyrimidine herbicide used for selective broadleaf weed control in wheat, barley, and oats, but is included in this experiment as a positive standard because it is rapidly metabolized in the test system. Azoxystrobin *(12)* serves as a negative standard because it metabolizes slowly in the test system. These standards provided positive and negative controls for the system, and helped put the metabolism rates of the other compounds into perspective.

Results of Metabolism Study

Media-only Controls

The media controls (medium without added cells) played two roles, providing information on those compounds which are not stable in aqueous conditions, and also determining if the compound under test was soluble under aqueous conditions. As shown in Figure 3, the level of pyraclostrobin in the incubations showed a decline over a 72 hr period. In this case, no breakdown products were observed and it is likely that the pyraclostrobin precipitated out of solution. Azoxystrobin, on the other hand, remained in solution, although there was some variation in the amounts observed at the different time points indicating that there was some variability in the assay. Due to the qualitative nature of this assay, a high level of precision is not required. None of the other compounds tested were either unstable or insoluble under the incubation conditions.

Metabolism of Commercial Standards in Wheat Cell Culture

Florasulam and trifloxystrobin are both observed to metabolize rapidly in the wheat cell culture system (Figure 4), with half lives calculated using a non-linear fit at 15.4 and 15.5 hours, respectively. Azoxystrobin was also observed to be metabolized, but the rate of metabolism was much slower than that of florasulam and trifloxystrobin (84% parent remaining 48 hours after treatment). It was not possible to accurately calculate the half life for azoxystrobin (the half life exceeded the incubation time), but it was extrapolated to be approximately 230 hours. All the other fungicides tested were stable over the 48 hour

incubation period. These results show that of the commercial fungicides tested, only trifloxystrobin would be considered to metabolize too quickly to give good
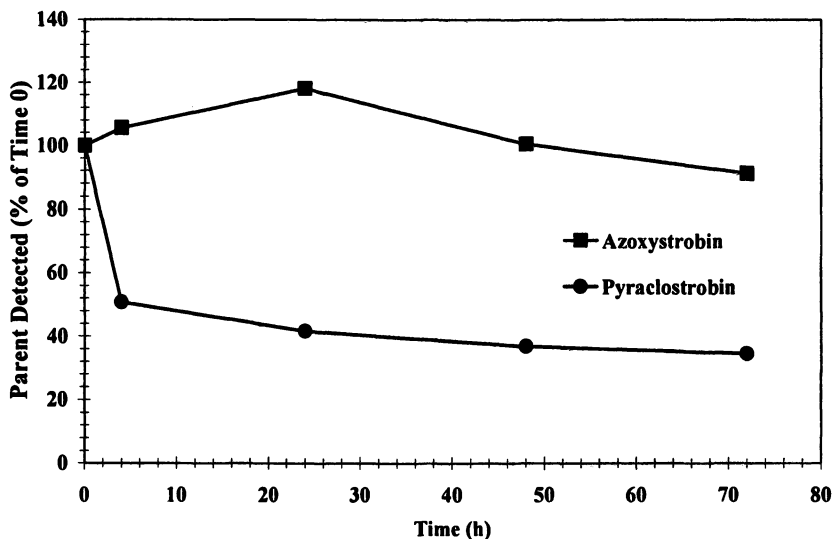
Figure 3. Solubility Limitations of Pyraclostrobin in the Media

residual disease control if its mechanism of movement and action was within the plant. However, the mechanism by which trifloxystrobin distributes around the plant is primarily via the vapor phase, thus, the rapid metabolism observed does not negatively impact its performance in the field.

Identification of Metabolites

Common Metabolic Reactions in Plants

Prior to discussing the identification of the metabolites found in these experiments, it is worth reviewing some of the common metabolic reactions that occur in plants. Metabolism in plants generally results in the formation of more polar compounds and insoluble bound residues. These metabolic processes are generally classified into three phases. Phase I is primary metabolism, which is

the conversion of active agrochemicals to less active molecules mainly via oxidation and hydrolysis. Many primary reactions actually originate from oxidation, usually catalyzed by mixed function oxidases and peroxidases *(13)*. Hydrolysis can occur either enzymatically via esterase activity or can be chemical in nature. In Phase II metabolism, primary metabolites are
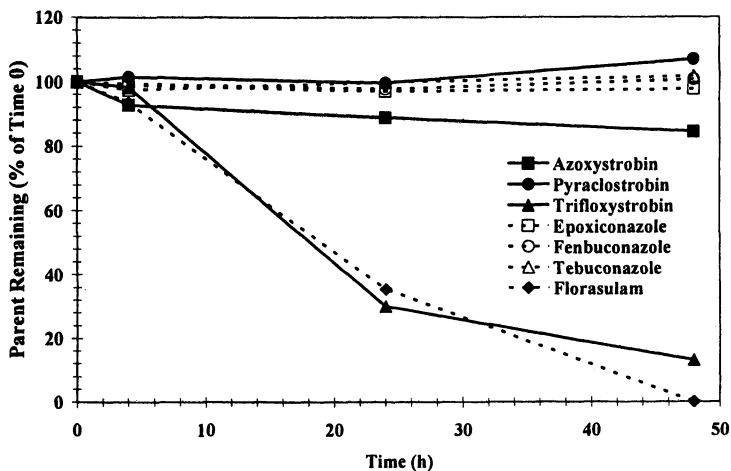
Figure 4.   Metabolic Degradation of the Fungicides Under Test Over 48 H
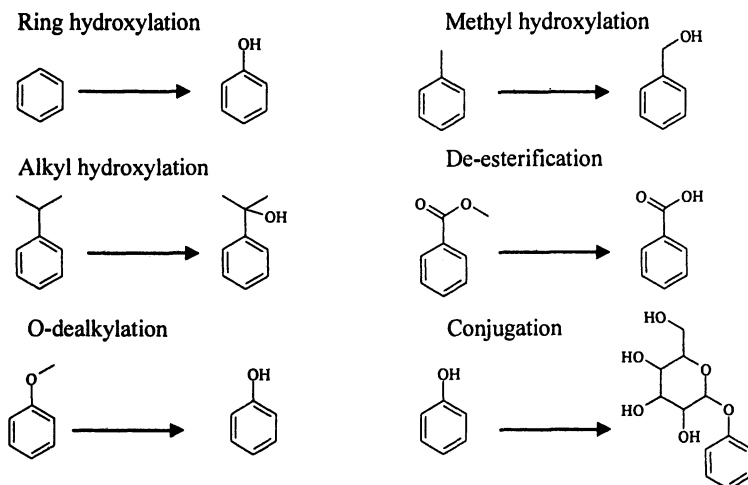
Figure 5.   The Most Common Metabolic Reactions in Plants

linked to glucose, glutathione, or amino acids to produce more water soluble conjugates which are removed to the plant vacuoles. Of these conjugates, the glucose conjugates are most common and catalyzed by glucosyltransferases. Phase III metabolism in plants involves conversion of the products of Phase II metabolism to secondary conjugates or insoluble bound residues. Figure 5 shows examples of the different types of primary and secondary metabolites that are commonly found in plants. Because we are concerned with the early stages of metabolism in this assay, examples of Phase III metabolism are rare.

Metabolism of Florasulam in Wheat Cell Culture

Florasulam is rapidly metabolized in the wheat cell culture system used in this experiment and is the basis for herbicide selectivity in this crop. The HPLC analysis of florasulam extracted from the cell culture incubation at 24 hours is shown below (Figure 6). Reverse phase HPLC conditions and a Phenomenex Luna C18(2) 150 x 4.6 mm, 5 µm column were used to separate the parent florasulam molecule from the metabolites. Conditions included a 1.0 mL/minute flow rate and a gradient of 10% acetic acid (1% v/v), 30% acetonitrile, and 60% water running to 10% acetic acid (1% v/v) and 90% acetonitrile over 20 minutes. In this experiments the metabolites formed were identified by comparison to standards. The parent molecule (Compound 1, Peak 1) undergoes ring hydroxylation, an example of Phase I metabolism, to give Compound 2 which is then linked to a glucose molecule to give the glucose conjugate (Compound 3). The HPLC chromatogram clearly shows the three components in the metabolic route and demonstrates that the cell culture system is clean enough to not only see the parent molecule but also the metabolites formed.

Metabolism of Azoxystrobin

The metabolism of azoxystrobin in whole plants results in numerous metabolites *(12)*. Three of the major metabolites generated from the parent molecule in whole plants are shown in Figure 7. Despite the slow rate of azoxystrobin metabolism in the wheat-cell culture (beyond the duration of the experiment), three metabolites were observed in the 48-hour extracts. Two of the metabolites were identified to be the same as metabolites, 1 and 2, observed in whole plants (Figure 7). The third was a benzoic acid metabolite which could be a precursor to metabolite 3. All three are results of Phase 1 metabolism. Metabolite 1 was the result of a ring hydroxylation, metabolite 2 was formed by O-dealkylation and metabolite 3 by de-esterification. These metabolites were
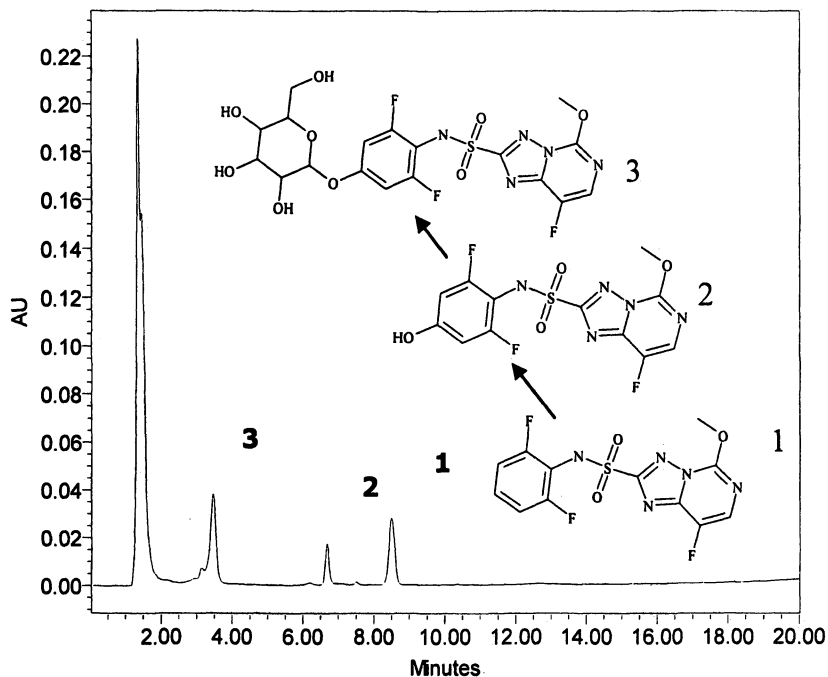
Figure 6. Metabolism of Florasulam in the Extract of 24 h Sample

identified using LC/MS on a linear ion trap mass spectrometer with electrospray ionization (ESI). For each metabolite, the protonated molecule, [M+H]$^+$, was observed by ESI/MS. The MS, MS/MS and MS^3 spectra for each metabolite were acquired in data-dependent mode. These spectra were all consistent with the metabolite structures shown in Figure 7.
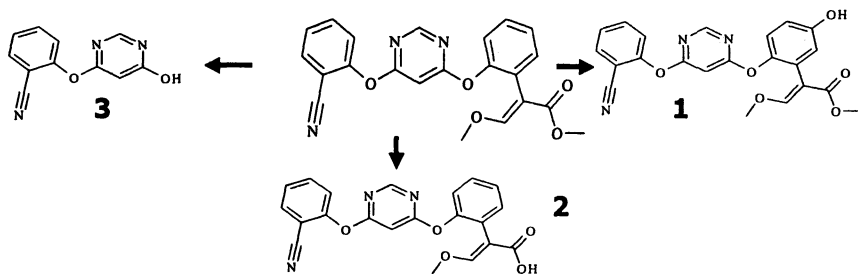
Figure 7. Major Early Metabolites of Azoxystrobin in Whole Plants (12)

Metabolism of Trifloxystrobin in Wheat

In whole plants, trifloxystrobin also produces a number of metabolites via fairly rapid metabolism *(15)*. In the cell culture experiments, trifloxystrobin was also metabolized rapidly, but only a single metabolite was detected and identified by LC/MS: de-esterified trifloxystrobin, (retention time = 10 minutes (Figure 8). This metabolite was also one of the major metabolites found in whole plants.

RT-17.8 min
MW-409

RT-10.0 min
MW-395
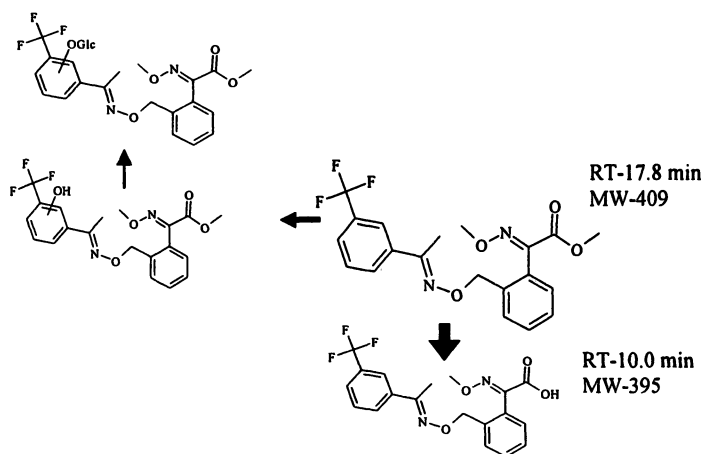
Figure 8.   Metabolism of Trifloxystrobin in Whole Plants (15)

Conclusions from the Metabolism Experiment

These results demonstrate that a cell culture system is able to generate metabolites via both Phase I and Phase II metabolic reactions. Examples of Phase I and II reactions were given for the three pesticides discussed here. It was also observed that the cell culture produced metabolites similar to those produced in whole plants. These observations suggest that the wheat cell culture assay is a good method for evaluating the initial metabolic fate of molecules in the early stages of Discovery. As the validation of the assay has been conducted with commercial fungicides, it has not been possible to demonstrate the loss of activity of a given fungicide by metabolism. In early stages of Discovery where this assay is used, many examples have been found where loss of activity of experimental fungicides can be attributed to metabolism *in planta*.

This experiment has demonstrated that cell cultures are not only suitable for determining the relative rates of metabolism, but also for determining where metabolism is occurring on a molecule. This provides the Discovery chemist a precise 'site of instability' so that synthetic modifications can be targeted to overcome metabolic instability in the molecule.

References

1. Cole D.J.; Detoxification and Activation of Agrochemicals in Plants; *Pesticide Science*; **1994**, *42*, 209.
2. Menéndez, J.; De Prado, R.; Detoxification of Chlorotoluron-resistant Biotype of Alpecurus Mysuroides. A Comparison between Cell Cultures and Whole Plants. *Physiologia Plantarum*, **1997**, *99*, 97.
3. *Metabolism of Agrochemicals in Plants*; Roberts, T. Eds.; Wiley Series in Agrochemicals and Plant Protection; 2000; p 5-42.
4. *Plant Cell Cultures; Introduction to Biotecniques*; Rickwood D.; Howe, C. Eds.; Bios, Scientific Publishers; 1998
5. Vanisree, M.; Lee, C-Y.; Lo, S-F; Nalawade, S. M.; Lin, C. Y.: Tsay, H-S.; *Studies on the Production of Some Important Secondary Metabolites from Medicinal Plant Tissue Culture.*; Bot.Bull. Acad. Sin.; **2004**, *45*; 1-22.
6. Oksman-Caldentey, K-M.; Dirk, I.; Plant Cell Factories in the Post-Genomic Era: New Ways to Produce Designer Secondary Metabolites.; Trends in Plant Sci.;**2004**, 9, 433.
7. Dubelman, A.M.; Solsten, T.R.; Fujiwara, H; Mehrsheikh, A.; *Metabolism of Halosufuraon-methyl by Corm and Wheat*; J. Agric. Food Chem.;**1997**; *45*;2314-21
8. Van der Krol, D.; Schuphan, I.; Schmidt, B.; *Metabolism of [ring-2,6-14C]Parathion in Plant Cell Suspension Cultures of Carrot (Daucuc carota), Purple Foxglove (Digitalis purpurea), Soybean, Thorn Apple (Datura stramonium) and Wheat (Triticum aestivum)*; Pestic. Sci.; **1995**; *45*, 143-52.
9. Murashige, T.; F. Skoog.; *A Revised Medium for Rapid Growth and Bio Assays with Tobacco Tissue Cultures*. Physiol. Plant; **1962**;*15*; 473-497.
10. Widholm, J.M.*; The Use of Fluorescein Diacetate and Phenosafranine for Determining Viability of Cultured Plant Cells*; Stain Tech.; **1972**; *47*; 189-194.
11. Florasulam EF-1343 Suspension Concentrate Herbicide. *Proposed Regulatory Decision Document;* Pest Management Regulatory Agency, Regulatory note 2004-4; Health Canada; **2004**; p 102.
12. Metabolic Pathways of Agrochemicals; Part 2: Insecticides and Fungicides; Eds.; Roberts, T. R.; Hutson, D.H.; *Azoxystrobin*; **1999**; 1329-1333.

13. *Metabolism of Agrochemicals in Plants*; Roberts, T. Eds.; Wiley Series in Agrochemicals and Plant Protection; **2000**; p 43-106.
14. *Metabolism of Agrochemicals in Plants*; Roberts, T. Eds.; Wiley Series in Agrochemicals and Plant Protection; **2000**; p 107-154.
15. *Proposed Regulatory Decision Document;* Pest Management Regulatory Agency, Regulatory note 2004-03; Health Canada; **2004**; p 119.

Chapter 4

Antagonism of the GABA Receptor of Dieldrin-Resistant Houseflies by Fipronil and Its Analogues

Yoshihisa Ozoe[1], Shigekazu Ishikawa[1], Soichiro Tomiyama[1], Fumiyo Ozoe[1], Toshinori Kozaki[2], and Jeffrey G. Scott[2]

[1]Department of Life Science and Biotechnology, Faculty of Life and Environmental Science, Shimane University, Matsue, Shimane 690–8504, Japan
[2]Department of Entomology, Comstock Hall, Cornell University, Ithaca, NY 14853

[³H]EBOB binding to the head membranes of the dieldrin-resistant (OCR) strain of houseflies was investigated. The OCR houseflies had an alanine-to-serine mutation at the 299-position of the RDL subunit. Scatchard analysis showed that EBOB bound to the head membranes of the OCR houseflies with 4-fold lower affinity than to those of the susceptible (WHO/SRS) strain. The membranes of the OCR strain were found to have 45-fold lower affinity for dieldrin than those of the WHO/SRS strain. By contrast, the membranes of the OCR strain showed only 2-fold lower affinity for fipronil than those of the WHO/SRS strain. The alanine-to-serine mutation does not hinder the binding of fipronil to the housefly GABA receptor.

39

γ-Aminobutyric acid (GABA) is a major inhibitory neurotransmitter in the nervous system of animals. The fast type of inhibitory neurotransmission is mediated via the ionotropic GABA receptor in postsynaptic neurons. The ionotropic GABA receptor is a chloride channel that is gated by the binding of GABA released from the terminal of presynaptic neurons. Chloride ions flow into the postsynaptic neuron through the GABA-gated channel to cause hyperpolarization, by which nerve excitation is suppressed. The mammalian channel is composed of five subunits, i.e., the α, β, γ, etc., subunits. A total of 16-19 cDNAs encoding these subunits have been cloned to date, not including the splice variants of the subunits (*1*). In the case of the insect GABA receptor, the RDL (resistant to dieldrin) subunit is the only known subunit that forms a robust chloride channel (*2*). However, it is not known whether the insect GABA receptor is formed as a homo-oligomer of the RDL subunit in neurons. The *Rdl* gene mutation underlies the resistance of insects to the chlorinated insecticide dieldrin. In the fruit fly (*Drosophila melanogaster*), the GRD (GABA$_A$ and glycine receptor-like subunit of *Drosophila*) and LCCH3 (ligand-gated chloride channel homologue 3) subunits have recently been shown to form a hetero-oligomeric GABA-gated cation channel, but this channel is not sensitive to dieldrin and lindane (*3*).

The GABA receptor is the site of action of a variety of drugs, including benzodiazepines, barbiturates, as well as other agents (*3*). Sites expected to be of particular interest to agrochemists would be those for noncompetitive antagonists. Noncompetitive antagonists bind to a site within the channel to stabilize the closed conformation of the channel and cause excitation in animals. Picrotoxinin, which is used as a reagent to block GABA-gated chloride channels, is probably the best known among such antagonists. The bicyclophosphorothionate TBPS and the bicycloorthobenzoate EBOB are not only convulsants, but are also useful ligands for labeling the antagonist site of GABA receptors. Insecticides such as lindane, cyclodienes (e.g., dieldrin, α-endosulfan, etc.), and fipronil are all noncompetitive GABA antagonists. In addition to these compounds, numerous others have been identified as antagonists (*4*). Although it is thought that these structurally diverse compounds all bind to the same site, it remains to be determined in what orientation these antagonists bind to this putative site. In particular, there remains considerable controversy regarding the binding site of fipronil (*5-7*). In the current study, we examined the binding site of fipronil and its analogues by investigating their inhibition of [^{3}H]EBOB binding to the head membranes of a dieldrin-resistant strain of houseflies.

Housefly Strains Used

We used dieldrin-resistant (OCR) and susceptible (WHO/SRS) strains of houseflies (*Musca domestica*) in the current study. Houseflies possess an RDL

subunit, the encoding DNA and deduced amino acid sequences of which have been submitted to the DNA Data Bank of Japan (Accession No. AB177547). The OCR strain of houseflies has an alanine-to-serine mutation at the 299-position of the RDL subunit, which corresponds to the RDL (A301S) mutation of the fruit fly. OCR houseflies were confirmed to be homozygous for the A299S mutation by direct sequencing of *Rdl* from individual houseflies.

Resistance of the OCR Strain to Dieldrin, Fipronil, and EBOB

We first examined the resistance of the OCR strain to three GABA antagonist/insecticides, i.e., dieldrin, fipronil, and EBOB. Figure 1 shows the dose-mortality curves for the insecticidal activity of dieldrin and fipronil determined 24 h after topical application to the OCR and WHO/SRS strains without any synergist treatment. When estimated using the 24-h LD_{50} values, the OCR strain was found to be 1800-fold more resistant to dieldrin than was the WHO/SRS strain (LD_{50}^{OCR} = 19.7 µg/fly; $LD_{50}^{WHO/SRS}$ = 10.9 ng/fly), whereas the former was 32-fold more resistant to fipronil than the latter (LD_{50}^{OCR} = 103 ng/fly; $LD_{50}^{WHO/SRS}$ = 3.26 ng/fly). These values approximate the reported values (*8*). Note that the OCR strain was resistant to fipronil, but that the resistance ratio was 56 times smaller than that to dieldrin. The resistance of the OCR strain to EBOB was low compared to that to dieldrin (Figure 2, left). The resistance ratio was 60 (LD_{50}^{OCR} = 1.69 µg/fly; $LD_{50}^{WHO/SRS}$ = 28.1 ng/fly). This ratio was identical to that previously reported based on a dieldrin-resistant strain and the SCR (susceptible) strain (*9*).

[³H]EBOB Binding to the Head Membranes of the OCR Houseflies

We next examined the binding of EBOB to the housefly GABA receptor. Figure 2 (right) compares the Scatchard plots of specific [³H]EBOB binding to the head membranes of the OCR and WHO/SRS strains of houseflies. The OCR houseflies exhibited a slightly increased number of binding sites with a decreased affinity for EBOB as compared to those of the WHO/SRS houseflies (OCR: B_{max} = 2.45 pmol/mg protein, K_d = 28.9 nM; WHO/SRS: B_{max} = 1.81 pmol/mg protein, K_d = 6.9 nM). However, the reduction of affinity in the OCR strain was by a factor of only 4. This 4-fold reduction in affinity is consistent with a previous finding (*9*). However, these findings contradict previous results of studies using fruit flies demonstrating that the RDL mutation led to either a marked reduction or a loss of [³H]EBOB binding (*10,11*). In this context, the difference between fruit flies and houseflies is elusive, as these two species of insect have the same amino acid sequence of the second transmembrane region, in which the binding site of GABA antagonists is thought to exist.
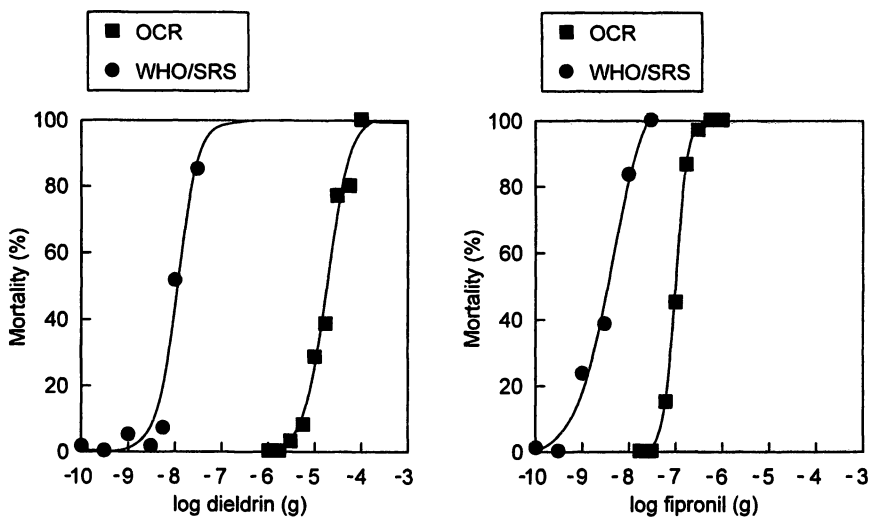
Figure 1. Insecticidal Activity of Dieldrin (left) and Fipronil (right) against OCR and WHO/SRS Strains of Houseflies.
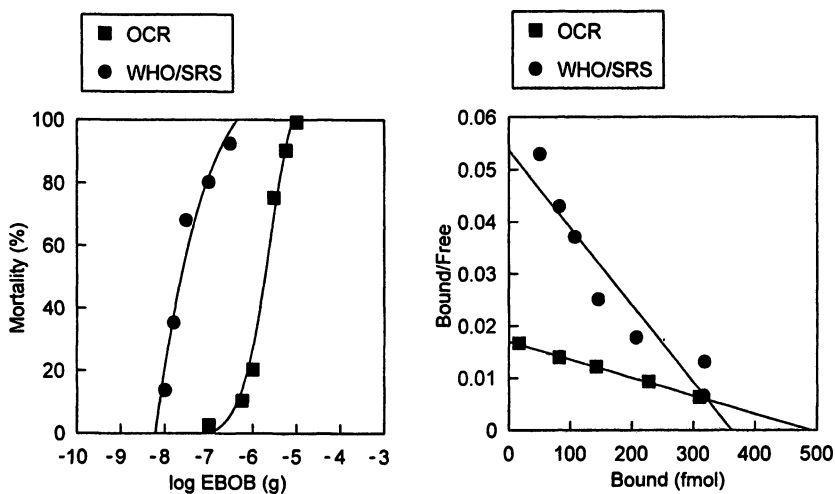
Figure 2. Insecticidal Activity of EBOB against the OCR and WHO/SRS Strains of Houseflies (left) and Scatchard Plots of [³H]EBOB Binding to the Head Membranes of OCR and WHO/SRS Houseflies (right).

Inhibition of [³H]EBOB Binding by Dieldrin and Fipronil

Since EBOB was found to bind to the GABA receptor of OCR houseflies, we performed binding assays to determine the potencies of dieldrin and fipronil in inhibiting [³H]EBOB binding to the head membranes. Figure 3 shows their respective concentration-inhibition curves for inhibiting [³H]EBOB (1 nM) binding to the head membranes of OCR and WHO/SRS houseflies. Comparison of the IC_{50} values revealed that the OCR receptor had a 45-fold lower affinity for dieldrin than the WHO/SRS receptor (IC_{50}^{OCR} = 1.40 µM; $IC_{50}^{WHO/SRS}$ = 31.1 nM). In contrast, the OCR receptor showed only 2-fold lower affinity for fipronil than the WHO/SRS receptor (IC_{50}^{OCR} = 5.51 nM; $IC_{50}^{WHO/SRS}$ = 2.83 nM).
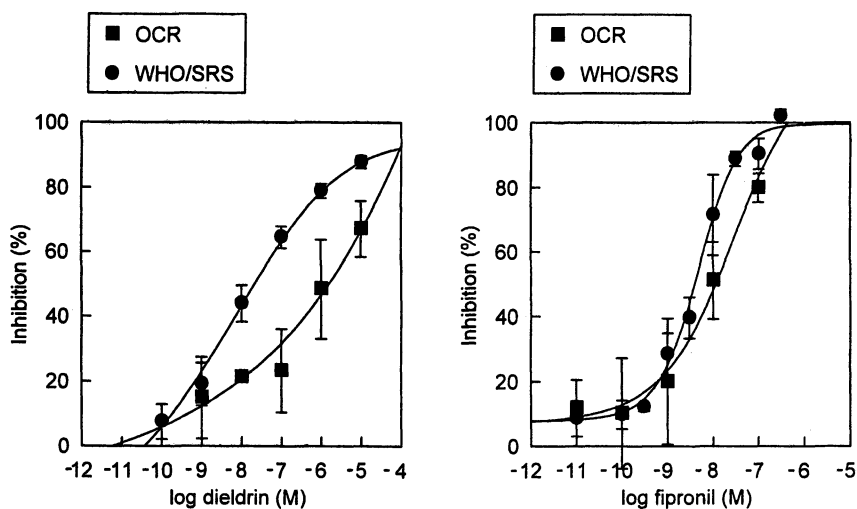
Figure 3. Inhibition of [³H]EBOB Binding to the Head Membranes of OCR and WHO/SRS Houseflies by Dieldrin (left) and Fipronil (right).

Inhibition of [³H]EBOB Binding by Fipronil and Its Analogues

We determined the pK_i values of fipronil and its analogues in the inhibition of [³H]EBOB binding to the head membranes of the OCR and WHO/SRS strains of houseflies. First, we assayed fipronil (1) and closely related analogues (2-4) in which only the 4-substituent differs from that of fipronil. As shown in Figure 4, not only fipronil (1) but also the analogues showed high potencies; moreover the potency was almost the same in both strains of houseflies. The

trifluoromethylthio (**2**), the ethylsulfinyl (**3**, ethiprole), and the thiocyanato (**4**) groups apparently confer properties similar to the trifluoromethylsulfinyl group of fipronil in terms of their high effect on the GABA receptor of the OCR strain. In contrast to fipronil and closely related analogues, 1-(2,6-dichloro-4-trifluoromethylphenyl)-5-methyl-4-nitropyrazoles with a variety of groups at the 3-position (**5-9**) exhibited only low levels of potency in the OCR strain, with K_i values in the micromolar range, whereas they showed high potency in the WHO/SRS strain (Figure 5). The selectivity ratios of these compounds were 151-565 or more. This high level of selectivity holds true of **10**, an analogue that has an amino group in place of the 5-methyl group of **5**. 1-(2,6-Dichloro-4-trifluoromethylphenyl)-3-difluoromethoxy-5-methylpyrazoles with a variety of groups at the 4-position (**11-14**) showed high levels of potency in the WHO/SRS strain, but low potency was observed in the OCR strain (Figure 6). Replacement of the 3-difluoromethoxy group of **12** with a methylsulfonyloxy group to produce **15** proved ineffective at increasing potency in the OCR receptor, although **15** was the second most potent among the compounds tested in the WHO/SRS receptor, with a K_i value of 5.54 nM. We also tested the potencies of three other phenylheterocycles (Figure 7). All of these compounds showed lower levels of potency in the OCR strain than in the WHO/SRS strain. These findings led us to speculate that fipronil and its closely related analogues belong to a class of compounds that differs from other tested phenylheterocyclic GABA antagonists in terms of their mode of action or binding.
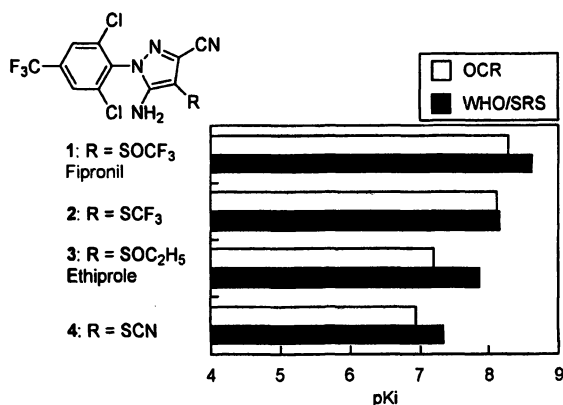
Figure 4. Potencies of Fipronil and Closely Related Analogues in the Inhibition of [³H]EBOB Binding to the Head Membranes of OCR and WHO/SRS Houseflies.
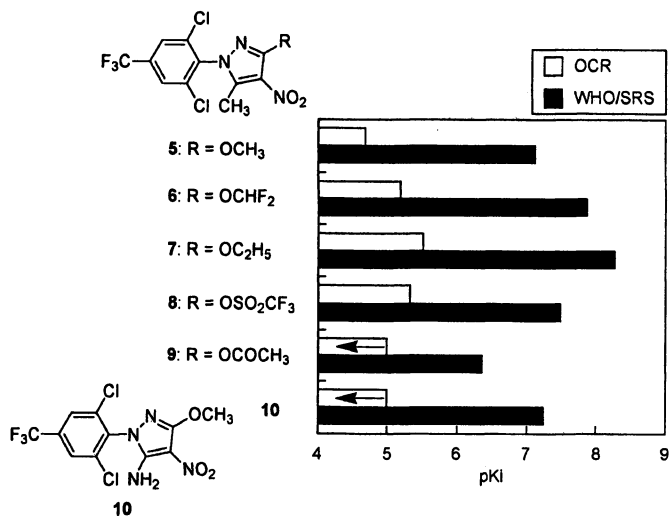
Figure 5. Potencies of Phenylpyrazoles in the Inhibition of [³H]EBOB Binding to the Head Membranes of OCR and WHO/SRS Houseflies. Arrows Indicate That K_i Values Are over 10 µM.
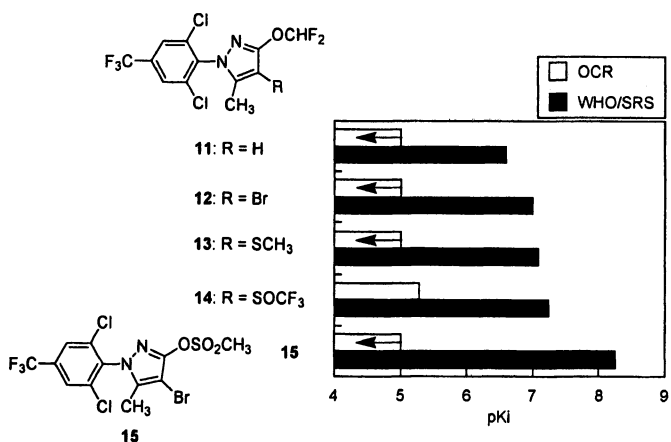
Figure 6. Potencies of Phenylpyrazoles in the Inhibition of [³H]EBOB Binding to the Head Membranes of OCR and WHO/SRS Houseflies. Arrows Indicate That K_i Values Are over 10 µM.
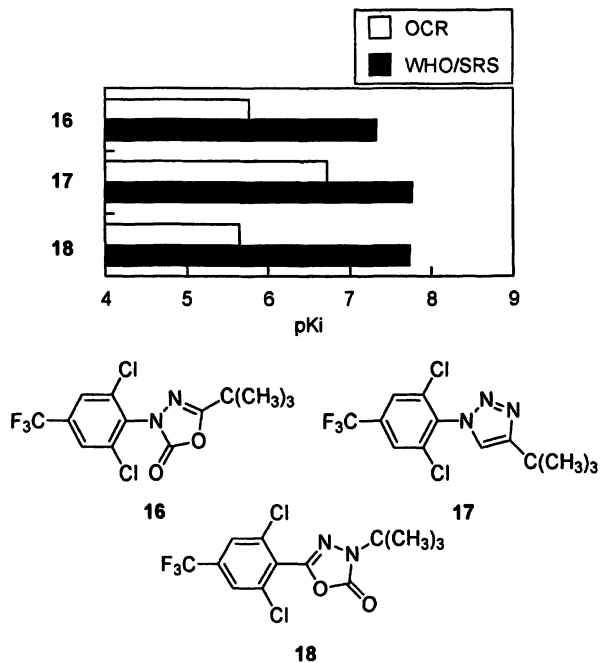
Figure 7. Potencies of Phenylheterocycles in the Inhibition of [³H]EBOB Binding to the Head Membranes of OCR and WHO/SRS Houseflies.

Fipronil Binding Site

The three-dimensional structural information of the GABA receptor, as analyzed by X-ray, has not yet been made available. Hence, we previously studied the structure-activity relationships of noncompetitive antagonists to determine whether or not structurally diverse antagonists bind to the same site (*12*). Based on the results of our three-dimensional quantitative structure-activity relationship (3D-QSAR) studies, we proposed a binding-site model that can accommodate a variety of antagonists (Figure 8). Subsite 1 most likely accepts an electronegative portion of the ligands. On both sides of Subsite 1, there may be spaces of definite size that accommodate hydrophobic and electronegative moieties on the ligands. In addition, the existence of an additional subsite, designated as Subsite 2, is speculated. The electronegative moieties of the antagonists would be expected to play a crucial role in the interaction with Subsite 1, because all antagonists have putative electronegative moieties thought to interact with this site.
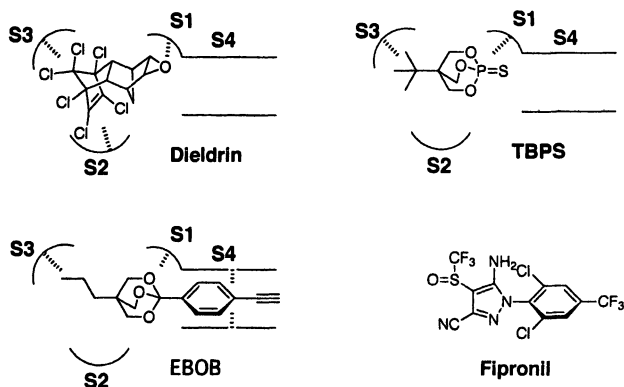
Figure 8. A Model of the Binding Site for Noncompetitive GABA Receptor Antagonists. The Orientation of Fipronil Remains to Be Determined.

In this context, it would be of interest to determine whether or not our model could be applied to the investigation of the binding mode of fipronil. In our model, the electronegative moiety on the antagonists plays a key role in the interaction with Subsite 1. In the case of fipronil, the nitrogen atoms of the pyrazole ring might play this role, and fipronil has a benzene ring similar to EBOB. It, therefore, seems reasonable to expect that the pyrazole ring and the benzene ring of fipronil interact with Subsites 1 and 4, respectively. Sammelson and colleagues (*13*) recently proposed that phenylpyrazoles interact with the binding site in the orientation described here. The main reason for proposing this binding mode was that a phenylpyrazole with a *tert*-butyl group at the 4-position and an ethynyl group at the *para*-position is highly active at the GABA receptor, and also because the phenylpyrazole is superposable on the bicycloorthobenzoate GABA antagonist. Meanwhile, the present study demonstrated that fipronil has high affinity for the receptor in OCR houseflies. Our data indicate that the alanine-to-serine mutation in the OCR houseflies does not exert a deteriorating effect on the binding of fipronil to the binding site, although it hinders the binding of dieldrin. Furthermore, it should also be noted that the orientation of fipronil at the binding site might be quite different from that of other antagonists, as an additional mutation was recently identified in the third transmembrane domain of a fipronil-resistant strain of *Drosophila simulans* obtained by laboratory selection (*14*). More work would be needed to determine the binding mode (or site) of fipronil.

Figure 9 compares the amino acid sequences of the second transmembrane α-helix region of GABA receptor subunits. The alanine-to-serine mutation of the pore-lining amino acid of the housefly RDL subunit accounts for the

resistance to dieldrin. On the basis of this finding and other site-directed mutagenesis data, the site of action of noncompetitive antagonists is believed to be around this amino acid residue on the cytoplasmic side within the channel formed by five subunits. An electrophysiological study using the fruit fly RDL subunit expressed in *Xenopus* oocytes indicated that the alanine-to-serine mutation reduced the potency of fipronil (*15*), although a conflicting experimental result was also reported using the same assay system (*16*). The reduced potency of fipronil in the mutant receptor is inconsistent with our results from binding assays, namely, that the mutation does not hinder fipronil binding. This discrepancy might indicate that the mutation may lead not only to the structural alteration of the binding site, but also to changes in the gating mechanisms. Zhang and colleagues (*17*) proposed that the mutation causes both a structural change at the binding site that leads to the unfavorable binding of antagonists and the destabilization of the antagonist-favored (desensitized) conformation by an allosteric mechanism. The latter cause has been postulated to contribute to the resistance to the antagonists by a factor of 29, independently of the structures of the antagonists. Our present findings suggest that the resistance of the OCR strain to fipronil is not due to a structural change at the binding site, but rather to the destabilization of the antagonist-favored conformation by an allosteric mechanism.

Rat α1	PARTVFGVTTVLTMTTLSIS
Rat β2	AARVALGITTVLTMTTINTH
Rat γ2	PARTSLGITTVLTMTTLSTI
Md RDL	PARVALGVTTVLTMTTLMSS
Md RDL (OCR)	PARVSLGVTTVLTMTTLMSS
Hv α1	PARVQLGVTTVLTMTTLMSS
Hv α2	PARVSLGVTTVLTMTTLMSS
Hv α3	PARVALGVTTVLTMTTLMSS
Md GluCl	PARVSLGVTTLLTMATQTSG
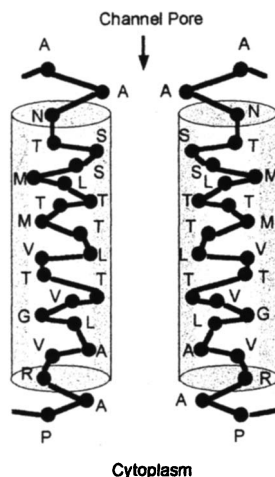
Figure 9. Amino Acid Sequences of the Second Membrane-spanning Region of GABA and Glutamate (GluCl) Receptor Subunits. Md: Musca domestica. Hv: Heliothis virescens.

Recently, Ikeda et al. (*18*) reported that fipronil acts on glutamate-gated chloride channels as well. The α-subunit of the inhibitory glutamate receptor of WHO/SRS houseflies has a serine at a position equivalent to that of the alanine-to-serine mutation of the RDL subunit, although another unidentified subunit(s) might contribute to the formation of the channel in insect neurons. Fipronil is known to have low affinity for rat GABA receptors (*6*). The major subunits of the rat GABA receptor are α1, β2, and γ2, which have valine, alanine, and serine, respectively, at the equivalent positions. Meanwhile, fipronil has high insecticidal activity against the tobacco budworm (*Heliothis virescens*). The tobacco budworm has three RDL-type subunits with glutamine, serine, and alanine, although it is not known whether the receptor in the neuron is a homo- or hetero-oligomer. It might be of interest in future studies to determine how the valine of the rat receptor or the glutamine of the *Heliothis* receptor affects the sensitivity to fipronil.

Conclusions

In the present study, we investigated the inhibition of [^{3}H]EBOB binding to the head membranes of dieldrin-resistant houseflies by fipronil and related phenylheterocycles. Fipronil and structurally closely related analogues inhibited [^{3}H]EBOB binding as potently as they inhibited the binding to the head membranes of the susceptible houseflies, whereas other phenylpyrazoles and phenylheterocycles were remarkably less potent in the resistant houseflies than in the susceptible houseflies. The alanine-to-serine mutation does not hinder the binding of fipronil and its closely related analogues to the binding site. Detailed 3D-QSAR and molecular biological studies would be needed to reveal the binding orientation of fipronil, which might in turn lead to novel discoveries in terms of the chemistry of third-generation GABA antagonist/insecticides.

Acknowledgments

References

1. Korpi, E. R.; Gründer, G.; Lüddens, H. *Prog. Neurobiol.* **2002**, *67*, 113-159.

2. Hosie, A. M.; Aronstein, K.; Sattelle, D. B.; ffrench-Constant, R. H. *Trends Neurosci.* **1997**, *20*, 578-583.
3. Gisselmann, G.; Plonka, J.; Pusch, H.; Hatt, H. *Br. J. Pharmacol.* **2004**, *142*, 409-413.
4. Ozoe, Y.; Akamtatsu, M. *Pest Manag. Sci.* **2001**, *57*, 923-931.
5. Cole, L. M.; Nicholson, R. A.; Casida, J. E. *Pestic. Biochem. Physiol.* **1993**, *46*, 47-54.
6. Gant, D. B.; Chalmers, A. E.; Wolff, M. A.; Hoffman, H. B.; Bushey, D. F. *Rev. Toxicol.* **1998**, *2*, 147-156.
7. Perret, P.; Sarda, X.; Wolff, M.; Wu, T.-T.; Bushey, D.; Goeldner, M. *J. Biol. Chem.* **1999**, *274*, 25350-25354.
8. Scott, J. G.; Wen, Z. *J. Econ. Entomol.* **1997**, *90*, 1152-1156.
9. Deng, Y.; Palmer, C. J.; Casida, J. E. *Pestic. Biochem. Physiol.* **1991**, *41*, 60-65.
10. Cole, L. M.; Roush, R. T.; Casida, J. E. *Life Sci.* **1995**, *56*, 757-765.
11. Lee, H.-J.; Zhang, H.-G.; Jackson, M. B.; ffrench-Constant, R. H. *Pestic. Biochem. Physiol.* **1995**, *51*, 30-37.
12. Akamatsu, M.; Ozoe, Y.; Ueno, T.; Fujita, T.; Mochida, K.; Nakamura, T.; Matsumura, F. *Pestic. Sci.* **1997**, *49*, 319-332.
13. Sammelson, R. E.; Caboni, P.; Durkin, K. A.; Casida, J. E. *Bioorg. Med. Chem.* **2004**, *12*, 3345-3355.
14. Le Goff, G.; Hamon, A.; Bergé, J.-B.; Amichot, M. *J. Neurochem.* **2005**, *92*, 1295-1305.
15. Hosie, A. M.; Baylis, H. A.; Buckingham, S. D.; Sattelle, D. B. *Br. J. Pharmacol.* **1995**, *115*, 909-912.
16. Wolff, M. A.; Wingate, V. P. M. *Invertebr. Neurosci.* **1998**, *3*, 305-315.
17. Zhang, H.-G.; ffrench-Constant, R. H.; Jackson, M. B. *J. Physiol.* **1994**, *479*, 65-75.
18. Ikeda, T.; Zhao, X.; Kono, Y.; Yeh, J. Z.; Narahashi, T. *NeuroToxicology* **2003**, *24*, 807-815.

Chapter 5

Thiamethoxam: A Neonicotinoid Precursor Converted to Clothianidin in Insects and Plants

Peter Jeschke[1] and Ralf Nauen[2]

[1]BCS-RD-R-I-CI, Building 6240, [2]BCS-RD-R-I-BI, Bayer CropScience AG, Alfred-Nobel-Strasse 50, D–40789 Monheim am Rhein, Germany

Neonicotinoid insecticides act agonistically on insect nicotinic acetylcholine receptors (nAChRs). Like imidacloprid (IMI), all neonicotinoids bind with high affinity (I_{50}-values ~ 1 nM) to [^{3}H]IMI binding sites on insect nAChRs. One notable omission is thiamethoxam (THIAM), showing binding affinities up to 10,000-fold less potent than other neonicotinoids, using housefly head membrane preparations. Clothianidin (CLOTHI) exhibits high activity as an agonist on isolated neurons at concentrations as low as 30 nM. Pharmacokinetic studies in different insect species revealed that THIAM was rapidly metabolized to CLOTHI, which shows high affinity to nAChRs in both binding assays and whole cell voltage clamp studies. When applied to cotton plants, THIAM was also quickly metabolized, with CLOTHI being the predominant neonicotinoid *in planta* briefly after application, as indicated by LC-MS/MS analyses. Our studies show that THIAM is likely to be a neonicotinoid precursor for CLOTHI and not active by itself.

51

Neonicotinoids are insecticides acting on insect *n*AChRs *(1)*. For a long time they are very effective on commercially important *Hemipteran* pest species such as aphids, whiteflies and planthoppers, but also control *Coleopteran* and some *Lepidopteran* pests *(1)*. The biochemical mode of action (MoA) of neonicotinoids has been studied and characterized extensively in the past 10 years. All neonicotinoids act selectively as agonists at the insect *n*AChRs and they are part of a single MoA group as defined by the Insecticide Resistance Action Committee (IRAC; an Expert Committee of Crop Life) for resistance management purposes *(2)*. Today the neonicotinoids are:

- The fastest growing group of insecticides introduced to the market since the launch of pyrethroids *(3)*, with wide-spread use in most countries in many agronomic cropping systems - especially against sucking pests, but also against ectoparasitic insects.

- An important class of insecticides - the estimated marked share in 2005 will be approximately 15 %.

- Relatively low risk and target-specific products combined with a suitability for a range of application methods, which will maintain them as important insecticides also in Integrated Pest Management (IPM) strategies.

Therefore, handling of resistant management strategies in pest control using neonicotinoid insecticides is essential *(4)*. A conversion of neonicotinoid sub types, so-called precursors, into an active neonicotinoid could have a significant impact on this matter.

Different Structural Types of Proneonicotinoids

Pharmaceutical conceptions in prodrug design generally focus on its potential in overcoming pharmacokinetic problems and poor oral absorbtion *(5)*. Prodrug activation occurs enzymatically, non-enzymatically, or also sequentially (enzymatic step followed by non-enzymatic rearrangement) *(6)*. Depending on both the drug and its prodrug, the therapeutic gain may be modest, marked or even significant *(7)*.

The literature of neonicotinoid chemistry reflects some significant examples for so-called proneonicotinoids in crop protection (Figure 1).

1. 5-Ring systems like *N*-methyl-IMI **2** (I; R=H, R'=Me), which is an *in vitro* inactive precursor of IMI **1** (I; R, R'=H), show low binding affinity to

nAChR with a pI_{50}-value at 5.8. As described by Yamamoto *et al. (8)* its *N*-demethylation occurs in microsomal fractions.

2. The metabolism of IMI **1** *(9)* is strongly influenced by the method of application *(10)*. Whilst in foliar application most of the residues on the leaf surface display unchanged parent compound, most of the IMI **1** administered to plants by soil application or seed treatment is metabolized more or less completely *(11)*, depending on plant species and time *(12)*. According to the metabolic pathway of IMI **1** in *Bemisia tabaci* (cotton whitefly) *(13)* it is known, that hydroxylation of the imidazolidine 5-ring in 4- and/or 5-position leads in general to the *mono* and *bis*-hydroxylated derivatives (pI_{50}-value 5.5) with reduced binding affinity. On the other hand, the metabolite 5-hydroxy-IMI **3** (**I**, R=OH, R'=H) reflects a higher level of efficacy with a pI_{50}-value of 8.5 *(14, 15)* than 4-hydroxy-IMI (pI_{50}-value 7.6). Interestingly, the olefinic metabolite **4** (**I**, R, R'=H; HC=CH-bond in 4- and 5-position) which is formed only in minor amounts by dehydratization showed a higher pI_{50}-value for nAChR from housefly head membranes (pI_{50}-value 9.6) than IMI **1** (pI_{50}-value 9.3) and provides superior toxicity to some *Hemipteran* pests after oral ingestion *(10)*.

CPM = 6-chloro-pyrid-3-ylmethyl
CTM = 2-chloro-1,3-thiazol-5-ylmethyl
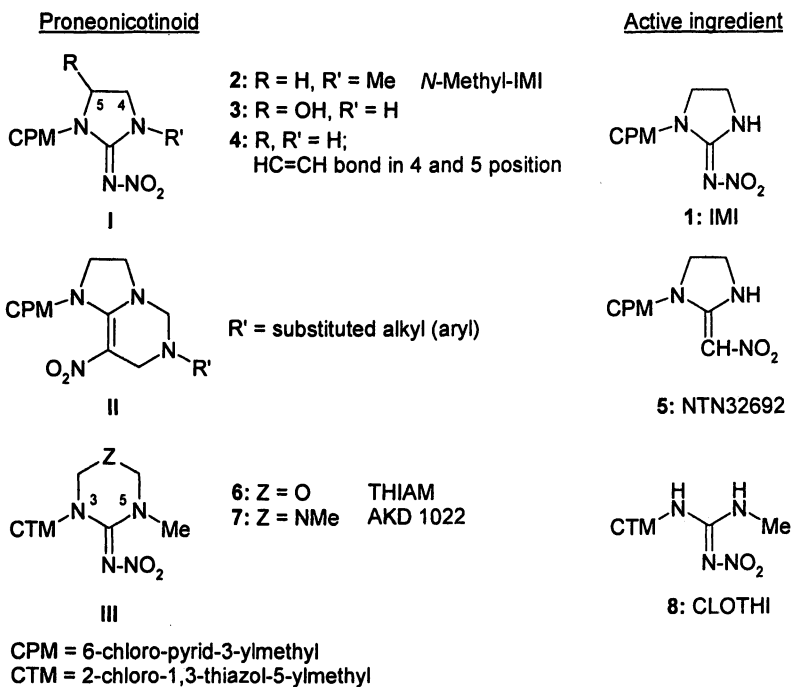
*Figure 1. Proneonicotinoids **I-III** and Their Active Ingredients **1**, **5** and **8**.*

3. Certain insecticidally active nitromethylenes so-called Mannich adducts were published in 1988 *(15)*. At different pH-values, hydrolysis of the cyclic Mannich adducts (**II**) forming the imidazolidine 5-ring **5** (NTN32692) can be observed. Utilizing this cleavage assay, the pH-dependence of the 6-ring cleavage reaction was investigated in order to identify the formed cleavage product. The analytical data (HPLC, NMR) clearly show that the nitromethylene **5** is formed and obviously responsible for activity. It was discovered, that all the Mannich adducts (**II**) exhibit the same insecticidal activity against *Myzus persicae* (green peach aphid) and *Nephotettix cincticeps* (green rice leafhopper) at 40 ppm and 8 ppm similar to the parent nitromethylene **5**.

4. Kagabu *(16)* has studied the hydrolysis (ring cleavage) of neonicotinoids having a 6-ring system (**III**), like the core heterocyclic perhydro-1,3,5-oxadiazines (Z=O), perhydro-1,3,5-thiadiazines (Z=S) and hexahydro-1,3,5-triazines (Z=NMe) *(cf.* AKD1022 **7**) containing *e.g.* a CTM or CPM moiety in physiological salt solution at 25 °C (pH 7.3). Recently, it was demonstrated that THIAM **6**, having a perhydro-1,3,5-oxadiazine (Z=O) structure, is also an *in vivo*, easy-to-cleave neonicotinoid precursor of the highly active non-cyclic neonicotinoid CLOTHI **8** *(17)*. This suggests a prodrug principle in the MoA of THIAM **6**, rather than differences in the binding site *(18)*.

Thiamethoxam as Neonicotinoid Precursor of Clothianidin

In recent studies it was described, that the *N*-demethylation of THIAM **6** (pI$_{50}$-value 5.3) *in vivo* may result in a metabolite - *N*-desmethyl-THIAM **9** - which shows much stronger binding affinity to insect *n*AChR with a pI$_{50}$-value of 8.7 (Figure 2).

9: *N-*Desmethyl-THIAM   6: THIAM   8: CLOTHI

[a] *N*-demethylation
[b] perhydro-1,3,5-oxadiazine ring cleavage
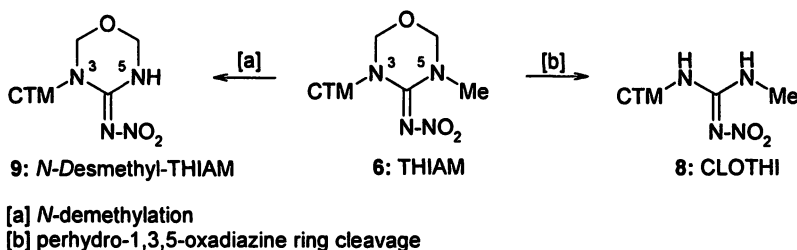
Figure 2. Possible Formation of the Active Metabolite of THIAM 6.

Therefore, it was speculated that this metabolite **9** may have potential to contribute to the insecticidal activity of THIAM **6** administered to insects. The biological efficacy of *N*-desmethyl THIAM **9** against *Aphis gossypii* (cotton aphid) is approximately 25-fold less compared to THIAM **6**, suggesting either pharmacokinetic or much more likely toxicodynamic constraints. However, besides *N*-demethylation, it could also be assumed that under metabolic conditions the cleavage of the 6-ring system in THIAM **6** leads to the non-cyclic and highly active CLOTHI **8** (pI_{50}-value 9.2) as metabolite, which is today commercialized by Sumitomo Chemical Takeda Agro Company and Bayer CropScience AG, *e.g.* as Dantotsu[TM] for foliar treatment and Poncho[TM] for seed treatment *(19)*. Therefore, it was interesting to check the metabolic pathway of THIAM **6** experimentally.

Isosurface of the Fukui Function - Electrophilic Attack

In this connection the usefulness of local reactivity descriptors for understanding drug metabolism of neonicotinoids, the electrophilic Fukui function of THIAM **6** was investigated *(20)*.

The Fukui function is a three dimensional function calculated quantum chemically from electron densities. It exhibits maxima in regions of space, where a molecule prefers to be attacked by a nucleophile/electrophile or radical. It can be shown *(21)* that local maxima of the electrophilic Fukui function relate to preferred sites of oxidative metabolic attack in many cases. One has to keep in mind that the Fukui function describes reactivity against an isotropic, abstract "reactivity bath". Any enzyme specific effects are not accounted for within the Fukui framework.

Visual inspection of the maxima of the electrophilic Fukui function of IMI **1** shows that the 5-position of the imidazolidine 5-ring system (*cf.* arrow in Figure 3) corresponds to the major site of electrophilic, oxidative metabolic attack as displayed by the level of isosurface. This fact may serve as a hint, why IMI **1** is metabolized in 4- and/or 5-position forming the hydroxylated metabolites such as 5-hydroxy-IMI **3** (I, R=OH, R'=H; *cf.* Figure 1).
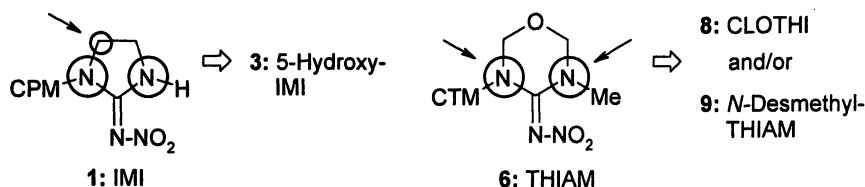
Figure 3. Fukui Function for Electrophilic Attack on IMI 1 and THIAM 6.

To broaden up the usefulness of local reactivity descriptors for understanding drug metabolism of neonicotinoids, the electrophilic Fukui function of THIAM **6** is also considered. It was found that in this case the electrophilic Fukui function showed maxima at experimentally observed sites of metabolism for this 6-ring compound. The Fukui functions are focused at the 3,5-positions of the core heterocyclic perhydro-1,3,5-oxadiazine (**III**, Z=O) ring system (Figure 1), which could correspond to the major site of metabolic attack. In other words, this result may serve also as a hint that THIAM **6** is metabolized in 5-position and/or 3,5-position of the 6-ring system forming *N*-desmethyl-THIAM **9** and/or CLOTHI **8** (Figure 2 and *cf.* two arrows in Figure 3).

Displacement of [³H]IMI by Different Neonicotinoids from nAChRs

Displacement of [³H]IMI **1** by different neonicotinoids from *n*AChR is generally described as I_{50}-value. The I_{50}-value (in nM) represents the concentration needed to displace half of the radioligand from its binding site at the *n*AChR.

It was found, that *N*-methyl IMI **2** (I_{50}-value 1600 nM) and THIAM **6** (I_{50}-value 5000 nM) showed only weak activity in displacing [³H]IMI **1** from its *n*AChR binding site in housefly head membrane preparations. In contrast, CLOTHI **8** (I_{50}-value 0.60 nM) and IMI **1** (I_{50}-value 0.79 nM) showed the highest affinity, both in the sub-nanomolar range, whereas *N*-desmethyl THIAM **9** (I_{50}-value 8 nM) was approximately 10-fold less active. The binding affinity of CLOTHI **8** to housefly *n*AChR preparations was comparable to that of IMI **1** and more than 8000-fold higher than that of THIAM **6**. In other words, THIAM **6** is up to 10,000-fold less active than other neonicotinoids such as thiacloprid (I_{50}-value 0.50 nM).

Very recently an alternative explanation for the obvious lack of THIAM **6** competition with all known tritiated *n*AChR ligands was presented by Wellmann *et al. (22)*. The authors were able to demonstrate:

- Binding of [³H]THIAM **6** to aphid membrane preparations - however, no correlation between aphid toxicity and binding was conclusively shown.
- The K_d-values for THIAM **6** were in the upper nM range - but still more than 100-fold higher than those found for IMI **1** for the same aphid species.
- IMI **1** turned out to be a non-competitive blocker at the THIAM **6** binding site, which is temperature sensitive and disappeared after freezing and thawing.

Interestingly the authors were not able to obtain consistent data for specific binding of [³H]THIAM **6** to *Aphis craccivora* (cowpea aphid) membranes at 22 °C, but at 2 °C. However, for *M. persicae* (green peach aphid) they obtained binding at both temperatures.

Insecticidal Efficacy of Selected Neonicotinoids

(a) M. persicae: The neonicotinoids IMI **1**, THIAM **6** and CLOTHI **8** showed similar effects against *M. persicae* in leafdip bioassays. This is demonstrated when comparing the efficacy of these neonicotinoids as LC_{95}-values 6 days after treatment. The LC_{95}-values were between 1.1 and 1.3 mg l^{-1}. Furthermore it was found, that *N*-methyl IMI **2** (LC_{95}=5.93 mg l^{-1}) and *N*-desmethyl THIAM **9** (LC_{95}=31 mg l^{-1}) were 4-5-fold and up to 30-fold less active than the three other neonicotinoids, respectively.

(b) Noctuid larvae: In order to check the toxicological relevance of electrophysiological measurements and metabolic studies using *Heliothis virescens* (tobacco budworm) neurons and *Spodoptera frugiperda* (fall army worm) larvae, the efficacy of THIAM **6**, CLOTHI **8** and *N*-desmethyl THIAM **9** was tested against both of these noctuid pests. All compounds showed insecticidal activity, and the observed symptomology of poisoning was consistent with the known agonistic action on insect *n*AChR - excitatory symptoms were usually observed already after one hour exposure.

The most potent neonicotinoid insecticide in feeding bioassays with *H. virescens* and *S. frugiperda* was CLOTHI **8**. THIAM **6** was considerably less active against larvae of both lepidopteran pests, and *N*-desmethyl-THIAM **9** was the least active compound, being 25-fold less active than CLOTHI **8** *(17)*.

Whole Cell Current Responses of Neurons Isolated from *Heliothis virescens*

A comparison was carried out of neonicotinoid efficacy regarding the whole cell current responses of neurons, isolated from the central nervous system (CNS) of tobacco budworm. In excellent correlation to the weak activity in larvae displacing [³H]IMI **1** from its *n*AChR binding site as already shown, *N*-methyl-IMI **2** demonstrates no activity on *Heliothis* nerve cells in our study (Figure 4).
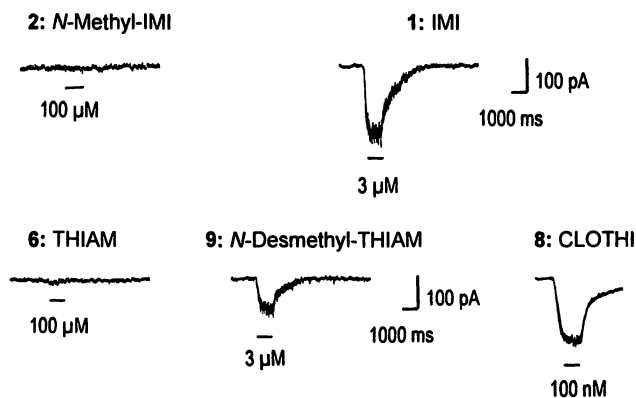
*Figure 4. Whole Cell Current Response of Neurons
Isolated from H. virescens (17).*

Whereas IMI **1** has considerable activity on *Heliothis* nerve cells. Similar to *N*-methyl IMI **2** mentioned before, THIAM **6** showed only weak activity in displacing [^{3}H]IMI **1** from its *n*AChR binding site in housefly head membrane preparations, and no response of nerve cells was observed (Figure 4). In contrast, CLOTHI **8** reflected the highest affinity, in sub-nanomolar range, whereas *N*-desmethyl THIAM **9** was approximately 10-fold less active.

THIAM **6** and *N*-methyl IMI **2** (although toxic to larvae) failed to induce whole cell currents at concentrations as high as 0.3 mM. Whereas *N*-desmethyl THIAM **9** and IMI **1** induced a fast inward current at a test concentration of 0.003 mM, and CLOTHI **8** at concentrations as low as 30 nM, *i.e.*, 10,000-times less than the highest THIAM **9** concentration tested.

The conclusion which can be drawn from the study was that THIAM **6** and *N*-methyl IMI **2** as well does not act on *Heliothis* *n*AChRs present on neuronal cell bodies isolated from the CNS, even at very high concentrations unlikely to be found by LC-MS/MS in intoxicated insects.

Metabolism of Thiamethoxam in Cotton Plants

True leaves of cotton plants treated with an aqueous solution of 100 ppm THIAM **6** by soil drench application were analyzed by LC-MS/MS three days after treatment and were shown to contain large quantities of CLOTHI **8**. (Figure 5).
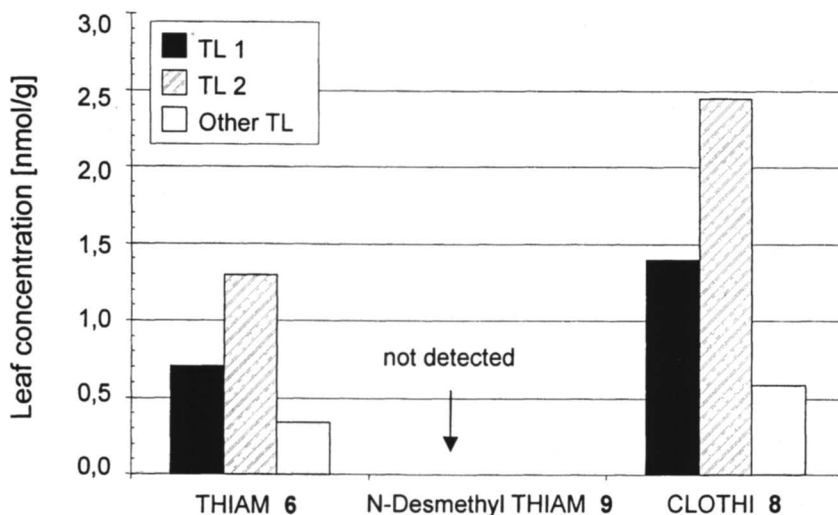
Figure 5. True Leaf Concentrations of THIAM 6, CLOTHI 8 and N-Desmethyl-THIAM 9 in Cotton Plants 3d After Drench Application of THIAM 6 (17).

The CLOTHI **8** concentration in the true leaf extracts was approximately twice as high as the THIAM **6** concentration, this indicates considerable metabolism of THIAM **6**. The amount of *N*-desmethyl THIAM **9** found in cotton true leaves was below the detection limit, *i.e.* 1 ng ml^{-1} extract.

In other words, the study of Nauen *et al. (17)* demonstrated for the very first time that the non-cyclic CLOTHI **8** is one of the most prominent metabolites in true leaves of THIAM **6** treated cotton plants. CLOTHI **8** concentrations after soil drench application of THIAM **6** render it as a very important neonicotinoid-equivalent *in planta*, undoubtfully responsible for the control of many leaf feeding and sucking pests infesting cotton plants. This displays an important finding, particularly considering resistance management strategies in pest insect control using neonicotinoid insecticides, because selection for THIAM **6** resistance actually means selection for CLOTHI **8** resistance.

Metabolism of Thiamethoxam in Insects

(a) S. frugiperda: Haemolymph samples taken at different elapsed time intervals from *S. frugiperda* larvae which were orally fed with THIAM **6** dosed mini leaf disks contained high amounts of CLOTHI **8**. Only those larvae which consumed the entire leaf disk within 20 min were taken for the analysis. The

maximum amount of CLOTHI **8** found on THIAM **6** treated leaf disks was 1 ng (*vs.* 10,000 ng THIAM **6** applied), suggesting no degradation of THIAM **6** on the leaf disks.

Twenty minutes after consumption of a leaf disk the haemolymph concentrations of THIAM **6**, *N*-desmethyl-THIAM **9** and CLOTHI **8** were 24, 0.067 and 3.9 nmol mL^{-1}, respectively. Haemolymph concentration of THIAM **6** reached its maximum one hour after application. Finally, the haemolymph concentration of all neonicotinoids did not rise proportionally: 24 hours after treatment, CLOTHI **8** concentrations were with 0.36 nmol per ml higher than THIAM **6** levels (0.20 nmol mL^{-1}).

In addition to haemolymph sample analyses, whole larvae of *S. frugiperda* were homogenized in order to determine the proportion of THIAM **6**, CLOTHI **8** and *N*-desmethyl THIAM **9** at two different time intervals. Just four hours after oral dosing of 1 μg THIAM **6** 30% of neonicotinoid equivalents in larvae represent CLOTHI **8**. From the biological point of view, this small amount of CLOTHI **8** should be sufficient for the strong insecticidal activity observed after oral application of THIAM **6** (Figure 6).

After 24 hours, the non-cyclic CLOTHI **8** represented even 90 % and the cyclic ring systems *N*-desmethyl THIAM **9**, and THIAM **6** only 5 % each, suggesting either metabolic break-down or faster elimination of THIAM **6** compared to CLOTHI **8**. The very same experiments using 5 μg THIAM **6** revealed similar results as shown before. The data obtained provided strong evidence that the parent THIAM **6** is not only rapidly metabolized in plants but also (within minutes) converted to CLOTHI **8** in noctuid larvae.

However, it could be argued, that THIAM **6** is not especially developed for control of chewing pests such as *S. frugiperda*. Therefore, similar investigations were carried out using:

- *Agrotis segetum* (wireworm larvae)
- *Diabrotica balteata (*corn root worm*)* and
- *Leptinotarsa decemlineata* (Colorado potato beetle).

In order to identify CLOTHI **8** as a possible metabolite, oral or topical application of THIAM **6** on either insect larvae or adults were done. In one case THIAM **6** was injected. Whole larvae or beetles were washed after elapsed time intervals and then homogenized in order to determine the proportion of neonicotinoids.
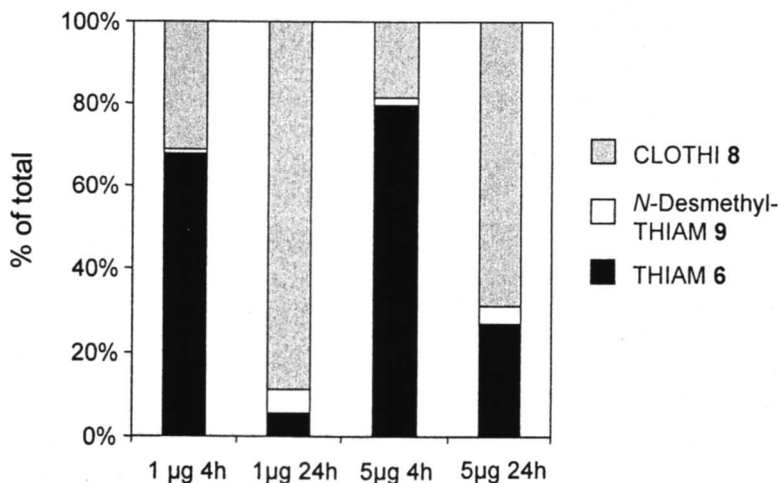
Figure 6. Extraction of THIAM 6, N-Desmethyl-THIAM 9 and CLOTHI 8 from Whole Larvae of S. frugiperda, 4h and 24h After Oral Administration of Different Doses of THIAM 6 (17).

(b) A. segetum: It was found, that directly after oral dosing of 1 μg THIAM **6** per wireworm larvae, the 6-ring system THIAM **6** is cleaved to the non-cyclic CLOTHI **8** (Figure 7).

(c) D. balteata beetles: In another experiment we applied 5 μg of THIAM **6** topically to *D. balteata* beetles. After different elapsed time intervals beetles were washed with acetonitrile in order to remove adhering THIAM **6**. In no case a conversion of THIAM **6** to CLOTHI **8** on the cuticular surface was observed. The wash solution always contained only THIAM **6**. Subsequently beetles were homogenized in acetonitrile, centrifuged and the supernatant analyzed for THIAM **6** and CLOTHI **8**. It was found, that THIAM **6** is rapidly taken up by the beetles and a reasonable portion is also rapidly converted to CLOTHI **8**. After 24 h one-fifth of the neonicotinoid equivalents detected in beetles is CLOTHI **8** and the concentration is well in the micromolar range, suggesting that the observed symptomology of poisoning is due to CLOTHI **8** rather than THIAM **6** (Figure 8).
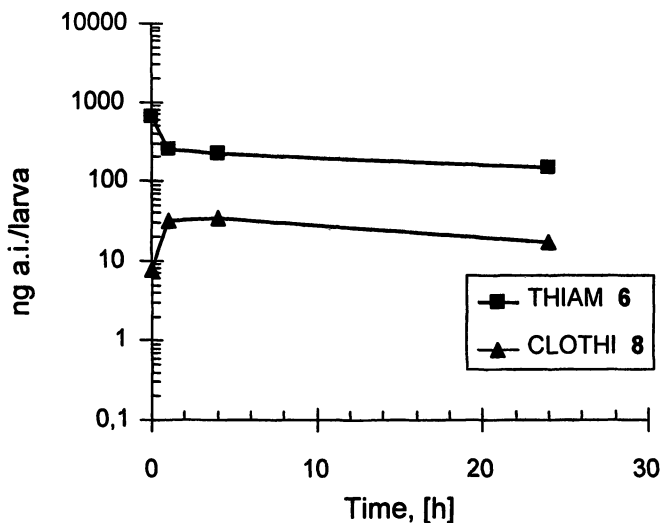
Figure 7. Conversion to CLOTHI 8 of THIAM 6 in A. segetum After Oral Application of 1 µg THIAM 6 per Larva.

Evidence for CLOTHI **8** being the responsible active ingredient is also demonstrated by the following experiment: 5 ng were injected of either THIAM **6** or CLOTHI **8** per *D. balteata* larva in order to identify if THIAM **6** acts less rapidly than CLOTHI **8**. If it has to be converted, even though it is a rapid process, one would expect a delayed onset of activity. And indeed, CLOTHI **8** action is fast and 10 min after application nearly 80% of the larvae showed strong intoxication symptoms (Figure 9). Whereas THIAM **6** treated larvae did not show any symptoms of poisoning after 10 min. That means, there is a delayed onset of activity with THIAM **6** compared with CLOTHI **8**, which is either due to pharmacokinetic constraints or more likely due to its conversion to CLOTHI **8**. Once it is present in reasonable amounts larvae started to show symptoms of poisoning.

(d) L. decemlineata: Another major target organism for neonicotinoid insecticides is *L. decemlineata*. After topical treatment of THIAM **6**, larvae were washed and afterwards homogenized as already explained for *D. balteata*. THIAM **6** was readily taken up by the larvae and 24 h after application at least one-third of the neonicotinoid equivalents measured by LC-MS/MS was CLOTHI **8**. The onset of symptoms of poisoning coincided with the presence of sub-micromolar amounts of CLOTHI **8**. Again this suggests CLOTHI **8** rather than THIAM **6** responsible for *L. decemlineata* larvae intoxication. Similar results were also obtained for adult beetles.
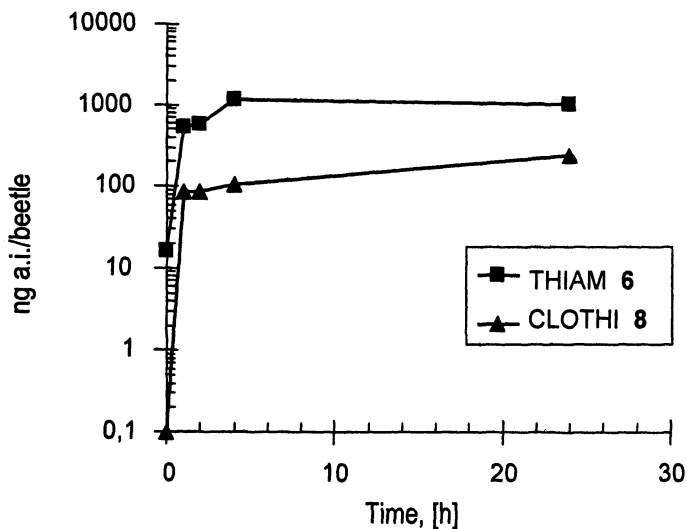
Figure 8. Metabolism of THIAM 6 After Topical Application of 5 µg THIAM 6 per D. balteata Beetle.
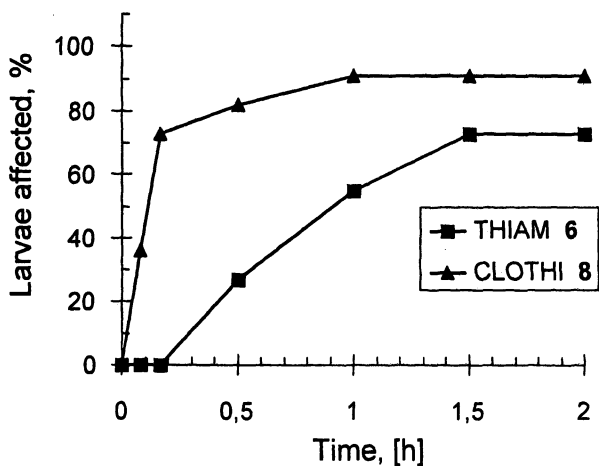
Figure 9. Speed of Action - Injection of 5 ng of Either THIAM 6 or CLOTHI 8 per D. balteata Larvae.

Concluding Remarks

The investigations demonstrate that THIAM **6** is an easy to cleave 6-ring neonicotinoid precursor of the non-cyclic and highly active CLOTHI **8**, which acts with high affinity on the same receptor site as IMI **1** and all other neonicotinoids. Our studies suggest a prodrug principle in the MoA of THIAM **6** *(17)* rather than binding site differences as suggested by other authors *(22, 23)*. According to the results high amounts of CLOTHI **8** found in cotton and insects after THIAM **6** treatment clearly interact with the IMI **1** binding site on *n*AChR *(17)*. Thus CLOTHI **8** is likely to be responsible for the insecticidal potency of THIAM **6** and not the parent compound itself, as demonstrated for important and relevant insects. This is of relevance in resistance management strategies as IMI **1** and CLOTHI **8** act on the same site, so THIAM **6** is no option for the alternation with other neonicotinoids.

Acknowledgements

References

1. Ohkawara, Y.; Akayama, A; Matsuda, K.; Andersch, W. *Proc. Brighton Crop Protection Conf. Pest Dis.* **2002**, *1*, 51-58.
2. Jeschke, P.; Schindler, M.; Beck, M. E. *Proc. Brighton Crop Protection Conf. Pest Dis.* **2002**, *1*, 137-144.
3. Nauen, R.; Bretschneider, T. *Pesticide Outlook* **2002**, *12*, 241-245.
4. Nauen, R.; Denholm, I. *Arch. Ins. Biochem. Phys.* **2005**, *58*, 200-215.
5. Testa, B.; Mayer, J. M. In: *Pharmacokinetic Optimization in Drug Research: Biological, Physicochemical, and Computational Strategies,* **2001**, 85-95, Editor(s): Testa, B.; van de Waterbeemd, H.; Folkers G.; Guy, R. Verlag Helvetica Chimica Acta, Zurich, Switzerland.
6. Testa, B.; Mayer, J. M. *Drug Metab. Rev.* **1998**, *30*, 787-807.
7. Balant, L. P.; Doelker, E. In: *Burger's Medicinal Chemistry and Drug Discovery*, **1995**, 949-982, 5th Edition, Vol. 1, Editor: Wolff, M. E. Wiley-Interscienece, New York.

8. Yamamoto, I.; Tomizawa, M.; Saito, T.; Miyamoto, T.; Walcott, E. C.; Sumikawa, K. *Arch. Insect Biochem. Physiol.* **1998**, 37, 24-32.
9. Jewess, P. J.; Lee, P. W.; Nicholls, P. H.; Plimmer, J. R. In: *Metabolic pathways of agrochemicals, Part 2, Insecticides and Fungicides*, Editor(s): Roberts, T. R.; Hutson, H. D. **1999**, Cambridge University Press, Cambridge.
10. Nauen, R.; Tietjen, K.; Wagner, K.; Elbert, A. *Pestic. Sci.* **1998**, 52, 53-57.
11. Tröltzsch, M. C.; Führ, F.; Wienecke, J.; Elbert, A. *Pflanzenschutz-Nachrichten Bayer* **1994**, 47, 249-303.
12. Araki, Y.; Bornatsch, W.; Brauner, A.; Clark, T.; Dräger, G. *et al.*, In: *Proc. IUPAC Congress*, Washington **1994**, 2B-157.
13. Rauch, N.; Nauen, R.; *Arch. Ins. Biochem. Physiol.* **2003**, 54, 165-176.
14. Sarkar, M. A.; Roy, S.; Kole, R. K.; Chowdhury, A. *Pest Manag. Sci.* **2001**, 57, 598-602.
15. Nauen, R.; Ebbinghaus-Kintscher, U.; Elbert, A.; Jeschke, P.; Tietjen, K. In: *Biochemical Sites Important in Insecticide Action and Resistance*, **2001**, 77-105, Editor: Ishaaya, I., Springer, Berlin, Germany.
16. Kagabu, S. In: *Chemistry of crop protection: progress and prospects in science and regulation*, **2003**, 193-212, Editor(s): Voss, G., Ramon, G. Wiley-VCH, New York.
17. Nauen, R.; Ebbinghaus-Kintscher, U.; Salgado, V. L.; Kaussmann, M. *Pest. Biochem. Physiol.* **2003**, 76, 55-69.
18. Kayser, H.; Lee, C.; Wellmann, H. In: *Proc. 10th IUPAC Int. Congr. Chem. Crop Protection* **2002**, Abstracts, 1, 305.
19. Jeschke, P.; Uneme, H.; Benet-Buchholz, J.; Stölting, J.; Sirges, W.; Beck, M. E.; Etzel, W. *Pflanzenschutz-Nachrichten Bayer* **2003**, 56, 5-24.
20. Parr, R. G.; Yang, W. *J. Am. Chem. Soc.* **1984**, 106, 4049-4050.
21. Beck, M.E. *J. Chem. Inf. Model.* **2005**, 45, 273-282.
22. Wellmann, H.; Gomes, M.; Lee, C.; Kayser, H. *Pest Manag. Sci.* **2004**, 60, 959-970.
23. Kayser, H.; Lee, C.; Decock, A.; Baur, M.; Haettenschwiler, J.; Maienfisch, P. *Pest Manag. Sci.* **2004**, 60, 945-958.

Chapter 6

Thiamethoxam: High-Affinity Binding and Unusual Mode of Interference with Other Neonicotinoids at Aphid Membranes

Hartmut Kayser[1], Henning Wellmann[1], Connie Lee[1],
Arnaud Decock[1], Marilyne Gomes[1], Ben Cheek[2], Rob Lind[2],
Markus Baur[1], Joerg Hattenschwiler[1], and Peter Maienfisch[1]
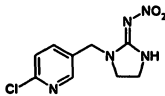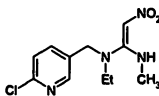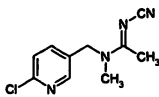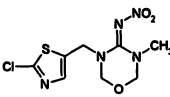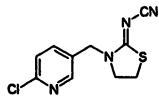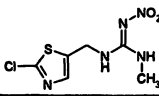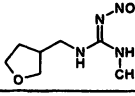
[1]Syngenta Crop Protection AG, Research & Technology, WRO-1004.4.46,
4002 Basel, Switzerland
[2]Syngenta Crop Protection AG, Research & Technology,
Jealotts Hill, Bracknell, Berkshire RG42 6EY, United Kingdom

Neonicotinoids do not act as a homogenous class of insecticides. Radioligand receptor binding assays revealed two classes of neonicotinoids described here as 'competitive' and 'non-competitive', respectively, relative to [^{3}H]imidacloprid. Differences in affinity, mode of displacement, number of binding sites and temperature sensitivity suggest that thiamethoxam binds in a way unique among the commercial neonicotinoids. Metabolic transformation is not relevant for its insecticidal effects.

Neonicotinoid insecticides have experienced a most remarkable and steady increase in use since their market introduction in 1991, now exceeding 10% of the total insecticide market (*1-3*). An overview of these products is given in Table I (cf. *4*). The major advantages of the new products over the previously preferred organophosphates are a novel chemistry, a new mode of action, systemic action and human safety. The systemic activity makes them the insecticide class of choice for the control of plant sucking pests.

© 2007 American Chemical Society

67

Table I. Overview of Presently Marketed Neonicotinoids.

Common Name	Structure	Company	Year of Market Intro.	Sales 2003 Mio $[a]
Imidacloprid		Bayer	1991	665
Nitenpyram		Takeda	1995	45
Acetamiprid		Nippon Soda	1996	60
Thiamethoxam		Syngenta	1998	215 298[b]
Thiacloprid		Bayer	2000	<30
Clothianidin		Takeda, Bayer	2002	<30
Dinotefuran		Mitsui Chemicals	2002	<30

[a] Data from *Phillips McDougall*
[b] *Sales 2004;* Data from *Syngenta Annual Report 2004*

Neonicotinoids have been shown by radioligand binding studies with isolated insect membranes, as well as by functional assays with neuronal preparations to act on nicotinic acetylcholine receptors with a high preference to those from insects compared to those of vertebrates. This property translates into the highly positive safety profile of this class of insecticides (5, 6). Receptor binding of neonicotinoids results in agonistic action, that is opening of the receptor-integrated ion pore and consequent influx of predominantly sodium ions. Depending on the type of neuron, this agonist action may rapidly lead to

receptor desensitation or inactivation (*7*), which is believed to be the basis for the insecticidal action of the neonicotinoids.

Synthesis of Neonicotinoids

Imidacloprid, nitenpyram, thiacloprid, acetamiprid, dinotefuran and nithiazine were synthesized at Syngenta following literature procedures. The preparation of the other neonicotinoids is described in the following publications: Clothianidin (*8, 9*); *N*-methyl Clothianidin (*8*); *N*-desmethyl Clothianidin (*8-10*); Chloropyridyl analog of Clothianidin (*9*); *N*-methyl Imidacloprid (*8*); Chlorothiazolyl analog of Imidacloprid (*11*); Thiamethoxam (*2, 10, 12*), *N*-desmethyl Thiamethoxam (*2, 10*); Chloropyridyl analogue of Thiamethoxam (*10*).

Chemical Features of Neonicotinoids

While members of the neonicotinoid class of insecticides share a number of structural and physico-chemical properties, the individual compounds provide a remarkable diversity of structural details, which may confer biological differences in their action (*13*).

Regarding the structural features of neonicotinoids, the pharmacophore part is characterized by a polar group represented by either a nitro group or a cyano group (*13*). Based on neighboring structural differences in the pharmacophore and on the heterocycle that typically is aromatic and mono-substituted by chlorine, neonicotinoids can be grouped as presented in Table II.

Table II. Chemical Classification of Commercial Neonicotinoids.

Pharmacophore	Heterocycle		
	Chloropyridyl	Clorothiazolyl	Tetrahydrofuryl
Nitroamidines	Imidacloprid	Thiamethoxam Clothianidin	Dinotefuran
Cyanoamidines	Acetamiprid Thiacloprid		
Nitroenamines	Nitenpyram		

Thiamethoxam was the first marketed chorothiazolyl-type neonicotinoid, a second-generation neonicotinoid (*10, 14*) that, as another specific and unique structural detail, is differentiated by an oxadiazine pharmacophore with an N-Methyl group. Thiamethoxam is used for seed treatment under the trademark CRUISER® and for foliar and soil application as ACTARA® and PLATIMUM®. It is highly effective against sucking pests (e.g. aphids, jassids, whiteflies, rice hoppers), beetles (e.g. the Colorado potato beetle), as well as Thysanoptera and some Lepidoptera.

Comparative Receptor Binding Studies of Neonicotinoids

Studies with [³H]imidacloprid

Different Modes of Binding Interaction with Other Neonicotinoids

Binding of [³H]imidacloprid to membrane preparations from whole aphids has been studied to determine its affinity and number of binding sites (*8, 15*). The affinity (K_d) of imidacloprid was 1.7 nM and 6.1 nM with *Myzus persicae* and *Aphis craccivora*, respectively. The binding capacities (B_{max}) were 915 fmol/mg protein and 1330 fmol/mg protein, respectively.

Other insecticidal neonicotinoids compete with [³H]imidacloprid for binding. In a detailed structure-activity study (*8*), the IC_{50}, or K_i, values as measures for the relative affinities of competitors, covered a range of about three orders of magnitude from nanomolar to micromolar concentrations. Remarkably, the IC_{50} values were grouped into those ≤10 nM and those ≥1000 nM. Moreover, the Hill coefficients (n_H), describing the steepness of the competitor displacement curves, were around unity (as expected for normal competitive behavior at a single site) with all strong competitors, while some of the weak competitors exhibited Hill values significantly below unity. The latter behavior is indicative for unusual (not pure competitive) displacement or for more than one binding site of the competitor. Thiamethoxam was the only commercialized neonicotinoid with a high (micromolar) IC_{50} value and a n_H value significantly below unity when measured with [³H]imidacloprid on membranes from both *M. persicae* and *A. craccivora* (*8*).
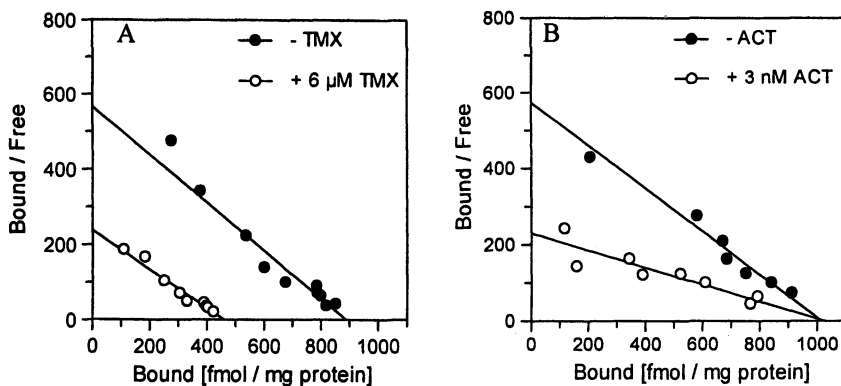
Figure 1. Scatchard representations of the effects of (A) thiamethoxam (TMX) and (B) acetamiprid (ACT) on [³H]imidacloprid displacement from membranes of M. persicae as examples for the 'non-competitive' (A) and 'competitive'(B) modes of displacement or inhibition.

In extending the determinations of IC_{50} values for displacement potencies of competitors we analyzed in detail also their mode of displacement of [³H]imidacloprid (8). As a most remarkable result, we identified two types of displacement of the labeled compound, which we described as 'competitive' and 'non-competitive', respectively (Figure 1; Table III). 'Non-competitive' displacement of [³H]imidacloprid was found with thiamethoxam and a number of other neonicotinoids that were all characterized by a common structural feature, namely an N-Methyl group in the pharmacophore.

As thiamethoxam is the only N-Methyl compound on the market, its 'non-competitive' behavior contrasted to all other commercial neonicotinoids, which all displayed a 'competitive' mode. The N-Methyl rule was not applicable to acetamiprid, thiacloprid and nithiazine (no tyical neonicotinoid); a possible interpretation has been given in a recent publication (8).

On the other side, among the class of 'non-competitive' compounds, the Hill coefficients were either around unity or significantly less. This is best demonstrated by the thiazolyl compound thiamethoxam and its pyridyl analog exhibiting n_H values of 0.38 and 1.0, respectively (data with *M. persicae*). This indicates differences in binding that might be due to sites discriminating even between pyridyls and thiazolyls (8). Hence, two subgroups of 'non-competitive' neonicotinoids may be discriminated, as depicted in Table IV.

Table III. The Two Classes of Neonicotinoids as Defined by Their Mode of Displacement of [³H]imidacloprid

'Competitive' Class	'Non-competitive' Class
• Imidacloprid[1]	• Thiamethoxam
• Acetamiprid	• N-methyl Imidacloprid
• Clothianidin	• N-methyl Clothianidin
• Nitenpyram	• N-desmethyl Clothianidin
• Thiacloprid	• Pyridyl resp. thiazolyl
• Dinotefuran	analogs of above
• Nithiazine	compounds
• N-desmethyl Thiamethoxam	

[1]Imidacloprid behaves competitively by the experimental design

The mechanism behind the 'non-competitive' mode of displacement is open to speculation. In descriptive words, it means that the presence of thiamethoxam, for example, lowers the number of accessible binding sites for imidacloprid, while its affinity is unchanged.

Table IV. Consensus Data of Neonicotinoids for Their Mode of Displacement of [³H]imidacloprid

	'Competitive' neonicotinoids	'Non-competitive' neonicotinoids	
Potency of displacement (IC_{50} and K_i, respectively)	≤ 10 nM	≥ 1000 nM	
		Subgroup A	Subgroup B
Hill coefficients (n_H)	~1	~1	<1
Common substructure	-NXH	-NXMethyl	

X = Methyl or ring methylene

On the Difference between Studies of Receptor Binding and of Enzyme Action

The terms 'competitive' and 'non-competitive' used here to describe modes of inhibition in receptor binding studies are established terms in enzymology to

describe modes of inhibition. In enzyme studies, the effect of an inhibitor is examined by measuring the quantity of the product(s) of enzyme action. In receptor binding assays, only the first step, binding of the radioligand, is measured, not its impact on receptor activity requiring a functional assay. Consequently, the meanings of 'competitive' and 'non-competitive' are different in the two fields. Based on theory, it has been argued that any displacement of a radioligand from the receptor site is expected to be 'competitive' and that 'non-competitive' results therefore indicate irreversible processes or artifacts (*16*). As we show below, however, this interpretation does not apply for our results on thiamethoxam and structurally related compounds.

Studies with [³H]thiamethoxam

Thiamethoxam Binding is Sensitive to Temperature Under In Vitro Conditions

Binding experiments revealed unusual properties of thiamethoxam at the target site (*17*). The optimal assay conditions to demonstrate thiamethoxam binding to aphid membranes are different and more strictly defined than those for imidacloprid. Highest specific binding of thiamethoxam is observed at low assay temperature (2°C) with freshly prepared membranes. Furthermore, preparations stored frozen prior to the assay are as good as fresh ones for studies with imidacloprid but not with thiamethoxam.

Saturation binding studies revealed the following data for affinity (K_d) and binding capacity (B_{max}) for the two compounds with fresh membranes from *M. persicae* assayed at 2°C (Fig. 2):

- Thiamethoxam: K_d = 11.4 nM; B_{max} = 700 fmol/mg protein
- Imidacloprid: K_d = 2.5 nM; B_{max} = 1400 fmol/mg protein

Non-specific binding was fairly low with both radioligands, typically around 10% with [³H]thiamethoxam and 5% with [³H]imidacloprid.

At temperatures ≥20°C, binding capacity for thiamethoxam was significantly lower by 40-60% compared to 2°C. This was typically not the case with imidacloprid though variation was observed. It should be noted that non-specific binding was not affected by temperature with both compounds.

For *A. craccivora*, specific binding of [³H]thiamethoxam was similarly sensitive to temperature and membrane quality as in *M. persicae* (*17*). The data for affinity and capacity at 2°C were about 90 nM and 1000 fmol/mg protein. Higher values for *A. craccivora* compared to *M. persicae* were also obtained with imidacloprid (*8, 15*).
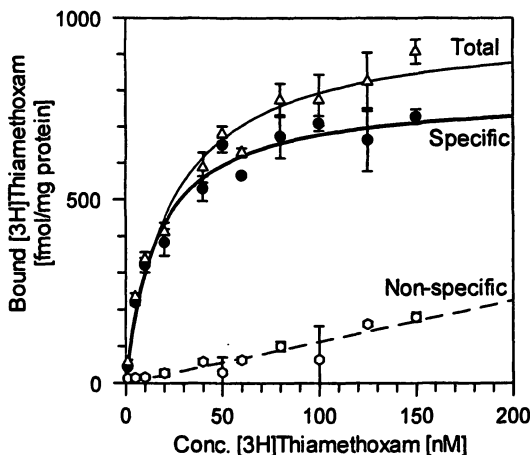
Figure 2. Saturation binding of [³H]thiamethoxam to membranes from M. persicae at 2°C. The curves represent total, specific and non-specific binding.

A number of experiments were performed aiming at the understanding of the temperature effect on thiamethoxam binding (*17*). The absence or presence of a cocktail of protease inhibitors during preparation and assaying of the membranes did not show any difference. In confirming this, the level of imidacloprid binding was relatively constant even over long incubation times (up to 3 h) hence destruction (by residual proteases, for example) of the membranes did not take place or was not relevant. Furthermore, both neonicotinoids proved to be stable even under extreme assay conditions (at 30°C; 3 h), as shown by liquid chromatography (HPLC) analysis of assay supernatants.

The Temperature Effect on Thiamethoxam Binding is Reversible

The experiments, described above, did not reveal any artifactual cause for the reduced binding capacity of aphid membranes for thiamethoxam at elevated temperatures. This was confirmed by applying other experimental schemes involving repeated changes (after 10-min periods) of assay temperature between 2°C and 22°C or 30°C. Briefly, after initial incubation of [³H]thiamethoxam at 2°C to achieve maximal saturation of the binding sites (*17*) samples were transferred to 30°C for 10 min, then again transferred to 2°C for 10 min followed again by a 30°C period and so forth. Bound radioactivity was counted 2 min after each transfer. Studies were performed with membranes from *M. persicae* (Fig. 3) and *A. craccivora* (*18*). In all these experiments, binding of [³H]thiamethoxam was high after a shift to low temperature and significantly lower after a shift to

high temperature. These rapid temperature changes were repeated many times (up to eight times) with no significant change of the high and low levels of binding reached after each transfer. Comparable results were obtained with [^{3}H]imidacloprid (*18*) the affinity of which is similarly sensitive to temperature (*17*). Surprisingly, these changes of binding capacity took place rather fast, within a few seconds.
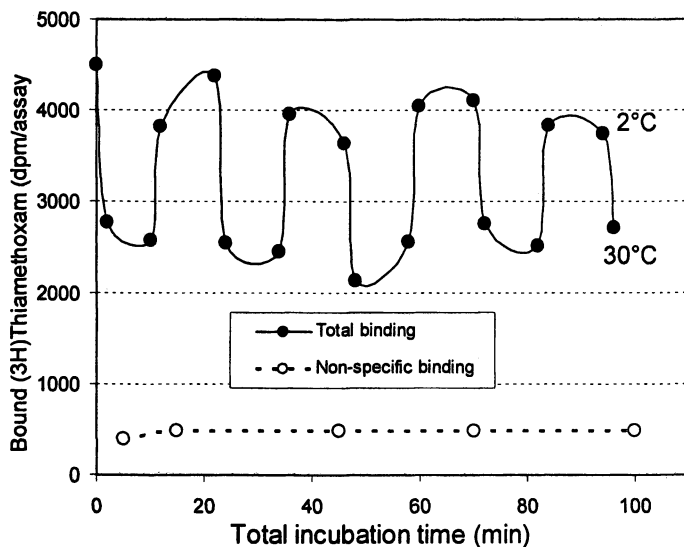
Figure 3. Repeated reversal of the effects of low (2°C – high binding) and elevated (30°C – low binding), respectively, temperature on [^{3}H]thiamethoxam (15 nM) binding to membranes from M. persicae. The incubation temperature was changed every 10 min and binding was measured 2 min thereafter.

In conclusion, temperature affects binding of thiamethoxam as well as imidacloprid in a reversible way, though the former compound is clearly stronger affected. This also suggests that the binding modes or sites of the two neonicotinoids at the target receptor are obviously not identical.

Thiamethoxam Like Imidacloprid, Binds to a Nicotinic Receptor Site

As previously demonstrated (*15*), thiamethoxam, like the other examined neonicotinoids and known natural nicotinic ligands, competes with the binding

of [³H]imidacloprid as well as of [³H](-)nicotine and [³H]α-bungarotoxin for binding to insect membranes. Subsequent studies revealed that both [³H]thiamethoxam (*17, 18*) and [³H]imidacloprid (*8*) are in competition by established nicotinic agonists and antagonists (nicotine, epibatidine, methyllycaconitine and dihydro-β-erythroidine), though with different potencies and different modes of inhibition (details will be published elsewhere). Taken together, the results of competition studies strongly suggest that thiamethoxam binds to a site (or sites) on nicotinic acetylcholine receptors; otherwise, mutually inhibition of these nicotinic ligands could not be readily understood.

To obtain conclusive evidence of the interpretation of the results from receptor binding studies, as summarized above, functional studies of nicotinic receptors by electrophysiological techniques would be essential. Such studies have mainly been performed with imidacloprid, as it was available first, using established lab model insects such as cockroaches or other non-target insects, lepidopteran larvae, for example (*5, 6, 19*). Comparable studies with receptors from true target pests (sucking insects) have yet to be performed; they are likely hampered by technical difficulties related to their small size.

Metabolism of Thiamethoxam and Its Relevance to Toxicology

Time Course of Toxicology and Metabolism of Thiamethoxam

Like other insecticides, thiamethoxam is transformed in the insect, crop, soil and other compartments to variable degrees to yield products that may not or may be active in their own right. An example for the latter case from the neonicotinoid class is imidacloprid, which is metabolized via hydroxylated intermediates to an olefin product that is more active than the parent compound by one order of magnitude in aphids screens and in receptor binding (*20, 21*).

Thiamethoxam has been reported to yield *N*-desmethyl thiamethoxam as well as clothianidin, the latter representing the dominant product (*19*). The metabolic conversion of thiamethoxam to clothianidin has been implied for its toxicology. To address this claim, we conducted an analytical study in which a 1000 ng (1 µl dose of 1000 ppm) dose of thiamethoxam was injected into tobacco budworm *Heliothis virescens* 5th instar larvae and symptoms monitored at time points of 15, 30, 60 and 120 minutes after exposure. Symptoms of thiamethoxam toxicity were reliably observed 30 minutes after injection thus this time period was chosen for further experiments. Symptoms recorded were uncoordinated locomotion and rapid mandibular motion at a frequency of 3-4 jaw movements per second.

Four replicate caterpillars were then analytically measured for amounts of thiamethoxam at these time points of 15, 30, 60 and 120 minutes and any subsequent production of clothianidin using liquid chromatography mass spectrometry (LCMS). Briefly, caterpillars were macerated in acetonitrile. After centrifugation, the supernatant was recovered for LCMS analysis. Known quantities of both thiamethoxam and clothianidin were used to generate a calibration plot over a range of weights encountered in the experiments to convert peak area generated by LCMS into actual weights of compound.

Figure 4 demonstrates that very low levels of clothianidin are metabolically produced equating to 23 ng or 2.3% of the parent at 30 min. A 30 min assessment also reflects that thiamethoxam is a rapidly acting insecticide in the field and this would be a realistic time point to study.
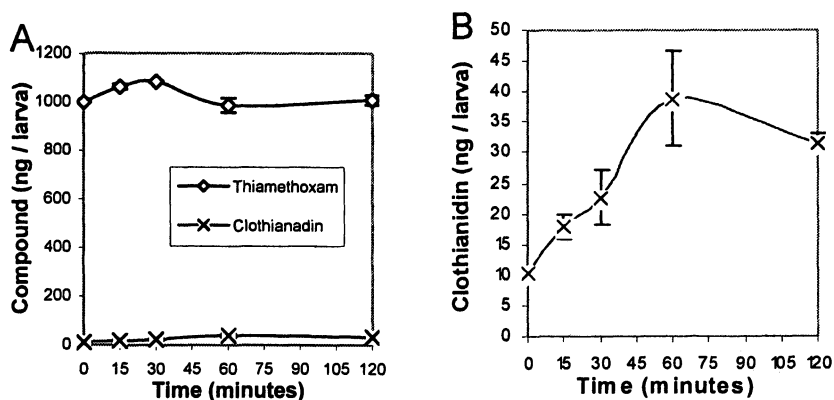
Figure 4. Formation of clothianidin from thiamethoxam in H. virescens. A mass of 1000 ng thiamethoxam was injected into 5th instar larvae. In Figure B, the concentration of clothianidin from Figure A is shown at an enlarged scale.

Insecticidal Relevance of Metabolism

Next, we focused on whether the amounts of clothianidin produced as a metabolite of thiamethoxam at 30 min could induce the symptoms observed. Therefore known amounts of clothianidin, namely 50, 100, 500, and 1000 ng were injected into four replicates of *H. virescens* larvae to determine symptoms

induced at 30 min. Symptoms of clothianidin were identical to those of thiamethoxam reflecting that both have the same mode of action (Table V).

There is a clear mismatch between the mass of clothianidin produced by metabolism of thiamethoxam, namely 23 ng, and the 100-500 ng of clothianidin needed to exhibit toxicity symptoms in *H. virescens* after 30 minutes. Therefore, it is extremely unlikely that the mechanism of action of thiamethoxam is propesticidal via clothianidin, as claimed (*19*). The most parsimonious hypothesis is that thiamethoxam is biologically active in its own right.

Table V. Physiological Effects of Clothianidin Injected into *H. virescens* 5th Instar Larvae at Different Masses

Mass (ng)	Physiological Effect after 30 minute Exposure
50	None
100	None
500	Uncontrolled mandibular movement, lack of general co-ordination
1000	Uncontrolled mandibular movement, lack of general co-ordination

This interpretation is supported by data from radioligand studies (*8*). According to saturation binding assays with [³H]thiamethoxam and competition assays with [³H]imidacloprid, all the compounds under discussion exhibit about the same affinity to aphid membranes. The data, given as K_D and K_i values, respectively, for *M. persicae* are (*8*):

- Thiamethoxam $K_D = 11.4 \pm 0.9$ nM
- Desmethyl thiamethoxam $K_i = 6.7 \pm 0.5$ nM
- Clothianidin $K_i = 7.2 \pm 0.8$ nM

From the above receptor-affinity data, obtained with aphids, formation of even relatively high amounts of the two metabolites from thiamethoxam are not expected to change at all or even increase the aphicidal effect. If this conclusion also applies to non-target insects, such as *Heliothis* and *Spodoptera* larvae, which have been used to postulate a propesticidal action of thiamethoxam (*19*), is presently unknown; an answer will crucially depend on functional receptor studies from aphids, as discussed above.

In supporting our view, a recent cockroach study by Kagabu et al. (*22*) combining biological, neurophysiological and stability tests came to the conclusion that "the prodrug concept does not necessarily apply to thiamethoxam."

Conclusions

This review documents that thiamethoxam shows properties distinct from those of other neonicotinoids under a number of aspects. Chemically, it represents the first commercialized chlorothiazolyl-type neonicotinoid. The combination of an oxadiazine ring with a N-Methyl group is unique and seems to shape the biological properties of thiamethoxam.

Neonicotinoids target nicotinic acetylcholine receptors as is mostly known from studies with imidacloprid and conveniently sized lab model insects; real target pests have not yet been used for technical reasons. Hence, conclusions, especially those on receptor sensitivity, should be taken with care. On the other hand, radioligand binding studies, which usually do not impose technical hurdles, have been widely performed with neonicotinoids using membranes from target and non-target insects.

Our studies with aphids clearly suggest that thiamethoxam, like the other examined neonicotoinoids, binds to nicotinic receptors. However, there are clear differences to the other commercial neonicotinoids as documented by a 'kinetic' analysis of competition experiments. While thiamethoxam binds to receptors with nanomolar affinity, micromolar concentrations are required to displace imidacloprid. Further, the interaction between the two compounds is 'non-competitive' meaning that binding of thiamethoxam reduces the binding capacity of the receptor preparation for imidacloprid but not its affinity. Thiamethoxam shares this unusual mode of inhibition with other neonicotinoids (not commercialized) also featured by an N-Methyl group in the pharmacophore. In the 'competitive' mode, displayed by the other commercial neonicotinoids, the capacity is unchanged, while the affinity is reduced.

Another case of loss of binding capacity is observed with thiamethoxam when the assay temperature is increased, thus also resulting in 'non-competitive' data plots (not shown). This change is completely reversible in contrast to views that link 'non-competitive' results to irreversible processes or similar artifacts. It should further be kept in mind that the temperature effects were observed in vitro with isolated membranes and in a non-physiological medium; whether it takes place also in vivo and has a physiological or toxicological impact is unknown. Anyway, our binding studies revealed remarkable differences in the receptor binding behavior among the neonicotinoids.

As effects like those documented for thiamethoxam have not yet been described in the receptor binding field, the results, though based on thorough and self-critical experimentation, may be questioned. In our view, these novel results necessarily call for novel interpretations. A most evident conclusion from the present results is that binding of thiamethoxam has a different impact (as measurable in binding assays) on the receptor complex as binding of other, 'competitive' neonicotinoids. Whether this different mode of interaction is due

to spatially well separated binding sites, possibly even located on different receptor subunits, is open to speculation. It could also mean that imidacloprid and the other 'competitive' compounds bind to the very same site, as defined by the amino acid side chains providing contact, while thiamethoxam is (partially) bonded to neighboring residues resulting in a different impact on the conformation of the oligomeric receptor complex and thus also its function. Related to this view is the recent first demonstration of point-mutated nicotinic receptor subunits causing target-site insensitivity for imidacloprid in a plant hopper shedding new light on the role of single amino acids in the agonist binding pocket (*23*).

References

1. *Nicotinoid Insecticides and the Nicotinic Acetylcholine Receptor*; Yamamoto, I.; Casida J. E., Eds.*;* Springer-Verlag: Tokyo, 1999; pp 1-300.
2. Maienfisch, P.; Rindlisbacher, A.; Huerlimann, H.; Haettenschwiler, J.; Desai, A. K.; Ekkundi, V. S.; Gangan, V. D. ACS Symposium Series (2002), 800 (Synthesis and Chemistry of Agrochemicals VI), 219-230.
3. Jeschke, P.; Schindler, M.; Beck, M. E. BCPC Conference--Pests & Diseases (2002), Vol. 1, 137-144.
4. Maienfisch, P.; Haettenschwiler, J.; Rindlisbacher, A.; Decock, A.; Wellmann, H.; Kayser, H. *Chimia* **2003**, *57*, 710-714.
5. Matsuda, K.; Buckingham, S. D.; Kleier, D.; Rauh, J. J.; Grauso, M.; Sattelle, D. B. *Trends Pharmacol. Sci.* **2001**, *22*, 573-580.
6. Tomizawa, M; Casida, J. E. *Annu. Rev. Entomol.* **2003**, *48*, 339-364.
7. Salgado, V. L.; Saar, R. *J. Insect Physiol.* **2004**, *50*, 867-879.
8. Kayser, H.; Lee, C.; Decock, A.; Baur, M.; Haettenschwiler, M.; Maienfisch, P. *Pest Manag. Sci.* **2004**, *60*, 945-958.
9. Maienfisch, P.; Huerlimann, H.; Haettenschwiler, J. *Tetrahedron Letters* **2000**, *41*, 7187-7191.
10. Maienfisch, P.; Huerlimann, H.; Rindlisbacher, A.; Gsell, L.; Dettwiler, H.; Haettenschwiler, J.; Sieger, E.; Walti, M. *Pest Manag. Sci.* **2001**, *57*, 165-176.
11. Zhang, A.; Kayser, H.; Maienfisch, P.; Casida, J. E. *J. Neurochem.* **2000**, *75*, 1294-1303.
12. Maienfisch, P.; Gsell, L.; Rindlisbacher, A. *Pestic. Sci.* **1999**, *55*, 351-355.
13. Maienfisch, P.; Brandl, F.; Kobel, W.; Rindlisbacher, A.; Senn, R. In *Nicotinoid Insecticides and the Nicotinic Acetylcholine Receptor;* Yamamoto, I.; Casida, J. E., Eds. Springer-Verlag, Tokyo, 1999; pp 177-209.

14. Maienfisch, P.; Angst, M.; Brandl, F.; Fischer, W.; Hofer, D.; Kayser, H.; Kobel, W.; Rindlisbacher, A.; Senn, R.; Steinemann, A.; Widmer, A. *Pest Manag. Sci.* **2001**, *57*, 906-913.
15. Wiesner, P.; Kayser, H. *J. Biochem. Toxicol.* **2000**, *14*, 221-230.
16. Tomlinson, G. *Canad. J. Physiol. Pharmacol.* **1988**, 66, 342-349.
17. Wellmann, H.; Gomes, M.; Lee, C.; Kayser, H. *Pest Manag. Sci.* **2004**, *60*, 959-970.
18. Kayser, H. and co-workers, unpublished data.
19. Nauen, R.; Ebbinghaus-Kintscher, U.; Salgado, V. L. Kaussmann, M. *Pestic. Biochem. Physiol.* **2003**, *76*, 55-69.
20. Nauen, R.; Tietjen, K.; Wagner, K.; Elber, A. *Pestic. Sci.* **1998**, *52*, 53-57.
21. Nauen, R.; Reckmann, U.; Armborst, S.; Stupp, H. P.; Elbert, A. *Pestic. Sci.* **1999**, *55*, 265-271.
22. Kagabu, S; Murata, N.; Hibino, R.; Hanzawa, M.; Nishimura, K. *J. Pestic. Sci.* **2005**, *30*, 111-115.
23. Liu, Z.; Williamson, M. S.; Lansdell, S. J.; Denholm, I.; Han, Z.; Millar, N. S. *Proc. Natl. Acad. Sci. USA* **2005**, *102*, 8420-8425.

Chapter 7

Discovery of Insecticidal Cyanine Dyes

**Robert N. Henrie II, Thomas Cullen, Benjamin Dugan,
Larry Zhang, Yanli Deng, Sandra F. Simpson, Bruce Black,
Franz Schuler, and Seong Jae Yu**

Discovery Research Department, Agricultural Products Group,
FMC Corporation, P.O. Box 8, Princeton, NJ 08543–0008

Inhibition of chitin synthase (CS, EC 2.4.1.16) is widely
recognized as a largely untapped, intrinsically mammalian-
safe, arthropodicidal mechanism of action. Certain classes of
cyanine dyes were observed as hits in a high-throughput
Lepidopteran (tobacco budworm, *Heliothis virescens*) chitin
synthase assay. Optimization produced *in vivo*-active analogs;
however, ultimately these were shown to be off-target, active
instead as mitochondrial electron transport inhibitors (METI)
at Complex 1. An overview of the chitin synthase project and
chemistry is presented.

Chitin synthase (CS), Enzyme Commission number 2.4.1.16, is the enzyme
that converts uridine diphosphoryl-*N*-acetylglucosamine (UDP-GlcNAc) into
chitin, the β-1,4-linked polymer of *N*-acetylglucosamine. CS is a member of the
class of enzymes known as polymerizing glycosyltransferases which are
responsible for the synthesis of critical structural biopolymers, including
cellulose as well as chitin. It is a processive enzyme, adding successive GlcNAc

83

84

units onto a primer, cf. Scheme 1. Inhibition of chitin synthase is widely recognized as a largely untapped, intrinsically mammalian-safe, arthropodicidal mechanism of action (*1*). Since the exoskeleton of insects consists mostly of chitin, disrupting the formation, deposition, and/or cross-linking of chitin should lead to insect death, especially during molting. One of the attractive features of chitin synthase as an insecticidal target site is its absence in mammals, although its presence in crustaceans such as Daphnia could cause potential ecotoxicology issues. There are no known commercial insecticides that are *bona fide* inhibitors of chitin synthase, nor are there any in development to our knowledge.
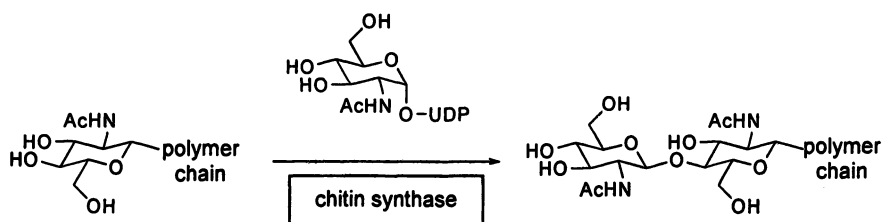
Scheme 1. Polymerization of N-acetylglucosamine by Chitin Synthase

The well-known insecticidal benzoyl phenyl ureas (BPUs), exemplified by diflubenzuron, are chitin biosynthesis disruptors, but at an uncharacterized site distinct from chitin synthase (*2*), Figure 1. The related bridge-cyclized oxazoline chemistries from DuPont and Yashima, represented by etoxazole, are also commercial or near-commercial insecticides with the same mechanism of action (*3*), Figure 1.

Uniroyal
Diflubenzuron

Dupont
experimental
(3)

Yashima
experimental
(3)

Yashima
Etoxazole
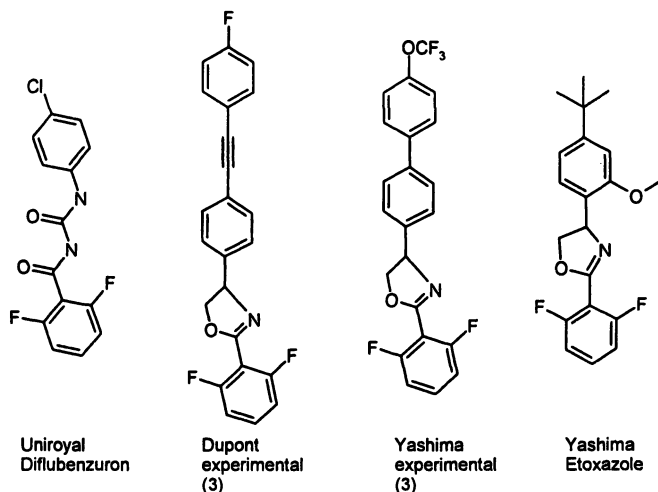
Figure 1. Chitin Biosynthesis Disruptors

The known *bona fide* CS enzyme inhibitors are natural product-derived substrate analogs, eg. polyoxin D, tunicamycin, and nikkomycin Z, Figure 2. These complex natural products inhibit the enzyme well, but express little *in vivo* insecticidal activity, presumably due to unfavorable ADME attributes.
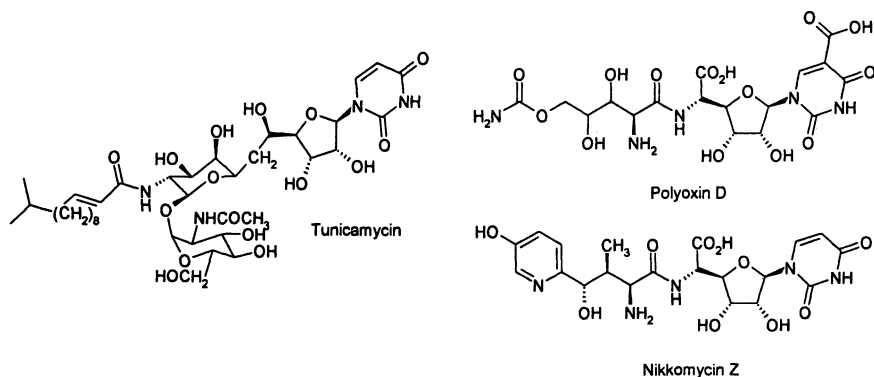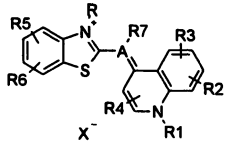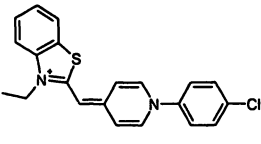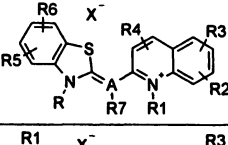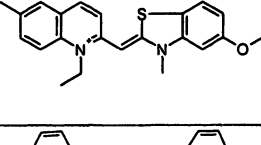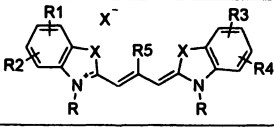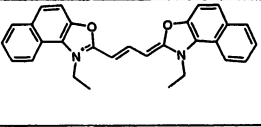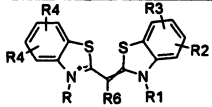
Figure 2. Bona Fide Chitin Synthase Inhibitors

Lead Identification

We have developed a proprietary CS assay using tobacco budworm (TBW, *heliothis virescens*) tissue, and automated the protocol for high-throughput screening in 96-well microtiter plates (*4*). During the screening phase of the CS project we defined a hit as a compound showing ≥30% inhibition of TBW CS at 10μM. Initial hits were confirmed in a second screen (overall confirmed hit rate = 0.55%), and the 366 confirmed hits were run through both the CS rate series and an *in vivo* surface-applied diet screen (*5*). Simultaneously, the chemical structures were confirmed using mass spectrometry and, if necessary, ^{1}H NMR. High-throughput screening required three months to process 67,000 compounds. A total of 210 compounds passed both the CS enzyme rate series test and structure confirmation. These actives were clustered into 30 chemical classes using HCA/Ward clustering on Daylight fingerprints. Thirty was the number of clusters observed to give good separation of scaffolds into chemically reasonable classes, yet still be manageable for lead optimization. These 30 chemical classes were prioritized, with 18 generics identified for synthesis; 3 out of the 18 were cyanine dye-related structures, Table I. A fourth symmetrical generic was also added. Prioritization criteria included preliminary literature and patent searches, level of biological activity, scaffold diversity, ADME properties, and perceived amenability to synthesis.

Table I. Cyanine Chitin Synthase Projects

Proj Code	Generic Structure	Lead Structure	CS Range pI_{50}	SRTD Range pI_{50} pLD_{50}
19			4.0 – 5.0	4.0 – 5.9 3.6 – 5.1
21B			4.0 – 5.4	3.6 – 5.6 3.6 – 4.1
40A			4.0 – 5.6	3.8 – 6.6 3.6 – 5.7
40B		designed	4.0 – 5.7	NM – 5.7 NM – 4.5

Optimization

We first defined the core. Both enzyme (CS) and *in vivo* (SRTD) data were generated for the analog sets in parallel biological testing. SAR was developed for each chemical class, attempting to correlate *in vitro* to *in vivo* activity. Our standard Discovery paradigm was followed. Scaffold probing was done with Cl, CH₃, and OCH₃ groups. Isosteric replacements were investigated simultaneously; eg., benzoxazoles as well as benzothiazoles were prepared. Specific sets of analogs were designed and prepared to answer questions and generate data for QSAR analysis. Anions explored included halides (Cl⁻, I⁻) and alkyl sulfates (⁻OSO3R, with R = CH₃, C₂H₅).

Classical Hansch 2D QSAR and Sequential Simplex Optimization (SSO) were utilized for optimization of the trimethine-bridged analogs, project 40A. Free-Wilson analysis of monomethine-bridged analogs showed the very positive effect of a 6-OEt on SRTD weight inhibition (pI₅₀). Results of the Hansch analysis are summarized in Figure 3. There appeared to be an optimum in lipophilicity (π). Electronically, the sum of the Swain and Lupton Resonance prarmeter, R, should be negative, making the substituents electron-donating.

Steric factors also appeared to be important around the aromatic rings, although there was cross correlation between the Sterimol parameters L, B1, and B5 and π. Also, steric and/or lipophilicity factors were important for the R/R' alkyls, with the most active being small (methyl or ethyl) groups.
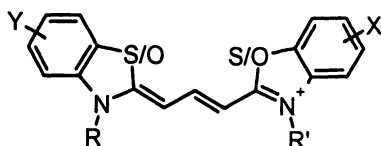
Bisbenzothiazoles:	Bisbenzoxazoles:	QSAR Summary:
X/Y: π_{SUM} opt: 0.9-2.0 R_{SUM} < -0.6 (e-donating) 4: B1 ≤ 1.5 5: B1 < 1.7 or B5 < 3.1 6/7: steric optimum? Nb. XCORR π/L/B1/B5	π_{SUM} > 2.0 5: B1 < 1.7, or B5 < 3.1 Nb. ΔCLogP = 1.0	Increase size or lipophilicity (cross-correlations) Small substituents

Figure 3.   QSAR Summary for Trimethylene Cyanines, Project 40A

We also developed 3-D QSAR (CoMFA) models for the various cyanine classes. These models were put to use identifying neutral, bridge-altered cyanine analogs with the greatest potential of being both enzyme- and in vivo-active. Representative generics are shown below.   Unfortunately all of the neutral analogs that we prepared were inactive.
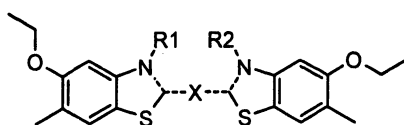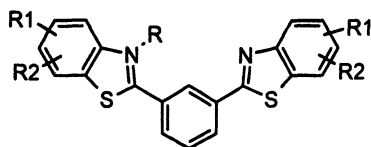
ADME of Cyanines

The photostability of the cyanine dye chemistries was initially thought to be surprisingly good, both on glass and leaf surfaces; however, reexamination showed that photo self-protection was taking place in the thin film deposits. The highly absorbent, deeply colored molecules were much less stable when dilute aqueous solutions containing a surfactant (Triton 100, to spread out the deposit into a thin film) were spotted onto microscope cover slips or leaf surfaces and photolyzed. This test modification gave leaf surface photolysis half-lives in the range 0.4 – 14 hours.

We observed a significant loss of activity proceeding from greenhouse to field. Examination of the factors involved in this translational loss included

- Aqueous hydrolysis testing at pH 10.5 (lepidopteran gut pH) revealed no particular labilities
- No synergism *in vivo* (SRTD) was revealed with either piperonyl butoxide (PBO) or DEF-6 (looking for oxidative or hydrolytic metabolism)
- No effect of foliage incorporated into synthetic diet was observed
- No effect of raising TBW larvae on foliage then transferring them to synthetic diet (testing for induced enzymes)
- No apparent *in vitro* metabolism was observed (non-radiolabeled samples) in isolated TBW microsomal preparations
- *In vivo* metabolism studies showed parent in frass, no obvious metabolites

However, we were able to demonstrate that powdered weak-cation exchange resin incorporated into synthetic diet greatly reduced the toxicity of representative cyanine dyes. Presumably the liphphilic organic cations are bound to the ion exchange resin resulting in reduced bioavailability. In the same way these cyanines should bind to anionic sites in leaf tissue causing them to become unavailable, hence the observation of less than expected potency in the foliar vs. SRTD assays. This observation is consistent with the use of certain cyanines as stains for membranes of acidic organelles and nucleic acids (*6*).

Mechanism of Action

Early in the program, plots of CS enzyme activity vs. SRTD weight inhibition pI_{50} values showed reasonably linear character; however, as more data was generated the correlations degraded until ultimately there appeared to be no correlation between *in vitro* and *in vivo* activity, even upon including additional factors such as LogP. Symptomology work identified a lethal phenotype in

TBW larvae characterized by rapid feeding cessation and absence of tarry frass (as seen with the IDDs), with the cuticle not impaired. This unique phenotype was not similar to that produced by juvenile hormone agonists, ecdysone agonists or the chitin biosynthesis disruptor classes represented by the BPUs.

Using an oxygen electrode, we discovered that representatives of our most active chemistries were mitochondrial electron transport inhibitors (METI) at NADH:ubiquinone oxidoreductase (Complex 1) in whole mouse liver mitochondria, with potencies sufficient to account for their *in vivo* activity. This was confirmed by demonstrating in bovine heart submitochondrial particles that the cyanine FMC4 is a slow potent blocker of Complex 1, with an IC$_{50}$ value of 330 nM, vs. 4.2 nM for the standard rotenone. Other analogs behaved similarly, Table II. It is quite likely that the insecticidal activity of these compounds is due to METI, although most commercial insecticidal Complex 1 inhibitors are actually acaricides, with little lepidopteran activity. Lipophilic organic cation inhibitors of Complex 1 are known in the literature (7), Figure 4. We assume that the cyanines are binding at the same cationic binding site.
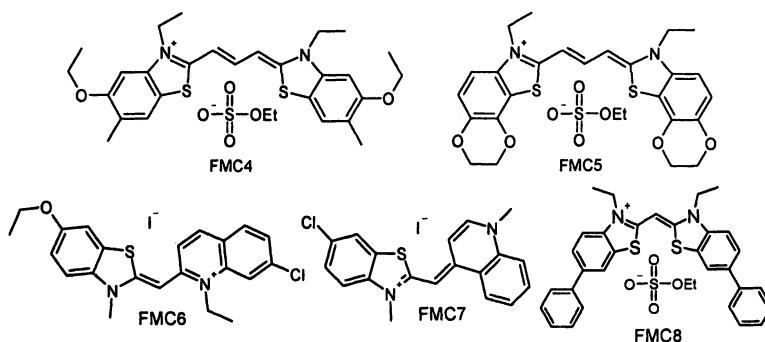
Table II. METI Complex 1 Activity of Cyanines

Compound	Project Code	CS pI$_{50}$	TBW SRTD pI$_{50}$/pLD$_{50}$	DBM Foliar, ppm	Complex 1* % Inh @ 10µM
FMC4	40A	<4	6.6/5.6	45	94 (330 nM)
FMC5	40A	<4	5.8/5.2	47	59
FMC6	21B	4.8	5.4/4.1	173	51
FMC7	19	4.5	5.9/5.1	118	49
FMC8	40B	5.0	5.2/4.5	88	65
Rotenone	Standard		4.1/<3.6		98 (4.2 nM)

* NADH oxidase (Complex 1), bovine submitochondrial particles, % inhibition at 10µM, 30-min preincubation. Values in parentheses are corresponding IC$_{50}$ values.
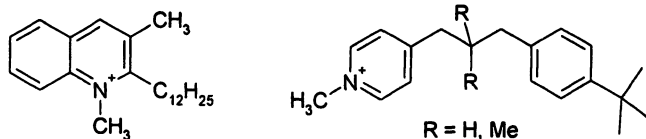
Figure 4. Lipophilic Organic Cationic Inhibitors of Complex 1(7)

Synthesis

Cyanine dyes are well-known in the photographic industry and their synthesis is well-characterized (*8*). The classical cyanine syntheses are flexible, allowing a variety of starting heterocycles to be used. In this convergent synthesis the acidic methyl group can be located on either the quinolinium or the benzothiazolium salt, with the SMe leaving group on the opposite partner, Scheme 2. The deeply colored product salts crystallize directly from the ethanolic reaction solution. Reactions could easily be run in parallel with 6 – 24 analogs being prepared simultaneously.
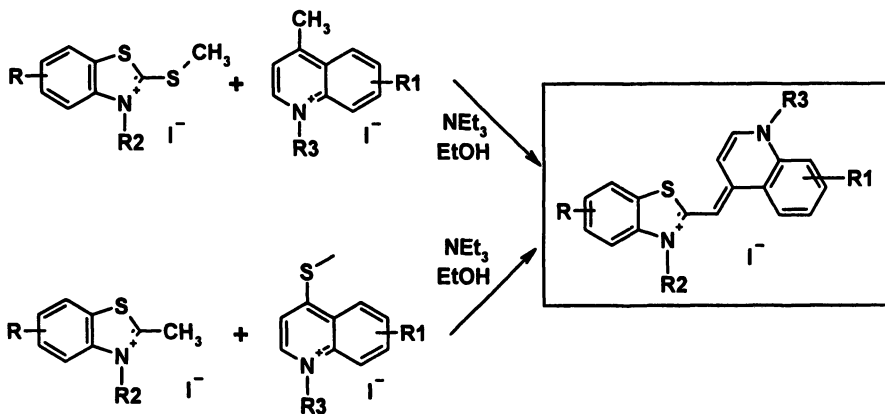
Scheme 2. General Synthesis of Cyanine Dyes

We discovered that this chemistry is quite amenable to microwave synthesis. Reaction times can be reduced from hours to seconds, giving cleaner products.
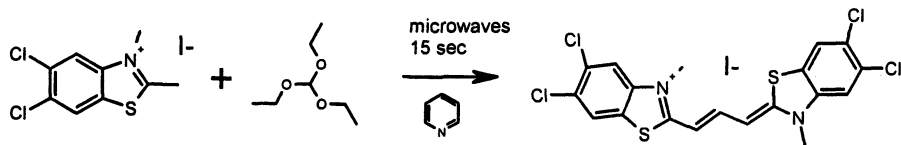
Conclusions

As the CS project concluded, our principle challenges were to determine whether the *in vivo*-active cyanine chemistries were on target, and to understand and overcome the physico-chemical property limitations of the cyanine organic cations. Our research had indicated that 1) the cyanine dyes were not CS inhibitors, but rather inhibited mitochondrial respiration at Complex 1, and 2) lipophilic organic cations are problematic in terms of bioavailability, with the cationic cyanines bound to anionic sites in leaf tissue thereby causing reduced bioavailability to the insect larvae. Therefore we focused synthesis briefly on chemically related uncharged scaffolds. The resulting analogs were devoid of CS activity as well as *in vivo* TBW activity.

It was not possible to overcome the inherent physico-chemical problems with the cyanine chemistries. A critical lesson learned was the value of exclusion assays early in a project, specifically in this case for the METI mechanism of action.

Acknowledgement

References

1. Ishaaya, I. in *Biochemical Sites of Insecticide Action and Resistance*, Ishaaya, I., Ed.; Springer-Verlag: Berlin, 2001; Chapter 1, pp 1-16; Reynolds, S. E. in *Progress and Prospects in Insect Control*, McFarlane, N.

R., Ed.; *British Crop Protection Council Monograph No. 43*; 1989, pp 73-87; Zoebelein, G.; Kniehase, U. *Pflanzenschutz-Nachrichten* **1985**, *38*(2-3), 203-304; Cohen, E. *Arch. Insect. Biochem. Physiol.* **1993**, *22*, 245-261.

2.   Cohen, E.; Casida, J. E. *Pesticide Biochem. Physiol.* **1980**, *13*(2), 129-136; Cohen, E.; Casida, J. E. *Pesticide Biochem. Physiol.* **1982**, *17*(3), 301-306; Palli, S. R.; Retnakaran, A. in *Chitin and Chitinases*; Jolles, P.; Muzzarelli, R. A. A., Eds.; Birkhauser Verlag: Basel, Switzerland, 1999; pp 87-98; Merz, R. A., et al., ibid, pp 9-37; Tripathi, A. K., et al. *J. Medicinal Aromatic Plant Sci.* **2002**, *24*, 104-122; Marks, E. P.; et al. in *Insecticide Mode of Action*; Coats, J. R., Ed.; Academic Press, Inc., 1982; pp 281-313; Cohen, E. *Pest Manag. Sci.* **2001**, *57*, 946-950; Londershausen, M.; Turberg, A. in *Applications of Chitin and Chitosan*; Goosen, M. F. A., Ed.; Technomic Publishing Co, Inc.: Lancaster, PA, 1997; pp 155-170; Kramer, K. J.; Koga, D. *Insect Biochem.* **1986**, *16*(6), 851-877.

3.   Ishida, T., et al. in *Brighton Crop Prot. Conf.—Pests Dis., Vol 1*; 1994; pp 37-44 (etoxazole); WO 9325079, Yashima Chemical Industries Ltd., 1993; WO 9322297, Yashima Chemical Industries Ltd., 1993; US 5663271, EI DuPont DeNemours and Company, 1997; US 5767281, EI DuPont DeNemours and Company, 1998; JK Long, et al., Paper 152, AGRO Division, 220th ACS National Meeting, Washington, DC, 2000 (DuPont); Stevenson, T. M., et al. *in Synthesis and Chemistry of Agrochemicals VI*; Baker, D. R.; Fenyes, J. G.; Lahm, G. P.; Selby, T. P.; Stevenson, T. M.; Eds., *ACS Symposium Series 800*; American Chemical Society: Washington, DC; 2002, pp 188-198.

4.   Sandra F. Simpson, FMC Corporation, manuscript in preparation.

5.   In this assay, which we call SRTD for SuRface TreateD, the surface of synthetic diet is treated with a solution of the test chemical, followed by drying and infestation with TBW larvae. Weight inhibition and mortality are scored after an appropriate period of time.

6.   Haugland, R. P. *Handbook of Fluorescent Probes and Research Chemicals, 6th Edition*; Molecular Probes, 1996; Chapter 12.3, pp 274-279; Ibid, Chapter 8.1, pp 144-156.

7.   Anderson, W. M., et al. *Biochem. Pharmacol.* **1993**, *45*(10), 2115-2122; Anderson, W. M., et al. *Biochem. Pharmacol.* **1995**, *49*(9), 1303-1311; Miyoshi, H., et al. *J. Biol. Chem.* **1997**, *272*(26), 16176-16183; Miyoshi, H., et al. *J. Biol. Chem.* **1998**, *273*(28), 17368-17374; Iwata, J., et al. *Biochim. Biophys. Acta* **1999**, *1413*(2), 63-69; Miyoshi, H. *J. Bioenergetics Biomembranes* **2001**, *33*(3), 223-231.

8.   Ficken, G.E., et al UK Patent 1,096,406; 1967; Mishra, A., et al. *Chem. Rev.* **2000**, *100*, 1973-2011.

Chapter 8

The Crocacins A and D: Novel Natural Products as Leads for Agrochemicals

Patrick J. Crowley, Christopher R. A. Godfrey, and Russell Viner

Syngenta, Jealott's Hill International Research Center, Bracknell, Berkshire RG42 6EY, United Kingdom

The naturally occurring respiration inhibitors crocacins A and D were used as leads for synthesis of a wide range of analogues. Some simplified analogues showed high activity in a mitochondrial beef heart respiration assay, and were also active against certain plant pathogens in glasshouse tests, and were much more stable than the natural products. However, it proved impossible to make analogues that were more active than the natural products.

Background

The discovery of new classes of agrochemicals is never an easy task, and the search for new leads is often a long and tortuous process. Despite the impact of combinatorial chemistry and high-throughput screening, traditional sources of agrochemical leads such as patents and natural products have continued to be widely exploited. In particular, naturally occurring chemicals are still of high interest, because they often have highly unusual structures, novel modes of action, and interesting biological activity. Sometimes however, they have

93

extremely complex structures, are unstable or are toxic. The challenge for chemists wishing to use these as leads for agrochemicals is usually to simplify the structures, raise biological activity, reduce toxicity or improve stability, often simultaneously. Examples of successes in this area include the pyrethroid insecticides *(1)* and the strobilurin fungicides *(2)*.

This story started in 1994 when Profs. Höfle and Reichenbach at GBF in Braunschweig, Germany isolated the new compounds crocacins A, B, C and D from the myxobacterium *Chondromyces crocatus (3)*, and identified their structures as the novel *Z*-enamides **1, 2, 3** and **4** (Figure 1). One of the features of particular interest to us in Zeneca Agrochemicals (as we were at the time) was their mode of action. Höfle and Reichenbach had showed that crocacins A and D inhibited the electron transport chain at complex III in a beef heart mitochondrial respiration assay, and that they inhibited the growth of several fungi *in vitro*. The acid crocacin B, and the truncated molecule crocacin C, were reported not to be active.
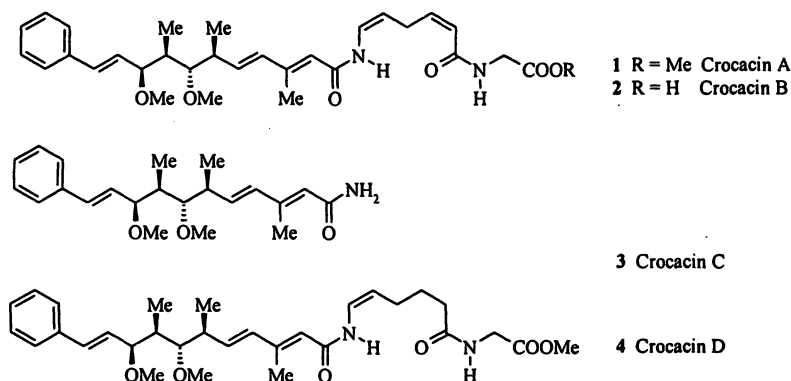
Figure 1. Structures of the Crocacin Natural Products

Inhibition of respiration at complex III was of strong interest at the time because of the very high and broad spectrum fungicidal activity achieved by the strobilurins, such as azoxystrobin **5** and kresoxim-methyl **6**, (Figure 2). The natural product stigmatellin **7** was also a complex III inhibitor, with reasonable activity on the beef heart NADH oxidase assay, although it showed no activity on our fungicide screens on plants. Stigmatellin had many similarities in structure to the crocacins, especially in its side chain, where the stereochemistry of the four contiguous chiral centers is identical to that of the crocacins.

5 Azoxystrobin

6 Kresoxim methyl

7 Stigmatellin
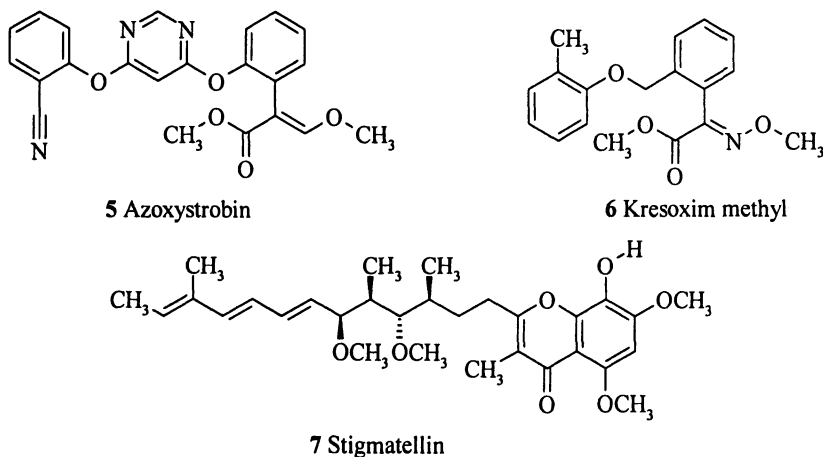
Figure 2. Structures of Other Inhibitors of the Cytochrome BC₁ Complex.

Potential as Agrochemical Leads

Professors Höfle and Reichenbach very kindly provided us with samples of crocacins A and D, and we confirmed their activity against certain fungi *in vitro*, with crocacin D being slightly more active than crocacin A. We also found that they showed activity by foliar spray against *Plasmopara viticola* (vine downy mildew), *Phytophthora infestans* (potato late blight), *Puccinia recondita* (wheat brown rust), and *Septoria nodorum* (wheat glume blotch) on plants.

Table 1. Activity of Respiration Inhibitors on Beef Heart NADH Oxidase and on Fungi on Plants

	EC90 (ppm)					IC50 (nM)
	Wheat Powdery Mildew	Wheat Glume Blotch	Potato Late Blight	Vine Downy Mildew	Wheat Brown Rust	NADH oxidase
Crocacin A	>100	>100	100	25	25	56
Crocacin D	>100	25	25	25-5	5	36
Azoxystrobin	<1	<1	<1	<1	<1	120
Stigmatellin	>100	>100	>100	100	>100	81

We confirmed that crocacins A and D inhibited beef heart mitochondrial respiration at complex III, and that they were significantly more active than

azoxystrobin in a beef heart NADH oxidase assay. We also showed that crocacin A had little or no cross-resistance with the strobilurins. It was fully active against a strobilurin resistant strain of *Plasmopara viticola* in the glasshouse, and against a strain of yeast that had been engineered with the G143A mutation responsible for fungicide resistance.

A major problem with crocacins A and D was their poor photostability, with 50% of parent compound being lost in 7 and 37 minutes respectively, in a simulated sunlight test in the laboratory using thin films on glass slides. Additionally, although they were stable at pH 4 and 7 at 39°C, treatment with pig liver esterase under these conditions rapidly hydrolysed the glyine methyl ester, suggesting that they might be metabolised in plants or fungi.

In summary, we had leads with novel structures, a well-proven mode of action and significant fungicidal activity on plants. On the negative side the compounds had poor stability, only moderate activity, and rather complex structures. However, we believed we could tackle these issues, and started a programme of chemistry.

Design of Analogues of Crocacins A and D - Key Considerations

An important element of our strategy was the assumption that more stable analogues would be more biologically active, both in the glasshouse and the field. We hoped that the lipophilic side chain of the crocacins, with its array of four contiguous chiral centres and three double bonds, could be replaced by stable aromatic groups, and that the unstable Z-enamide could be mimicked by a more stable linking group. In addition, the glycine ester might also need replacing with groups that were more resistant to hydrolysis, to reduce potential degradation by esterases in plant or fungal cells. These changes would also make analogues easier to make and therefore cheaper. The synthetic chemistry to make the various analogues has already been published *(4)* and will not be repeated here. We also carried out extensive molecular modeling, which will be published separately.

First Attempts

Our first attempt was to synthesis some libraries, where we replaced the Z-double bonds with benzene rings, and the complex side chain with simpler groups. Typical examples were Compounds **8** and **9**, (Figure 3). All the compounds were tested on a cascade consisting of the beef heart mitochondrial respiration assay and application to fungi on leaf disks, with the most active compounds then being tested on fungi on small plants. Unfortunately, none of the compounds showed activity in any of these tests.

8　　　　　　**9**
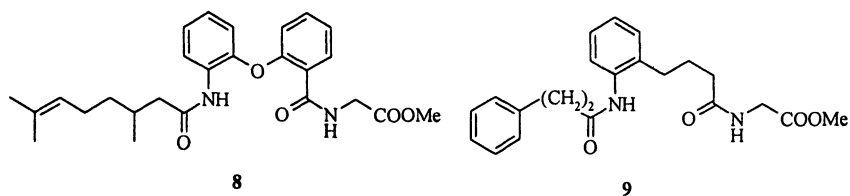
Figure 3. Examples of Library Compounds

Replacement of the Side Chain

Since the *Z*-enamide glycine ester appeared to be very important in keeping the structure rigid, we decided to keep this moiety constant in our initial set of analogues, and to replace the complex side chain of crocacin D with simpler groups. The first analogues we synthesised had just simple n-alkyl chains, e.g. **10**, as shown in Table 2. Several of these were very active in the beef heart mitochondrial respiration assay, but were not fungicidal. Replacement of the carboxamide with a benzamide substituted with alkoxy groups, such as in Compound **11**, also produced good respiration inhibitors, which were again inactive on fungi. However, substituting the benzamide in the 4-position with chains containing aryl groups, such as the 4-bromobenzyl Compound **12**, iodobenzyl Compound **13** and ethylbenzyl Compound **14** gave not only potent inhibition of respiration, but also activity on vine downy mildew both on leaf disks and plants, at a level similar to that of the crocacins. Benzamides substituted in the 4-position were much more active than those substituted in the 3-position.

As also shown in Table 2, there was also a considerable improvement in photostability, with some analogues such as **15** being very much more stable than the natural products.

Replacement of the *Z*-Enamide

The *Z*-enamide 'linking' group is unusual in that it imparts rigidity but is sterically undemanding, and it was consequently always likely to be difficult to mimic with other groups. A set of analogues with relatively rigid linking groups were synthesised (see Figure 4), for example Compounds **16-21** all with the same n-decyl side chain, but they showed very little activity on the beef heart mitochondrial assay or on fungi on leaf disks.

**Table 2. Activity of Side Chain Analogues on Beef Heart NADH Oxidase
and Vine Downy Mildew on Plants**

No.	Side Chain R	IC50 NADH Oxidase (nM)	EC90 Vine Downy Mildew (ppm)	T_{50} Glass Slides (Hours)
4	Crocacin side chain	36	25	0.6
10	$n\text{-}C_{12}H_{21}\text{-}$	24	>100	NT
11	$4\text{-}(n\text{-}C_6H_{11}O)\text{-}C_6H_4\text{-}$	21	>100	5
12	$4\text{-}(4\text{-}Br\text{-}C_6H_4CH_2)\text{-}C_6H_4\text{-}$	17	10	12
13	$4\text{-}(4\text{-}I\text{-}C_6H_4CH_2)\text{-}C_6H_4\text{-}$	18	10	NT
14	$4\text{-}(4\text{-}C_2H_5\text{-}C_6H_4CH_2)\text{-}C_6H_4\text{-}$	16	<10	NT
15	$4\text{-}(4\text{-}EtO\text{-}C_6H_4O)\text{-}C_6H_4\text{-}$	9	25	20

NT: not tested

16 **17** **18**

X = O, C

19 **20** **21**

R = n-C$_{10}$H$_{21}$
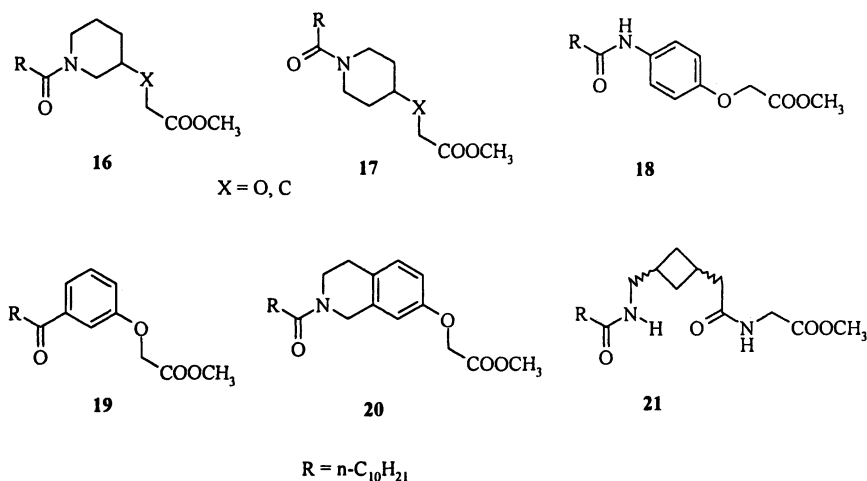
Figure 4. General Structures of some Potential Z-enamide Mimics.

An interesting exception was the benzoxazolone **22**, (see Table 3) which contained a more optimized side chain and showed rather better activity in the NADH Oxidase assay, although it was almost inactive on fungi on plants.
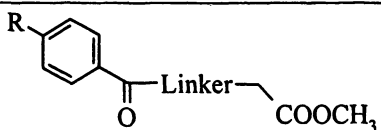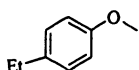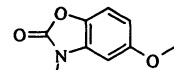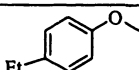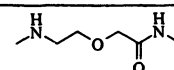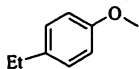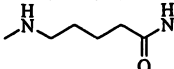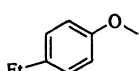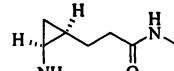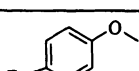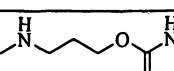
We then tried more flexible linkers, in the hope that they might be better able to adapt their structures to the requirements of the active site. Of these **23**, with an oxygen-containing chain was most intrinsically active, but again it was inactive on fungi. The compound with the Z-olefin replaced by a cis-cyclopropane **25** was poor on the NADH Oxidase assay, but surprisingly showed some weak activity on fungi. This disparity between activity on the respiration assay and on fungi is hard to explain, and either suggests that **25** has a different mode of action, or casts doubt on the reliability of the correlation between the beef heart mitochondrial assay and antifungal activity.

At this point it became clear that it is was going to be very difficult to find active analogues with alternative groups to the Z-enamide. We concluded that the problem was maintaining the rigidity of the Z-enamide without increasing steric bulk, and modeling studies confirmed that space in the active site is very restricted.

Replacement of the Glycine Ester

Simple esters can be prone to hydrolysis by esterases in plants, and indeed tests using maize cell and liquid fungal cell cultures showed that the methyl ester of several analogues was cleaved very rapidly. The glycine methyl ester was found to be important for activity, and some effort was devoted to looking for groups that might mimic the methyl ester but be more resistant to hydrolysis, as

Table 3. Activity of Z-Enamide Analogues on Beef Heart NADH Oxidase and Vine Downy Mildew on Plants
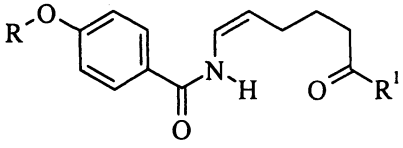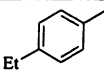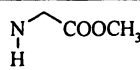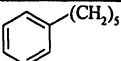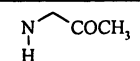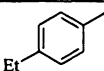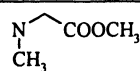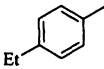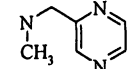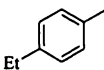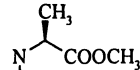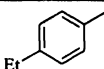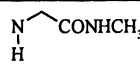
No.	R	Linker	IC50 NADH Oxidase, (nM)	EC90 Vine Downy Mildew (ppm)
22			140	>100
23			230	>100
24			400	>100
25			900	100
26			1600	>100

shown in Table 4. The *N*-methylamide **32** was inactive, but the methyl ketone **28** did show some activity. Certain heterocycles have been shown to be good methyl ester replacements *(5)*, and several were tried. Of these the pyrazine **30** was the best, but although it was resistant to hydrolysis, it was only weakly active in the respiration assay and on fungi.

Conclusions

The project was successful in that we were able to make synthetic analogues of crocacin D, which were active both in an *in vitro* respiration assay, as well as on fungi on plants, and which were significantly more stable than the natural compounds.

Table 4. Activity of Glycine Ester Analogues on Beef Heart NADH Oxidase and Vine Downy Mildew on Mini Plants

No.	R	R¹	IC50 NADH oxidase (nM)	EC90 Vine Downy Mildew (ppm)
27	Et— (phenyl)—	N(H)—CH₂—COOCH₃	9	25
28	(phenyl)—(CH₂)₅	N(H)—CH₂—COCH₃	49	30
29	Et— (phenyl)—	N(CH₃)—CH₂—COOCH₃	70	>100
30	Et— (phenyl)—	N(CH₃)—CH₂—(pyrazine)	110	100
31	Et— (phenyl)—	N(H)—CH(CH₃)—COOCH₃	210	>100
32	Et— (phenyl)—	N(H)—CH₂—CONHCH₃	880	>100

Unfortunately, the best analogues were only moderate active against vine downy mildew and were rather weak against potato blight on tomatoes, and were thus not active enough to progress. We were disappointed not to be able to improve on the activity of the natural products, despite finding analogues with high activity in the beef heart NADH oxidase assay, and with substantially more stability than the natural products. The reasons for this are not certain, but may be several.

Firstly, we had hoped that if we could find really good mimics of the Z-enamide, that were also stable, then we would achieve high fungicidal activity. In the event we were unable to find alternative groups to the Z-enamide with any significant fungicidal activity.
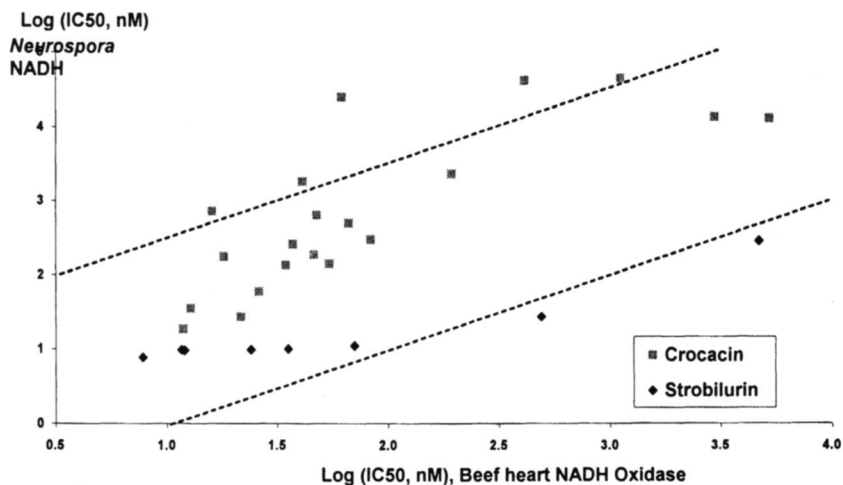
Figure 5. Graph of Activity against Neurospora Crassa versus Beefheart Mitochondrial NADH Oxidase.

Secondly, there were concerns about whether the beef heart NADH oxidase assay used to measure the intrinsic activity of analogues was a valid model for fungal systems. This was highlighted when late in the project we tested a range of analogues on NADH oxidase in mitochondria from the model fungus *Neurospora crassa*, which were difficult to prepare and use compared to beef heart mitochondria. It was found that the crocacin analogues were all significantly less active in *Neurospora* than in beef heart. In contrast, a range of strobilurin analogues were if anything more active in *Neurospora* than in beef heart, (Figure 5).

References

1. Elliott, M., *Pesticide Science* **1989**, *27*, 337.
2. Clough, J. M.;Godfrey, C. R. A.; Godwin, J. R.; Joseph, R. S. I.; Spinks, C. *Pesticide Outlook* **1996**, *4*, 16.
3. Kunze, B.; Jansen, R.; Höfle, H.; Reichenbach, H. *J. Antibiot.* **1994**, *47*, 881.
4. Crowley, P. J.; Aspinall, I. H.; Gillen, K.; Godfrey, C. R. A.; Devillers, I. M.; Munns, G.; Sageot, O-A.; Swanborough, J.; Worthington, P. A.; Williams, J. *Chimia*, **2003**, *57*, 685.
5. Lipinski, C. A. *Annual Reports in Medicinal Chemistry*, **1986**, *21* 283.

Chapter 9

A Structure-Based Design Approach to Plant Selective 4-Hydroxyphenylpyruvate Dioxygenase Inhibitors

Debra L. Camper and Marshall H. Parker

Dow AgroSciences R&D, 9330 Zionsville Road, Indianapolis, IN 46268

A high degree of selectivity toward the target site of the pest organism is a desirable attribute for new safer agrochemicals. To assist in the design of novel herbicides, we determined the crystal structures of the herbicidal target enzyme 4-hydroxyphenylpyruvate dioxygenase (HPPD; EC 1.13.11.27) from the plant *Arabidopsis thaliana* with and without herbicidal inhibitors and from a mammalian (rat) HPPD in complex with an inhibitor. Detailed comparisons of the plant and mammalian HPPD-ligand structures suggest a structural basis for the high degree of plant selectivity of certain HPPD inhibitors and point to design strategies to obtain potent and selective inhibitors of plant HPPD as agrochemical leads. The design, synthesis, and testing of a set of novel tetramic acid inhibitors will be described.

© 2007 American Chemical Society

105

Molecular target sites that are of interest for the design of new agrochemicals often occur in both the pest species (weed, fungus, insect) and vertebrates. Undesirable affects on off-target species are often alleviated through mechanisms of differential metabolism. The advancements in the collection of detailed structural information and the development of sophisticated target site-based computational tools have provided a rich environment for improving potency and selectivity toward the target pest and away from nontarget organisms. One enzyme of interest for herbicide design is 4-hydroxyphenylpyruvate dioxygenase (HPPD) *(1, 2)* which is the target site for a family of bleaching herbicides including the commercial herbicides isoxaflutole (Balance®), mesotrione (Callisto®) and pyrazolate.

HPPD catalyzes the oxygenation of 4-hydroxyphenylpyruvate (HPPA) to form homogentisic acid (HGA) (Figure 1). It is found in microbes, mammals and plants with differing enzyme functions. In plants, HGA is a precursor for plastoquinone, an important cofactor in the biosynthesis of photoprotectant carotenoids *(1, 3)*. Loss of carotenoids results in characteristic intense bleaching of new plant growth and eventually plant death. In mammals, the enzyme functions in tyrosine catabolism in the liver. Deficiency of the enzyme in humans causes tyrosinemia, a rare disorder characterized by elevated serum tyrosine levels. *(4, 5, 6, 7, 8)*
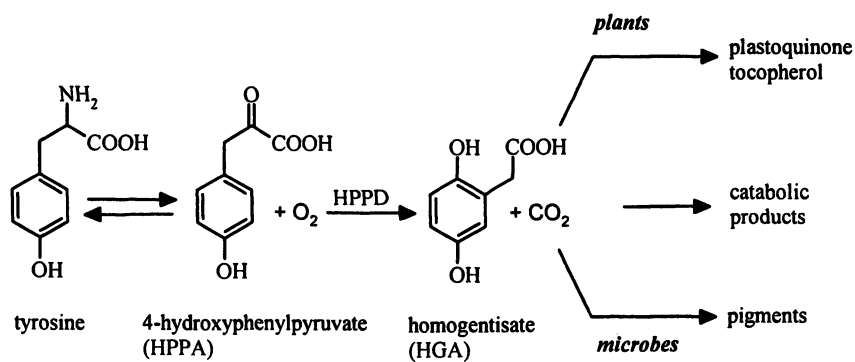
Figure 1: Scheme for the HPPD Catalyzed Reactions in Multiple Species

Potent HPPD inhibitors have a common structural feature in the form of a 1,3-diketone moiety *(9, 10, 11)*. Kinetics experiments show that these potent inhibitors exhibit the characteristics of slow-tight binding inhibitors *(12, 13, 14, 15)*. Figure 2 contains examples of various structural classes of inhibitors all with the 1,3-diketone motif. Mesotrione and the diketonitrile form of isoxaflutole are commercial herbicides, (-)-usnic acid is a natural product inhibitor isolated from lichen *(16)*, and DAS645 and DAS869 are experimental herbicides from the Dow AgroSciences (DAS) collection. DAS869 is a potent
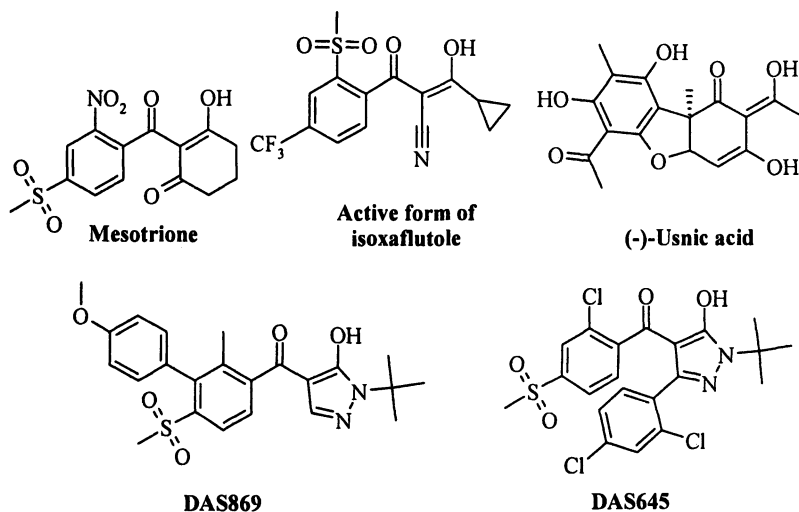
Figure 2: Examples of Various Structural Classes of HPPD Inhibitors.

inhibitor of both plant and mammalian HPPDs whereas DAS645 is highly selective for the plant enzyme.

Most of the initial work at DAS in this area focused on the benzoylpyrazole class of HPPD inhibitors that deliver potent enzyme inhibition and excellent herbicidal activity. The majority of HPPD inhibitors inhibit both plant and mammalian HPPDs. We wished to determine mechanisms to confer a high degree of plant selectivity for HPPD inhibitors and utilize this structural information to design novel, potent inhibitors of Plant HPPD. To identify compounds with differential inhibition, a microplate-based assay was developed to screen about 1,000 HPPD inhibitors from the DAS collection against both plant and mammalian HPPDs. From this screen 6 selective inhibitors were identified. The I50's for plant and rat HPPD were 7nM and <20nM for DAS869 and 12nM and >>50μM for DAS645, respectively. The x-ray crystal structures for non-selective inhibitor DAS869 and selective inhibitor DAS645 were determined to provide structural details relevant to the difference in selectivity of these similar compounds. The crystallography work is described in detail elsewhere *(17)*.

Most of the binding site residues are conserved in the plant and rat enzymes and the x-ray structures of the different enzyme-inhibitor complexes are very similar, with little movement of the protein backbone (Figure 3). In the apo structure, two histidines, a glutamic acid and three water molecules coordinate the active site metal ion. In the inhibitor bound structures, the 1,3-diketone of the inhibitor chelates the metal ion, replacing two of the water molecules. There

AtHPPD-869　　　　　**RnHPPD-869**　　　　　**AtHPPD-645**
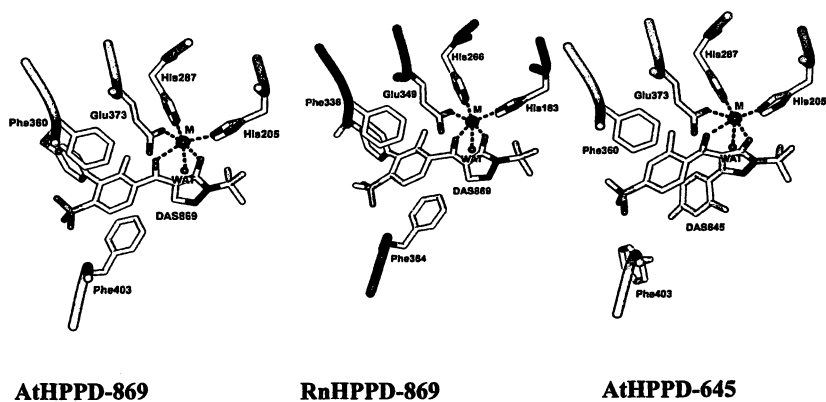
Figure 3: AtHPPD-869 1.8 Å Arabidopsis HPPD + DAS869 pdb code 1TFZ; RnHPPD-869 2.15 Å Rat HPPD + DAS869, pdb code 1SQI; AtHPPD-645 1.9 Å Arabidopsis HPPD + DAS645, pdb code 1TG5; At HPPD 1.8 Å Native HPPD from Arabidopsis, pdb code 1SQD (not shown).


```
AtHPPD:(376) ...QRVGCMMKDEEGKAYQSGGCGGFGKGNFSELFKSIE...

RnHPPD:(352) ...QRHNH---------------QGFGAGNFNSLFKAFE...
```
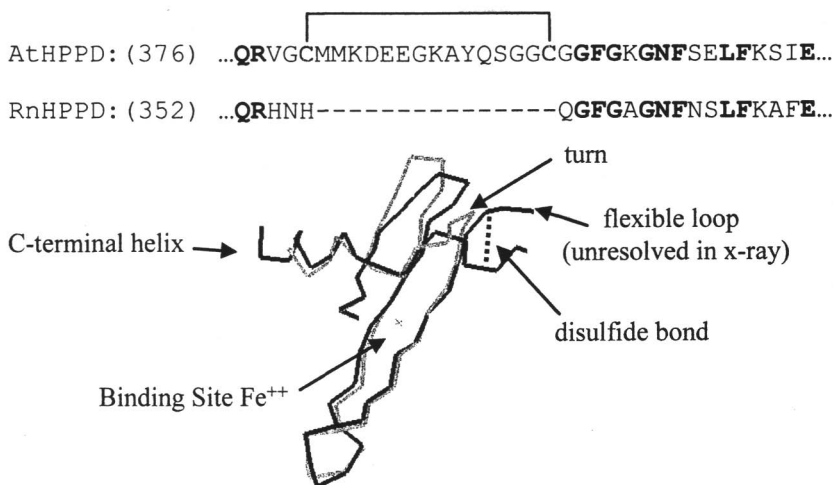

Figure 4: Sequence alignment and C-α trace of AtHPPD (dark) and RnHPPD (light) in the C-terminal helix. The dotted line represents a disulfide bond in AtHPPD which aligns with a shorter turn in the RnHPPD structure.

is an important π-stacking network between the inhibitor and the protein. Specifically the π-stacking of two Phe residues (*Arabidopsis* (At) Phe360 and Phe403; Rat (Rn) Phe336 and Phe364) with the benzoyl ring of the inhibitor is important to binding. The plant-selective inhibitor DAS645 displaces one of these Phe residues (AtPhe403) to achieve binding. After careful analysis of the different enzyme-inhibitor complexes, several structural features were found which, when combined, confer selectivity. The first feature is a plant-specific loop which leads to flexibility of the C-terminal helix in AtHPPD whereas RnHPPD has a shortened, restricted turn (Figure 4). The second feature (Figure 5) is the ability of a specific Phe residue to rotate away to accommodate a bulky ligand. AtPhe403/RnPhe364 in the C-terminal helix must reorient to accommodate the 2,4-dichlorophenyl substitution on the pyrazole of the ligand.
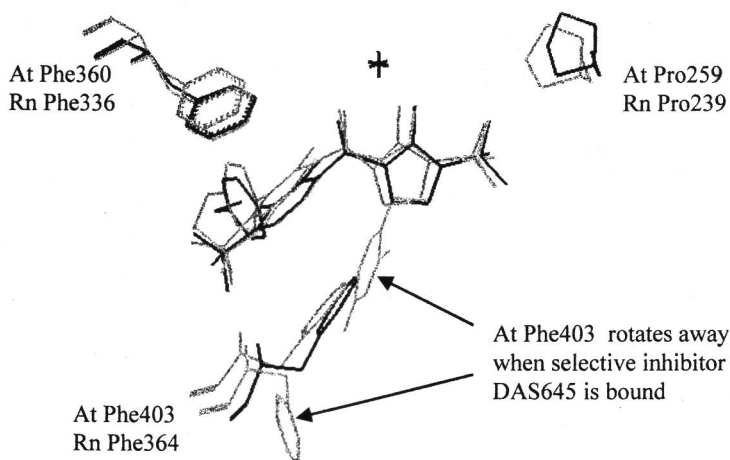
At Phe360
Rn Phe336

At Pro259
Rn Pro239

At Phe403 rotates away when selective inhibitor DAS645 is bound

At Phe403
Rn Phe364

Figure 5: π-stacking network. AtPhe403 rotates away when DAS645 binds to the enzyme. AtHPPD-869 in dark blue, AtHPPD-645 in cyan, RnHPPD-869 in green (See page 2 in color inserts.)

The flexible loop of AtHPPD allows C-terminal helix movement whereas the RnHPPD C-terminal helix is less flexible and cannot readily accommodate this rotation. The third important feature involves position and flexibility of the backbone near a proline residue which interacts with the pyrazole portion of the ligands. DAS869 and DAS645 with *N*1-tert-butylpyrazoles butt up to AtPro259/RnPro239 and require rearrangement. In AtHPPD, the protein backbone shifts away to accommodate this bulky substitution. For RnHPPD it

appears the equivalent RnPro239 cannot be readily repositioned resulting in a slightly smaller ligand binding region. RnHPPD must accommodate the ligand by displacement of the inhibitor toward the middle of the ligand binding domain to avoid steric clash with RnPro239, causing additional detrimental C-terminal helix interactions (Figure 6).

backbone shifts to accommodate *t*-butyl group in plants

backbone cannot shift, ligand moves ~0.5Å in rat enzyme
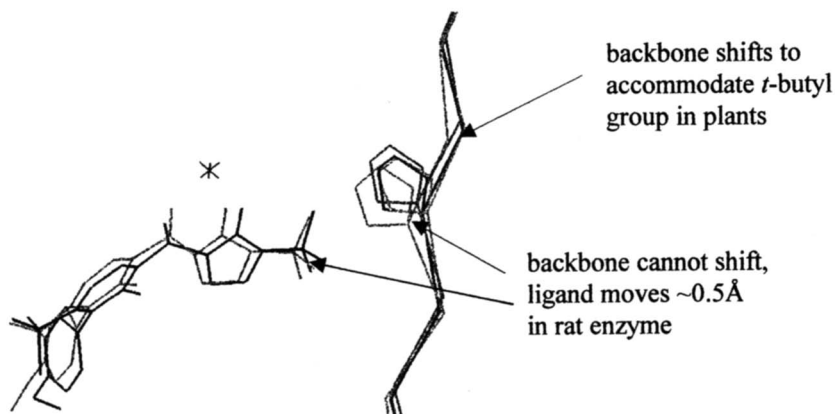
Figure 6: Shifting of the ligand towards the middle of the binding site to accommodate the position of RnPro239 resulting in a more crowded binding site. AtHPPD with DAS869 in dark blue; RnHPPD with DAS869 in green; AtHPPD with DAS645 in cyan; At HPPD with no bound ligands in purple (See page 2 in color insert.).

Design of New Inhibitors

With the mechanisms of affinity and selectivity well understood, the goal of the synthetic effort was to discover novel plant selective bioactive templates. A lysine tetramic acid template (Figure 7) was selected as the focus of our synthesis for several reasons: the tetramic acid core is found in bioactive molecules *(18, 19, 20, 21, 22),* had the correct shape to include the appropriate bulky groups to increase target selectivity, could accommodate hydrogen-bonding groups, had good physical properties, and was associated with a library synthesis that capitalized on previously reported protocol *(23, 24).* The synthesized tetramic acid library incorporated these observations by including substituted *N*-benzyl groups on the tetramic acid ring as well as both cyclopropyl and cyclobutyl groups adjacent to the chelation site.

R2 =

R3 =
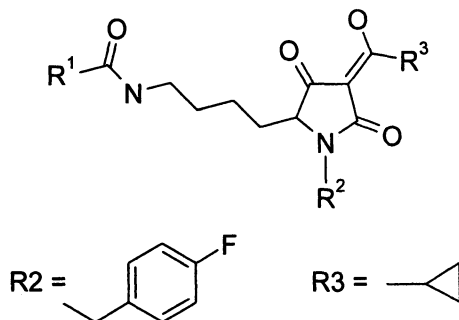
Figure 7: Lysine tetramic acid core template. The inputs shown for R2 and R3 were used to facilitate docking and exploration of the R1 lysine tail.
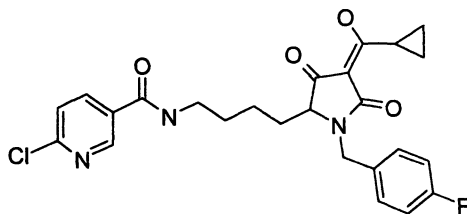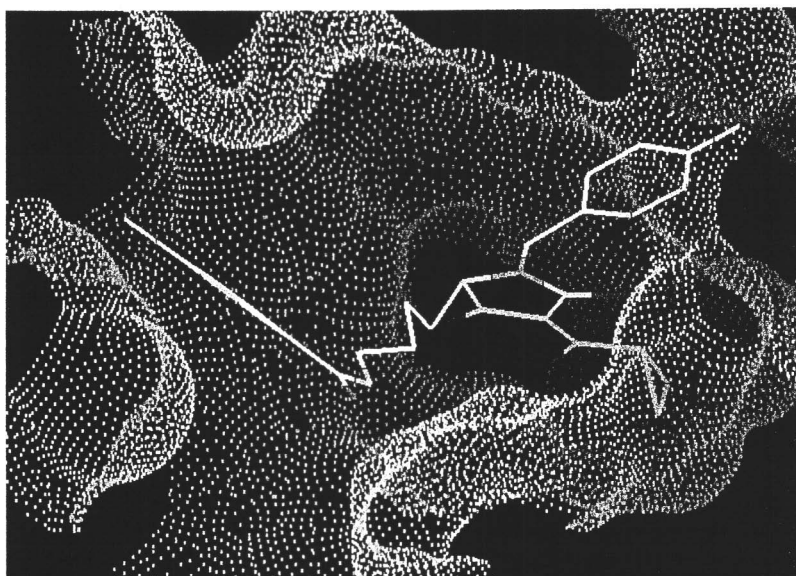
Figure 8: Dot surface indicates the van der Waals surface of the AtHPPD protein. Proposed inhibitor DAS432 shown with good fit to protein surface and the chloro-pyridine amide tail occupies a previously unexplored channel.

The tetramic acid core, as shown in Figure 8, was docked into the x-ray crystal structure of AtHPPD and aligned with the bound benzoylpyrazole ligand using FlexX within the Sybyl program *(25)*. The designed inhibitors and the protein were minimized using Charmm within the InsightII program *(26)*. The cyclopropyl group and the benzyl group attached to the tetramic acid structure overlapped well with the known active benzoylpyrazole inhibitors. This allowed for docking studies and structure-based design tools to be used for exploration of R1 tails (Figure 7). In particular, examination of the binding pocket led to the conclusion that libraries with either the amide or urea linkages would be potentially beneficial for increasing enzyme efficacy through a hydrogen bond with a glutamine residue AtHPPD - Gln272 (Figure 9). Examination of the enzyme structure revealed a previously unexploited channel reachable with the
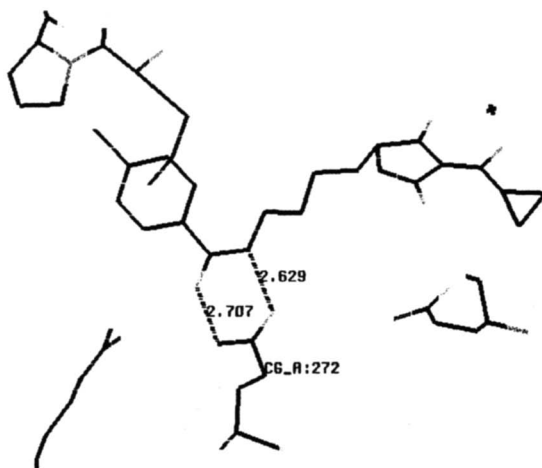
Figure 9: Much of the protein and side chains have been clipped for a better view of the proposed inhibitor. The amide tail linkage appears to hydrogen-bond with the side-chain of glutamine 272. The star is the location of the chelating metal ion.

substituted lysine tail. Building off literature protocol previously reported, a small library of functionalized lysine tetramic acids (Scheme 1) was prepared *(23, 24, 27)*. The computational docking work highlighted several compounds from this library to be evaluated in the in vitro enzyme assay. Specifically several interesting inhibitors including DAS432 and DAS531 were re-synthesized and purified to provide sufficient sample for characterization in our in vitro assay (Figure 10). Both of these inhibitors displayed high levels of
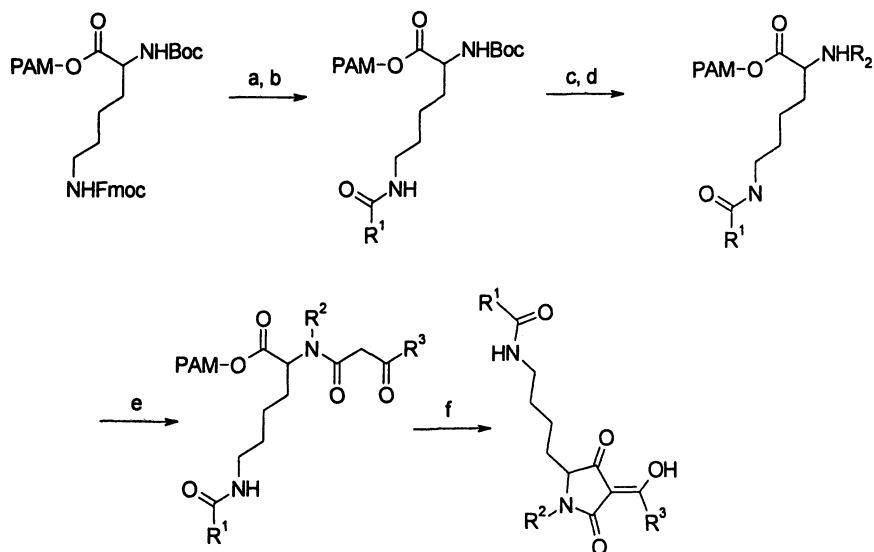
Scheme 1 : Lysine ATA Library Protocol: (a) Piperidine, DMF; (b) DIC, DMAP, a carboxylic acid or an isocyanate, DMF; (c) 25% TFA, CH2Cl2; (d) Aldehyde, TMOF; NaCNBH3, DMF, 1% AcOH; (e) AcylMeldrum's acid, BSA, 50 °C; (f) DIEA, Dioxane, 70 °C.

selectivity for the plant enzyme over the rat enzyme. DAS531 with the larger cyclobutyl group helped confirm the role the protein backbone rearrangement near AtHPPD – Pro259 plays in determining selectivity. These compounds were tested in greenhouse studies but despite the identification of these potent inhibitors, the *in vivo* activity was not compelling.

Conclusions

Based on the mechanism of selectivity identified for *Arabidopsis* versus Rat HPPD, potent, selective inhibitors were designed which contained new chemical scaffolds. The combinatorial methodology for the lysine tetramic acids allowed for broad and rapid exploration of multiple hypotheses simultaneously. DAS432 and DAS531 had the required substitution patterns to exhibit the desired plant selectivity. Specifically, both the cyclopropyl and the cyclobutyl R^3 groups provided the necessary bulk to bump into AtPro259/RnPro239 which require rearrangement similar to that described for the *N*1-tert-butyl group on the pyrazoles of DAS869 and DAS645. The *N*-benzyl substitutions at R^2 on the
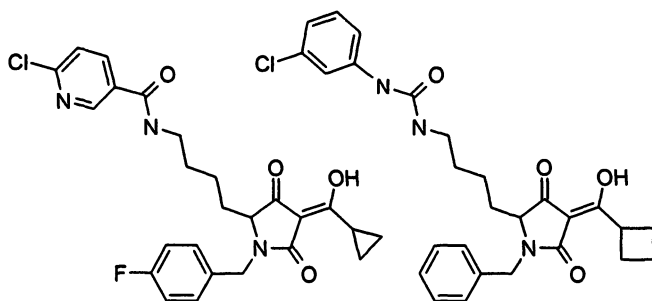
	DAS432	DAS531	DAS645
Arabidopsis I_{50}(nM)	20	158	12
Rat I_{50}(nM)	3870	>10,000	>50,000

Figure 10: Inhibitors Resynthesized and Purified with Enzyme Inhibition Data

tetramic acid core correspond to the 2,4-diclorophenyl on DAS645. This substitution drives the rotation of the AtPhe403/RnPhe364 away from the ligand which is hindered in the Rat structure due to the restricted turn in the c-terminal helix. These features combined to provide the high degree of selectivity observed for DAS432 and DAS531. This work on the tetramic acids confirmed the hypothesis that the size, geometry, and substitution patterns of the inhibitor strongly influence binding affinity and validates the structural preferences for this class of inhibitors. These mechanisms of selectivity were very subtle and must all be present to confer high levels of selectivity. The x-ray crystal structures with inhibitors from both *Arabidopsis* and Rat were vital to identification of these selectivity mechanisms. Despite identification of potent inhibitors with high levels of plant selectivity, the *in vivo* activity was not compelling.

Methods

Synthesis

Commercially available, orthogonally protected, lysine on PAM resin was selectively deprotected with piperidine to liberate the epsilon amine. This amine was then utilized in one of two ways. In the first instance, a dehydrative coupling with an acid produced a series of amides (exemplified by DAS432). In the second case, direct reaction with an isocyanate yielded the urea (exemplified by DAS531). The resulting ureas and amides were treated as a single point of diversity (R^1) throughout the rest of library production with no apparent

difference in their reactivity. Formation of the tetramic acid was initiated by deprotecting the remaining amine with a 25% solution of trifluoroacetic acid. Reductive amination with a variety of aldehydes introduced a second point of diversity (R^2). The resulting secondary amine was then reacted with several preformed Meldrums acids to introduce the third point of diversity (R^3) and set the stage for a cyclitive cleavage that forms the tetramic acid ring system. It is important to note that even with the optimized conditions and reduced temperatures afforded by the introduction of bistrimethylsilylacedamide (BSA), premature ring formation and cleavage of the product from the resin was noted at this stage. Finally, the resin was thoroughly washed and the treated with Diisopropylethylamine (DIEA) in dioxane to induce the cyclization and liberate the targeted compounds from the resin. Filtration and concentration of the resulting wash gave the desired tetramic acids in good yields (45-90%) and high purities (>85%) as determined by coupled LCMS. Finally, compounds of high interest were purified via reverse phase chromatography for *in vitro* enzyme studies and crystallography.

References

1. Pallett, K. E., Little, J. P., Sheekey, M., and Veerasekaran, P. (1998) Pestic. Biochem. Physiol. 62, 113-124.
2. Mitchell, G., Bartlett, D. W., Fraser, T. E. M., Hawkes, T. R., Holt, D. C., Townson, J. K., and Wichert, R. A. (2001) Pest Manag. Sci. 57, 120-128.
3. Norris, S. R., Barrette, T. R., and DellaPenna, D. (1995) Plant Cell 7, 2139-2149.
4. Cerone, R., Holme, E., Schiaffino, M. C., Caruso, U., Maritano, L., and Romano, C. (1997) Acta Paediatrica 86, 1013-1015.
5. Endo, F., Kitano, A., Uehara, I., Nagata, N., Matsuda, I., Shinka, T., Kuhara, T., and Matsumoto, I. (1983) Pediatric Research 17, 92-96.
6. Sanchez-Amat, A., Ruzafa, C., and Solano, F. (1998) Comp. Biochem. Biophys. B 119B, 557-562.
7. Tomoeda, K., Awata, H., Matsuura, T., Matsuda, I., Ploechl, E., Milovac, T., Boneh, A., Scott, C. R., Danks, D. M., and Endo, F. (2000) Mol. Genet. Metab. 71, 506-510.
8. Holme, E. and Lindstedt, S. (1998) J. Inherited Metab. Dis. 21, 507-517.
9. Pallett, K. E., Cramp, S. M., Little, J. P., Veerasekaran, P., Crudace, A. J., and Slater, A. E. (2001) Pest Manag. Sci. 57, 133-142.
10. Lee, D. L., Knudsen, C. G., Michaely, W. J., Chin, H. L., Nguyen, N. H., Carter, C. G., Cromartie, T. H., Lake, B. H., Shribbs, J. M., and Fraser, T. (1998) Pestic. Sci. 54, 377-384.
11. Meazza, G., Scheffler, B. E., Tellez, M. R., Rimando, A. M., Romagni, J. G., Duke, S. O., Nanayakkara, D., Khan, I. A., Abourashed, E. A., and Dayan, F. E. (2002) Phytochemistry 60, 281-288.

12. Garcia, I., Job, D., and Matringe, M. (2000) Biochem. 39, 7501-7507.
13. Ellis, M. K., Whitfield, A. C., Gowans, L. A., Auton, T. R., Provan, W. M., Lock, E. A., Lee, D. L., and Smith, L. L. (1996) Chem. Res. Toxicol. 9, 24-27.
14. Lock, E. A., Ellis, M. K., Gaskin, P., Robinson, M., Auton, T. R., Provan, W. M., Smith, L. L., Prisbylla, M. P., Mutter, L. C., and Lee, D. L. (1998) J. Inherited Metab. Dis. 21, 498-506.
15. Lee, D. L., Prisbylla, M. P., Cromartie, T. H., Dagarin, D. P., Howard, S. W., Provan, W. M., Ellis, M. K., Fraser, T., and Mutter, L. C. (1997) Weed Sci. 45, 601-609.
16. The Phytotoxic Lichen Metabolite, Usnic Acid, Is A Potent Inhibitor of Plant P-Hydroxyphenylpyruvate Dioxygenase. Romagni, J. G.; Meazza, G.; Nanayakkara, N. P. D.; Dayan, F. E. Natural Products Utilization Research Unit, USDA/ARS, University of Mississippi, Lafayette, MS, USA. FEBS Lett. (2000), 480(2,3), 301-305.
17. Camper, D. L., Pernich, D. J., Walsh, T. A., Foster, M., Pflugrath, J., Yang, C. "Structural Basis For Herbicidal Inhibitor Selectivity Revealed by Comparison of Crystal Structures Of Plant And Mammalian 4-Hydroxyphenylpyruvate Dioxygenases", Biochemistry, (2004), 43(32), 10414-10423.
18. Graupner, Paul R.; Carr, Andy; Clancy, Erin; Gilbert, Jeffrey; Bailey, Karen L.; Derby, Jo-Anne; Gerwick, B. Clifford. The Macrocidins: Novel Cyclic Tetramic Acids with Herbicidal Activity Produced by Phoma Macrostoma. Journal of Natural Products (2003), 66(12), 1558-1561.
19. Parker, Marshall H.; Ruiz, James M.; Schmitzer, Paul R. Outside the Matrix: The Combinatorial Exploitation of Acyl Tetramic Acids. Abstracts, 36th Central Regional Meeting of the American Chemical Society, Indianapolis, IN, United States, June 2-4 (2004).
20. Ono, Makoto; Sakuda, Shohei; Suzuki, Akinori; Isogai, Akira. Aflastatin a, A Novel Inhibitor of Aflatoxin Production by Aflatoxigenic Fungi. Journal of Antibiotics (1997), 50(2), 111-118.
21. Takahashi, Atsushi; Igarashi, Masayuki; Tamamura, Takeshi; Tezuka, Yasuyuki; Sato, Sei; Kutsuma, Seiichi; Arita, Kazuyoshi; Osanawa, Hiroshi; Takeuchi, Tomio. Preparation of Antibiotic PF 1052 Derivatives As Agricultural and Horticultural Fungicides. Jpn. Kokai Tokkyo Koho (1996), 11 pp., JP 08059612 A2 19960305.
22. Sasaki, Toru; Takagi, Masayuki; Yaguchi, Mayumi; Nishiyama, Kazuko; Yaguchi, Takashi; Koyama, Masao. Novel aAntibiotic PF1052 and Its Manufacture with Phoma Species. Jpn. Kokai Tokkyo Koho (1992), 6 pp.. JP 04316578 A2 19921106.
23. Weber, Lutz; Iaiza, Patrick; Biringer, Gerard; Barbier, Pierre. Solid-Phase Synthesis of 3-Acyltetramic Acids. Synlett (1998), (10), 1156-1158

24. Nefzi A; Giulianotti M A; Houghten R A   Solid-phase Synthesis of *bis*-heterocyclic Compounds from rResin-bound Orthogonally Protected Lysine. Journal of Combinatorial Chemistry (2001), 3(1), 68-70.

25. Sybyl Interface to FlexX, Receptor-Based Design Manual, Tripos, Inc. Version 6.81, May 2002. http://www.tripos.com.

26. http://www.accelrys.com

27. PPD, Inc., 3151 South 17th Street, Wilmington, NC 28412-6461, http://www.ppdi.com.

Chapter 10

Fungicidal Properties of Acivicin and Its Derivatives

**Hans-Georg Brunner, Phillippe Chemla, Marcus R. Dobler,
Anthony C. O'Sullivan[*], Paul Pachlatko, Christian Pillonel,
and Daniel Stierli**

Chemistry Research, Syngenta AG, 4002 Basel, Switzerland

Acivicin is a fermentation product with antitumour activity
isolated at Upjohn in 1973. The herbicidal activity was
claimed by Rohm and Haas in 1985. We found it has
interesting oomycete activity, and prepared analogs varying at
positions 3, 5, 2', NH_2 and COOH. Acivicin inhibits
glutaminases, so we tested known glutaminase-inhibitors, and
glutamine derivatives with cysteine protease pharmacophores,
some of which also showed interesting oomycete activity.

Acivicin **1** (AT-125, U-42126) was isolated by scientists at Upjohn in the
early 1970s on account of its anticancer activity (*1*). Upjohn workers also
described acivicin's activity against Candida (*2*). Later in 1996 Rohm and Haas
chemists claimed the herbicidal activity of acivicin (*3*).

In the Syngenta heritage company Ciba-Geigy the agricultural fungicidal
activity was found after a semi-random screen. While searching for the mode of
action of the herbicide hydantocidin **2**, it was found to inhibit purine
biosynthesis.

121

A number of purine biosynthesis inhibitors were therefore submitted for screening, of which acivicin showed a promising fungicidal activity (Table 1), with a broad spectrum and good control of oomycetes. It was later shown that hydantocidin **2** inhibits adenylosuccinate synthetase (*4*), which is a different mode of action to that of acivicin, which is a glutamine antimetabolite (Figure 4). Although the glasshouse results were promising, acivicin (as a racemate) was ineffective in two field trials at high dose rates. Against Phytophthora infestans (late blight) in potato with a dose of 500 g/Ha, 6% control was observed and with a dose of 750 g/Ha 32% control. Against Puccinia recondita (leaf rust) on wheat at 250 g/Ha 10% control and at 750 g/Ha, 18% control was observed. Despite the weak field results, the glasshouse results were so promising that a synthesis program was started.

Acivicin 1 (AT-125, U-42126)

Hydantocidin 2
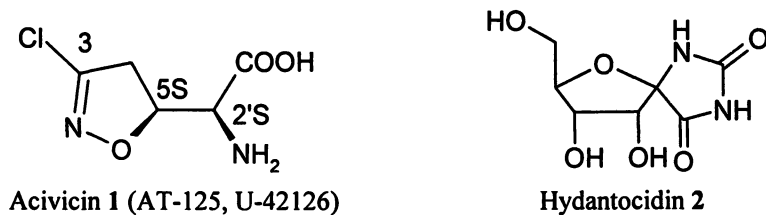
Table 1. Fungicidal Activity of Acivicin (Foliar Application).

Fungus	Host	Common Name	EC80 (ppm)
Phytophthora infestans	tomato	late blight	5[a]
Phytophthora infestans	potato	late blight	3[a]
Plasmopara viticola	grape	downy mildew	100
Erysiphe graminis	barley	powdery mildew	20[b]
Podosphaera leucotricha	apple	powdery mildew	>200
Uncinula necator	grape	powdery mildew	5
Helminthosporium teres	barley	net blotch	50
Septoria nodorum	wheat	glume blotch	50
Puccinia recondita	wheat	leaf rust	50
Botrytis cinerea	tomato	grey mold	>200
Botrytis cinerea	grape	grey mold	>200
Venturia inaequalis	apple	apple scab	20
Pyricularia oryzae	rice	rice blast	>200

a. >20 ppm on soil application
b. 20 ppm on soil application

Synthesis

Many synthetic approaches have been described to acivicin and its derivatives. The first route was reported by Upjohn chemists involving an N-C(3) ring closure (5). Other routes involving O-C(5) ring closures were later reported (6,7,8). Routes involving cycloaddition with halonitrile oxides (9,10,11) and nitrones (12,13) were reported. Furthermore several derivatives were prepared using nitrile oxide cyclisations (14,15,16,17,18,19).

To prepare field amounts and intermediates for a derivatisation program a route suitable for amounts of several hundred grams was needed. The Bristol-Myers procedure (11) was used (Figure 1), as it is direct and scalable. The erythro isomer resulting in naturally occurring acivicin was separated from its threo isomer at the stage of the alcohol 7 through crystallisation.
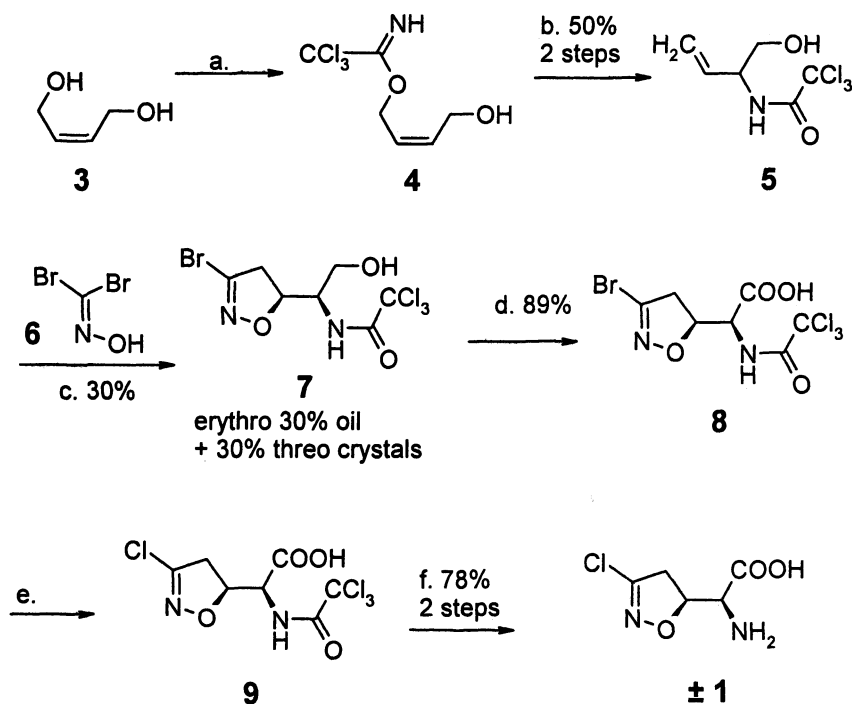
a. CCl₃CN, Na (cat.) –23° - 0°C, THF   b. t-BuPh 170 °C >50% (2 steps)   c. KHCO₃, H₂O RT d. Jones reagent e. HCl, MeOH   f. Ba(OH)₂, 78% (2 steps)

Figure 1. Bristol-Myers Synthesis of Racemic Acivicin 1.

Table 2 Fungicidal Activity of the Racemate, Threo and Homo Derivatives of Acivicin

fungus	common name	host	application	1 lead	1 racemic	10 erythro	11 threo	12 homo	13 homo
B. cinerea	grey mold	tomato	leaf	65	75	35	0	0	0
E. graminis	powdery mildew	barley	leaf	0	0	0	0	35	0
E. graminis	powdery mildew	barley	soil	95	0	0	0	0	35
P. infestans	late blight	tomato	leaf	95	100	97	97	85	0
P. infestans	late blight	tomato	soil	0	95	0	95	85	65
P. viticola	downy mildew	grape	leaf	97	100	0	95	0	0
P. recondita	leaf rust	wheat	leaf	65	65	0	0	0	0
P. recondita	leaf rust	wheat	soil	0	0	0	65	0	0
P. oryzae	rice blast	rice	leaf	65	35	32	35	0	0
S. nodorum	glume blotch	wheat	leaf	95	85	65	35	0	0
F. culmorum	root rot	tomato	soil	0	75	75	0	0	0
R. solani	foot rot	rice	soil	65	35	0	0	0	0

Values are % control after treatment with 200ppm (leaf) or 20 ppm (soil)

erythro
X = Cl 1
X = Br 10

threo 11

X = Cl 12
X = Br 13
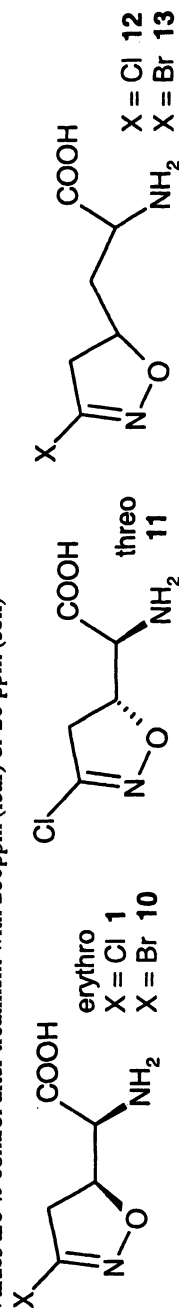
The bromo derivative **8** was deprotected to the bromo derivative **10** of acivicin and the threo derivative **7b** was converted as above to threo acivicin **11**. The homoacivicin analogs were prepared by cycloaddition to allyl glycine derivatives (*15*). The bromo analog **10** and the threo derivative **11** both showed fungicidal activity but less than that of acivicin **1** (Table 2).

C(3) Derivatives

Substitution of the bromide **14** gave Nu = imidazole **17** (75%), CN **18**, MeO **19** (63%). Thiolate gave a bromophilic attack and ring opening to the hydroxy-nitrile **16** 62%, but the chloride **15** gave the sulfide Nu = MeS **20** (68%). Oxidation of the sulfide with H_2O_2, AcOH led to the sulfoxide **21** in 86% yield and then to the sulfone **22** in 100% yield. Treatment of the chloride **15** with silver fluoride gave the fluoride **23**, which led to the trifluoroacetate **24** on deprotection. Another approach to 3-substituted acivicins was by cycloaddition of various nitrile oxides to the alkene **25** followed by oxidation and deprotection leading to X = PhCO **27**, EtOCO **28**, Me_2NCO **29** , $ClCH_2$ **30**, i-Pr **31**. Finally the trifluoromethyl derivative **32** was prepared via a nitrone cycloaddition. None of these compounds showed fungicidal activity in our screens.

C(5) and C(2') Derivatives

Protected vinyl glycine derivatives were prepared by Steglich's method (*20*) from vinyl Grignard reagents and *O*-t.butyl-*N*-Boc-bromoglycine. $CH_2=C(TMS)MgBr$, $PhCH=CHBr$, and $CH_2=C(TMSCH_2)MgBr$ did not yield vinylglycine derivatives. The cycloaddition reaction is sensitive to steric hindrance (Table 3). Substituents at the terminal position, which becomes *C(4)* are not tolerated. Unprotected vinyl glycines, prepared by Heinzer and Bellus (*21*) also react well, but again subsituents R2 and R3 hinder the cycloaddition. Compounds **33**, **34**, and **35**, prepared by this method were fungicidally inactive.

NH$_2$ and COOH Derivatives

A series of *N*-substituted derivatives (Table 4) were prepared by acylating racemic acivicin, and the derivatives at the carboxylic acid (Table 5) were prepared by EDC amination of Boc-acivicin. Many of them showed moderate fungicidal activity, which may be due to pro-cidal hydrolysis to the parent acivicin **1**.

As shown in the summary (Figure 3) we were able to make fungicidally active analogs. However no improvement in potency was observed, and the amide analogs may be active due to their pro-cidal behaviour. We therefore took a broader approach to the derivatising program.
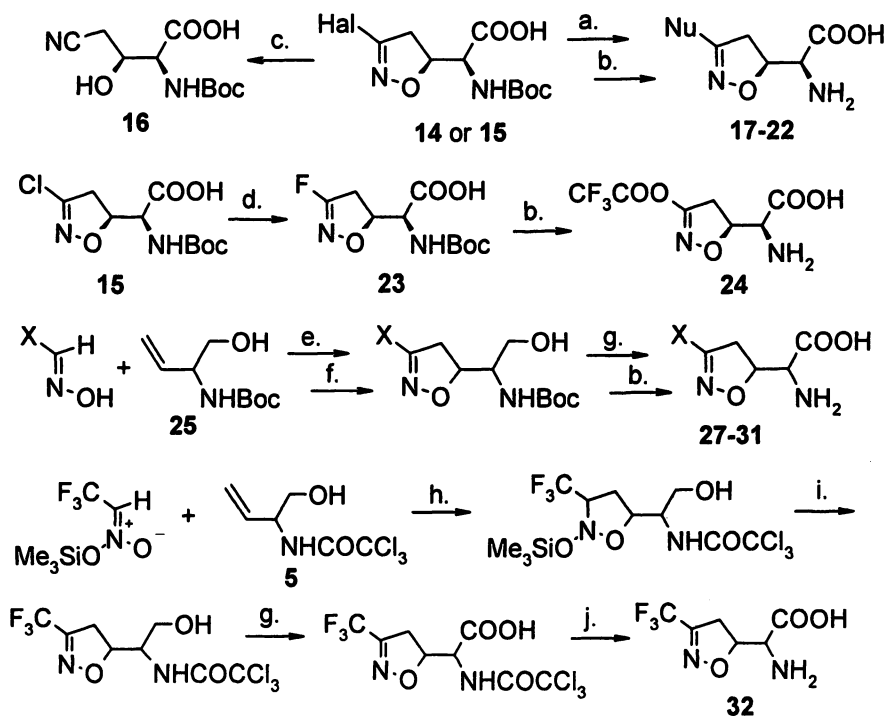
a. nucleophile (Nu), DMF or MeCN b. TFA c. NaSMe, DMF d. AgF, pyridine
e. NCS, DME, f. KHCO$_3$, DME, H$_2$O g. Jones h. Et$_2$O 23% i. TsOH, TFA,
100% j. Ba(OH)$_2$ 82%

Figure 2. Synthesis of 3-substituted Acivicin Derivatives.

Table 3. Cycloadditions Leading to C(5)-, and C(2')-substituted Acivicins
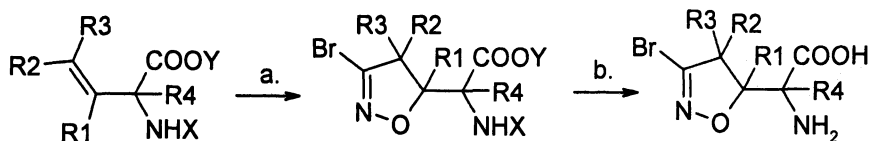
a. dibromoformaldehyde oxime, NaHCO$_3$, H$_2$O b. TFA

X	Y	R1	R2	R3	R4	yield (a)	yield (b)	Cpd
Boc	tBu	Me	Me	Me		0%		
Boc	tBu	H	Me	H		0%		
Boc	tBu	Et	H	H		59%	62%	33
H	H	Me	H	H	H	54%		34
H	H	Me	H	H	Me	26%		35
H	H	Me	Me	H	H	0%		

Cl	+++
Br	+
MeO	-
MeS	-
MeSO	-
EtOCO	-
PhCO	-
Me$_2$NCO	-
i-Pr	-
CF$_3$COO	-
NC	-
ClCH$_2$	-
F$_3$C	-

Me	-
Et	-

PhCH$_2$NH	+
n-PrNH	+
PhNH	-
H$_2$N	+

erythro	+++
threo	+

Cl$_3$CCO	+
t-BuOCO	+
Fmoc	+
BnOCO	+
i-PrOCO	+
TolSO$_2$	-
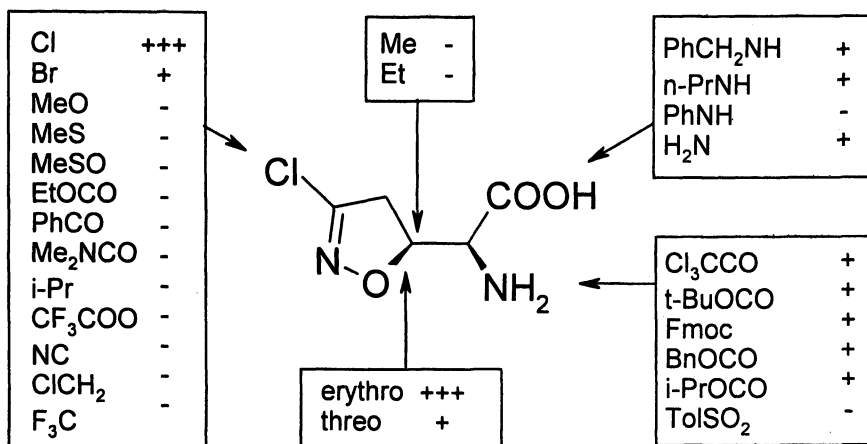
Figure 3. Summary of the Observed Structure Activity Relationships of Acivicin Derivatives. (+++ good activity, + weak activity, - inactive)

Table 4. Fungicidal Activity of Compounds Derivatised at the NH₂-Group

common name	host	appl.	H	Cl₃CCO erythro	Cl₃CCO threo	tBuOCO erythro	tBuOCO threo	Fmoc erythro	BnOCO erythro	iPrOCO erythro	TolSO₂ erythro
grey mold	tomato	leaf		0	0	65	95	75	0	0	0
powdery mildew	barley	leaf	65	0	0	0	0	0	0	0	0
powdery mildew	barley	soil	0	35	0	0	0	0	0	0	0
late blight	tomato	leaf	95	65	65	95	35	90	85	65	0
late blight	tomato	soil	0	95	95	95	0	0	75	75	0
downy mildew	grape	leaf	97.5	0	0	0	0	55	90	0	0
leaf rust	wheat	leaf	65	0	35	35	0	0	35	65	0
leaf rust	wheat	soil	0	0	35	0	0	0	0	0	0
rice blast	rice	leaf	65	0	0	0	75	85	85	0	0
glume blotch	wheat	leaf	95	85	65	65	35	65	65	35	0
root rot	tomato	soil	0	0	55	0	45	0	65	0	0
foot rot	rice	soil	65	55	65	0	0	0	0	0	0

Values are % control after treatment with 200ppm (leaf) or 20 ppm (soil)

Table 5. Fungicidal Activity of Derivatives (amides) at the COOH Group

fungus	common name	host	appl.	OH	PhCH₂NH-	nPrNH-	PhNH-	H₂N-
B. cinerea	grey mold	tomato	leaf		0	0	0	50
E. graminis	powdery mildew	barley	leaf	65	0	0	0	0
E. graminis	powdery mildew	barley	soil	0	0	0	0	0
P. infestans	late blight	tomato	leaf	95	65	75	65	90
P. infestans	late blight	tomato	soil	0	85	75	35	65
P. viticola	downy mildew	grape	leaf	98	0	0	0	50
P. recondita	leaf rust	wheat	leaf	65	35	35	0	0
P. recondita	leaf rust	wheat	soil	0	35	0	0	0
P. oryzae	rice blast	rice	leaf	65	0	65	0	0
S. nodorum	glume blotch	wheat	leaf	95	0	85	0	75
F. culmorum	root rot	tomato	soil	0	70	45	65	45
R. solani	foot rot	rice	soil	65	55	0	0	45

Values are % control after treatment with 200ppm (leaf) or 20 ppm (soil)

Mode of Action

Acivicin   X   Glutamine
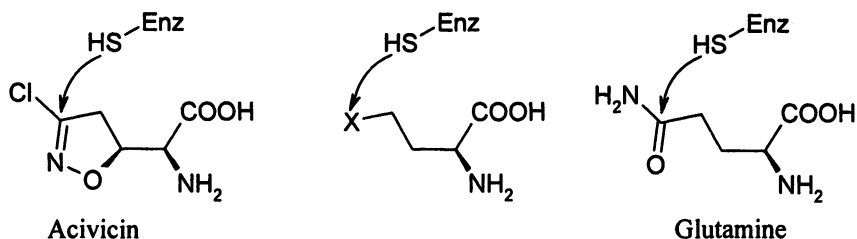
Figure 4. Schematic representation of Acivicin's mode of action as well as that of other amidotransferase inhibitors, where X is the pharmacophoric moiety of cysteine protease inhibitors.

Acivicin was found to act as a mimic and antimetabolite of glutamine and to inhibit many glutamine amidotransferases (*22*) (Figure 4). A crystal structure of acivicin covalently bound into the active site of one of these enzymes exists (*23*). These are important enzymes which cleave ammonia from glutamine and attach it to various substrates, and are thus responsible for introducing some or all of the nitrogen atoms into amino-acids, amino sugars, and nucleotides among others (*24,25*). Acivicin is also known to inhibit γ-glutamyl-transpeptidase (*26*) and glutaminase (*27*).

Several other inhibitors of amidotransferases are known (*24,25*), and several are also known to have fungicidal activity (*28*). They fit into the scheme shown above, where X is part of a cysteine protease inhibitor (*29*).

Some of these compounds were purchasable and we were pleased to see that DON and azaserine showed a similar activity to acivicin albeit somewhat weaker (Table 6). We then prepared a series of nitrogen or oxygen bridged compounds from serine or aminoalanine by conventional means, but the activity was very weak (Tables 7 and 8).

In summary, although we were successful in preparing fungicidally active analogs, we never reached the level of potency required for a commercial fungicide.

References

1. Upjohn US 3856808, 1973 and US 3878047, 1973.
2. Martin, D.G et al.*Tet. Lett.* **1973** (*27*) 2549-52.
3. Rohm and Haas EP 640286, 1996 and US 5489562, 1996.

Table 6. Fungicidal Activity of Amidotransferase Inhibitors

fungus	common name	host	appl.	acivicin	DON	azaserine	albizzin	cpd 4	cpd 5
B. cinerea	grey mold	tomato	leaf	65	100	0	0	0	0
E. graminis	powdery mildew	barley	leaf	0	65	75	0	0	0
E. graminis	powdery mildew	barley	soil	95	0	35	0	65	0
P. infestans	late blight	tomato	leaf	0	85	0	0	0	0
P. infestans	late blight	tomato	soil	98	65	32	65	65	0
P. viticola	downy mildew	grape	leaf	65	0	0	0	0	0
P. recondita	leaf rust	wheat	leaf	0	65	0	0	0	0
P. recondita	leaf rust	wheat	soil	65	0	0	0	0	0
P. oryzae	rice blast	rice	leaf	95	0	0	0	0	0
S. nodorum	glume blotch	wheat	leaf	0	0	75	75	0	0
F. culmorum	root rot	tomato	soil	65	0	75	0	0	0
R. solani	foot rot	rice	soil	0	0	0	0	0	0

Values are % control after treatment with 200ppm (leaf) or 20 ppm (soil)

DON
1

azaserine
2

albizzin
3

DNP-hydrazone
4

5
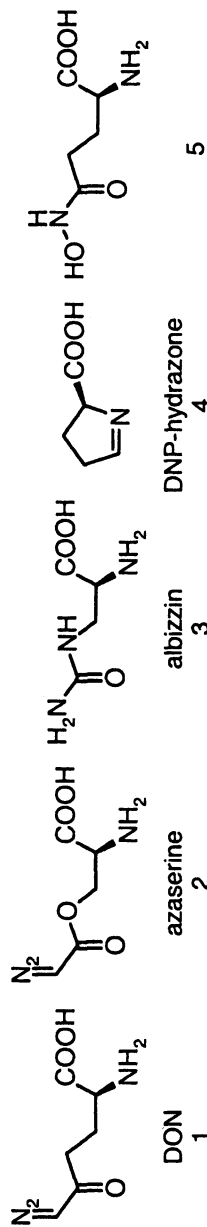
Table 7. Fungicidal Activity of Amidotransferase Inhibitors Derived from β-Amino-alanine.

fungus	common name	host	appl.	acivicin	ClCH₂	BrCH₂	Me₂SCH₂	epoxide
B. cinerea	grey mold	tomato	leaf		80	0	0	0
E. graminis	powdery mildew	barley	leaf	65	65	0	0	0
E. graminis	powdery mildew	barley	soil	0	0	0	0	0
P. infestans	late blight	tomato	leaf	95	65	0	0	0
P. infestans	late blight	tomato	soil	0	70	0	0	32
P. viticola	downy mildew	grape	leaf	97	0	0	0	0
P. recondita	leaf rust	wheat	leaf	65	0	0	0	65
P. recondita	leaf rust	wheat	soil	0	0	0	0	0
P. oryzae	rice blast	rice	leaf	65	65	0	35	0
S. nodorum	glume blotch	wheat	leaf	95	85	0	0	85
F. culmorum	root rot	tomato	soil	0	70	55	0	0
R. solani	foot rot	rice	soil	65	0	0	0	0

Values are % control after treatment with 200ppm (leaf) or 20 ppm (soil)
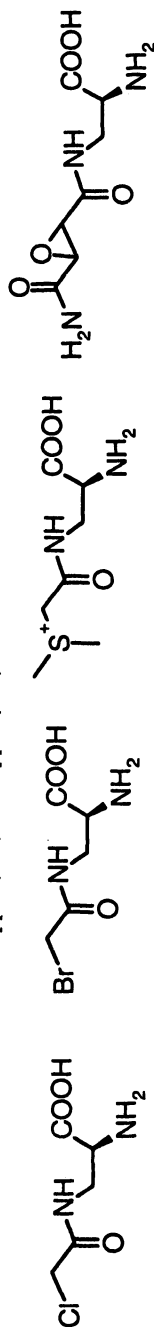
Table 8. Fungicidal Activity of Amidotransferase Inhibitors Derived from Serine.

fungus	common name	host	appl.	acivicin	Me_2SCH_2	$ClCH_2$	Y_1	Y_2	Y_3	Y_4
B. cinerea	grey mold	tomato	leaf		0	0	0	0	0	0
E. graminis	powdery mildew	barley	leaf	65	0	0	0	0	0	0
E. graminis	powdery mildew	barley	soil	0	0	0	0	0	0	0
P. infestans	late blight	tomato	leaf	95	0	0	0	0	0	0
P. infestans	late blight	tomato	soil	0	0	0	0	0	0	75
P. viticola	downy mildew	grape	leaf	97	0	0	0	0	0	0
P. recondita	leaf rust	wheat	leaf	65	0	0	0	0	0	0
P. recondita	leaf rust	wheat	soil	0	0	0	0	0	0	0
P. oryzae	rice blast	rice	leaf	65	0	0	0	0	0	0
S. nodorum	glume blotch	wheat	leaf	95	0	0	0	75	0	0
F. culmorum	root rot	tomato	soil	0	0	0	0	55	0	0
R. solani	foot rot	rice	soil	65	0	0	0	0	0	22

Values are % control after treatment with 200ppm (leaf) or 20 ppm (soil)

$Y_1 = MeO$

$Y_2 = H_2N$

$Y_3 = MeO$

$Y_4 = H_2N$

acivicin   DON   azaserine   chloroketone

albizzin

anticapsin   chlorotetaine
(R = alanyl)   A-19009   Sch 37137
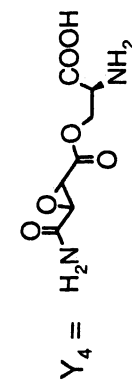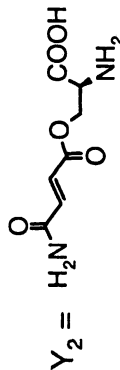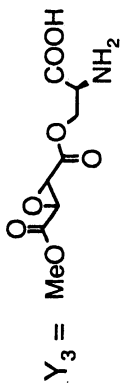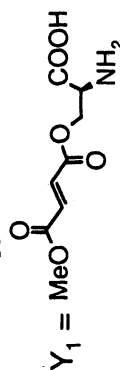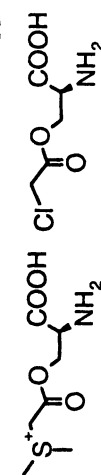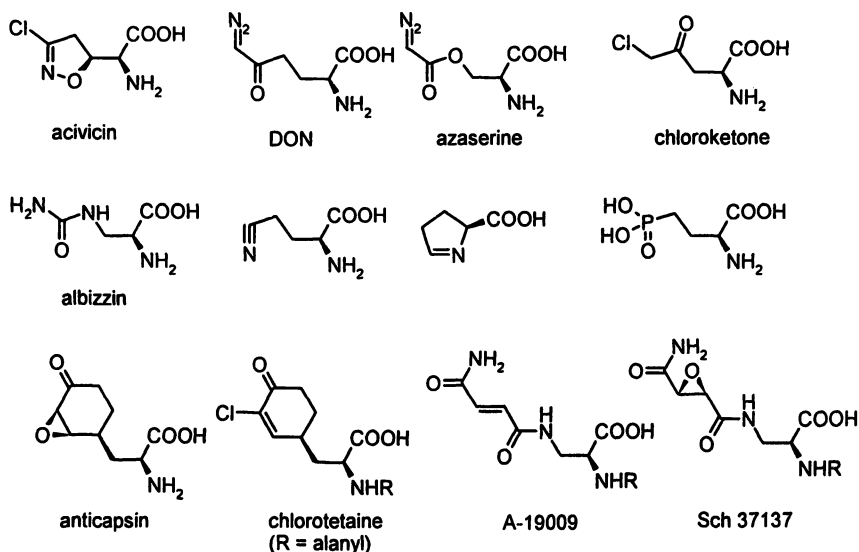
Figure 5. Known Glutamine Transaminase Inhibitors

4. Fonne-Pfister, R. et al. *PNAS* **1996**, *93*, 9431-6.
5. Kelly, R. C.; Schletter, I,; Stein. S. J.; Wierenga, W. *J. Am. Chem. Soc* **1979**, *101*, 1054-6 (BE-876-261, US 4275214 and US 4298744).
6. Silverman, R. B. Holladay, M. W. *J. Am. Chem. Soc.* **1981**, *103*, 7357-8.
7. Baldwin, J. E.; Cha, J. K.; Kruse, L. I. *Tetr.* **1985**, *41*, 5241-60.
8. Hanessian, S.; Vanasse, B. *Can. J. Chem.* **1987**, *65*, 195-9.
9. Hagedorn, A. A.; Miller, B. J.; Nagy, J. O. *Tet. Lett.* **1980**, *21*, 229-30.
10. Wade, P. A.; Pillay, M. K.; Singh, S. M. *Tet. Lett.* **1982**, *23*, 4563-6.
11. Vyas, D. M.; Chiang, Y.; Doyle, T. W. *Tet. Lett.* **1984**, *25*, 487-90. (US 4692538)
12. Mzengeza, S.; Yang, C. M.; Whitney, R. A. *J. Am. Chem. Soc.* **1987**, *109*, 276-7.
13. Mzengeza, S.; Whitney, R. A. *J. Org. Chem.* **1988**, *53*, 4074-81.
14. Gombos, Z.; Nyitrai, J; Kolonits, P.; Kajtar-Peredny M. *Perkin 1*, **1989**, 1915-21.
15. Nam, G. S.; Lee, Y. Y.; Goo, Y. M. *J. Korean, Chem. Soc.* **1991**, *35*, 262-7.
16. Rohloff, J. C. Robinson, J.; Gardner, J. O. *Tet. Lett.* **1992**, *33*, 3113-6.
17. Keum, G.; Chung, Y. J.; Kim, B. H. *Bull. Korean. Chem. Soc.* **1992**, *13*, 343-4.
18. Griesbach, A. G.; Hirt, J.; Peters, K.; Peters, E-M.; von Schnering, H-G. *Liebigs Ann.* **1995**, 619-25.

19. Conti. P.; Roda, G.; Stabile, H.; Vanoni, M. A.; Curti, B.; De Amici, M. *Il Farmaco*, **2003**, *58*, 683-90.
20. Münster, P.; Steglich, W. *Synthesis* **1987**, 223-5.
21. Heinzer, F.; Bellus, D. *Helv. Chim. Acta* **1981**, *64*, 2279-97
22. Jayaram, H. N.; Cooney, D. A.; Ryan, J. A.; Neil, G.; Dion, R. L.; Bono, V. H. *Cancer. Chemother. Rep.* **1975**, *59*, 481-91.
23. Chaudhuri, B.; Lange, S. C.; Myers, R. S.; Davisson, V. J.; Smith, J. L. *Biochemistry*, **2003**, *42*, 7003-12.
24. Massière, F.; Badet-Denisot, M.-A. *Cell. Mol. Life. Sci.* **1998**, *54*, 205-222.
25. Zalkin, H.; Smith, J.L. *Adv. Enzymol.* **1998**, *72*, 87-144.
26. Taniguchi, N.; Ikeda, Y. *Adv. Enzymol. Relat. Areas Mol. Biol.* **1998**, *72*, 239-78.
27. Purich, D. L. *Adv. Enzymol.* **1998**, *72*, 9-43
28. Andruszkiewicz, R.; Chmara, H.; Zieniewa, T.; Borowski, E. *Eur. J. Med. Chem.* **1994**, *29*, 61-7.
29. Otto, H-H.; Schirmeister, T. *Chem. Rev.* **1997**, *97*, 133-171.

Chapter 11

Factors Involved in the Field Translation of a Class of Mitochondrial Q_i Inhibitor Fungicides

W. J. Owen, Y. Adelfinskaya, Z. Benko, and C. T. Schobert

Dow AgroSciences LLC, 9330 Zionsville Road, Indianapolis, IN 46268

Translation of fungicidal efficacy from laboratory to field can be quite complex, being influenced by factors such as potency, spectrum, stability, formulation, application frequency and physical properties and their impact on rainfastness and redistribution in host plants or crop canopies. A number of these factors will be illustrated with examples from within a series of Oomycete-active fungicides, the N-formylaminosalicylamides, that are potent inhibitors of mitochondrial electron transport. This class of chemistry inhibits respiration at the Q_i site, orientated towards the inner surface of the inner mitochondrial membrane. Both laboratory and field trial data indicated inconsistent foliar uptake and plant distribution as a significant translation barrier for this chemistry, supported by the necessary use of penetrating adjuvants to deliver curative efficacy *vs. Plasmopara*. Data generated on the physical properties and membrane permeation of individual analogs suggest a clear basis for their poor redistribution in grape-vines. Further studies pointed to xylem unloading rather than bioavailability of 'in tissue' active ingredient as a key obstacle for delivery of robust disease control with this chemistry.

137

Introduction

While naturally-occurring microorganisms have proven a rich source of novel structures for Ag Discovery, it is rare for one to be commercialized without subsequent synthetic modification. One recent example is Dow AgroSciences's Spinosad, produced from a soil actinomycete fermentation broth, which has potent insecticidal activity *vs.* chewing insects in particular (*1,2*). The reasons for this are no doubt complex and include: single mode of delivery by foliar application; significant residuality challenges such as UV stability & rainfastness in addition to metabolic susceptibilities; multiple host and target disease combinations and their impact on required physical properties and compound placement. However, there have been several excellent success stories in which an initial natural product active has been successfully exploited as a scaffold for synthetic modification aimed at correcting attribute limitations while simultaneously retaining or enhancing target potency. Notable examples include the pyrethroid insecticides (*3,4*) and strobilurin fungicides (*5,6*). In each case synthetic approaches successfully addressed significant limitations in the natural product starting points, and delivered a plethora of products for a number of agrochemical companies.

The strobilurin fungicides, exemplified by kresoxim-Me, azoxystrobin, trifloxystrobin, picoxystrobin and pyraclostrobin, were determined to be potent inhibitors of mitochondrial electron transport at the Q_o site of ubiquinone binding in Complex III (cytochrome bc_1 complex), clearly establishing this as a highly commercially validated target site (*6-8*). On the other hand, a second ubiquinone binding site (Q_i) located on the inner surface of the cytochrome bc_1 complex, facing the mitochondrial matrix, has remained commercially unexploited as a fungicide target until very recently with the development of cyazofamid, active against Oomycete fungi (*9*). While cyazofamid is the only commercial product whose activity results from Q_i-site binding, the antibiotic Antimycin A (Figure 1), which has long been recognized as a potent inhibitor of mitochondrial Complex III, is now known to involve Q_i binding and has been a valuable experimental tool in mitochondrial research (*10*). Antimycin A's are produced as fermentation products by various Streptomyces species, and form a series that differ primarily in the structure of the alkyl chain linked to the bis-lactone ring system. Antimycins A_1 and A_3 were first identified in the mid 1950's, but novel variants continue to be discovered, the most recent being Antimycin A_{17} (*11*) Antimycins A_1 and A_3 have been used experimentally as fungicides with activity against *Pyricularia oryzae, P. grisea* and *Penicillium* spp. in particular, while Antimycin A_{17} is claimed to have significant activity against 11 fungal species, including *Curvularia lunata, Rhizopus nigricans* and *Colletotrichum nigrum.*

Despite their demonstrated abilities to inhibit growth of a number of fungi, none of the Antimycins have been commercialized as fungicides, presumably because they are deficient in one or more of the necessary key attributes. These might include shortcomings in residuality, limited spectrum, lack of curative efficacy or poor redistribution within the host plant or crop canopy. However, earlier uncertainties regarding the commercial utility of the Q_i target site have now been largely addressed by the introduction of cyazofamid (*12*).

It was against this background that Dow AgroSciences initiated an effort around the synthetic exploitation of the Antimycin A scaffold, aimed at addressing an optimum balance between desirable attributes and fungicidal potency and spectrum for this chemistry and MOA.

Synthesis

Opportunities for making structural modifications to Antimycin A isolated from fermentation broths is rather limited. Replacement of the ester external to the bislactone ring with either another ester or with ether substitutions offers the most obvious opportunity. However, the presence of three ester functionalities (two in the bislactone plus the exocyclic ester) in the Antimycins was considered to pose a potential issue limiting residuality, given the known propensity for plants to hydrolyze esters. Furthermore, the various modifications to substituents on the bislactone ring within the naturally-occurring Antimycin A's have not incorporated the right mix of attributes to support commercialization, though they have seemingly impacted selectivity and spectrum. These inputs, together with a desire to simplify the bislactone structure, led to the decision to shape a synthetic strategy around holding the *N*-formylaminosalicylamide (FSA) "head' portion of the molecule constant while replacing the bislactone ring and its attachments (the 'tail') with more synthetically accessible alternatives (*13-16*).

In all, some 750 analogs were prepared based on aromatic, aliphatic (both cyclic and non-cyclic), hetero, bicyclic and tricyclic ring systems, some of the more significant milestones en route to the optimized 3-methylethyl, 5-gem dimethylcyclohexyl tail (**V**) being depicted in Figure 1. Initially, interesting levels of efficacy seen for the norbornane derivative (**I**) were later surpassed in the cyclohexyl series exemplified by (**II**) and (**III**), as well as (**V**), which gave the best activity overall. Attempts to improve in planta redistribution led to the synthesis of targets with heterocyclic ring systems such as the tetrahydropyran (**IV**), but although enhanced systemicity was achieved this was not at a level sufficient to compensate for reduced intrinsic potency relative to their cyclohexyl counterparts.

R = -(CH$_2$)$_5$CH$_3$: Antimycin A$_1$
R = -(CH$_2$)$_3$CH$_3$: Antimycin A$_3$

chemistry optimization

I

II

III

IV

V

optimized structure
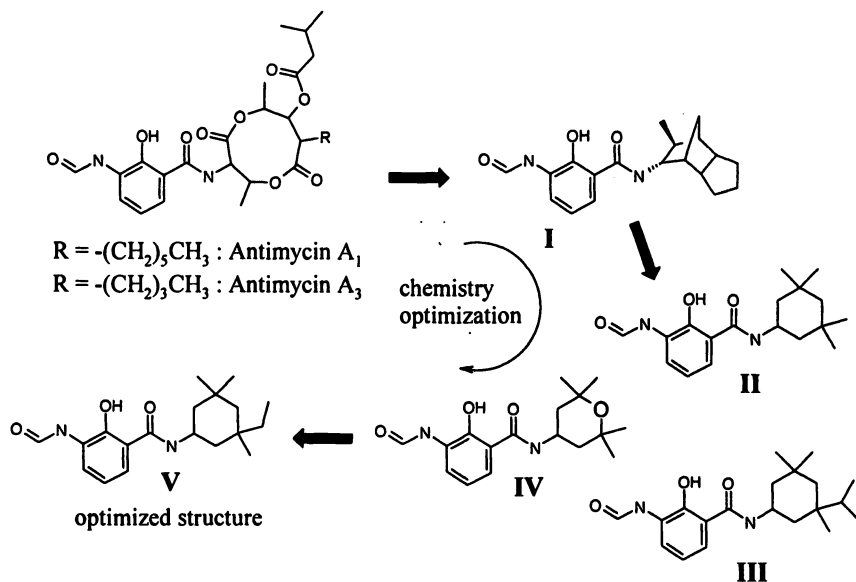
Figure 1. Synthetic Milestones in the Optimization of N-formylaminosalicylamide analogs

Mode of Action

Synthetic analogs were evaluated for potency as mitochondrial electron transport inhibitors in a 96-well plate assay, based on oxidation of NADH by mitochondrial fragments and the associated reduction in absorbance at 340 nm. Table I shows that, based on I$_{50}$ values, **V** is a potent mitochondrial inhibitor across a broad spectrum of fungal pathogens, including the important cereal

Table I. Inhibition (I50's) of Mitochondrial Electron Transport in Pathogenic Fungi by *N*-formylsalicylamide (FSA) V

Species	MET Activity (I$_{50}$ in µg/mL)	
	FSA **V**	Azoxystrobin
BOTRCI	0.002	
LEPTNO	0.0005	0.003
SEPTTR	0.001	
PLASVI	0.00009	0.0015
PHYTIN	0.0071	0.0002

diseases *Leptosphaeria nodorum* (LEPTNO) and *Septoria tritici* (SEPTTR), grey mold of grapes and vegetables, *Botrytis cineraria* (BOTRCI) and the Oomycetes *Phytophthora infestans* (PHYTIN) and *Plasmopara viticola* (PLASVI). Potency overall is comparable to that of the Q_o site inhibitor azoxystrobin, though **V** stands out as being particularly potent *vs.* the mitochondrial electron transport system of *P. viticola*. Relative to Antimycin A_1, *N*-formylsalicylamide **V** either showed improvements in inhibitory potency or was of comparable activity, depending on pathogen. Although differences in sensitivity exist, these results indicated that **V** had sufficient intrinsic potency across the five pathogens tested to support good broad-spectrum activity at both the whole organism and greenhouse levels of testing, provided that efficacy translation was not impeded by other factors, such as rapid metabolism or physical property limitations. Binding of the *N*-formylsalicylamides at the Q_i site was inferred from their demonstrated cross-resistance to an yeast (*Saccharomyces cerevisiae*) strain resistant to Antimycin A, but not to a strobilurin-resistant isolate (unpublished results, D.Young, Dow AgroSciences LLC, Indianapolis, IN).

Biological Activity

Biological efficacy of synthesized analogs was initially evaluated against a small number of key target pathogens, both *in vitro* (96-well plate assays) and in the greenhouse. *In vitro* growth inhibition was assessed as the minimum concentration (μg/mL) required to inhibit fungal growth by 70% relative to untreated controls, typical values for analog **V** lying in the range of 0.1-0.93, 0.31-2.8, 0.93-2.8 and < 0.1 *vs. S. tritici, L. nodorum, P. Oryzae* and *P. infestans,* respectively. Although the *N*-formylsalicylamide showed good broad spectrum activity, the substantially greater growth inhibition potency (at least 10X) *vs.* the Oomycete pathogen *P. infestans* would not have been predicted based on the respective target site sensitivities (Table I). This clearly indicates a significant cell-free to whole organism efficacy translation barrier in the case of the three ascomycete fungi. The reason for this is unclear, but either the *N*-formylsalicylamides are unable to accumulate at the Q_i binding site of the ascomycete fungi in quantities sufficient to elicit fungitoxicity, or the consequences of Q_i site binding are more detrimental to Oomycetes.

Corresponding greenhouse data for **V** is shown in Table II, the host plants being tomato for *P. infestans*, grape seedlings for *P. viticola*, and wheat for *Puccinia recondita, S. tritici* and *L. nodorum*. In the 1 day protectant protocol (1 DP, Table II), host plants received spray applications of *N*-formylsalicylamide at various rates 24 hours prior to inoculation with spores of the respective pathogens. In contrast, in a 1 day curative test (1 DC), plants were treated

Table II. Greenhouse Efficacy Translation – FSA V

1 DP Efficacy	Rate (ppm)	% Disease Control
PHYTIN	6.25	25-100
PLASVI	1.56	37-100
PLASVI TL	100	85-100
PUCCRT	25	87
SEPTTR	100	89
LEPTNO	100	90-100
1 DC Efficacy		
Curative efficacy is poor *vs*. PHYTIN and *vs*. PLASVI is dependent on a penetrating adjuvant e.g. Crop Oil		
PLASVI	100	~20 (-CO); 90 (+CO)

with the experimental fungicides 24 hours after spore inoculation. The 1 day protectant greenhouse data reflect very well the efficacy differential between oomycete and ascomycete pathogens observed in growth inhibition testing, with disease control levels of 100 % frequently being observed for *P. viticola* and *P. infestans* at application rates of 6.25 ppm. *P. viticola* was consistently the most sensitive pathogen, disease free plants being achieved by 1.56 ppm treatments in some tests, whereas for *S. tritici, L. nodorum* and the basidiomycete pathogen *P. recondita* (wheat leaf rust), compound **V** seldom achieved 100 % disease control even at 100 ppm in the spray application. From a curative standpoint, efficacy of **V** vs. *P. infestans* was very poor, whereas in the case of *P. viticola* curativity was substantially dependent on application in conjunction with a strongly penetrating adjuvant such as Crop Oil Concentrate. In view of the demonstrated potency of **V** at the level of the mitochondrial target site of both pathogens, these data were indicative of foliar penetration issues for this chemistry. Attempts to broaden the potency spectrum to achieve greenhouse levels of control *vs*. ascomycete and basidiomycete fungi comparable to commercial standards met with limited success. Therefore, further greenhouse characterization and field evaluation of the most efficacious chemistries was only warranted for the Oomycete diseases.

Field evaluation of **V** in multiple potato and grape-vine trials yielded data that was generally consistent with relative performance against the driver Oomycete pathogens in the greenhouse, and is represented in Table III for two trials. The data for *vs*. *P. infestans* represent disease control assessments averaged over 39-47 days after first application of the fungicide treatments, when the level of disease in untreated controls was determined to be 85%. Compared to two commercial Oomycete fungicides applied at their label rates, **V** failed to deliver acceptable levels of disease control even at the 250 g a.i./H rate.

Table III. Field Efficacy of FSA V in Grape-Vines and Potatoes

Pathogen	Treatment	Rate (g a.i./Ha)	% Disease Control	
PHYTIN	FSA V	125	49	
		250	66	
	Standard 1	Label	93	
	Standard 2	Label	86	
		(g a.i./HL)	Foliage	Bunches
PLASVI	FSA V	10	62	76
		20	72	91
	Standard 1	Label	82	79
	Standard 2	Label	78	94

Although performance was better in some trials where the prevailing disease pressure was lower, the compound did not display the necessary robustness under conditions of severe disease infestation frequently encountered with *P. infestans*. By contrast, in grapes, performance *vs. P. viticola*, at the 20 g a.i./HL rate, was closer to grower expectations, especially on bunches. The data in Table III depict assessments averaged over 50-70 days after the first fungicide treatment, when disease levels were 60% and 35% for foliage and bunches, respectively. While the level of bunch disease control was consistently encouraging over a number of trials, performance on leaves appeared less consistent, particularly in regard to disease control on foliage emerging subsequent to fungicide treatment. A basis for this and other translational issues limiting performance of the *N*-formylaminosalicylamide chemistry was sought via a number of approaches for understanding activity delivery.

Efficacy Translation

Potential barriers to biological efficacy translation from mitochondrial cell-free assays to whole organism and greenhouse testing scenarios include compound stability (metabolic, photostability) and physical properties as they impact compound delivery, leaf coverage, foliar/membrane penetration and interactions and *in planta* redistribution. Some of these parameters were investigated for the *N*-formylsalicylamides to assist in the interpretation of biological data and help formulate hypotheses for addressing spectrum and performance optimization within the series.

144

Stability

Metabolism

The compound most well characterized for metabolic stability was *N*-formylsalicylamide **II** (Figure 1), differing from **V** by possessing a second *gem*-dimethyl in place of the ethyl-methyl substitution at C_3 of the cyclohexyl ring. In studies involving extraction (80% aqueous acetonitrile) and analysis of radioactivity 72 hr after stem injection of seedlings with [carboxamide-^{14}C]-labeled compound **II**, the fraction representing metabolites was determined to be 26 %, 21 % and 52 %, respectively, for wheat, grapevine and tomato. Although metabolites were not characterized further, their more extensive formation in tomatoes likely contributes to the weaker greenhouse performance of *N*-formylsalicylamides *vs.* the Oomycete pathogen *P. infestans* compared to *P. viticola*. Of perhaps even greater significance, however, were the very low percentages of injected radioactivity recovered in the organic extracts, amounting to only 36 %, 35 % and 17 % for wheat, grapevine and tomato at the 72 hr time point. The remaining material was determined by sample oxidation and scintillation counting to be associated with the non-extractable residues. On the assumption that the *N*-formylsalicylamide-derived material rendered non-extractible by unknown sequestration mechanisms (that could include covalent linkage) may be of very limited bioavailability to pathogenic fungi colonizing leaf tissues, this rapid immobilization likely contributes to poor curative efficacy, residuality and systemicity within the series as a whole. Studies with radiolabeled **V** in grape seedlings found similar levels of sequestration but little evidence of extractable metabolite formation even seven days after injection of the radiolabel.

Photolysis

The potential for various *N*-formylsalicylamides to degrade in sunlight, as spray droplets deposited on leaf surfaces dry, was assessed by exposing aqueous solutions to simulated sunlight conditions and analyzing samples by HPLC at various time intervals. Percentage photolytic breakdown varied among analogs, ranging from 6-62 % after continuous 4 hr exposure to simulated sunlight, with the most efficacious analog **V** degrading 36 %. Under identical conditions, the commercial fungicides azoxystrobin and iprovalicarb degraded 3 % and 13 %, respectively. These data suggested that UV stability had the potential to negatively impact field performance of **V**, depending on the prevailing conditions during and immediately following application, coupled with rate and extent of cuticular penetration.

Downloaded by CORNELL UNIV on June 16, 2012 | http://pubs.acs.org
Publication Date: February 1, 2007 | doi: 10.1021/bk-2007-0948.ch011

These laboratory observations were subsequently verified by data generated (Table IV) using cucumber plants treated with analogs **II** and **V** and exposed continuously for 24 hr to simulated sunlight (a bank of 115 W fluorescent lamps delivering a balance of wavelengths in the visible spectrum, supplemented with UV emissions consisting predominantly of UV-A, peaking at 355 nm) prior to

Table IV. Effect of UV Exposure on Efficacy *vs.* Cucumber Downy Mildew

FSA Analog (25 ppm)	% Disease Control		% Loss
	No UV	24 hr UV	
II	65	40	38%
V	53	7	87%
Dimethomorph (6 ppm)	87	78	9%

inoculating with downey mildew. Comparison of disease expression on plants treated identically apart from UV supplementation revealed substantial efficacy losses for both compounds, particularly for **V** (87 % loss). Identical UV exposure impacted performance of the Oomycete product dimethomorph by only 9 %.

Physical Properties

Log K_{ow}, pK_a and water solubility (ppm) values were routinely determined for newly synthesized analogs using micro-electrokinetic chromatography (MEEKC), capillary zone electrophoresis (CZE) and HPLC analytical methodologies, respectively, as described previously (*17,18*). Log K_{ow} and water solubility values for the series as a whole generally fell within the ranges of 4.0 – 4.5 (**V** – 4.36) and <1 – 10 (**V** – 3 ppm), respectively. While these log K_{ow} values were on the high end of the range of values for commercialized fungicides, this was not considered to be a key limitation for efficacy translation. This is supported by the fact that successful broad-spectrum fungicide products such as trifloxystrobin and pyraclostrobin have published logK_{ow} values in this range (*19*). On the other hand the measured pK_a's for the salicyl – OH pointed to a potential issue, in that they generally fell within the range pK_a 6.0 – 6.5. This meant that under many physiological conditions, including leaf surfaces, this acidic–OH would be largely deprotonated thus imparting a negative charge to the *N*-formylsalicyamides that may negatively impact foliar penetration. Derivatization of acidic herbicides, such as the auxinics, to various esters has historically been used as a means of achieving the desired cuticular and foliar uptake by avoiding delivery of the charged active ingredient to the leaf surface.

In addition to its likely impact on cuticular penetration, the salicyl-O⁻ species may also impede passive membrane permeation. This particular aspect was investigated using pION's PAMPA technology for assessing permeation through an artificial membrane (*20*). At pH 7.5, the permeation rate for **V** was determined to be $9 \cdot 10^{-6}$ cm/s, compared to $35 \cdot 10^{-6}$ and $34 \cdot 10^{-6}$ cm/s respectively for azoxystrobin and the Oomycete-specific dimethomorph, suggesting that physical properties indeed may limit the accumulation of sufficient *N*-formylsalicylamide to the inner surface of the inner mitochondrial membrane, at least in the less sensitive fungi, to deliver the desired fungicidal effect.

In Planta Redistribution

Uptake and redistribution of carboxamide ^{14}C-labeled *N*-formylsalicyl-amides **II**, **III** and **IV** was studied 24 hr after both hydroponic and stem injection application to vine seedlings (Figure 2). In the case of hydroponic treatment with compound **III** (measured $\log K_{ow}$ 4.3), the resulting phosphorimages indicate that the only detectable radioactivity was associated with the treated root system, with little or no evidence of xylem movement into foliage. This contrasts with hydroponic application of dimethomorph (published $\log K_{ow}$ 2.63) which resulted in the foliar translocation of significant amounts of radioactivity. Lowering $\log K_{ow}$ of the *N*-formylsalicylamides by one unit, as in the less efficacious tetrahydropyran analog **IV**, improved uptake and xylem distribution into foliage though vascular unloading appeared impeded relative to dimethomorph (Figure 2). Inefficient xylem unloading is also clearly evident following application of compound **II** by stem injection, the resulting phosphorimage (Figure 2) visualizing the majority of the radiolabel as being associated with the vasculature.

The impact of this limited vascular unloading on biological performance is effectively illustrated in Figure 3, which compares the redistribution of radiolabel and *P. viticola* disease control of **V** after petiole injection with that of an experimental strobilurin with more desirable attributes. In the case of the strobilurin the vasculature appears white indicating that the majority of the injected radiolabel has unloaded into the leaf tissue to deliver complete disease control. In contrast, the majority of the radiolabeled **V** remains associated with the leaf vasculature with the result that the downy mildew was essentially uncontrolled in the inter-veinal regions of the leaf.

The likely impact of the acidic salicylic OH on uptake and *in planta* re-distribution of *N*-formylsalicylamides was explored in comparative phytokinetic studies using **II** and its neutral des-OH (**VII**) and methoxy (**VI**) analogs, all of which were radiolabeled in the amide carbonyl. Reference to Figure 4, which shows redistribution patterns 24 hrs after radiolabel treatments, indicates that methylation of the salicylic-OH resulted in much improved xylem movement and
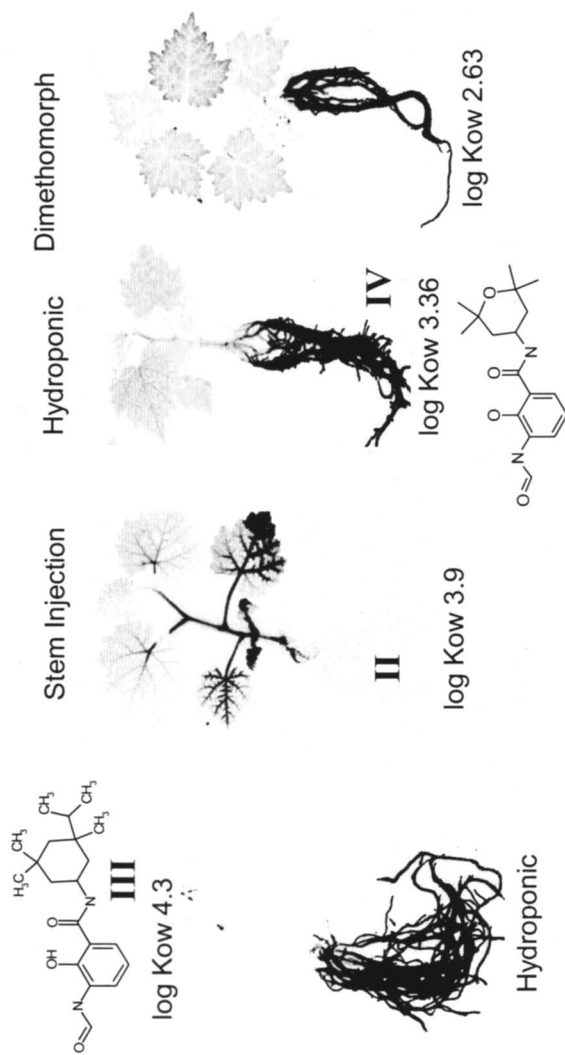
Figure 2.   In Planta Redistribution of N-formylsalicylamides
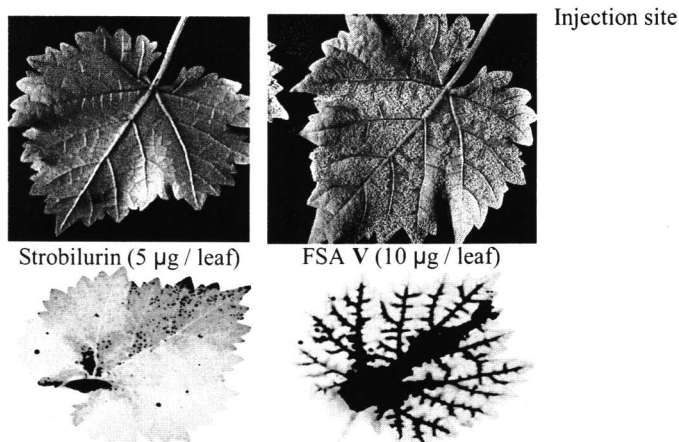
Figure 3. *Distribution and Efficacy of V after Petiole Injection*
(See page 3 in color insert.)

vascular unloading following topical application of radiolabeled compound to the stems of vine seedlings. Measured log K_{ow} values for protonated **II** and **VI** were found to be almost identical (3.9 and 3.8, respectively) clearly attributing the poor redistribution properties of the former to its ionizability at physiogiocal pH values. Similarly, acropetal movement of the corresponding des-OH compound, **VII**, following droplet application to the mid-section of the leaves of wheat seedlings was very comparable to that of the commercial fungicide azoxystrobin. Although these studies with **VI** and **VII** served to confirm the negative impact of the salicyl-OH on the performance of this series of chemistry, their improved attributes could not adequately compensate for the reduction in intrinsic activity associated with these chemical modifications.

Despite the redistribution issues that these radiolabel studies served to identify as a significant performance limitation, **V** and closely related *N*-formylsalicylamides generally performed very well *vs. P. viticola* in vineyard trials (see Table III). However, there appeared to be inconsistent robustness of disease control assessed on foliage that emerged subsequent to fungicide treatment. The data presented in Figures 2–4 would imply that the *N*-formylsalicylamide chemistry would be unlikely to deliver adequate 'new-growth' disease protection under vineyard conditions, at least if vascular transport were the only vehicle for re-distribution.
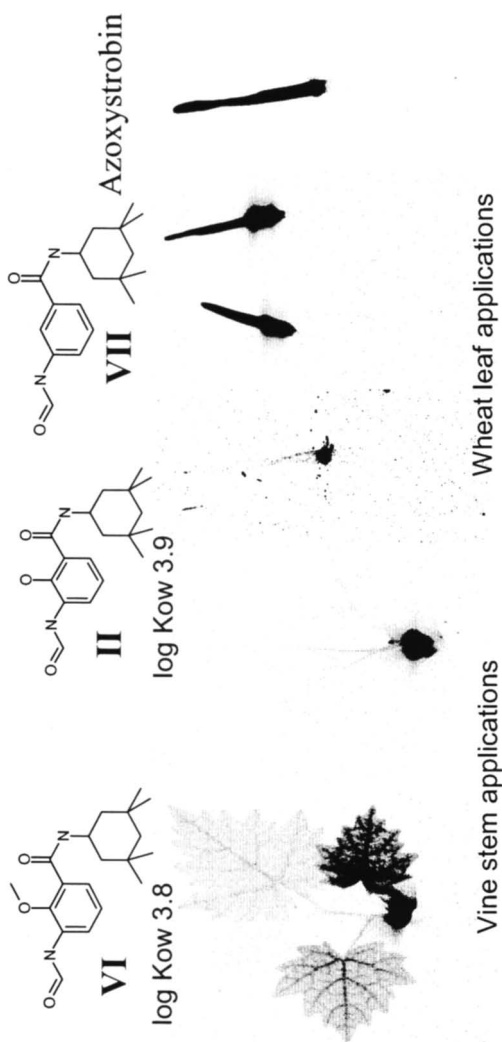
Figure 4. Impact of FSA-OH on in planta Redistribution

The fact that data reported from vineyard trials were very variable in this regard prompted a study involving spray application of a radiolabeled SC formulation of V to vine seedlings, the results of which are captured in Figure 5. Plants were sprayed with either the apical meristems exposed (Figure 5(a)) or shielded from the incident spray by wrapping in aluminum foil (Figure 5(b)). In each case, the plants are displayed on the left and their corresponding phosphorimages to their right, the arrows indicating the first leaves to emerge from the apical meristems subsequent to fungicide application. The two darkest leaves in each phosphorimage represent the youngest unfolded leaves immediately below the meristem region at the time of application. The leaf above these developed several days later and clearly has radioactivity distributed throughout, albeit at a relatively low level, when the meristem received fungicide. However, when the apical meristem was covered (Figure 5b), no radioactivity was evident in the next leaf to emerge. Based on the earlier phyokinetic studies, this latter result was not unexpected.

The extreme potency of N-formylsalicylamides as P. viticola mitochondrial Q_i-site inhibitors suggests that the amount of material associated with at least the initial leaf to unfold from treated meristems is sufficient for disease control. The variable performance vs. newly emerged foliage across trials may be a reflection of the thoroughness of targeting of the apical tissues at time of application.

Conclusion

The N-formylaminosalicylamides clearly illustrate that properties such as stability and redistribution contribute substantially to successful field translation and impact the potential commercial value that can be extracted from highly potent fungicidal chemistries. Development of a clear understanding of properties responsible for limiting field performance is critical to the success of future project efforts, as they potentially benefit from leveraging this knowledge earlier in the discovery process.

References

1. Crouse, G.D.; Sparks, T.C.; Schoonover, J.; Gifford, J.; Dripps, J.; Bruse, T.; Larson, L.L.; Garlich, J.; Hatton, C.; Hill, R.L.; Worden, T.V.; Martynow, J.G. Pest. Management Sci. 2001, 57, 177-85.
2. Sparks, T.C.; Crouse, G.D.; Durst, G. Pest Management Sci. 2001, 57, 896-905.
3. Casida, J.E. Current Themes in Tropical Sci. 1983, 2, 109-25.
4. Elliott, M. Critical Reports on Applied Chemistry 1996, 35, 254-300.

(a) Apical Meristem Uncovered
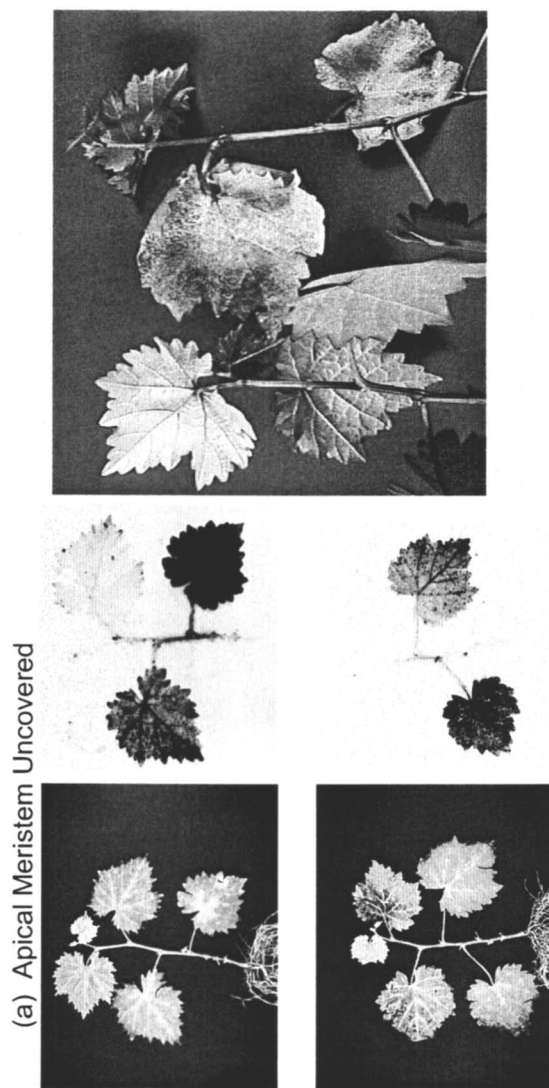
Figure 5. Importance of Delivery to Apical Meristems for Control of P. viticola by V in newly emerged Vine shoots (See page 3 in color insert.)

5. Sauter, H.; Steglich, W.; Anke, T. *Angewandte Chemie,* Int. Ed. **1999**, *38,* 1329-49.
6. Bartlett, D.W.; Cluffe, J.M.; Godwin, J.R.; Hall, A.A.; Hamer, M.; Parr-Dobrzanski, R. *Pest Management Sci.* **2002,** *58,* 649-62.
7. Becker, W.F.; von Jagow, G.; Anke, T.; Steglich, W. *FEBS Lett.* **1981,** *132,* 329-33.
8. Sierotzki, H.; Parisi, S.; Steinfeld, U.; Tenzer, I.; Poirey, S.; Gisi, U. *Pest Management. Sci.* **2000,** *56,* 833-41.
9. Mitani, S.; Araki, S.; Takii, Y.; Ohshima, T.; Matsuo, N.; Miyoshi, H. *Pest. Biochem. Physiol.* **2001,** *71,* 107-115.
10. Gao, X.; Wen, X.; Esser, L.; Quinn, B.; Yu, C-A.; Xia, D. *Biochemistry* **2003**, *42,* 9067-80.
11. Chen, G.; Lin, B.; Lin,Y.; Xie, F.; Lu, W.; Fong, W-F. *J. Antibiotics* **2005,** *58,* 519-22.
12. Mitani, S. *Agrochemicals Japan* **2001,** *78,* 17-20.
13. Fitzpatrick, G M.; Orth, A. B.; Yap, M. C. H.; Rogers, R. B.; Werk, T. L.; Davis, G. E. U.S. Patent 6,333,432, 2001.
14. Ricks, M. J.; Dent, W. H., III; Rogers, R. B.; Yao, C.; Nader, B.S.; Miesel, J.L.; Fitzpatrick, G. M.; Meyer, K. G.; Niyaz, N. M.; Morrison, I. M.; Henry, M. J.; Adamski, B. J. L.; Gajewski, R. P. WO Patent 2,001,014,339, 2001
15. Ricks, M. J.; Dent, W. H., III; Rogers, R. B.; Yao, C.; Nader, B. S.; Miesel, J. L.; Fitzpatrick, G. M.; Meyer, K. G.; Niyaz, N. M.; Morrison, I. M.; Gajewski, R. P. WO Patent 2,001,005,769, 2001
16. Miesel, J. L.; Benko, Z. L.; Dent, W. H., III; Durst, G. L.; Fitzpatrick, G. M.; Johnson, D. D.; Kaster, S. V.; Kemmitt, G. M.; Lo, W. C.; McKennon, M. J.; Orth, A. B.; Ricks, M. J.; Rogers, R. B.; and Werk, T. L. WO Patent 9,927,783, 1999.
17. Gluck, S.J.; Cleveland, J. A. *J. Chromatogr.* **1994**, *A 680,* 43-8.
18. Gluck, S.J.; Benko, M. H.; Hallberg, R. K.; Steele, K. P. *J. Chromatogr.* **1996,** *A 744,* 141-46.
19. *The Pesticide Manual,* 13th Edition, Tomlin, C.D.S., Ed.; BCPC: Alton, UK, 2003.
20. Avdeef, A. *Methods and Principles in Medicinal Chemistry* **2003,** *18* (Drug Bioavailability), 46-71.

Chapter 12

Discovery of 3-Arylpyrimidin-2,4-diones as GABA-Gated Chloride Channel Insecticides: Translation from Target Site to Field

John W. Lyga, Syed F. Ali, Lyle P. Kinne, F. Larry Marek, Mark A. Wusaty, Charles A. Staetz, and James Willut

Discovery Research Department, Agricultural Products Group, FMC Corporation, P.O. Box 8, Princeton, NJ 08543

An insecticide screening program using an [^{3}H]EBOB binding assay resulted in the discovery of 3-(4-chlorophenyl)-1-methyl-6-trifluoromethylpyrimidin-2,4-dione (1), an early lead acting at the GABA-gated chloride channel. Compound 1 was one of the many analogs contained in the FMC corporate archives synthesized as part of the protox herbicide program. Compound 1 had moderate activity in the GABA assay measurable whole organism activity against mosquito (*A. aegypti*), however, it caused severe phytotoxicity. Through a series of optimization steps, we were able to increase the *in-vitro* activity to nM levels, reduce phytotoxicity, and achieve whole organism activity below 10 ppm against southern corn rootworm in the greenhouse. Poor translation to the field due to metabolism was partially overcome but lack of spectrum and mammalian toxicity was not.

153

154

The global value of chloride channel insecticides in 2003 for both crop and non-crop use was in excess of $1.5 B. This includes insecticides acting at the GABA and glutamate chloride channels; primarily the avermectins, aryl pyrazoles, and chlorinated hydrocarbons.(*1*). The quest for new chloride channel insecticides has relied primarily on screening strategies using radioligand binding assays, especially for those acting at the GABA-gated chloride channel; fipronil being the most recent success (*2*). GABA (γ-aminobutyric acid) is a major inhibitory neurotransmitter in the insect nervous system. GABA receptors are coupled to ligand-gated chloride channels; activation of the channel leads to increased membrane permeability towards chloride. Insecticidal compounds acting at the GABA-gated chloride channel exert their effect by blocking chloride movement through the channel. Although there is significant structural diversity among the known insecticidal GABA chloride channel blockers, most are thought to interact at or near the same site within the channel pore.(*3*) Recent reports indicate that insecticidal action may be a more complex interaction, however, with the discovery that fipronil is also a potent blocker of the glutamate-activated chloride channel.(*4*)

There were a number of radioligands available to evaluate new chemistry acting at the GABA chloride channel blocker site in the mid 1990's.(*5*) We initiated a high throughput screening program at FMC using a [^{3}H]EBOB binding assay using house fly head tissue for the insect screen and rat brain tissue as a check for mammalian selectivity.(*6*) An early lead in our program was 3-(4-chlorophenyl)-1-methyl-6-trifluoromethylpyrimidin-2,4-dione, **1**, one of the many analogs in our corporate archives synthesized as part of our Protox herbicide program.

1
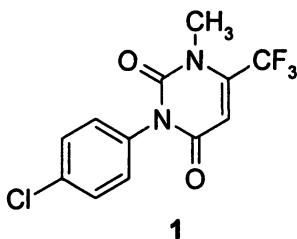
A search of the literature revealed several patent applications and patents claiming arylpyrimidin-2,4-dione as insecticides. A recent publication from Nissan claimed substituted arylpyrimidin-2,4-diones to be insecticidal against planthopper, rice leafhopper, twenty-eight-spotted lady beetle and two-spotted spider mite in the 10-100 ppm range, with no MOA disclosed.(*7*) Ozoe et al. recently reported that 2,4,6-trisubstituted arylpyrimidin-2,4-diones were weakly active in a GABA EBOB assay.(*8*) We found that Compound **1** had moderate activity in the EBOB assay (IC$_{50}$ = 10 μM) with measurable whole organism

activity against yellow fever mosquito (YFM, *A. aegypti*), a model insect used in our HTS screen, however, compound **1** caused severe phytotoxicity in our herbicide screen.

Lead Definition

The first goal was to optimize GABA activity and eliminate the protox herbicidal activity. During the validation phase of the EBOB binding assay we prepared a series of arylpyrazole analogs and obtained an acceptable correlation between EBOB binding with whole organism activity against YFM (see Graph 1) and TBW (tobacco budworm, *Heliothis virescens*).(*9*) We felt confident we could drive the initial optimization using the GABA intrinsic assay and at least

Graph 1. Correlation between GABA pKi and YFM for a Set of Aryl Pyrazole ($r^2 = 0.79$)
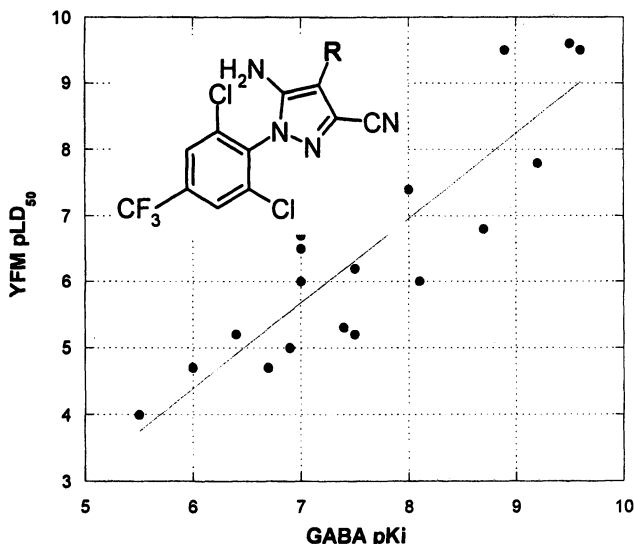
maintain the level of insect activity. Our initial strategy was to use a Free-Wilson approach (*10*) to probe the aryl substitution pattern for optimal GABA and minimal protox activity by synthesizing a set of mono- di- and tri-chloro substituted analogs. Substitution at the aryl positions which increase GABA activity and reduce herbicidal activity would be selected for further

optimization. The 6-subtituted-3-uracils were prepared from either the arylisocyanate or arylcarbamate and substituted aminocrotonates in the presence of NaH and DMF according to Scheme 1.(*11*)
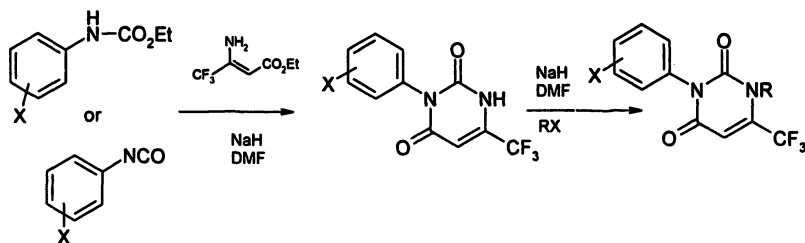
Scheme 1. General Synthesis Methods for Substituted Aryluracils

The set of 11 mono, di, and tri substituted chloro analogs were prepared and compared to the unsubstituted analog (Table 1). Analysis of this chlorine probe set indicated that substitution at Positions 3 and 5 with chlorine favored GABA activity and substitution and Position 4 disfavored herbicidal activity. The 3,4,5-trichloro analog, Compound **7**, had the greatest GABA activity and weakest herbicidal activity. This intrigued us since the pattern was quite different from the 2,4,6 substitution pattern reported by Yagi et al. (*7*) and Ozoe et al.(*8*). It was also fortuitous that the most active pattern in the GABA assay was only weakly phytotoxic.

Lead Optimization Phase

With a lead identified, the goal during this phase of the optimization was to improve activity at the target site by at least an order of magnitude (Compound 7 was still an order of magnitude less active than the standard, fipronil) and to demonstrate good control of at least one economically important insect under lab conditions. Positions 3 and 5 were kept fixed with Cl while and optimizing the aryl para position and pyimidin-2,4-dione positions 1 and 6.

Optimization of N-1 and C-6. A set of *N*-substituted compounds were selected that were orthogonal in electronic (σ), steric (MR), and lipophilic (π) properties

(*12*). For this set, the uracil Position 6 was fixed with CF_3 and the aryl ring fixed with 3,4,5-trichloro (Table2). Regression analysis of the set using the GABA data and the descriptors (π, σ, and MR) indicated the best compounds were substituted with a small group (small MR) but not H (eq. 1). The YFM activity correlated with GABA data similar to the aryl pryazole set with a $r^2 = 0.81$.

Eq. 1   GABA pKi = 8.77 - 1.38 ($\pm$ 0.46) MR   n=8, r = 0.78, F = 9.5 (p = 0.02)

Table 1. Chlorine Probe Set SAR
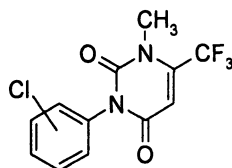
Cmpd #	2	3	4	5	6	GABA pKi[1]	AGU pI$_{50}$[2]	HC pI$_{50}$[3]
1			Cl			5.4	6.9(+)	6.8
2		Cl				5.8	5.1(+)	5.3
3		Cl		Cl		6.8	4.5(+)	4.7
4		Cl	Cl			6.6	6.7(+)	6.7
5	Cl	Cl				6.6	4.3(+)	4.8
6	Cl				Cl	5.6	<4(-)	3.9
7		Cl	Cl	Cl		8.0	<4(-)	5
8	Cl	Cl		Cl		7.4	<4(-)	<5
9	Cl		Cl		Cl	5.2	not tested	5.3
10	Cl	Cl			Cl	7.6	4.2(+)	4.7
11	Cl		Cl	Cl		7.1	6.7(+)	6.0
12						<4	4.9(+)	<4

[1] GABA refers to the [3][H] EBOB binding assay using housefly head tissue. Ki is calculated from the IC_{50} value using the Cheng- Prushoff equation: Ki = IC_{50} / (1 + [ligand concentration / Kd of the ligand])

[2] −log [M] causing 50% inhibition of greening of algae, *Chlamydomonas reinhardtii* y-1 mutant; (+) indicates the presence of the 405 nm peak in the UV, indicative of a protox MOA; (-) indicates the 405 nm peak was not observed

[3] −log[M] causing 50% growth inhibition of hydroponically grown cucumber

There was one positive outlier in the GABA vs. YFM plot, the N-NH$_2$. Both had similar GABA activity but the N-NH$_2$ was more active in the YFM assay. Another measure of the uracils acting at the GABA EBOB target was the use of a mutant strain of YFM resistant to dieldrin (*13*). Compound **22** was much less active on rdlYFM compared to native, evidence that the compounds were acting at the GABA chloride channel blocker site.

A diverse set of uracil Position 6 analogs were prepared again spanning a range of electronic, steric, and lipophilic properties (Table 2). The CF$_3$ group remained the most active. A small set of Position 5 analogs were also prepared, including F, CN, NO$_2$; all were less active than H. Compound **22** remained the most active compound in both the GABA assay and against YFM after optimization of the uracil N-1, C-5 and 6 Positions. The most significant outlier was the *t*-butyl analog, Compound **30**, which was almost as active as the CF$_3$ analog in the GABA assay but virtually inactive in the YFM assay. This was one of the first indications of a lack of translation between the GABA assay and whole insect. The CF$_3$ and *t*-butyl differ in lipophilicity (π, 0.9 vs. 2.0), electronics (σ, 0.5 vs. -0.2) and sterics (MR, 0.5 vs. 2.0) so the lack of activity in YFM could be due to either agrokinetic effects or target site differences between HF and YFM.

Reoptimization of the Aryl with the Best Substituents. Since the N-NH$_2$ was slightly more active than the N-CH$_3$ in most cases, we wanted to see if the 3,4,5-aryl substitution pattern was still optimal for insect activity. A second probe set was prepared and screened against an expanded group of insects including southern corn rootworm (SCR, *Diabrotica undecimpunctata howardi*), cotton aphid (CA, *Aphis gossypii*) and tobacco budworm (TBW, *Heliothis virescens*). None of the compounds were active against TBW at 3.5 μM in a feeding assay or against CA at 100 ppm in a contact assay although many showed phytotoxicity to the cotton plants. Several compounds were found to be quite active against SCR. The 3,4,5-trichloro analog, Compound **22** (Table 3) remained the most active in both the GABA assay and against SCR in the feeding assay and was very close in activity to fipronil. Two additional analogs stand out in this set. The 2,3,4 trichloro analog, Compound **48**, was as active as the 3,4,5-trichloro analog in GABA but was much less active against SCR and the 2,4,6-trichloro analog, having the fipronil aryl substitution pattern, was less active in both the GABA and SCR assays.

Due to the similar response in both GABA and SCR between Compound **22** and fipronil, a study was initiated to compare structural and electronic properties. In several different molecular modeling programs (*14*), both compounds overlayed well with the aryl ring of fipronil overlaying the uracil ring of Compound **22** and the aryl ring of Compound **22** overlaying the pyrazole

of fipronil. Aligned in this way, the dipoles, the HOMO/LUMO maps (Figure 1) and electrostatic potential maps were quite similar. The bio-isosteric relationship between uracils and a 2,4,6-aryl or heteroaryl ring has been previously observed and exploited in the herbicide area.(*15*) This suggested to us that both compounds are interacting with the GABA chloride channel at or near the same site and offers an explanation about the differing optimal aryl substitution pattern.

Table 2. In-vitro and In-vivo Data for the N-1 and C-6 Substituted Set
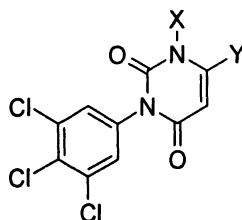
#	X (Y=CF$_3$)	GABA pKi	YFM	#	Y (X=CH$_3$)	GABA pKi	YFM
7	CH$_3$	8.1	6.2	24	i-Pr	6.3	5.3
13	iPr	6.5	4.8	25	CF$_2$CF$_2$CF$_3$	7.3	6.3
14	CH$_2$-t-Bu	6.2	4.3	26	CH$_2$OCH$_3$	5.1	4.3
15	CH$_2$CF$_3$	7.2	6.0	27	Ph	<4	<4
16	CH$_2$COCH$_3$	<4	4.1	28	CH$_2$SO$_2$CH$_3$	<4	<4
17	CH$_2$CN	7.4	5.7	29	CH$_3$	<4.6	<4
18	CH$_2$Ph	<4	<4	30	t-butyl	7.5	<4
19	CH$_2$CH$_2$OMe	6.6	4.6	31	CH$_2$SCH$_3$	<4.6	<4
20	Bu	<4	<4	32	CO$_2$H	<4	<4
21	H	5.5	4.9	33	CN	6.2	4.6
22	NH$_2$	8.8	7.6	34	CH$_2$CH$_2$CF$_3$	6.4	4.0
23	NHCOCH$_3$	5.3	4.4	35	propyl	6.2	3.9
				36	CF$_2$CF$_2$CF$_2$CF$_3$	5.0	6.1
				37	2-F-phenyl	<4	4.56
				38	4-F-phenyl	5.0	4.6
				39	Cl	5.6	-

160

Table 3. Chlorine Probe set for the _N_-Amino Pyrimidin-2,4-dione
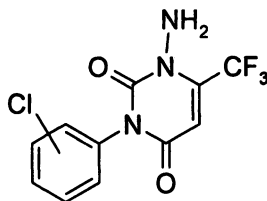
Cmpd #	2	3	4	5	6	GABA pKi	SCRD pI$_{50}$[1]
22		Cl	Cl	Cl		8.7	6.0
40			Cl			6.7	4.5
41	Cl		Cl			7.5	4.0
42		Cl		Cl		7.7	5.5
43		Cl	Cl			7.7	5.3
44	Cl		Cl	Cl		7.5	4.0
45	Cl		Cl		Cl	7.5	4.2
46	Cl				Cl	7.1	4.0
47		Cl				6.5	5.1
48	Cl	Cl	Cl			8.5	4.2
49						<5	<4

[1]   -log [M]causing 50% mortality of SCR in a diet assay

Optimization of the aryl 3,4,5-positions. Optimization continued with an analog set at Position 4 of the aryl ring; Positions 3 and 5 were fixed with Cl and the uracil with N-NH$_2$ (Table 4). Southern corn rootworm topical data was used to drive the optimization checking _in-vitro_ GABA potency as a guide. There was a general trend of increasing SCR activity with increasing GABA. Analyzing the set using cluster significance analysis with rank ordered SCR data[16] found that all of the more active compounds had Position 4 substituents that were clustered around a length (L) between 3.5 and 4.3 Å and a F value [electronic field effect] of around 0.43. At this stage of the optimization, we achieved target site potency equivalent to fipronil with the iodo analog, Compound **50**, being the most potent.
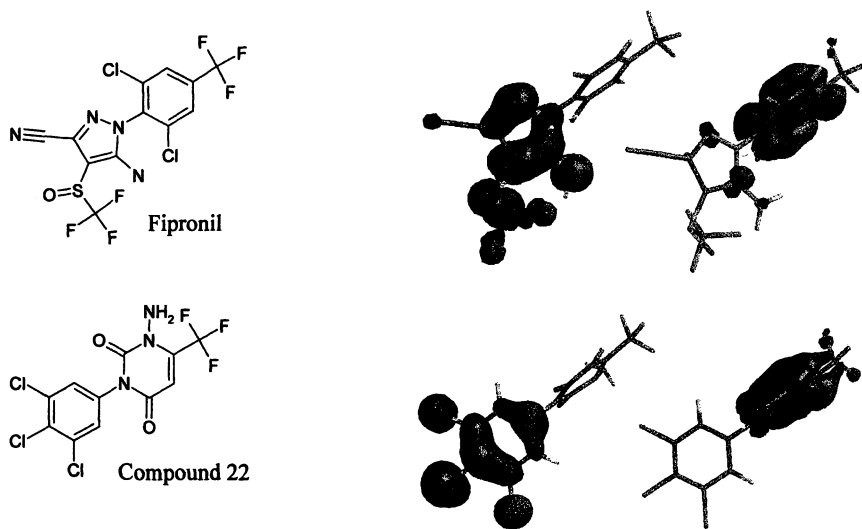
Figure 1. Comparison of the HOMO (left) and LUMO (right) of Compound 22 with Fipronil

Compound **50** was tested against SCR in a full greenhouse trial including bioactive soil including fipronil as a standard. In sterile soil, Compound **50** was about 3X less effective than fipronil at controlling SCR, consistent with the earlier data. In bioactive soil, there was a significant reduction in activity with Compound **50** compared to fipronil (Table 5). A follow-up soil metabolism study indicated that Compound **50** degrades readily in bioactive soil with a $T_{1/2}$ = 5.9 d. Of the potential sites for degradation (Figure 2), mass spectral analysis of the metabolites from the soil study indicated that Compound **50** is degrading by uracil reduction and by loss of the 4-iodo group (Figure 2, solid circles). The 3,5-dichloro analog (4-H) and the dihydrouracil both were inactive against SCR in a soil applied test. The de-amino metabolite was not found in the soil study but was a key metabolite in TBW frass. In looking for analogs with greater soil residual activity, we went back to the results of the cluster significances analysis of the Position 4 substituent set and selected additional substituents having an L between 3.5 and 4.3 Å with F around 0.43, properties previously shown to be desirable. Examples of both 3,5-dichloro and 3,5-difluoro were prepared since F and Cl were both shown to be equal in activity against SCR and 3,5-difluoro simplified synthesis of some of the Position 4 analogs. Evaluation in active soil

indicated that the new analogs (Table 6) were more resistant to degradation and does suggest that we can improve the soil efficacy by modifying the substituent at Position 4. The 4-CF$_3$ (50) was the best.

Table 4. Optimization of Position 4 of the *N*-amino Aryl Uracils
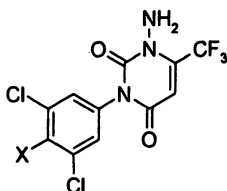
Cmpd #	X	GABA pKi	YFM pLC$_{50}$	SCR topical LC$_{50}$ ppm	SCR soil LC$_{50}$ ppm[1]
50	I	9.3	7.6	20	0.3
22	Cl	8.8	7.4	32	1
51	SOCH$_3$	7.5	5.1	>300	
52	SCH$_3$	8.7	5.6	>300	
53	Ph	8.9	6.1	>300	
54	OCH$_3$	8.5	5.9	100	
55	2-thienyl	9.1	6.7	>300	
56	N(CH$_3$)$_2$	8.8	5.7	>300	
57	i-PrO	9.0	5.4	300	
58	Br	9.3	7.0	<30	~2
fipronil		9.6	9.0		0.2

[1] Only the more active compounds were tested in the soil assay

Although the activity against SCR was excellent, the spectrum was disappointing with Compounds **59** and **60** showing excellent activity primarily against SCR with significantly weaker activity against CA and only poor activity against TBW. In addition, we had early indication that toxicity may be a major problem with this lead. The best compounds that were highly active in the GABA EBOB housefly binding assay were also very active in the GABA assay using rat brain. In fact, a plot of GABA HF vs. GABA rat for all of the aryl uracil analogs indicated little selectivity. Patterns with more target site selectivity, such as the 2,3,6-trichloro or the 2,3,5-trichloro were void of insect activity (Graph 2). A few aryl uracils, including Compound **50**, were also found to have a LD$_{50}$ <50 mg/kg in a rat toxicity screen.

Table 5. Evaluation of Compound 50 in Bioactive Soil Against SCR

	Percent Mortality							
	Fipronil - sterile		Fipronil- bioactive		Cmpd 50 - sterile		Cmpd 50 - bioactive	
rate (ppm)	Day 1	Day 10	Day 1	Day 10	Day 1	Day 10	Day 1	Day 10
3					100	100	90	100
1.0	100	97	100	100	97	97	53	37
0.3	97	90	100	97	97	90	3	23
0.1	60	97	40	83	80	60	0	23
0.03	30	60	0	27				
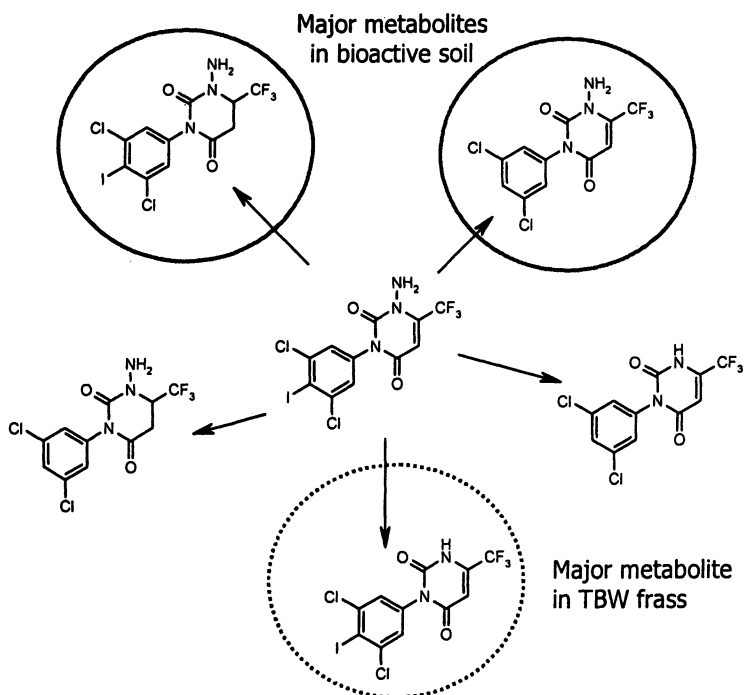
Figure 2. Metabolites of Compound 50

Table 6. Compounds Designed to have Improved Residual Activity
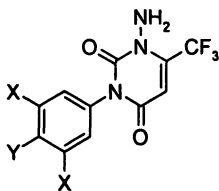
Cmpd #	X	Y	GABA pKi	SCR topical LC$_{50}$ ppm	SCR soil LC$_{50}$ ppm	#days residual in virgin soil
51	Cl	I	9.3	20	0.3	10
59	Cl	CF$_2$CF$_3$	8.8	22	0.3	>28
60	F	CF$_3$	8.7		0.3	>28

Conclusions

The 3-Arylpyrimidin-2,4-diones are a new class of insecticides that are active at the insect GABA chloride channel. A 3,4,5-substitution pattern was best for optimal insect activity and low phytotoxicity. The best compounds are equivalent to fipronil both *in vitro* in the GABA assay and *in vivo* against SCR. We were able to optimize target site activity and minimize phytotoxicity using the GABA EBOB data. Screening through our insect screens found that the aryluracils have excellent control against SCR. This was confirmed in the greenhouse and the SCR assay was useful to screen analogs for improved residual activity. The better compounds against SCR also were potent in the GABA assay. The GABA rat assay was also a useful predictor for toxicity . In the end, however, we were unable to significantly both improve toxicity and broaden spectrum for the aryluracils.

Graph 2. Correlation between GABA HF and GABA Rat

GABA rat pKi vs GABA HF pKi
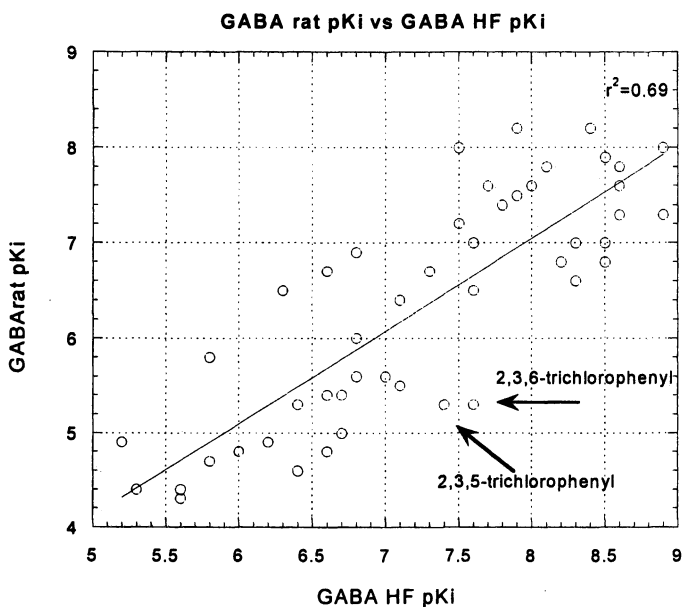
Acknowledgment

The authors would like to thank the members of the herbicide discovery effort at FMC for providing the initial lead and for the many helpful discussions from synthetic methods to biological testing.

References

1. Bloomquist, J. R. *Annu. Rev. Entomol,* **1996,** *42,* 163.
2. Gant, D. B.; Chalmers, A. E.; Wolff, M. A.; Hoffman, H. B.; Bushey, D. F. *Reviews in Toxicology,* **1998,** *2,* 147; for a new radioligand based on fipronil see, Meegalla, S. K.; Doller, D.; Silver, G. M.; Wisnewski, N.; Soll, R. M.; Dhanoa, D.; *Biorg. Med. Chem. Lett.* **2003,** *13,* 4035.

3. Sammelson, R. E.; Caboni, P.; Durkin, K.; Casida, J. Bioorg. Med. Chem., **2004**, *12*, 3345.; Ozoe, Y.; Akamatsu, M.; Pest. Manag. Sci. **2001**, *57*, 923; Calder, J. A.; Wyatt, J. A.; Frenkel, D. A.; Casida, J. E. *J. Comput. Aided Mol. Design.* **1993**, *7*, 45.

4. Zhao, X.; Yeh, J. Z.; Salgado, V. L.; Narahashi, T. *J. Pharmacol. Exp. Therapeutics*, **2004**, *310*, 192

5. Deng, Y, *Molecular Action of Insecticides on Ion Channels*, *ACS Symposium Series 591*, Clark, J. M., ed., Washington, D.C., 1995; pp.230-250.

6. Cole, L. M.; Casida, J. E. *Pestic. Biochem. Physiol.* **1992**, *44*, 1.

7. Yagi, K; Akimoto, K.; Mimori, N.; Miyake, T.; Kudo,M.; Arai, K.; Ishi, S. *Pest. Manag. Sci.* **2000**, 65.

8. Ozoe, Y.; Yagi, K.; Nakamura, M.; Akamatsu, M.; Miyake, T.; Matsumura, F. *Pestic. Biochem. Phys.*, **2000**, *66*, 92-104.

9. Eldridge, R.; Lyga, J. W. AGRO-019, 225th ACS National Meeting, New Orleans, March 23-27, **2003**

10. Free, S. M.; Wilson, J. W., *J. Med. Chem.*, **1964**, *7*, 395.

11. Maravetz, L. L; Theodoridis, G., *PCT Int. Appl.* WO 9712884 (1997), CAN 126:330612

12. Hansch, C.; Leo, A. *Exploring QSAR*, American Chemical Society, Washington, D.C., 1995, Chapter 2.

13. "YFM Resistant to Dieldrin" was obtained from the University of Wisconsin

14. Alchemy 2000 (Tripos), MedChem Explore (MDL), and C2 (MSI

15. Schafer, P.; Hamprecht, G.; Ouhl, M.; Westphalen, K-O.; Zagar, C. *Chimia*, **2003**, *57*, 715

16. McFarland, J. M.; Gans, D. J. *J. Med. Chem*, **1986**, *29*, 505.

Chapter 13

2,4-Diaminoquinazoline Insecticides

**Elizabeth G. Rowley, Thomas G. Cullen, John A. Dixson,
Sayed ElMarakby, Louis V. LaFrance, Saroj Sehgel,
and Dennis Warkentin**

**Agricultural Products Group, FMC Corporation, P.O. Box 8,
Princeton, NJ 08543**

2,4-Diaminoquinazolines are a new class of lepidopteran
insecticide that perform very well in an artificial diet assay, but
perform less well when the compounds are applied foliarly.
2,4-Diaminoquinazolines are readily prepared and optimized
to high activity against tobacco budworm larvae in an artificial
diet assay. 2,4-Dichloroquinazoline was treated with an
appropriately protected 4-aminopiperidine, followed by
reaction with an aniline at high temperature to prepare the
desired targets. These compounds are 10 to 100-fold less
active than expected in foliar assays of tobacco budworm and
other lepidoptera. A number of possible reasons for this poor
diet to foliar translation are explored including metabolism,
physical properties and formulations.

FMC developed a feeding assay using tobacco budworm (TBW) on semi-artificial diet as a method to rapidly screen our compound collection. In this surface-treated diet (SRTD) assay TBW larvae are fed a semi-artificial diet on which a top layer of test compound has been placed. The SRTD assay can be run in a 24-well plate format and is suitable for screening large numbers of compounds. Two measurements are taken for the SRTD assay: the weight-inhibition (pI_{50}) measures the dose required to reduce larval weight by 50%

© 2007 American Chemical Society

relative to the controls, and the mortality (pLD_{50}) measures the dose required to kill 50% of the larvae. Diaminoquinazoline **1** was discovered by screening FMC's corporate compound collection against tobacco budworm in the SRTD assay. Compound **1** was adopted as a lead with the goal of optimizing activity in SRTD and then testing the most active compounds in foliar assays against TBW and other lepidoptera.
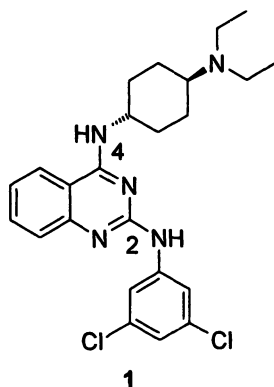
Table 1. Initial Lead Activity

Test	Activity
SRTD weight inhibition	$pI_{50} = 5.8$
SRTD mortality	$pLD_{50} = 3.6$

Initial Optimization

During the early phase of work on this lead, it was discovered that SRTD activity could be maintained by replacing the 4-diethylaminocyclohexylamino moiety at Position 4 with an unsubstituted cyclohexylamino group, thereby simplifying the synthesis. The simplified compounds are prepared in three steps from benzoyleneurea as shown in Scheme 1. Treatment of the benzoyleneurea **2** with POCl$_3$ and dimethylaniline gives 2,4-dichloroquinazoline **3** as described by Hess et.al *(1)*. The chlorine in Position 4 is readily displaced with cyclohexylamine at room temperature, while the chlorine in Position 2 requires forcing conditions to react with the aniline *(2)*. We found that for the final step the best yields of **5** were obtained by heating a neat mixture of chloroquinazoline **4** with excess aniline at 100 °C. The product **5** could be isolated by precipitation with dichloromethane, or by filtering the product mixture through a short plug of silica.

For the initial optimization we kept the cyclohexylamino group at Position 4 while the aniline and benzo rings were probed with chlorine, methyl, and methoxy groups. Figure 1 summarizes the results of these experiments. On
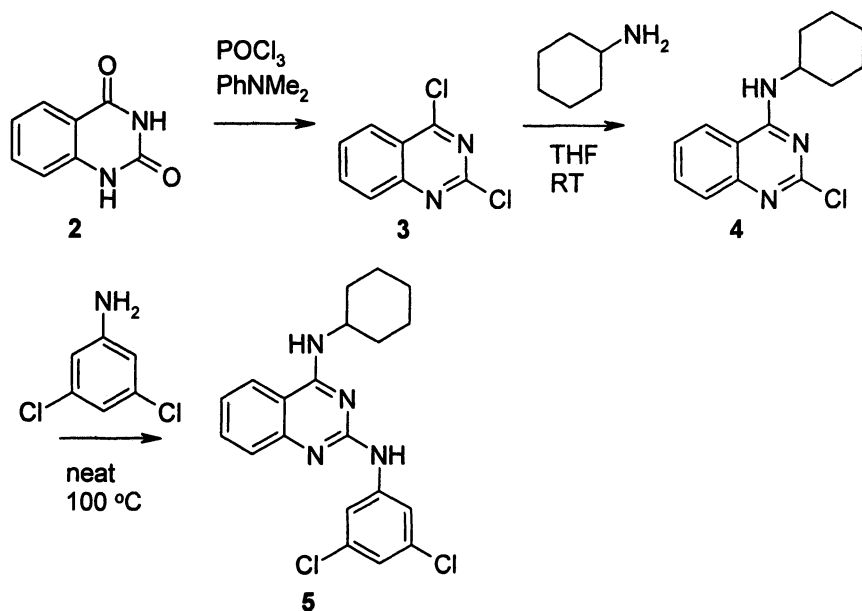
Scheme 1. Synthesis of Cyclohexylamino Substituted Quinazolines

the quinazoline core, the unsubstituted benzo ring gave the highest level of SRTD activity. Compounds with chlorine in Position 6 or 7 maintained a reduced level of activity, while the 5- and 8-chloro compounds were inactive. On the aniline, 3,5-dichloro substitution was found to give the highest SRTD activity while 3,4-dichloro substitution was slightly less active. At Position 2 other substituted anilines had reduced activity, and aliphatic amines were inactive. Figure 1 also shows the importance of the secondary amines at Positions 2 and 4. The nitrogen at Position 2 could be acylated with some loss of activity, presumably the TBW can metabolize the resulting amide back to the secondary amine, but methylating or replacing nitrogen with oxygen gives inactive compounds. A similar trend was observed at Position 4 where the *N*-methyl derivative is inactive.

Position 4 Optimization

More dramatic improvements in SRTD weight inhibition and mortality were achieved by varying the amino substituent at Position 4 while keeping 3,5-dichloroaniline fixed in Position 2. The 4-aminopiperidine derivatives were a particularly fruitful area of investigation. Scheme 2 shows how a variety of substituted piperidines could be readily made from a common intermediate. The
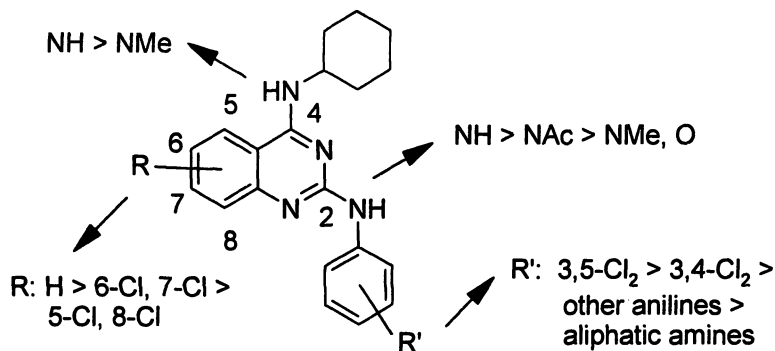
Figure 1. Structure-activity Relationships for 4-cyclohexylaminoquinazolines

initial synthesis scheme was modified by replacing cyclohexylamine with 4-amino-1-*tert*-butoxycarbonyl-piperidine to give Compound **6**. Reaction of **6** with neat 3,5-dichloroaniline at 100 °C gave intermediate **7** without any loss of the BOC group. Deprotection of **7** with trifluoroacetic acid gives Compound **8**, a common intermediate that could be reacted with alkyl and acyl halides, chloroformates, isocyanates and other electrophiles to give substituted aminopiperidine derivatives **9**.

While alkyl substituted piperidines have low levels of SRTD activity, the amides, carbamates, and ureas are much more active compounds (Table 2). The 4-fluorophenylurea, Compound **10**, has the highest SRTD activity of any compound in the diaminoquinazoline area. The substitution patterns on the aniline and benzo portions of the molecule were reinvestigated with the more active group in Position 4, but the structure-activity relationships were found to be the same as for the 4-cyclohexylamino compounds as described in Figure 1.
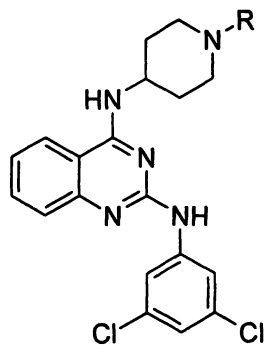
Table 2. SRTD Activity of 4-aminopiperidine Derivatives

R	SRTD pI_{50}	SRTD pLD_{50}
H	4.6	inactive
CH_3	4.7	inactive
$CH_2C_6H_5$	5.6	3.6
$CO_2C_2H_5$	6.1	4.5
$CO_2C_6H_5$	6.0	5.3
$CO_2C_6H_4$-4F	6.2	5.5
$COCH_2C_6H_4$-4F	6.6	5.4
$CONHC_6H_5$	6.6	5.6
$CONHC_6H_4$-4F	7.0	6.6
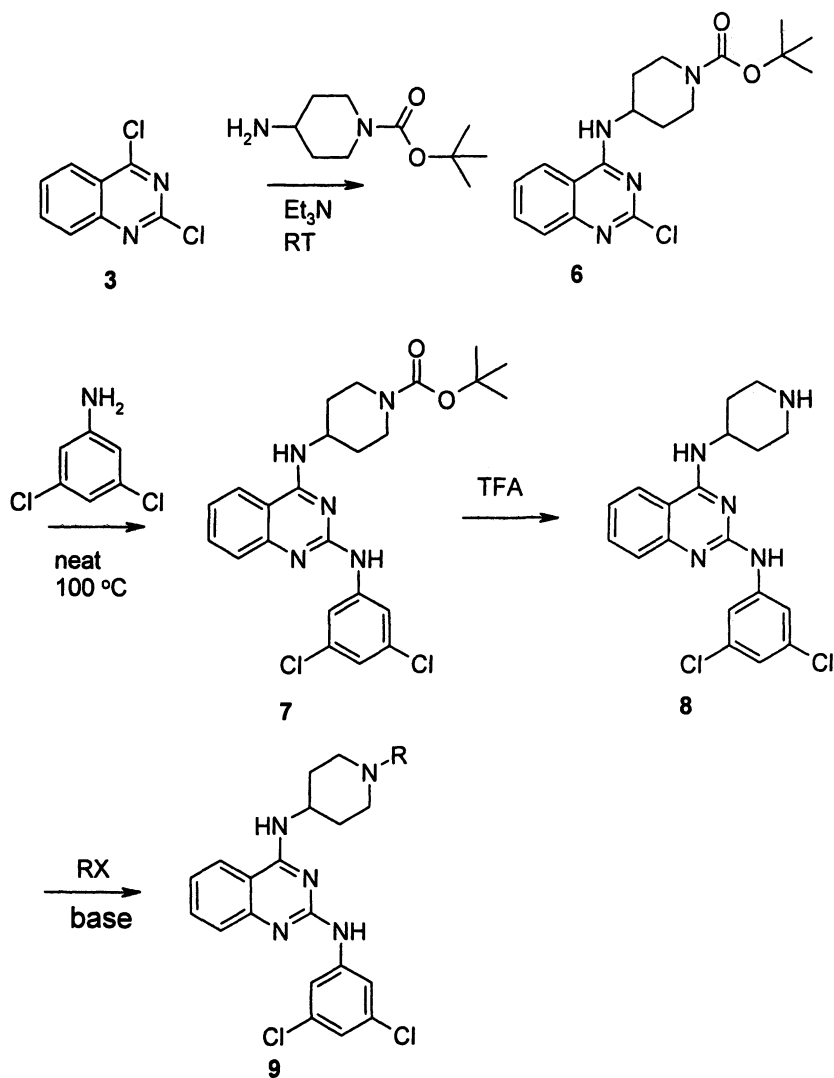
Scheme 2. Synthesis of 4-aminopiperidine Derivatives

Diet to Foliar Translation

Compound **10** has excellent potency in the SRTD assay, at levels often seen with commercial products, but it performed poorly in more advanced foliar tests against larvae of tobacco budworm, diamond back moth, and beet armyworm. The SRTD active amides and carbamates from Table 2 also failed to translate well to the foliar assays. It is expected that a compound with a pI_{50} of 7.0 in SRTD will translate to a foliar LC_{50} of less than 10 parts per million. This trend is observed in data derived from commercial and experimental lepidoptericides and was the basis for using the higher throughput SRTD as a screening assay. Figure 2 displays TBW foliar LC_{50} versus SRTD pI_{50} for a randomly selected set of pyrethroids and sets of compounds from experimental classes of lepidoptericides. A similar trend is observed with TBW foliar LC_{50} versus SRTD pLD_{50}. For these compound classes the SRTD assay is a valuable optimization tool because improving SRTD activity correlates well with improved foliar activity. However, this trend is not observed for the 2,4-diaminoquinazolines; the 2,4-diaminoquinazolines have a higher foliar LC_{50} value for a given SRTD pI_{50}, and the slope of the LC_{50} vs. pI_{50} line is shallower for the 2,4-diaminoquinazolines than it is for the other compounds classes.

We investigated the possibility that the lower than expected foliar activity of Compound **10** was due to its being bound up with the leaf surface and therefore not available to the tobacco budworm larvae as it is on the artificial diet. Compound **10** was applied to a pinto bean leaf surface and after two days was quantitatively recovered by rinsing the leaf with acetone, indicating that Compound **10** should be as accessible on the leaf surface as it is on the diet surface.

10
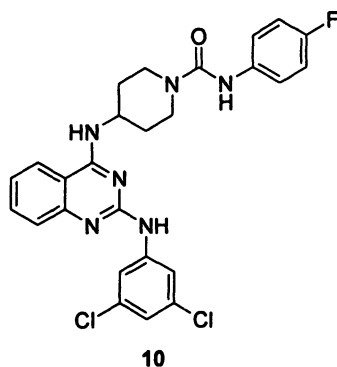
Table 3. Foliar Activity of Compound 10

Test	Activity
SRTD weight inhibition	$pI_{50} = 7.0$
SRTD mortality	$pLD_{50} = 6.6$
TBW foliar	$LC_{50} = 88$ ppm
BAW foliar	$LC_{50} \approx 100$ ppm
DBM foliar	$LC_{50} \approx 300$ ppm

TBW = tobacco budworm, *Heliothis virescens*

BAW = beet armyworm, *Spodoptera exigua*

DBM = diamondback moth, *Plutella xylostella*

ppm = parts per million
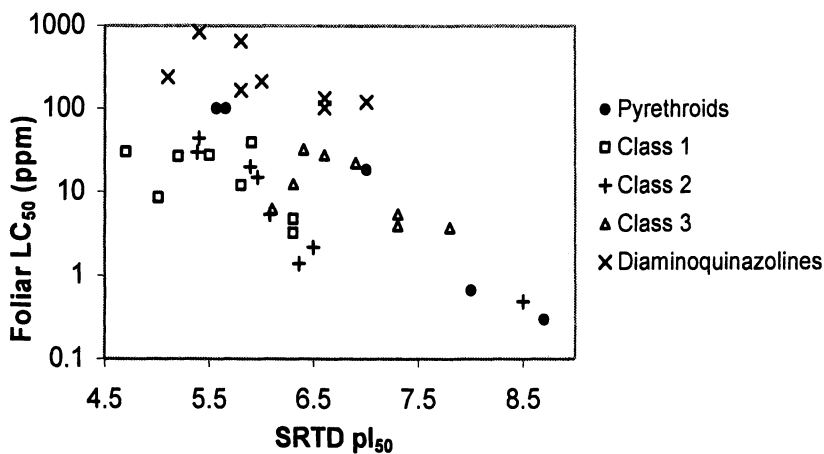
Figure 2. TBW Foliar LC$_{50}$ vs. SRTD pI$_{50}$ for Various Compound Classes

Next we considered that the plant material might induce the tobacco budworm to metabolize Compound **10** into an inactive form. TBW were fed Compound **10** on semi-artificial diet and on chickpea leaves. HPLC analysis of the gut, excrement, and carcass showed that the TBW did not metabolize Compound **10** from either food source. These experiments did not address the relative amounts of Compound **10** entering the larvae from the two food sources, but they do demonstrate that ingestion of plant material does not affect the insect's ability to metabolize Compound **10**.

Another possible explanation for the poor performance of Compound **10** in the foliar assay is that its physical properties are unsuitable for foliar application. The 2,4-diaminoquinazolines are high melting solids, and are expected to have poor solubility properties *(3)*. Material for the foliar assay is first dissolved in acetone and then diluted with Triton-water. Examination of the spraying equipment used for the foliar assay indicated that Compound **10** stays in solution long enough to be dispensed from the sprayer and on to the plant. However, Compound **10** might precipitate from the spray droplets on the leaf surface in a heterogeneous manner and provide a way for the larvae to avoid contact with a lethal dose of Compound **10** *(4)*.

Analogs of Compound **10** that were predicted to have a reduced melting point and improved solubility were investigated in an attempt to find a compound that had better translation from SRTD to the foliar assay (Figure 3). Compound **11** was expected to have a lower melting point because of reduced planarity of the center part of the molecule, but in fact melted at a higher temperature than Compound **10** and was not investigated any further. The

unsymmetrical 3,4-dichloroaniline found in Compound **12** did give an analog with a lower melting point as did the *N*-acetyl derivative, Compound **13**. While both of these lower melting analogs retained much of their SRTD weight inhibition activity, no improvement was seen in the translation to foliar activity. It is interesting to note that for the reduced melting point compounds the SRTD mortality has fallen off by an order of magnitude and is more in line with the observed levels of TBW foliar activity.

Finally, we investigated whether or not formulation could improve the foliar activity of Compound **10**. The standard formulation procedure for the foliar assay is to dilute an acetone solution of the compound with Triton-water. When DMSO was substituted for acetone a slight improvement in foliar activity was observed. Control experiments verified that this level of DMSO did not affect TBW mortality so it is possible that the increased solubility of **10** in DMSO is providing better coverage of the leaf surface or better penetration into the TBW gut. However, an agronomically more acceptable EC formulation gave decreased foliar activity compared to the acetone standard. While formulations may play a role in improving the foliar activity of the 2,4-diaminoquinazolines, it is clear that a compound with more intrinsic activity than Compound **10** will be required in order to reach the goal of a foliar LC_{50} of less than 10 ppm.

Table 4. Effect of Formulation of Compound 10 on Foliar Activity

Formulation	TBW foliar activity
Acetone/Triton/water	LC_{50} = 88 ppm
Dimethylsulfoxide/Triton/water	LC_{50} = 40 ppm
5% EC	LC_{50} = 160 ppm

Summary

2,4-Diaminoquinazolines were readily optimized to a high level of activity against TBW larvae in a surface-treated diet assay. The most potent analog, Compound **10**, was expected to translate to a foliar LC_{50} of less than 10 ppm, but in fact was an order of magnitude less active. We determined that the insect is able to get a dose of Compound **10** from the leaf surface, and that the plant material does not affect larval metabolism of Compound **10**. We were unsuccessful in using alternate formulations or lower melting analogs to increase foliar activity. As we lacked the opportunity to increase the intrinsic activity of the 2,4-diaminoquinazolines, the project was stopped.
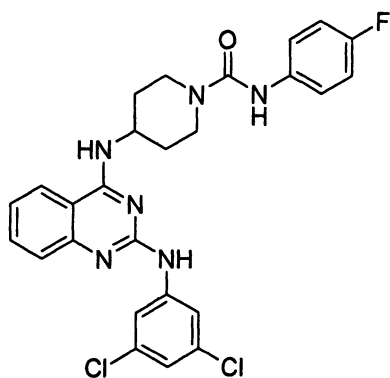
10
SRTD pI_{50} = 7.0
SRTD pLD_{50} = 6.6
TBW foliar LC_{50} = 88 ppm
m.p. = 231-233 °C
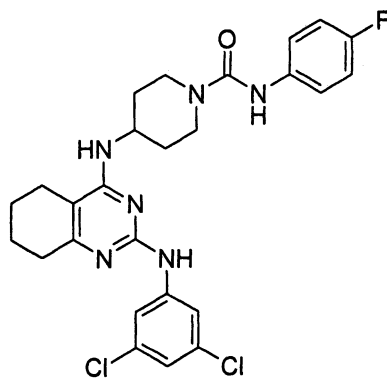
11
SRTD pI_{50} = 6.0
SRTD pLD_{50} = 4.9
m.p. = 245-246 °C
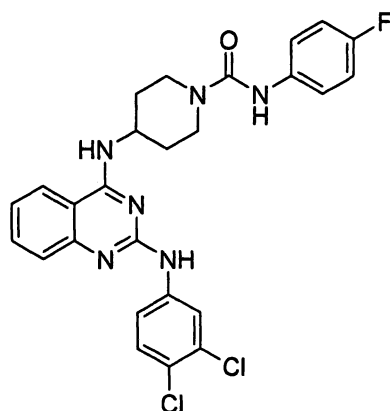
12
SRTD pI_{50} = 6.6
SRTD pLD_{50} = 5.6
TBW foliar LC_{50} = 354ppm
m.p. = 185-190 °C
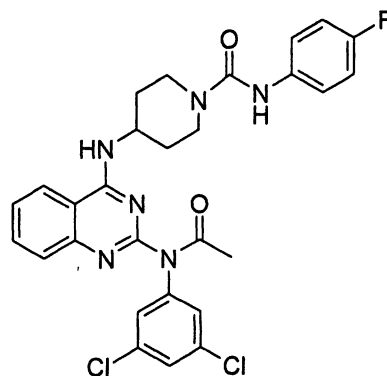
13
SRTD pI_{50} = 7.2
SRTD pLD_{50} = 5.5
TBW foliar LC_{50} = 100 ppm
m.p. = 169-172 °C

Figure 3. Lower Melting Analogs of Compound 2

Acknowledgements

The authors are indebted to Zeinab Elshenawy and Mike Wyle for compound synthesis; to Joe Argentine, Lisa Cornell, Leo Dungan, Larry Faehl, Elena Goodell, Larry Marek, Jim Willut, and Linda Varanyak for biological testing; and to Barbara Collura for assistance with this manuscript.

References

1. Hess, H.J.; Cronin, T.H.; Scriabine, A. *J.Med.Chem.* **1968**, *11*, 130.
2. Elslager, E.F.; Hess, C.; Johnson, J.; Ortwine, D.; Chu, V.; Werbel, L.M. *J.Med.Chem.* **1981**, *24*, 127.
3. Yalkowsky, S.H. *J.Pharm.Sci.* **1981**, *70*, 971.
4. Chowdhury, A.B.M.N.U.; Jepson, P.C.; Howse, P.E.; Ford, M.G. *Pest Management Science* **2001**, *57*, 403.

Chapter 14

New Termiticides Necessitate Changes in Efficacy Testing: A Case Study of Fipronil

Chris J. Peterson, Terence L. Wagner, Thomas G. Shelton, and Joe E. Mulrooney

Forest Service, Wood Products Insect Research Unit, U.S. Department of Agriculture, 201 Lincoln Green, Starkville, MS 39759

The US Forest Service has been conducting efficacy testing of soil-applied termiticides and other products since the 1930s. With the emergence of delayed-acting, non-repellent (DANR) termiticides in the 1990s, deficiencies in testing protocol became apparent. For one DANR, fipronil, an "area effect" was observed in field trials, where control plots adjacent to treated plots experienced reduced termite incidence, and the effect was observed only in the tests containing fipronil. The area effect had not been observed before with any of the other products tested in the testing program's 60-year history. An expanded test layout was developed where test methods and product concentrations were separated by 50 feet from each other and from control plots. The area effect was not observed in this layout, and this layout has since been used for other products, for example chlorfenapyr. However, the expanded layout is costly, time consuming and land intensive. A laboratory test is necessary to determine which products require the expanded layout, and which may be placed in a conventional layout.

179

Termites are wood-feeding insects that cause over $1.5 billion damage annually in the United States (*1*). Pest termites, of which there are several species in North America, can be divided into three general groups based on lifestyle. Subterranean termites are the most common, and therefore are the most damaging, ranging from the tropics to the southern part of Canada, with the heaviest infestations in the Southeast (from South Carolina to Oklahoma and south) and southwestern California. Subterranean termites (primarily *Reticulitermes* spp. in the United States) live in the soil but infest wood in contact with the soil, or construct protective shelter tubes over barriers to reach wood above ground. The invasive Formosan subterranean termite (*Coptotermes formosanus*), which was originally introduced into New Orleans, LA and is of major concern due to its rapid spread throughout the Southeast, is a subterranean termite. Drywood termites, unlike subterranean termites, live without contact to the soil and are not as dependent upon a source of moisture. They occur primarily along the Gulf Coast and Southern California, but may be more economically important than subterranean termites in localized areas. The third type of termite, the dampwood termite, requires a high amount of moisture, often nesting under decaying wood. They are mostly limited in distribution to Florida and northern California, although they do occur elsewhere. They are rarely of significant economic importance.

Several methods may be used to protect structures from subterranean termite damage. Because both subterranean and dampwood termites nest in the soil, the most common method is to treat the soil around and under a structure with a termiticide prior to construction, with subsequent applications as needed later. This provides a continuous chemical barrier of treated soil, preventing entry of the termites. Another popular method is the use of termite baits, where termites feeding on the baits pass toxic levels of a slow-acting active ingredient to nestmates, thereby reducing the termite population adjacent to the structure. The use of physical or chemically-impregnated physical barriers is a third approach used by some. Such barriers, if used properly and they remain intact, provide protection via termite exclusion.

The United States Environmental Protection Agency (EPA) regulates pesticide registration in the US. For soil-applied liquid termiticides, the EPA requires that products undergo efficacy testing prior to registration. Under Pesticide Registration Notice 96-7 (or PR 96-7), product registrants are required to provide efficacy testing data demonstrating that their product provides satisfactory protection from termites for five years (*2*). The EPA's Product Performance Test Guidelines OPPTS 810.3600 – Structural Treatments, further states that the performance testing must be conducted at a minimum of three geographically separated sites (*3*). Individual states may impose other guidelines as well.

The United States Department of Agriculture - Forest Service has provided efficacy testing of termiticides since 1939, long before the formation of the EPA,

and before the passage of the Federal Insecticide, Fungicide and Rodenticide Act (FIFRA) in 1947, which required pesticide products to be registered with the USDA. The Forest Service began testing termiticide products at the request of the Army to help protect ammunition boxes and installations around the world from termites (*4*). The Forest Service currently uses two tests to evaluate efficacy, the ground board test and the concrete slab test (called "modified ground board" in some literature). These tests will be described in more detail later. The EPA guidelines also allow the use of the stake test, which is not commonly used and will not be described here.

The Forest Service has tested every soil applied termiticide product registered in the US. Although registrants are required to submit efficacy data, they are not legally required to use the Forest Service. Figure 1 shows the number of products and sites by year installed since 1955. Currently, testing occurs at four locations: Panama City, FL, Tucson, AZ, Gulfport, MS and Union, SC. These sites represent different ecosystems, soil types and environments, and in the case of Arizona, a different termite genus, *Heterotermes* (the other three sites are dominated by *Reticulitermes* species). Historic locations no longer used include sites in Maryland, Oregon, Missouri, the Panama Canal Zone and Midway Island.

Each year the results of the testing studies are reported in *Pest Control Magazine*. This report is regarded as the industry standard for termiticide efficacy. It is used by manufacturers and pest management professionals.

In the 1990s, several new active ingredients emerged that were slow-acting and applied at less than repellent rates as soil termiticides. These will be referred to as the delayed-acting, non-repellent (DANR) termiticides. Three currently-registered DANR active ingredients are imidacloprid, fipronil and chlorfenapyr. Such products do not cause rapid mortality in termites, compared to older compounds such as the organochlorines, organophosphates and pyrethroids. They also do not result in avoidance of treated soil, unlike the pyrethroids which are repellent (*5*). These properties have the benefit of increasing the likelihood of termites encountering the active ingredient, the amount of time termites spend in association with the active ingredient, and the likelihood that toxic amounts of the compound will be transferred to other termites before the exposed individual succumbs to the toxic action.

This chapter describes, in narrative form, results obtained from Forest Service tests of one DANR, fipronil, the active ingredient of BASF's Termidor® products. In the first test of this product, diminished termite incidence at control plots adjacent to treated plots was observed, a phenomenon dubbed the "area effect." This presented a problem for regulatory officials, because termite presence is required to evaluate efficacy. The Forest Service has modified the test for subsequent testing of this and other products, and these efforts are described as well. In keeping with the symposium theme of "translation of
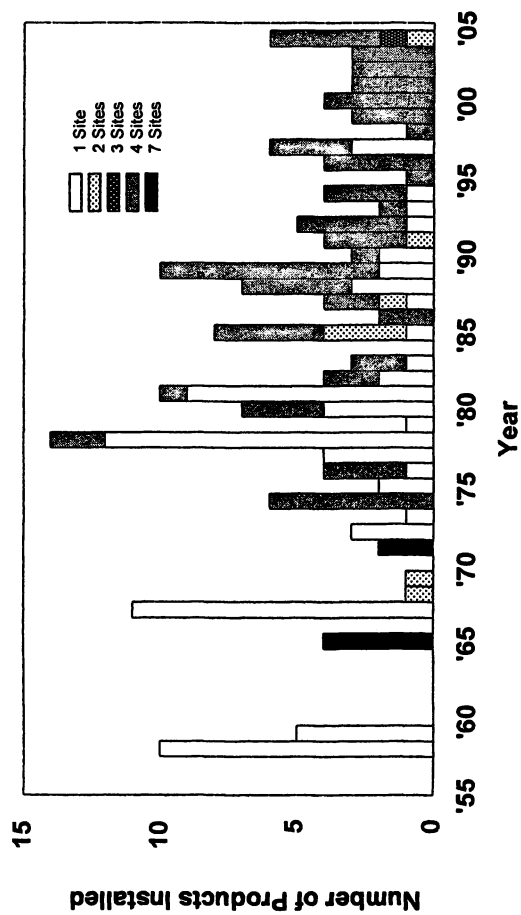
Figure 1. Number of Products Installed at Forest Service Testing Program Locations since 1955.

pesticidal activity from the laboratory to the greenhouse to the field," it illustrates the need for laboratory testing to determine how to test this and other products in the field more effectively.

Test Methods

The Ground Board Test

The ground board test is the older of the two currently used methods, introduced in 1943 (*4*). In this test, leaf litter and duff is removed from a 60 × 60 cm square of ground. Roots and stones are dug out of the ground to a depth of 5 cm. The soil is leveled and a 43 × 43 cm metal treatment frame is placed on the ground. Mixed formulation of the termiticide, 760 ml, is applied to the soil inside the treatment frame, corresponding to the label recommendations of one US gallon per ten square feet. Once the formulation has soaked in, the frame is removed and a 2 × 14 × 14 cm piece of southern yellow pine is centered on the treated soil. A brick is placed on the board to hold it in place (Figure 2) (*4*). The treated soil is left exposed to the environment and the wood is examined at one-year intervals for damage caused by termites. The presence of living termites is recorded if observed. Damage to the wood is rated by one of the scales described later.
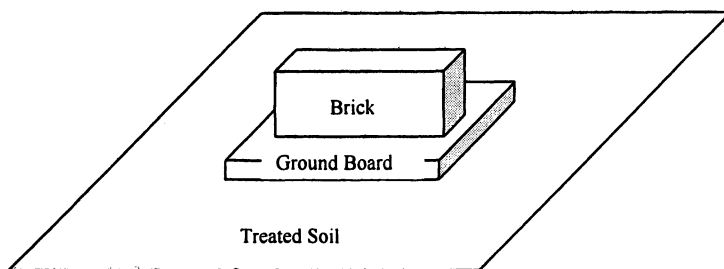
Figure 2. Schematic of the Ground Board Test

Concrete Slab Test

The concrete slab test was initiated in 1967 in response to the introduction of organophosphate, pyrethroid and carbamate insecticides (*4*). It was feared

that these products would be less persistent in the environment, and the new test would better approximate their actual use.

The test plot is prepared in the same way as the ground board test, except that a 53 × 53 cm wooden frame is installed around the worked ground before the termiticide is applied. The termiticide is mixed according to the label instructions, and 760 ml is applied to the soil. A 53 × 53 cm sheet of plastic is placed over the treated area as a vapor barrier. A 10 × 10 cm i.d. polyvinyl chloride (PVC) pipe is centered over the treated area to serve as an inspection port, and concrete is poured to cover the treated area to a depth of about 5 cm. After the concrete has dried, the vapor barrier within the PVC pipe is carefully removed to expose the treated soil beneath. Care is used to ensure that disturbance of the treated soil is limited. A 4 × 9 × 6 cm piece of southern yellow pine is placed in the PVC pipe and the pipe is capped (Figure 3) (4). The wood is inspected at one-year intervals for damage and the presence of termites, and the damage is rated according to one of the scales described below.
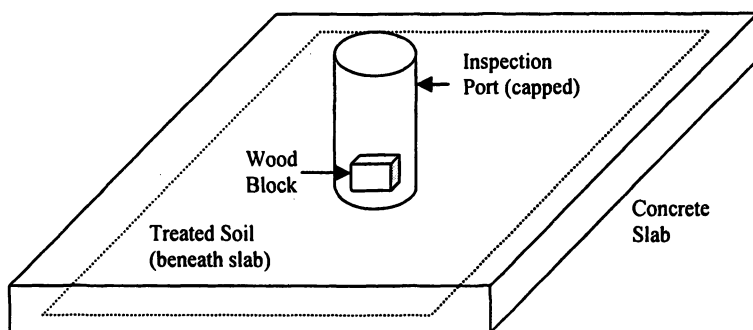
Figure 3. Schematic of the Concrete Slab Test.

Wood Damage Rating

Two scales are used for the evaluation of wood damage by termites. The older of the two scales, and the one most commonly used by the Forest Service, is the "Gulfport Scale," which was developed over 40 years ago. It has values of 0 (no evidence of termite attack), 1 (nibbles to surface etching, no penetration), 2 (penetration, limited damage), 3 (general damage), 4 (heavy damage) and 5 (destroyed) (6).

The other scale is the American Society for Testing and Materials (ASTM) scale. Unlike the Gulfport scale, which measures wood damage, the ASTM scale is a "wood soundness scale" measuring loss of cross-sectional area and has

values of 10 (sound), 9 (nibbles to 3% loss), 8 (penetration; 3 – 10% loss), 7 (penetration; 10 – 30% loss), 6 (penetration; 30 – 50% loss), 4 (penetration; 50 – 75% loss) and 0 (failure) (7). Table 1 shows the approximate equivalency of the two scales.

Test Plot Layout

Until the early 1990s, nearly all products were laid out in what is now referred to as the "conventional layout." In this layout, which is still used for most products, individual test plots (ground boards and concrete slabs) are separated in a grid on 1.5-m centers. Each of ten replications contains a mixture of rates, products, test methods and control plots arranged in a randomized block design (Figure 4). Replications are laid out in two tiers of five replications per tier. The conventional layout utilizes about 0.08 ha.

Tests of Fipronil (Termidor®)

In 1994, Termidor® 80 WG (Rhône-Poulenc), the active ingredient of which is fipronil, was installed in Forest Service field tests in a conventional layout. Figure 5 shows the number of years without termite attack for Termidor 80 WG in the concrete slab tests. As of 2003, there were no termite attacks at any of the plots at the four sites, down to the lowest labeled rate of 0.0625% a.i. However, it was noticed that termite pressure in the fipronil control groups at all four sites was less than expected (Figure 6, shaded bars). Termite attack in the control plots rarely surpassed about 30%. The simplest explanation for this was that it was simply a "bad time for termites" and termite pressures were low, leading to low attack rates at the control plots. If this were the case, it could not be said that the results in the test plots were due to the presence of fipronil; it may simply be that there were few termites present. This presented a significant problem for regulatory officials.

Examination of other tests at the same locations in the same years, however, revealed that termite attack on the control plots of other tests at the same site were, in all cases, notably higher than those in the fipronil test (Figure 6, open bars). So it seemed that the lower termite pressure was confined to the study containing fipronil, a phenomenon dubbed the "area effect."

One observation was that the study contained several doses of fipronil, many of them much higher than the labeled rate. Could it be that so much fipronil was applied to the area that it caused attrition of the local termite population? Figure 7 illustrates this possibility, the "coverage" hypothesis. In each replicate, 22 of the 49 available plots contained some dose of fipronil, and an additional 16 plots contained another product and four control plots. In many cases, control plots were nearly completely surrounded by fipronil-treated plots.

Table 1. Equivalency of the Gulfport Wood Damage Scale and the ASTM Wood Soundness Scale

Gulfport	ASTM
0 No attack	10 Sound
1 Nibbles to surface etching; no penetration	9 Nibbles to 3% loss
2 Penetration; limited damage	8 Penetration; 3-10% loss
3 General attack	7 Penetration; 10-30% loss
	6 Penetration; 30-50% loss
4 Heavy attack	4 Penetration; 50-75% loss
5 Destroyed	0 Wood failure
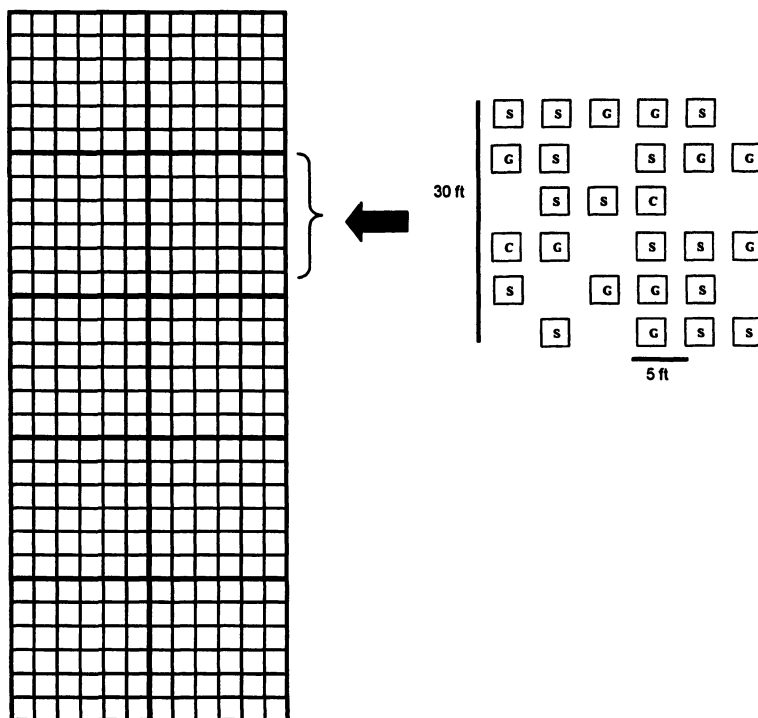
Figure 4. Conventional Layout of Ground Board (G), Concrete Slab (S) and Control Plots (C).
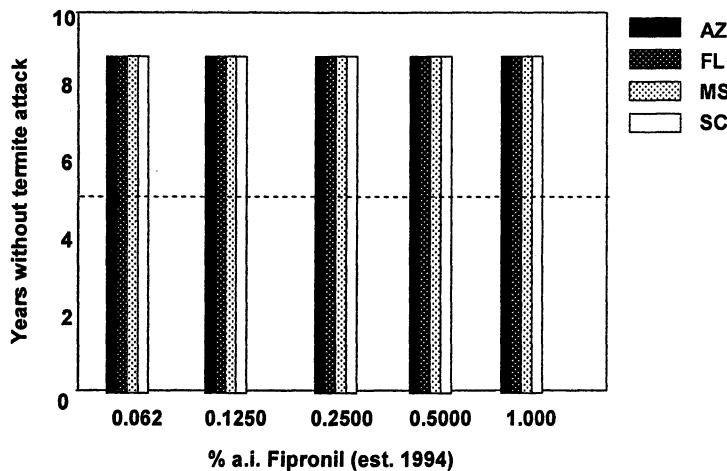
Figure 5. Years without termite attack as of 2003 for Termidor 80 WG for the concrete slab test in the conventional layout. The dashed line represents the EPA's five-year testing requirement. This product is labeled for use at the 0.0625 and 0.125% rates.
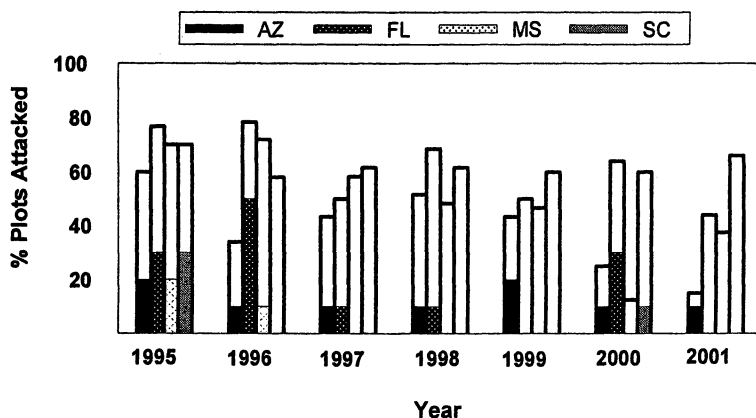
Figure 6. Percentage of concrete slab control plots hit at the four sites for fipronil (shaded bars) and for another product installed that same year separately (open bars).

Another hypothesis, not necessarily mutually exclusive of the coverage hypothesis, is that transfer of fipronil between individual termites could have led to the reduction of the local termite population, the "transfer" hypothesis. Lethal amounts of fipronil have been shown to transfer from one termite to another in laboratory tests (8). Termites encountering fipronil in treated soil in the field could have transferred lethal amounts to other termites, although this has never been demonstrated in the field. The coverage and transfer hypotheses are not mutually exclusive because mortality due to transfer may not be significant until a critical level of fipronil in the environment is reached. Other hypotheses exist in addition to these two. It may be possible, for example, that the presence of a repellent in one plot may increase the probability of termites occurring in an adjacent plot, one that contains a toxic level of a non-repellent. This is related to the coverage hypothesis, and has not been conclusively demonstrated in the field. Regardless of the cause of the area effect, the layout of the test was modified to eliminate this effect.

Expansion of Plot Layout

In 1998 and 1999, Termidor MEC and Termidor SC, respectively, were installed in field tests at the four testing sites in an "expanded layout." The test used the ground board and concrete slab tests, but individual groups (concentrations and test methods) were separated from one another. Each group contained all ten test plots (Plots A to J), with two internal control plots (Plots K and L) interspersed within the ten (Figure 8). In addition, there was one group of ten control plots, plus two internal controls of the control, included in the test. Each group was then separated by 15 m to ensure that an area effect caused by one concentration would not interfere with other concentrations (Figure 8) (9). This distance, 15 m, was confirmed by DeHeer and Vargo (10), who report that *Reticulitermes* foraging areas are small, e.g. the longest linear distance separating two sites used by the same colony averaged 5.6 m (or about 18.4 feet). A 23 m buffer was included around the study area to ensure that this test did not affect other tests in progress nearby.

Modification of the test layout yielded satisfactory results. Comparing the percentage of Termidor SC control plots attacked between the internal controls, the external controls, and the control plots of another study installed the same year, the same trends are observed for all three control groups. If the area effect was significant in this layout, we would expect the internal controls to have a lower percentage of plots attacked. This was not observed, and was always within 10% of the external controls or the controls for the other product (Figure 9).
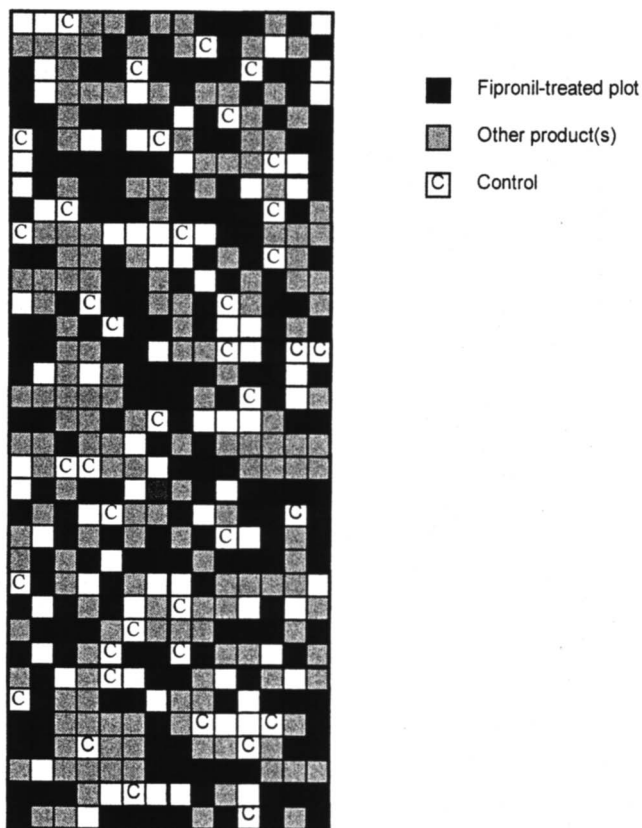
Figure 7. Coverage of Fipronil in the Conventional Layout at the Mississippi Test Site.
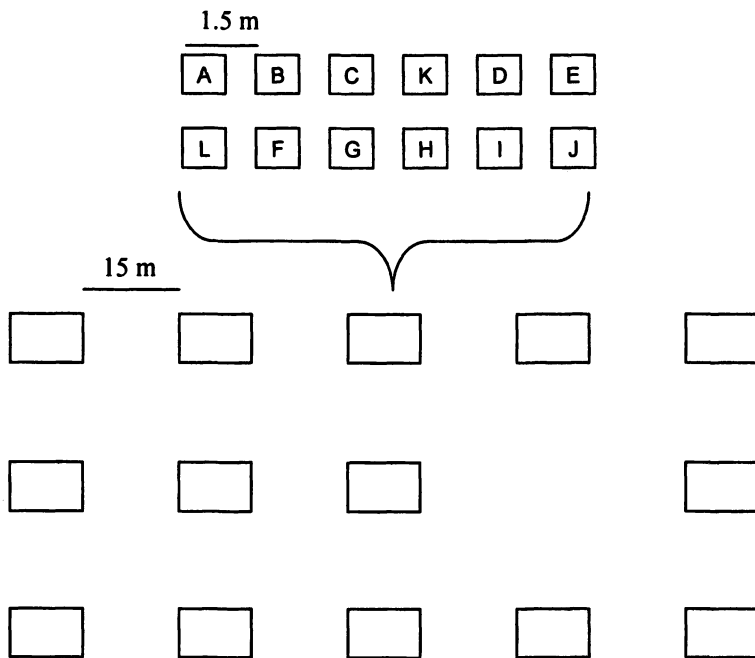
Figure 8. Expanded Layout used for DANR Products
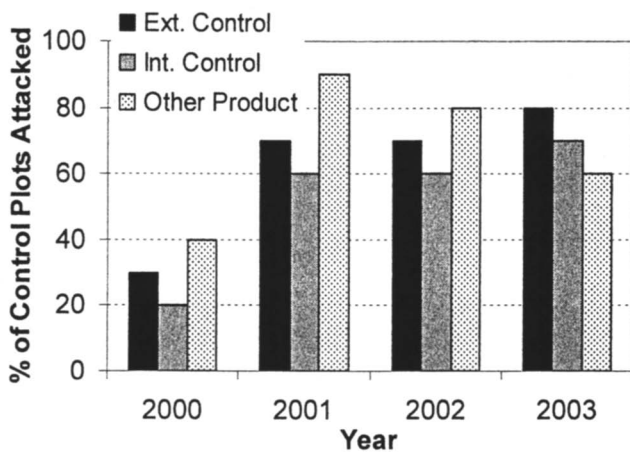
Figure 9. Percentage of control plots attacked by termites for Termidor SC in the expanded layout and for another product installed separately in the same year.

Limitations of the Expanded Layout

If the expanded layout solves the problem of the area effect, why not install all products in the expanded layout? The answer involves labor and land use. It requires about the same amount of labor to clear, prepare and treat one expanded layout with one product as it does to clear, prepare and treat a conventional layout, which can accommodate three products. Therefore, to install all products in an expanded layout would require about three times the labor.

Regarding land area, the conventional layout requires about 0.08 ha, and can usually accommodate three products at five concentrations, plus control plots. The expanded layout, however, including the 23-m buffer zone, requires about 1.8 ha, or 22 times the area of the conventional layout. Add this to the fact that only one product can be installed in a single expanded layout, installation of three products would require three expanded layouts and would use enough land to install conventional layouts for 66 years. In one year, we would use more land than that used in the entire history of the testing program! In addition, the tests must be installed on level ground due to erosion and runoff concerns and to better simulate a building site, and this further restricts the amount of suitable land. There is also the issue of public land use. The tests are conducted on public land, some in popular hunting areas, and although we have maintained amicable relations with local residents, this is likely to change if inordinate amounts of land are being used for testing.

Laboratory Tests for Area Effects

To determine if a new product requires an expanded layout, laboratory screening tests are helpful. The remainder of this chapter will examine several potential tests that may be modified for this purpose.

The first test is an insecticide transfer test such as that described by Shelton and Grace (8). In this test, "donor" termites are exposed for a short period of time to soil treated with the insecticide. These donors are then placed on untreated soil with naïve, or "recipient" termites. The mortality of recipient termites is recorded and a significant increase in recipient mortality is taken as evidence of insecticide transfer. It is possible to measure insecticide levels in recipient termites, but this has its limitations. Termites are soft-bodied and begin to decompose soon after death; recovery of dead termites from test apparatuses is very difficult. Sampling living termites only samples those that have not received a lethal dose. So even though transfer can be demonstrated, it does not indicate if enough of the material has been transferred to result in death of the insect. There would be a narrow window in which living termites receiving a lethal dose may be sampled before death. Currently, transfer is used by us as a

criterion for installing a new product in the expanded layout, as transfer is one factor that potentially contributes to an area effect. However, most active ingredients that transfer in the laboratory have not shown an area effect in the field test, so this test by itself is not a conclusive indicator of area effects.

A test similar to that reported by Esenther (*11*) may be helpful. In this test, a central reservoir or "nest" area is connected to two or more satellite foraging areas, one or more containing treated soil and the other(s) containing untreated soil. A decrease in the number of termites foraging in the untreated area or in the nest area could be used as an indication of an area effect. However, in small tests such as this, death of termites visiting the treated area may lead to false positive results due to the low number of termites used in the test. In the field, termite colonies may contain hundreds of thousands to millions of individuals, with reproduction by the queen (*1*), while a few thousand is the limit in laboratory tests. It is also rare to include a queen and accompanying males in a laboratory test due to the difficulty of obtaining queen termites.

A larger test with more termites may alleviate the problem of attrition. Portable swimming pools are filled with soil, with a central wood source for food, and can accommodate a much larger number of termites. An area of the pool could be treated with the insecticide of interest, and decreases in termite activity in monitoring stations placed elsewhere in the pool may indicate an area effect. This test has at least two limitations, however. First, termites must find both the treated area and the monitoring stations; this may not happen in all replications. Second, it provides only a qualitative endpoint; presence of a treatment here, are termites present over there, yes or no? The number of termites visiting a monitoring station is unreliable because it varies over time in the absence of any treatment (*12*). In addition, the concentration of active ingredient in termites recovered from monitoring stations is unreliable because it would fluctuate widely, depending upon the number of termites that have visited the treated plot and transferred the compound to nestmates. Finally, this test procedure would only measure insecticide levels in termites that have not received a lethal amount of the chemical.

Accelerated field tests have been proposed to determine area effects. These tests would resemble a conventional layout, and could be installed at sites convenient to the Unit headquarters in Starkville, MS. If area effects were noted within a few years in the reduced-scale test, then the product would be reinstalled in the expanded layout at the four regular testing sites. This would be the most reliable indication that the product may have area effects in the full conventional layouts. To be reliable, however, it would be necessary to determine the termite pressure at the accelerated field site beforehand, a process that takes at least several months. "Accelerated," furthermore, is a relative term. It may take two or three years to determine if a product has area effects in an accelerated test. Consequently, the registrant would be asked to wait up to eight years for five years of data.

Based on the number of requests we have received for testing, DANR compounds with potential area effects are increasing in popularity. Work is currently underway to develop efficient laboratory tests for area effects. The method used will likely be modifications of one or more of the tests described, as each method provides useful information. The transfer test is one such test currently in use. This work will increase the likelihood of effective products reaching the market in a timely fashion, serving both the consumer and the manufacturer.

Acknowledgments

References

1. Su, N-Y., Scheffrahn, R. H. In Termites: Evolution, Sociality, Symbioses, Ecology. Abe, T., Bignell, D. E., Higashi, M., eds.; Kluwer Academic Publ., Boston, MA, 2000, pp. 437-453.
2. United States Environmental Protection Agency. Pesticide Registeration (PR) Notice 96-7. Washington, DC, 1996, 16 pp.
3. Unites States Environmental Protection Agency. Product Performance Test Guidelines, OPPTS 810.3600, Structural Treatments. Washington, DC, 1998, 4 pp.
4. Beal, R. H. Pest Control Tech. **1984**, 12, 71-72, 74.
5. Wagner, T. L., Mulrooney, J. E., Peterson, C. J. Pest Control February 2002, pp. 24-25, 28, 30.
6. Wagner, T. L., Mulrooney, J. E., Peterson, C. J., Shelton, T. G. Pest Control February 2004, 3 pp.
7. American Society for Testing and Materials. Designation D 1758 – 96. American Society for Testing and Materials, West Conshohocken, PA, 1996, pp. 248-254.
8. Shelton, T. G., Grace, J. K. J. Econ. Entomol. **2003**, 96, 456-460.
9. Wagner, T. L. Sociobiology **2003**, 41, 131-141.
10. DeHeer, C. J., Vargo, E. L. Molecular Ecology **2004**, 13, 431-441.
11. Esenther, G. R. Proceedings of the 16th Annual Meeting of the International Research Group on Wood Preservation, May 12 – 17, 1985, Brazil. 14 pp.
12. Esenther, G. R., Beal, R. H. J. Econ. Entomol. **1974**, 67, 85-88.

Chapter 15

2-Acylimino-3-phenylthiazolines: A New Family of Bleaching Herbicides

Yuzuru Sanemitsu, Shinichi Kawamura, Junichi Satoh, Tadasi Katayama, and Shunichi Hashimoto

Agricultural Chemicals Research Laboratory, Sumitomo Chemical Company Ltd., 2–1, Takatsukasa, 4-Chome, Takarazuka, Hyogo, 665–0081, Japan

In our continuing effort to discover new heterocyclic compounds as useful agrochemicals, we disclosed a new bleaching herbicide lead represented by 5-methylene-3-phenylthiazolidine, **4**, which has demonstrated a weak herbicidal activity. Further structural optimization of this new lead led to the discovery of 2-(N-difluoroacetylimino)-5-methyl-3-(3-trifluoromethylphenyl)-1,3-thiazoline (**S-3085**) belonging to a new class of preemergent bleaching herbicides. **S-3085** demonstrated excellent control of a number of grass and broadleaf weeds with good selectivity on cotton. Physiological and biochemical properties of 2-acylimino-3-phenylthiazolines has been investigated. Their primary mode of action was direct inhibition of phytoene desaturase which resulted in decreased biosynthesis of colored carotenoides and subsequent photooxidation of chlorophyll in the light. A summary of the discovery, structure-activity relationships and mode of action of this new class of herbicides is reported.

197

$$F_3C \qquad \qquad Me$$

S-3085
(Preemergence Cotton Herbicide)
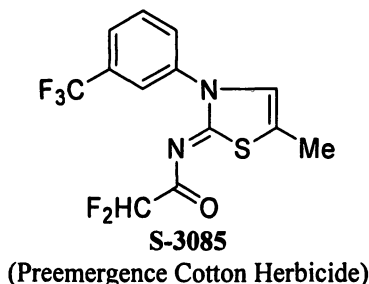
Recently, a variety of heterocyclic compounds containing nitrogen and sulfur atoms have been developed as useful and practical agrochemicals. Our attention was directed to these heterocycles as screening targets to create novel bioactive compounds (*1*).
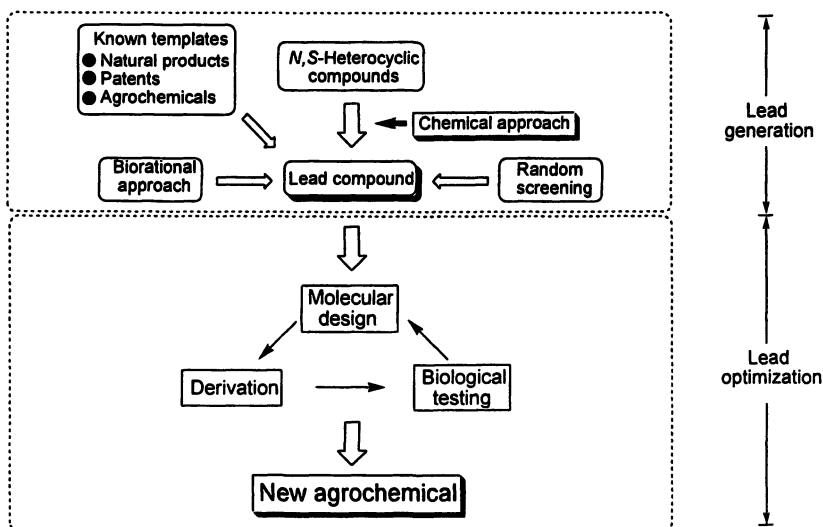
Figure 1. Process of Drug Discovery

In our methodology to search for a new lead, which we call lead generation, three approaches are possible as shown in Figure 1. The first is to use the structure of known templates, such as bioactive natural products, patents and commercial agrochemicals. The modification of these structures has resulted in the formation of compounds with desired properties, thus many researchers have

employed this approach. The second approach, often called biorational approach, is derived from the detailed structural knowledge of the receptor or the active site of an enzyme. However, this method has not led to any new agricultural leads, since the species tested are diverse and their biochemical information is lacking in agrochemical research. The third approach is random screening. The test compounds can be secured from numerous sources, including synthesis, commercial reagents, arrangements with other laboratories, and naturally occurring compounds. The more structurally novel, innovative leads are most often found in the latter sources. A recent example of success based on this method includes the strobilurin fungicides. In this work we selected a fourth approach, the chemical approach to *N*- and *N,S*- heterocyclic compounds with an expectation of discovering a new chemical class with a novel mode of action (*2*). This method has been used to find a number of heterocyles with the interesting biological activities (*3*).

While exploring the synthesis of *N,S*-heterocycles using heterocumulenes, such as the acyl isothiocyanates (*4*), we discovered weak herbicidal activity for 3-(3-chlorophenyl)-2-(*N*-ethoxycarbonylimino)-5-methylene-1,3-thiazolidine, (*4*). This new herbicide lead, 4, showed bleaching symptoms at 8000 g/are. Our interest in the structure and herbicidal activity of this novel heterocycle encouraged us to examine a systematic study on the thiazolidine herbicide.

Lead Discovery

The reaction of nucleophiles with various heterocumulenes, such as isothio-cyanates or acyl isothiocyanates, has been widely studied, and the scope and limitation of these reactions have been defined (*5*). The utility of heterocumulenes as building blocks to a variety of *N,S*-heterocycles prompted us to investigate the behavior of acyl isothiocyanates toward *N*-substituted anilines (*6*).

Starting with the commercially available ethoxycarbonyl isothiocyanate 2 as the heterocumulenes, we studied the cyclization reaction of the labile thiourea 3 formed by reaction with the *N*-propargyl anilines, 1 (Figure 2). As a result, we found new transformation reactions of thioureas 3 into the novel heterocycle, 2-(*N*-ethoxycarbonylimino)-5-methylene-1,3-thiazolidines, 4. This transformation was achieved through an one-pot reaction without isolation of the resultant thioureas 3 to generate 4 in excellent yields. Among the 1,3-thiazolidines prepared for the herbicidal evaluation test, 4 showed weak herbicidal activity at 8000 g/are with bleaching symptoms. This finding encouraged us to examine a systematic screening study of 4 as an initial lead of a new bleaching herbicide.
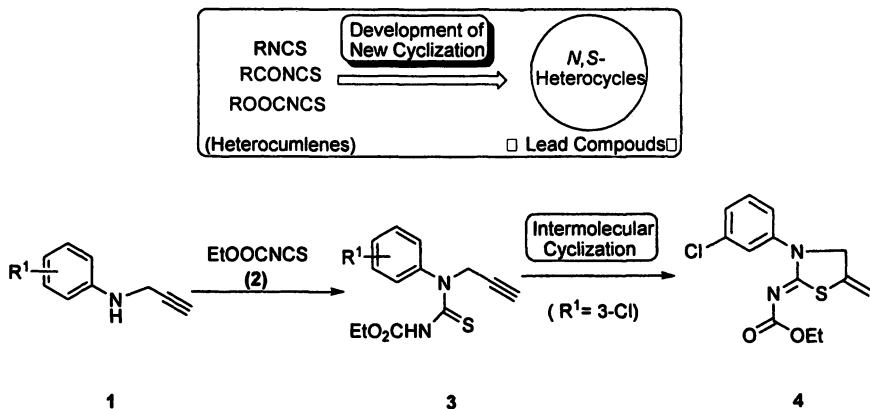
Figure 2. Synthetic Strategy for New Lead and Its Discovery

Considering the similarity of the structure and characteristic symptoms with known bleaching herbicides (7), the activity of the lead, 4 allowed us to propose the model for herbicidal activity shown in Figure 3. Namely, a key structure requirement for herbicidal activity is the presence of an acylimino group incorporating a nitrogen atom in conjunction with a carbonyl group through an imino function as indicated by the bold lines in the substructure .

To clarify the structural requirements of compound 4 for herbicidal activity, a systematic evaluation of the effects of changes in the acyl group and in the thiazolidine nucleus was undertaken. Replacement of the ethyl ester group by hydrogen,11, or phenyl, 12, resulted in the loss of herbicidal activity. Also, all compounds, which bear no acyl groups, Compounds 13 and 14, showed a complete loss of activity (Figure 4). From these results, we could clarify that the presence of the acyl groups conjugated with an imino function are essential for activity.

Based on our hypothesis, compounds incorporating an acylimino group in which the core thiazolidine ring was replaced with other 5- and 6-membered heterocycles were targeted for synthesis. As can be seen in Figure 4, Compound 6 in which the methylene unit in an initial lead was deleted, showed more potent herbicidal activity than 4. However, replacement of the ring sulfur atom in 6 with an oxygen, 8 or a nitrogen, 10 resulted in a lowering of activity, compared to that of 6. The 6-membered homolog of 9 showed very weak herbicidal activity.

Intrigued, we soon became aware of a great increase in activity when going from compound 4 to the thiazoline nucleus 5 as a second lead (8). The
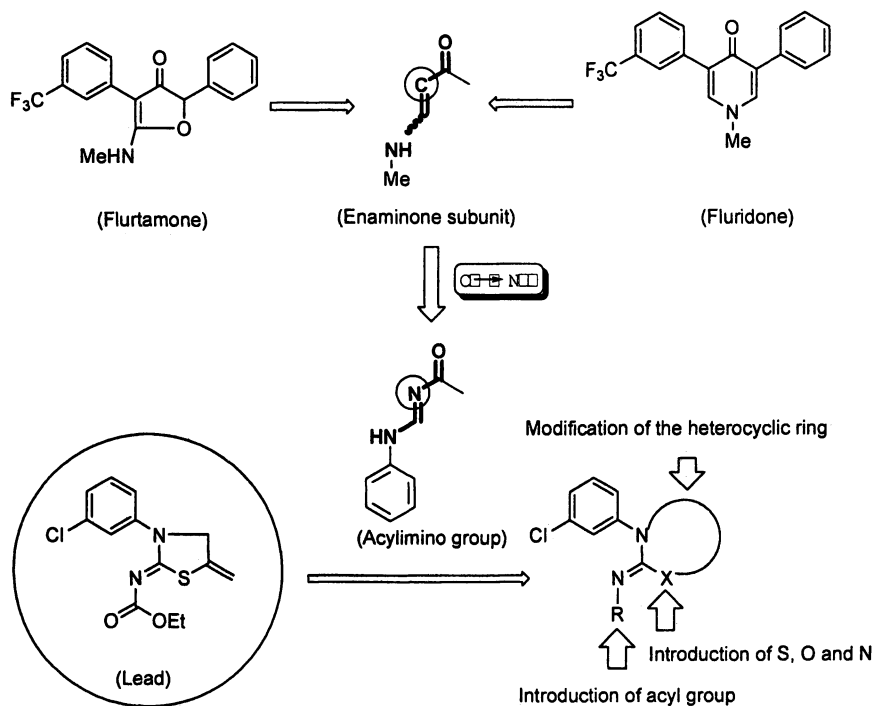
Figure 3. Structural Similarity with Known Herbicides and Design Plan

thiadiazole **7** was also active, but provided diminished activity relative to the most active thiazoline **5**. Our interest in the structure and herbicidal activity of this novel heterocyclic compound, **5** prompted us to examine further screening studies on thiazoline herbicides.

Optimization Development from a Second Lead

As a starting point for structural optimization of the second lead, we divided the core structure into three subsections, the phenyl (X), the imino group (Y), and the thiazoline nucleus (R^1 and R^2) (Figure 5). First, we synthesized the 2-(*N*-ethoxycarbonylimino)-1,3-thiazolines that possessed a variety of substituents at each position of the phenyl ring to examine the effect on herbicidal activity. Preemergence activities are summarized in Figure 6. Substitution on the phenyl moiety was preferred in the *meta* position and we observed a progressive

(Heterocyclic ring)

Active
(Acylimino group)

5 (Second lead)   6   7   8

Slightly active
(Acylimino group)

9   10   4 (Initial lead)

No active
(No acylimino group)

11   12   13   14
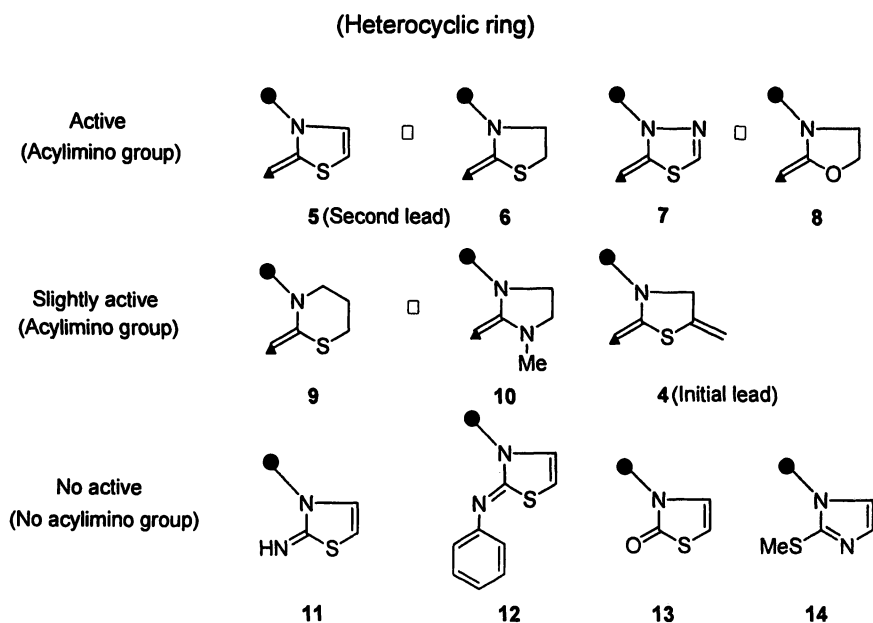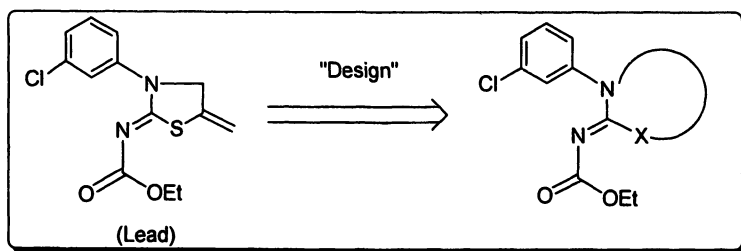
Figure 4. Effect of Heterocyclic Ring on Relative Preemergence Activity
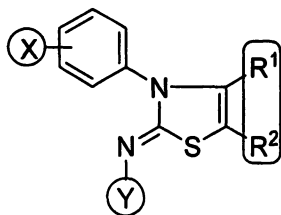
Figure 5. Optimization Strategy for Second Lead

decrease in activity as the substituent is moved to the *ortho* or *para*-position. When a trifluoromethyl group was introduced in the *meta*-position the activity was the greatest. The level of activity of the trifluoromethoxy derivative approached that of the trifluoromethyl, indicating that lipophilic electron-withdrawing groups provided optimum activity.

Secondly, the herbicidal effect at the imino *N*-subtituents was investigated. Relative activity of various 3-phenyl-1,3-thiazolines with optimum substitution in a phenyl ring is shown in Figure 6. As can be seen, the substitution requirements at this position was quite specific. Substituents incorporating a
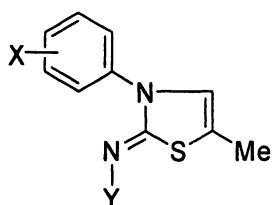
X = *m*-substituted >> *o*- and *p*-substituted

$3\text{-}CF_3 > 3\text{-}OCF_3 > 3\text{-}Br > 3\text{-}Cl$

Y = COMe > COOEt > CONHMe > CN >> H, Ph

$\boxed{COCHF_2 > COCF_3 > CO\ Me > COPh, COBn}$

(Aceyl group is the best)

Figure 6. Effect of X and Y Substituents on the Preemegence Activity

carbonyl function such as acyl groups greatly enhanced the activity. However, activity fell off rapidly when Y= hydrogen or phenyl. These results indicate that the conjugation with a carbonyl group through an imino double bond is key to the activity of the bleaching herbicides. The most active analog in this series was the *N*-acyl derivative. In particular, the highest activity was obtained when Y was a lipophilic electron-withdrawing group such as difluoroacetyl or trifluoroacetyl. When the difluoroacetylimino derivative was applied preemergently, excellent broadleaf control was achieved with cotton showing good tolerance.

Finally, our attention was directed toward the activity optimization at the 4- and 5-positions on the thiazoline ring (Figure 7). In the series of 4-substituted derivatives (where R^2 is methyl), introduction of various substituents, such as methyl, halogen and ester groups, resulted in diminished activity. In contrast, the excellent herbicidal activity of the 5-substituted derivatives was observed

when R^1 = hydrogen. When R^1 is held constant as hydrogen, R^2 equal to methyl gave the highest level of activity with lower efficacy observed for halogen, mercaptomethyl, hydrogen or larger alkyl.
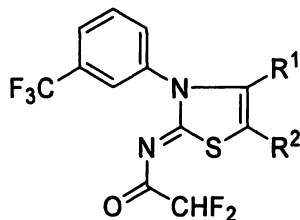
R^1 = H >> Me, Br > Et, COOMe

R^2 = Me > Et, Br, Cl > SMe >> H

Figure 7. Effect of R^1 and R^2 Substituents on Preemergence Activity

On the basis of the limited structure-activity relationships found here, great enhancement of activity was only achieved by the introduction of a *meta* substituent in the phenyl ring, the imino *N*-substituent, and a substituent at the thiadiazoline 5-position. From the viewpoint of the preemergence herbicidal efficacy and the selectivity on cotton, one of these compounds, 2-(*N*-difluoro-acetylimino)-5-methyl-3-(3-trifluoromethylphenyl)-1,3-thiazoline, **S-3085** was finally selected as a promising candidate for precommerciallization.

Mode of Action

The mode of action of the phenylthiazolines has been investigated by looking for the accumulation of metabolic intermediates in chlorotic cress leaves. Treated plants showed an increase in levels of a compound that can not be observed in controls, identified by UV spectroscopy and HPLC co-chromatography with an authentic phytoene. The latter has been produced by the application of the known carotenoid synthesis inhibitors such as flurtamon and identified independently by UV and mass spectroscopy. From these results, it can be assumed that chlorosis is caused by inhibition of carotenoid synthesis at the phytoene desaturase step.

In order to exclude the possibility that inhibition of phytoene desaturation is caused by indirect or regulatory mechanisms, direct interaction of substituted phenylthiazolines with phytoene desaturase was demonstrated by *in vitro* studies. As a result, with increasing concentrations, more phytoene is retained which means that less phytoene was desaturated. Therefore, less β-carotene is formed as the end product of this *in vitro* biosynthetic chain. Interaction of phenylthiazolines is very similar to inhibition of this enzyme by flurtamone. For the latter herbicide, it has been shown to be a reversible non-competitive inhibitor of phytoene desaturase (9).
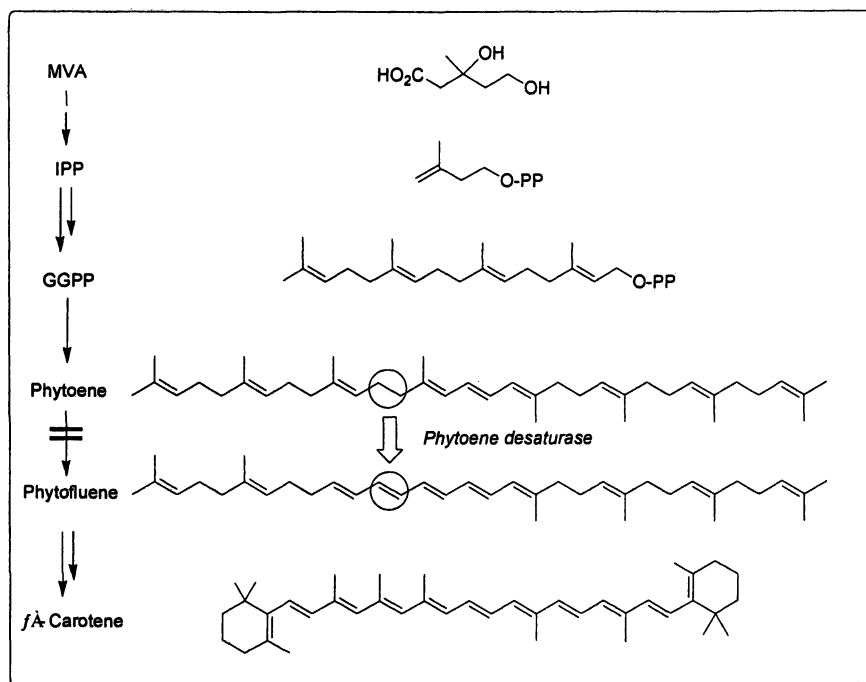
Figure 8. Inhibition of Cartenoid Biosynthesis by 2-Acylimino-thiazolines

With reduced carotenoid levels, the herbicidal effect of these compounds are the results of photooxidative damage of chlorophyll followed by chloroplast destruction. Loss of carotenoid and chlorophyll pigment results in the characteristic bleached appearance of the treated plants.

Cotton Field Testing

We were particularly interested in compounds of this class due to their cotton tolerance. **S-3085** was field tested as a cotton herbicide in postemergence application on a variety of weeds. These weeds were morningglory, velvetleaf, pigweed, lambsqarter, annual grasses, and yellow nutsedge. **S-3085** demonstrated excellent control of a number of broadleaf weeds while providing weed control of a number of grass weeds with good safety on cotton at rates as low as 100 g/ha. Nonetheless, raising the application rates to 300 g/ha gave outstanding control of broadleaf and grass weeds. However, commercial development of **S-3085** was not pursued due to a narrow margin of crop safety at high rates of application

Conclusions

As a methodology to search for a new lead, we focused on the chemical approach using *N,S*-heterocycles. This approach led to the evolution of 5-methylene-thiazolidines as the lead to bleaching herbicides. Further structural modifications based on the parent compound resulted in the creation of a new family of bleaching herbicides, 2-(*N*-difluoroacetylimino)-5-methyl-3-(3-trifluoromethylphenyl)-1,3-thiazoline, **(S-3085)** with potent preemergence herbicidal activity and selectivity on cotton crops. On the basis of biochemical studies, 3-phenylthiazolines have been characterized as a new inhibitor of phytoene desaturase. Facile syntheses of 1,3-thiazolines and the manufacturing process toward **S-3085** will be reported in future publications.

Acknowledgments

References

1. Sanemitsu, Y.; Mizutani, M.; Nakayama, Y. *J. Synth. Org. Chem.*(Japan). **1992**, 50: 875-886.
2. Kawamura, S.; Hamada, T.; Satoh, R.; Sanemitsu, Y.; Sandmann, G.; Babczinski, R. *Synthesis and Chemistry of Agrochemicals III*, Baker, D. R.; Feynes, J. G.; Steffens, J. J. Eds.; ACS Symposium Series No. 504; American Chemical Society : Washington, D. C. **1992**, pp 103-108.
3. Kawamura, S.; Satoh, J.; Sakaki, M.; Sanemitsu, Y. *J. Agric. Food Chem.* **1993**, 41: 288-291.
4. Nakayama, Y.; Sanemitsu, Y.; *J. Org. Chem.* **1984**, 49: 1703-1707.
5. Ulrich, H. *Cycloaddition Reactions of Heterocumulenes*, Blomquist, A. T. Eds.; Organic Chemistry, A Series of Monographs; Academic Press; New York and London; **1967**, Vol.9, pp 129-219.
6. Kawamura, S.; Sanemitsu, Y. *J. Org. Chem.* **1993**, 58: 414-418.
7. Boger, P.; Sandmann, G. *Target Sites of Herbicide Action*, Boger, P.; Sandmann, G. Eds.; CRC Press: Boca Roton, FL. **1989**.
8. Kawamura, S.; Izumi, K.; Satoh, J.; Sanemitsu, Y. European Patent EP 446,802, **1991**.
9. Sandmann, G.; Ward, C. E.; Lo, W. C.; Nagy, J. O.; Boger, P. *Plant Physiol.* **1990**, 94: 476-478.

Chapter 16

The Discovery of Proquinazid: A New and Potent Powdery Mildew Control Agent

Thomas P. Selby, Charlene G. Sternberg, James F. Bereznak, Reed A. Coats, and Eric A. Marshall

Stine Haskell Research Center, DuPont Crop Protection, Newark, DE 19714

Substituted pyrido[1,2-a]pyrimidin-4-ones, quinazolin-4-ones and thieno[2,3-d]pyrimidin-4-ones represent a new class of potent antifungal agents possessing high protectant activity against powdery mildew strains of fungi. These compounds provide plant protection by preventing pathogen penetration via potent inhibition of appressorial formation following spore germination. The lead compound showed interesting but weak powdery mildew activity. Optimization provided much more active analogs with proquinazid (DPX-KQ926) showing optimum efficacy. Proquinazid consistently gave outstanding powdery mildew control in field tests on cereals, grapes and other crops at very low rates of application. Field performance exceeded that of commercial protectants with excellent residual disease control. Proquinazid holds great promise for mildew control and will be a valuable tool for growers combating this disease. This paper focuses on the discovery of proquinazid with an emphasis on chemistry, biology, SAR and field activity of candidates from this class of chemistry.

209

Widespread use of commercial fungicides for powdery mildew control has generally been accompanied with the onset of resistance or reduced pathogen sensitivity. In an on-going effort to combat this problem, the crop protection industry remains committed to finding new products with novel modes-of-action for the marketplace.

We have found that substituted pyrido[1,2-a]pyrimidin-4-ones of formula 1, quinazolin-4-ones of formula 2 and thieno[2,3-d]pyrimidin-4-ones of formula 3 (where W is a heteroatom – preferably oxygen) represent a new class of antifungal agents possessing high protectant activity against powdery mildew fungi (*1-4*). Although non-toxic on the leaf surface, these compounds provide plant protection by preventing pathogen penetration via potent inhibition of appressorial formation following spore germination and germ tube development.

Pyridopyrimidinone 4, the lead compound, showed interesting but very weak powdery mildew activity at high concentrations. Early in our follow-up, we became aware of related quinazolinones discovered to have powdery mildew activity over thirty years ago at DuPont (*5,6*). Although active in greenhouse tests, quinazolinones such as 5 gave disappointing field results. Our findings with pyridopyrimidinones prompted the preparation of new quinazolinones and thienopyrimidinones that were found to maintain very high activity under field conditions. Providing excellent mildew control on cereals, grapes and other crops at very low rates, proquinazid was selected for commercial development.

Proquinazid (DPX-KQ926)
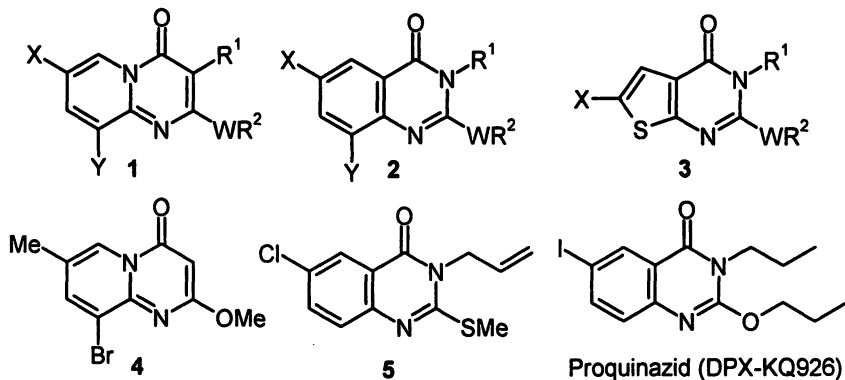
Chemistry

Pyridopyrimidinones 1a were made by the route shown in Figure 1. By a known thermal condensation method (*9*), aminopyridines of formula 6 were heated neat with substituted malonates (where generated ethanol was removed via distillation) to give intermediates of formula 7 (zwitterionic form shown). Alkylation of 7 in the presence of potassium carbonate in *N,N-*

dimethylformamide took place predominantly on oxygen to afford pyridopyrimidinones **1a** as major products. Some alkylation on nitrogen occurred, giving rise to the more polar mesoionic structures **8** (*10*). These isomers were readily separated by silica gel column chromatography (compounds of formula **8** had limited antifungal activity).
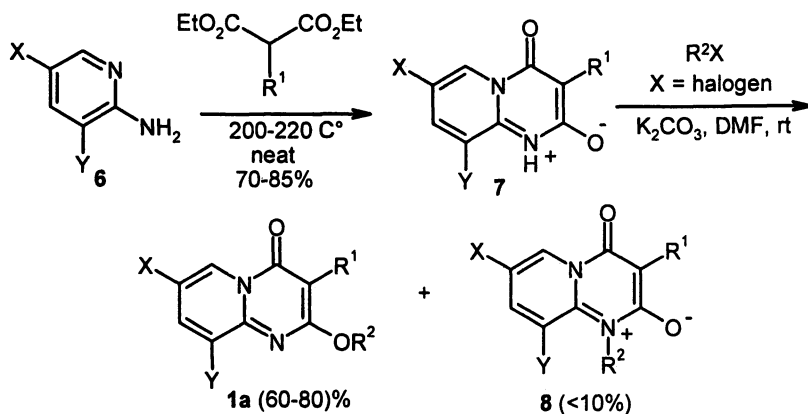
Figure 1. Synthesis of 2-Alkoxy Substituted Pyridopyrimidinones
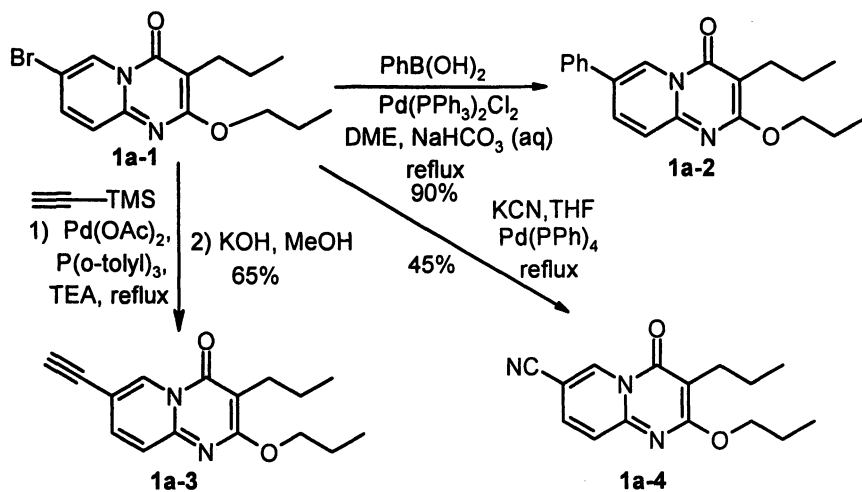
Figure 2. Introduction of Pyridopyrimidinone Substituents by Cross-Coupling

Substituents were also introduced on the pyridopyrimidinone ring via palladium-mediated cross-coupling reactions as outlined in Figure 2. Cross-coupling of 7-bromo-2-propoxy-3-propylpyridopyrimidinone **1a-1** (made by the method in Figure 1) with phenyl boronic acid, potassium cyanide or trimethylsilylacetylene (followed by desilylation with base) gave the phenyl, acetylenic and cyano substituted products **1a-2**, **1a-3** and **1a-4**, respectively.

The preparation of 2-*n*-propylthio and 2-*n*-propylamino substituted 7-chloro-3-*n*-propylpyridopyrimidinones **1b** and **1c** is outlined in Figure 3. Heating **7a** in phosphorous oxychloride gave a modest yield of the 3,7-dichloropyridopyrimidinone **8**. Displacement of the 2-chloro group on **8** with sodium *n*-propylmercaptide afforded *n*-propylthiopyridopyrimidinone **1b**. Alternatively, reaction of **7a** with triflic anhydride and pyridine gave the triflate **9**; displacing the triflate gourp with *n*-propylamine yielded *n*-propylaminopyridopyrimidinone **1c**.
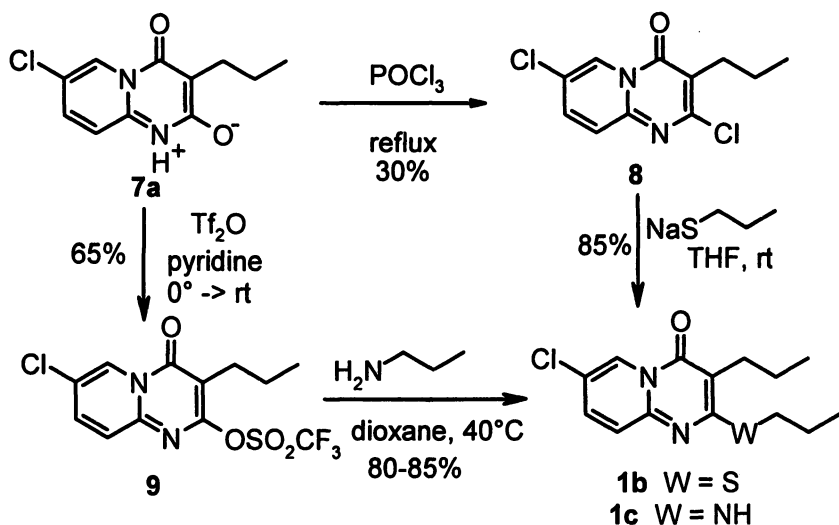
Figure 3. Synthesis of 2-Alkylthio and 2-Alkylamino Pyridopyrimidinones

Quinazolinones of formula **2a** were prepared as outlined in Figure 4. Reaction of halogen substituted anthranilic acids **10** (where X is halogen and Y is halogen or hydrogen) with alkylisothiocyanates in the presence of base provided intermediates of formula **11**. Methylation of **11** with methyl iodide under basic conditions gave 2-methylthioquinazolinones **2b**. Displacement of the methylthio group of **2b** with alkoxides afforded 2-alkoxyquinazolinones **2a** (where R^1 and R^2 are preferably *n*-alkyl) in good yield.
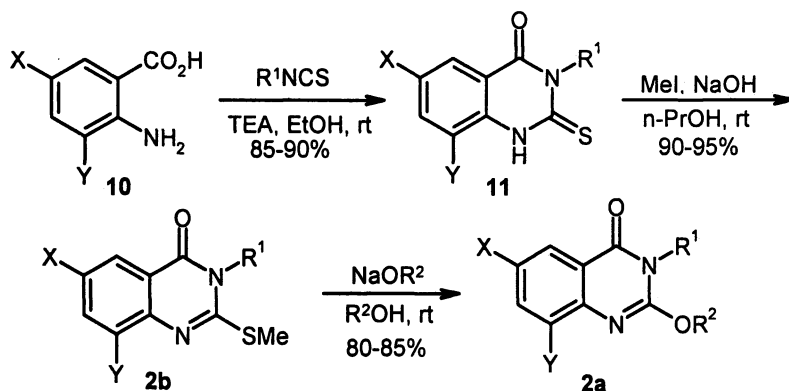
Figure 4. Synthesis of 2-Alkoxy Substituted Quinazolinones
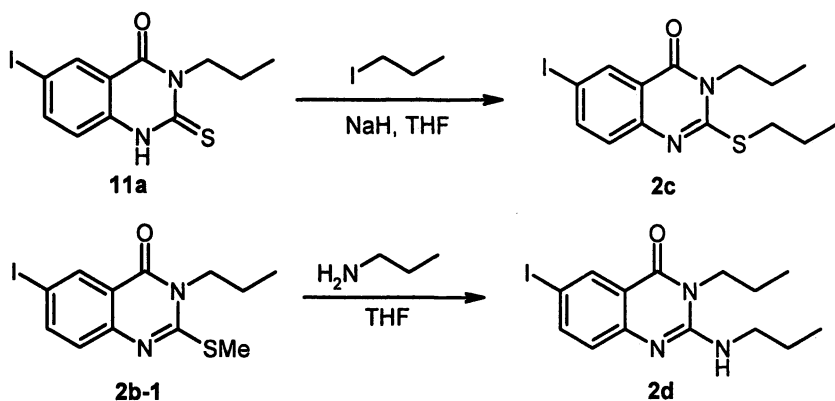
Figure 5. Synthesis of 2-Alkylthio and 2-Alkylamino Quinazolinones

The synthesis of 2-*n*-propylthio and 2-*n*-propylamino substituted 6-iodo-3-*n*-propylpyridopyrimidinones **2c** and **2d**, respectively, is outlined in Figure 5. Alkylation of the benzo-fused thiouracil **11a** with *n*-propyl iodide and sodium hydride afforded 2-*n*-propylthioquinazolinone **2c**. Reaction of 2-methylthio-quinazolinone **2b-1** with 2-*n*-propylamine resulted in mercaptan displacement to give 2-*n*-propylaminoquinazolinone **2d**.

Thienopyrimidinones of formula **3a** were made by the method shown in Figure 6. Methyl aminothiophene carboxylate **12** was condensed with thiophosgene followed by treatment with an alkylamine to provide thiophene

thioureas **13**. Cyclization with sodium hydride afforded thiophene fused thiouracils **14.** Alkylating with methyl iodide gave methylthio intermediates that were allowed to react with alkoxides *in situ* to provide alkoxy thienopyrimidinones **3b** (where R^1 and R^2 are preferably *n*-alkyl). Halogenation of **3b** with N-bromosuccinimide, N-chlorosuccinimide in pyridine or with chloroiodide in acetic acid gave the corresponding 6-halothienopyrimidinones **3a** (where X is halogen). Synthesis of substituted thienopyrimidinones has also been reported by Walter et al. at Syngenta (*7,8*).
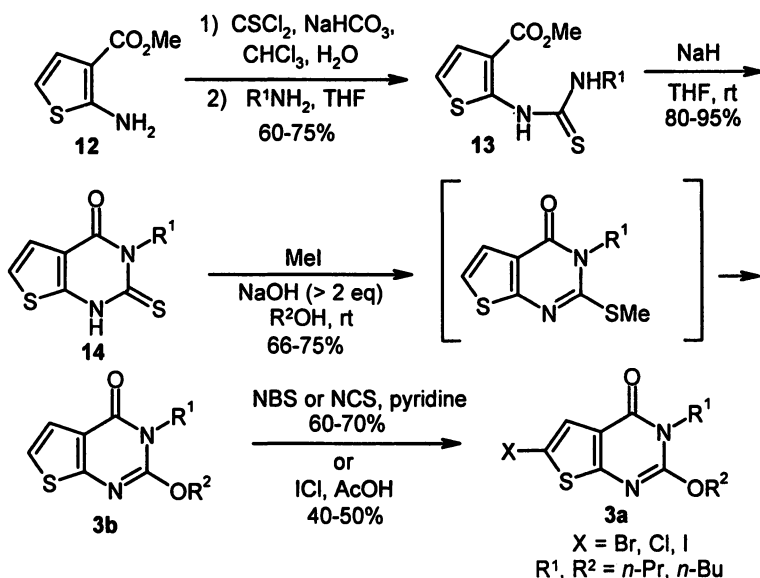
Figure 6. Synthesis of 2-Alkoxy Substituted Thienopyrimidinones

Biology

Although compounds from this chemistry class were active against many strains of powdery mildew, our studies focused on activity against wheat powdery mildew (*blumeria graminis f.sp. tritici*). Applied pre-infection, these compounds were primarily active as protectants, showing less curative efficacy when applied post-infection.A thorough study of structure-activity relationships (SAR) was undertaken on substituted pyridopyrimidinones with results from protectant tests summarized in Tables 1 and 2. Analogs are ranked according to

EC_{90} (effective concentration giving 90% preventive control of the pathogen) range values.

For 3-substituted 7-chloro-2-methoxypyridopyrimidinones in Table 1, R^1 = n-propyl at the 3-position provided optimum activity with an EC_{90} value of 25 ppm. This level of protectant activity was close but slightly less than that of the commercial standard fenpropidin. Lower activity resulted with R_1 equal to higher or lower alkyl versus n-propyl, branched alkyl, allyl, hydrogen, phenyl or benzyl.

Holding R_1 constant as n-propyl, substituent variations for R^2 on oxygen at the pyridopyrimidinone 2-position are also reported in Table 1. Surprisingly, n-propyl for R^2 also gave optimum activity showing an EC_{90} value of 0.5 ppm. This level of preventive potency was significantly better than that of fenpropidin (although fenpropidin provided higher curative efficacy post-infection). Lower activity was observed when R^2 was higher or lower alkyl versus n-propyl, branched alkyl, fluoroalkyl, allyl, propargyl, alkoxyalkyl or benzyl (Table 1).

Table 1. SAR: Protectant Activity of Substituted 7-Chloropyrido [1,2-a]pyrimidinones against Wheat Powdery Mildew

R^1	EC_{90} (ppm)	R^2	EC_{90} (ppm)
n-Pr	25	n-Pr	0.5
n-Bu, allyl, Et, Me	50 - 100	n-Bu, allyl	1 - 2
H, i-Pr, Ph, benzyl	> 100	3-fluoropropyl, Et, n-Hex	5- 10
Fenpropidin	10 - 20	Me, CH_2CF_3, i-Bu, propargyl, CH_2OMe	20 - 50
		benzyl	> 50

A summary of SAR for X and Y on the pyridopyrimidine ring is provided in Table 2. Substitution at the 7 and/or 9 positions generally favored higher activity. For analogs where Y is hydrogen, X = iodo and bromo gave optimum

protectant activity with EC_{90} values below 0.5 ppm. Although the activity exceeded the lowest concentration of this screen, advanced testing under more stringent conditions did reveal that iodo was preferred over bromo. Lower activity was observed where X = chloro or acetylene, with a further drop in activity for trifluoromethyl and methyl followed by hydrogen, cyano, phenyl and nitro.

Table 2. SAR: Protectant Activity of Substituted 2-Propoxy-3-propylpyrido[1,2-a]pyrimidinones against Wheat Powdery Mildew

X	EC_{90} (ppm)
I > Br	< 0.5
CCH, Cl	0.5 - 1
CF₃, Me	> 100
H, CN, Ph, NO₂	10 - 20

X	Y	EC_{90} (ppm)
I	I	
Br	Br	< 0.5
H	I	
Cl	Cl	
Br	Me	0.5 - 1
Me	Br	

Also shown in Table 2, diiodo and dibromo analogs (where X and Y = iodo or bromo) were both quite active with EC_{90} values less than 0.5 ppm. Interestingly, when X is hydrogen and Y is iodo, an EC_{90} value less than of 0.5 ppm was also obtained. However, none of these analogs were more potent than the mono iodo substituted derivative (where X = iodo and Y = hydrogen) in advanced tests. Slightly less activity was observed for analogs where X and Y were other combinations of substituents shown at the bottom of Table 2.

Summaries of SAR for protectant activity of substituted quinazolines are in Tables 3 and 4. In the case of iodo-substituted quinazolinones in Table 3 where R^1 is n-propyl, EC_{90} values were less than 0.5 ppm for all of the following R^2 groups: n-propyl, n-butyl, n-pentyl, allyl, ethyl and methyl. Likewise when R^2 is n-propyl, R^1 = n-propyl, n-butyl, cyclopropylmethyl, n-pentyl, allyl, ethyl or methyl all gave EC_{90} values less than 0.5 ppm. Although these analogs were more active than the lowest test concentration of this screen (EC_{90} values

therefore not determined), advanced tests did show that *n*-propyl and *n*-butyl were generally preferred substituents.

In the case of halogen-substituted 2-propoxy-3-propylquinazolinones in Table 4, iodo, bromo and chloro substitution all gave rise to EC_{90} values less than 0.5 ppm. However, iodo generally provided optimum levels of activity followed by bromo then chloro. Comparable activity was generally observed for mono halogenated analogs (where X = halogen and Y = hydrogen) and bis-halogened derivatives (where X and Y = halogen) for a given halogen series. In most cases, these substituted quinazolinones maintained excellent activity at much lower concentrations in follow-up preventative tests.

Table 3. SAR: Protectant Activity of Substituted Iodoquinazolinones against Wheat Powdery Mildew
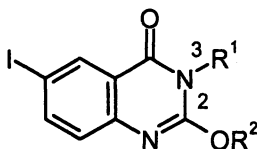
	EC_{90} Values
$R^1 = $ *n*-propyl $R^2 = $ *n*-Pr, *n*-Bu > *n*-pentyl, allyl > Et, Me, i-Pr	< 0.5 ppm
$R^2 = $ *n*-propyl $R^1 = $ *n*-Pr, *n*-Bu > *c*-PrCH$_2$, *n*-pentyl , allyl > Et, Me	

Table 4. SAR: Protectant Activity of Halogen-substituted Quinazolinones against Wheat Powdery Mildew
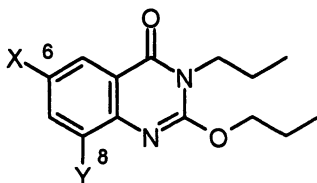
	EC_{90} Values
X, Y = I, H; I, I > Br, H; Br, Br > Cl, H; Cl, Cl	< 0.5 ppm

In Table 5, the protectant activity of proquinazid is compared to that of other commercial standards against wheat powdery mildew. Proquinazid

showed an EC_{50} value of 3 ppb, an order of magnitude more active than the listed standards.

Table 5. Protectant Activity of Proquinazid versus Commercial Standards against Sensitive Wheat Powdery Mildew Isolates

Compound	EC_{50} (ppm)	Compound	EC_{50} (ppm)
proquinazid	0.003	propiconazole	0.10
epoxiconazole	0.04	fenpropidin	0.4
quinoxyfen	0.05	kresoxim-methyl	2
tebuconazole	0.05	cyprodinil	4

Pyridopyrimidinones of formulae **1b** (where W = S) and **1c** (where W = NH) were significantly less active than the corresponding *n*-propylthio and *n*-propylamino quinazolinones **2c** and **2d**. However, *n*-propoxy substitution generally gave higher activity than either *n*-propylthio or *n*-propylamino groups for a given heterocyclic system.

Thienopyrimidinones of formula **3a**, where X is halogen and $R^1/R^2 = n$-propyl or *n*-butyl, were also highly active with EC_{50} values well below 0.5 ppm. Analogs where X = iodo or bromo and $R^1/R^2 = n$-propyl or *n*-butyl had optimum activity. Interestingly, bromo and iodo thienopyrimidinone analogs gave comparable levels of mildew control in advanced tests whereas iodo pyridopyrimidinones and quinazolinones tended to be more active than their bromo counterparts.

In follow-up tests, compounds from this chemistry class continued to show high activity against powdery mildew on a variety of other crops including barley, grapes and cucurbits. These compounds tended to show excellent residual control and protection of new plant growth.

Field Activity

Pyridopyrimidinones, quinazolinones and thienopyrimidinones were all evaluated in the field for powdery mildew control on wheat. Field candidates were applied early in the season as protectants (before substantial presence of the disease). Table 6 shows field efficacy of several substituted pyridopyrimidinones. Although highly active in greenhouse tests, these analogs were less effective than standards, e.g. flusilazole, under field conditions with only moderate levels of mildew control observed at 250-125 g/ha.

Table 6. Field Activity of Substituted Pyridopyrimidinones as Protectants Against Wheat Powdery Mildew
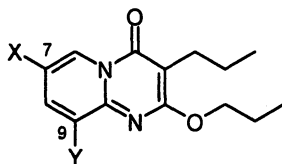
X	Y	Rate (g/ha)	Average % Control*
I	H	250	85
		125	40
Br	H	250	70
		125	20
Br	Br	250	60
		125	50
Flusilazole		250	> 90

* Ratings made 21 days after compound application.

Table 7. Field Activity of Substituted Quinazolinones as Protectants Against Wheat Powdery Mildew
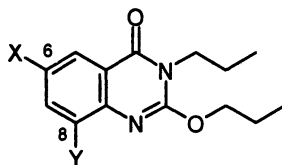
X	Y	Rate (g/ha)	Average % Control*
I	H	125	100
		50	99
		25	97
I	I	125	100
		63	98
Br	H	125	99
		63	85
Fenpropidin		750	95
Quinoxyfen		100	94
		50	76

* Ratings made 40 days after compound application.

Photostability was suspected to be an issue and pyridopyrimidinones were generally found to have short half-lives under UV irradiation, only several hours in some cases.

Table 8. Field Activity of Substituted Quinazolinones Against Grape Powdery Mildew
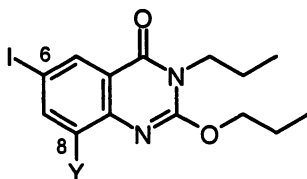
Y	Rate (oz/acre)	Average % Control
H	1.0	> 99
I	1.0	99
Myclobutanil	1.6	97

Table 9. Field Activity of Substituted Thienopyrimidinones versus Proquinazid Against Wheat Powdery Mildew
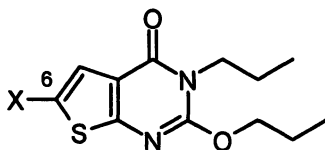
X	Rate (g/ha)	Average % Control*
I	50	98
	25	97
Br	50	99
	25	96
Proquinazid	50	99
	25	97

Ratings made 40 days after compound application.

Field activity of substituted quinazolinones, which generally had good photostability, is summarized in Table 7. Unlike pyridopyrimidinones, quinazolinones maintained very high activity under field conditions giving outstanding mildew control at 50-125 g/ha. Iodine analogs had optimum

activity with proquinazid (X = I, Y = H) still showing effective mildew control at 25 g/ha.

Proquinazid continued to provide excellent mildew activity in follow-up field evaluations on cereals, grapes, other fruits and vegetables at very low application rates. Table 8 shows that iodo quinazolinones also gave outstanding control of powdery mildew on grapes when applied at 1 ounce per acre.

Both thienopyrimidinones (where X = I or Br) in Table 9 were also highly active under field conditions with activity comparable to proquinazid at 25 – 50 g/ha on wheat. Neither showed an advantage over proquinazid. Unlike pyridopyrimidinones and quinazolinones, the bromo and iodo thienopyrimidinones were almost equal in activity.

Conclusion

Substituted pyrido[1,2-a]pyrimidin-4-ones, quinazolin-4-ones and thieno[2,3-a]pyrimidin-4-ones represent a unique class of potent antifungal agents showing high protectant activity against powdery mildew strains of fungi. Although pyrido[1,2-a]pyrimidin-4-ones showed disappointing field results (due possibility to photoinstability), quinazolin-4-ones and thieno[2,3-d]pyrimidin-4-ones maintained outstanding mildew activity under field conditions. Proquinazid consistently gave outstanding powdery mildew control in field tests on cereals, grapes and other crops at very low rates of application. Field performance exceeded that of commercial protectants with excellent residual disease control and protection of new growth. Proquinazid will be sold under the trade names Talius™ (for use in cereals) and Talendo™ (for use in grapes, fruits and vegetables). Setting a new standard for powdery mildew control, proquinazid will be a valuable tool for growers in their efforts to combat this disease.

Acknowledgments

222

References

1. Selby, T. P. World Patent Application WO 93/23398, 1993.
2. Bereznak, J. F.; Selby, T. P.; Sternberg, C. G. World Patent Application WO 94/26722. 1994.
3. Bereznak, J. F.; Chang, Z.-Y.; Selby, T. P.; Sternberg, C. G. U. S. Patents 6,245,770, 2001; 5,945,423, 1999; 5,747,497, 1998.
4. Bereznak, J. F.; Chang, Z.-Y.; Gross (Sternberg), C. G. World Patent Application WO 97/02262, 1997.
5. Bullock, G. A. U. S. Patent 3,755,582, 1973.
6. Bullock, G. A.; Sheeran, P. J. U. S. Patent 3,867,384, 1975.
7. Walter, H.; Zeun, R. *Chimia* **2003**, *57*, 692-696.
8. Walter, H. World Patent Applications WO 97/33890, 1997; WO 99/11631, 1999; WO 99/14202, 1999.
9. Lappin, G. R.; Petersen, Q. R.; Wheeler, C. E. *J. Org. Chem.* **1950**, *15*, 377-380.
10. Urban, R.; Grosjean, M.; Arnolds, W. *Helvetica Chimica Acta* **1970**, *53*, 905-922.

Chapter 17

The Novel Mode of Action of Anthranilic Diamide Insecticides: Ryanodine Receptor Activation

Daniel Cordova, Eric A. Benner, Matthew D. Sacher,
James J. Rauh, Jeffrey S. Sopa, George P. Lahm,
Thomas P. Selby, Thomas M. Stevenson, Lindsey Flexner,
Steven Gutteridge, Daniel F. Rhoades, Lihong Wu,
Rejane M. Smith, and Yong Tao

Stine Haskell Research Center, DuPont Crop Protection Products,
1090 Elkton Road, Newark, DE 19714

Development of insecticides with unique modes of action is necessary to combat resistance. DuPont Crop Protection has discovered a new class of insecticides which provides exceptional control through action on a novel target, the ryanodine receptor. Studies on native and recombinant insect ryanodine receptors demonstrate that the anthranilic diamides bind to a unique site on this receptor, potently releasing calcium from the sarcoendoplasmic reticulum. As this chemistry exhibits greater than 500-fold differential selectivity toward insect, over mammalian, receptors, anthranilic diamides offer an exciting alternative to existing pest-management strategies.

© 2007 American Chemical Society

223

224

Currently, 95% of commercial insecticides comprise molecules interfering with one of five targets: acetylcholine receptor, GABA receptor, sodium channel, mitochondrial respiration or chitin synthesis *(1)*. Calcium signaling plays a key role in multiple biological processes, including muscle contraction and neurotransmitter release. Contraction of insect muscle involves modulation of two distinct channels, voltage-gated Ca^{2+} channels, which regulate external calcium entry and ryanodine receptor channels (RyRs), which regulate release of internal calcium stores *(2)*. Although it has been speculated that calcium channels present a valid target for insect control, to-date no synthetic insecticides have been commercialized against such targets. Here we describe the mode of action of a new and highly effective class of insecticides, the anthranilic diamides, hence referred to as anthranilamides, which target RyRs.

Insecticidal Activity and Symptomology

The earliest anthranilamides, characterized by 2-methyl aryl or 2-methyl heteroaryl diamide of Formulae I and II (Figure 1, Table I), exhibit moderate lepidopteran toxicity. Optimization efforts led to the discovery of the phenylpyrazoles analogs of Formula III with considerable improvement in insecticidal potency. Further modification of the 1-phenylpyrazole to 1-pyridylpyrazole group (Formula IV) greatly increased the insecticidal potency with **DP-013** having an LD_{50} value of 0.02 and 0.03 ppm against *Heliothis virescens* and *Spodoptera frugiperda* larvae, respectively *(3)*. The insecticidal potency of **DP-013** is more than an order of magnitude greater than commercial standards such as cypermethrin or indoxacarb.

Lepidopteran larvae exposed to anthranilamides exhibit rapid feeding cessation, general lethargy, and partial paralysis. Further, dorsal vessel (heart) studies with **DP-012**, revealed a rapid cardio-inhibitory effect in *Manduca sexta* larvae. Contraction frequency was attenuated in a dose-dependent manor with injection of 3 ng/g (body weight) attenuating the contraction by 27%. As shown in Table II, the rank potency for anthranilamides is comparable to its lepidopteran toxicity with **DP-012** > **DP-010** > **DP-002**.
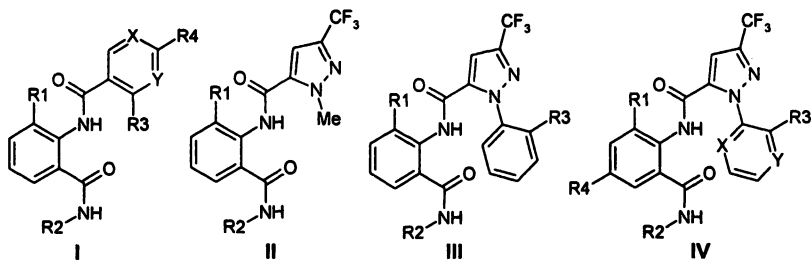
Figure 1. Structure Classes of Insecticidal Anthranilamides

Table 1. Comparative Biological Activity of Anthranilamides and Commercial Lepidopteran

Cpd	Formula	R1	R2	R3	R4	X	Y	S. frugiperda LD_{50} (ppm)	H. virescens LD_{50} (ppm)
DP-001	I	CH_3	iC_3H_7	H	OCF_3	N	N	51.60	>500
DP-002	I	CH_3	iC_3H_7	iC_3H_7	CF_3	N	N	45.20	51.4
DP-003	I	CH_3	iC_3H_7	C_2H_6	CF_3	C	N	51.30	77.5
DP-005	II	CH_3	iC_3H_7	-	-	-	-	48.80	130.1
DP-006	III	Cl	iC_3H_7	H	-	C	C	2.90	17.0
DP-007	III	Cl	iC_3H_7	Br	-	C	C	-	5.6
DP-008	III	Cl	iC_3H_7	Cl	-	-	-	0.44	3.5
DP-010	IV	CH_3	CH_3	F	-	N	C	0.52	2.3
DP-011	IV	CH_3	CH_3	Cl	H	N	C	0.26	0.8
DP-012	IV	CH_3	iC_3H_7	Cl	H	N	C	0.12	0.4
DP-013	IV	CH_3	iC_3H_7	Cl	Cl	N	C	0.03	0.02
Cypermethrin	Commercial standard							5.30	13.48
Indoxacarb	Commercial standard							0.33	0.6

Table II. Attenuation of Heart Contraction Frequency in *m. sexta* Larvae Injected with Anthranilamides

Cpd	Dose (ng/g body weight)	Heart Rate Change (%)
DP-002	100	-3.8
	300	0.5
	1000	-54.0
DP-010	10	1.2
	30	-61.0
	100	-62.8
DP-012	1	4.2
	3	-27.1
	10	-55.0

Measurements obtained 30 min after compound injection

Anthranilamides Stimulate Calcium Mobilization

As similar poisoning symptoms were observed in the cockroach, *Periplaneta americana*, the effect of anthranilamides on calcium homeostasis was investigated on embryonic neurons from this insect. Using calcium imaging it was found that anthranilamides induce a dose-dependent increase in intracellular calcium ($[Ca^{2+}]_i$) with rank potency of **DP-012 > DP-010 > DP-002** as shown in Figure 2. Upon comparing whole organism lepidopteran toxicity of the anthranilamides in Table I with calcium mobilization in *P. americana* neurons, a high degree of correlation was observed (Figure 3). These results, coupled with a lack of activity against other neuromuscular targets, strongly implicated a calcium signaling mechanism as the toxicologically relevant target.
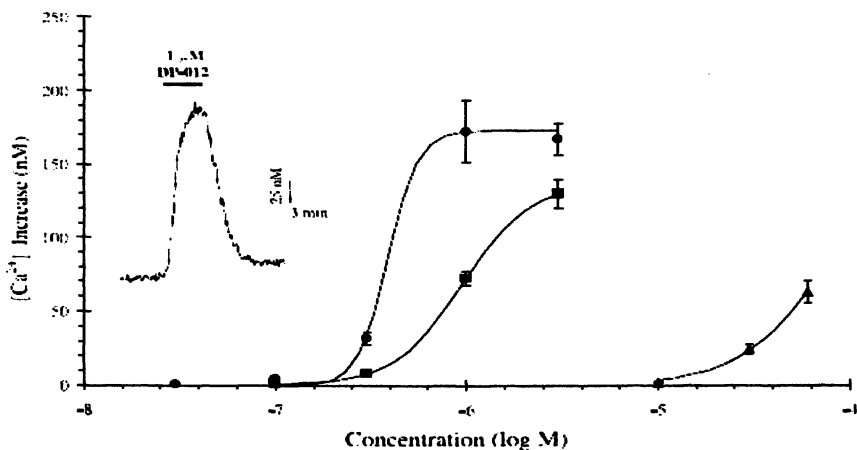
Figure 2. Ca^{2+} Mobilization Dose Response Curves for P. Americana Embryonic Neurons Challenged with Anthranilamides DP-012 (●), DP-010 (■), and DP-002 (▲). Inset: A Typical Ca^{2+} Response for DP-012. (Reproduced with permission from Reference 4. Copyright 2005 Elsevier)

The anthranilamide, **DP-012**, stimulates a rise in $[Ca^{2+}]_i$ under conditions of Ca^{2+}-free saline similar to that observed with standard saline, indicating that this chemistry mobilizes calcium from internal calcium stores rather than through external entry via voltage-gated Ca^{2+} channels. Three possible targets are involved in release of internal calcium stores, inositol trisphosphate receptors (IP$_3$Rs), ryanodine receptors (RyRs), and sarco-endoplasmic reticulum ATPase (SERCA). These *P. americana* neurons possess functional ryanodine receptors,

as demonstrated by their sensitivity to the receptor activator, caffeine, which stimulates a calcium response similar to that observed with **DP-012** (Figure 4). At micromolar concentrations, the plant alkaloid, ryanodine, for which the receptor is named, selectively locks RyRs in a "partially-open" state upon activation *(5)*. As shown in Figure 4, ryanodine treatment of *P. americana* neurons causes a prolongation of the initial anthranilamide-induced Ca^{2+} release, followed by an inability of subsequent anthranilamide or caffeine challenges to mobilize Ca^{2+}. Furthermore, insect cells, which possess both IP$_3$Rs and SERCA, but not ryanodine receptors, are completely insensitive to anthranilamide chemistry. Taken together, these findings strongly implicate RyR activation as the anthranilamide mode of action.

Anthranilamides Bind to a Unique Site on the RyR

The RyR is a tetramer composed of four identical subunits with a central pore region forming a channel through which Ca^{2+} flows (Figure 5). In addition
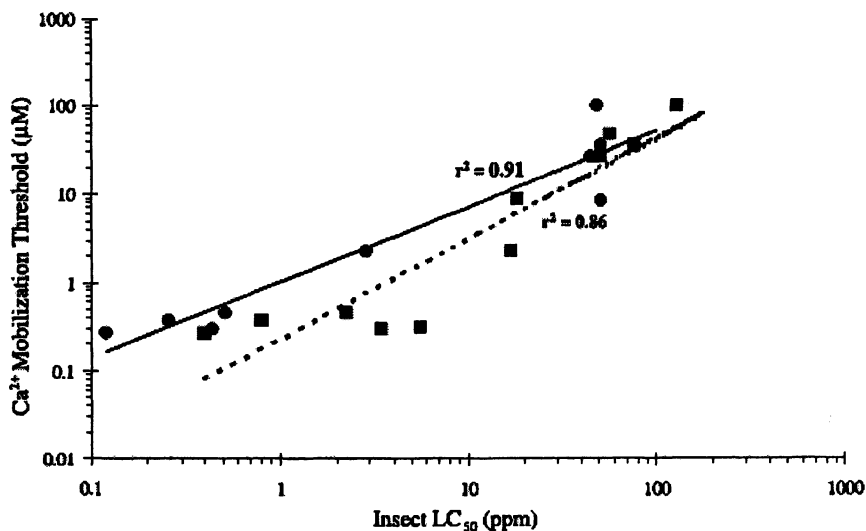
Figure 3. Correlation Between Ca^{2+} Mobilization Threshold for P. Americana Neurons and S. Frugiperda (●) or H. Virescens (■) Larval Toxicity for the Series of Anthranilamides Shown in Table I. (Adapted with permission from Reference 4. Copyright 2005 Elsevier)
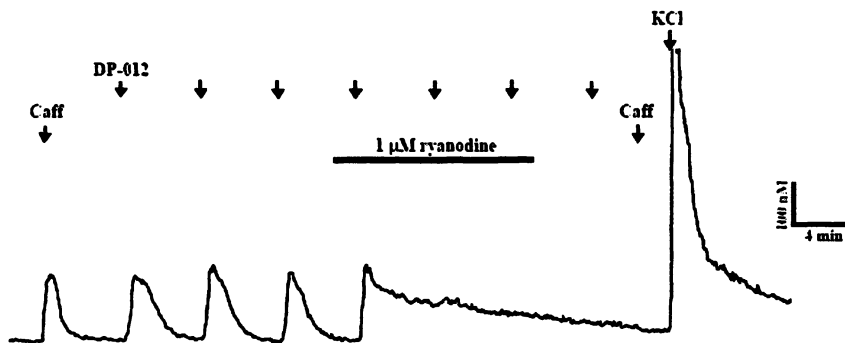
*Figure 4. Challenges with Caffeine (20 mM) or **DP-012** (1 μM) Stimulate
Similar Calcium Responses in P. Americana Neurons. Depletion of Internal
Calcium Stores with the Selective RyR Agent, Ryanodine, Inhibits Further
Responses to **DP-012** and Caffeine While Having No Effect on Voltage-gated
Ca²⁺ Channel Activation by KCl (100 mM). (Reproduced with permission from
Reference 4. Copyright 2005 Elsevier)*

to the RyR protein, additional proteins such as calmodulin, FK506-binding
protein, junctin, triadin, and calsequestrin comprise the ryanodine receptor
complex and have a role in channel regulation and calcium sequestration (6).
Ryanodine and caffeine, bind directly to the receptor protein, with ryanodine
binding to a site located in the pore region, whereas caffeine binds to a site
distant from the pore (7). To characterize the anthranilamide-binding site,
radioligand studies were conducted on membranes prepared from *P. americana*
leg muscle. It was found that various anthranilamides, including **DP-012**, fail to
displace or enhance ^{3}H-ryanodine binding, revealing that the anthranilamide-
binding site is distinct from that of ryanodine.

Further biochemical characterization was conducted using a radiolabeled
anthranilamide, ^{3}H-**DP-010**. In *P. americana* muscle, ^{3}H-**DP-010** was found to
exhibit specific, saturable binding to a single site. While both caffeine and
ryanodine fail to displace ^{3}H-**DP-010**, binding is enhanced in the presence of
ryanodine as shown in Figure 6. Scatchard transformation of ^{3}H-**DP-010**
binding data obtained in the presence of ryanodine yields K_d and B_{max} values of
44 nM and 9,687 fmol mg^{-1} protein, respectively. While the mechanism of
binding enhancement remains unclear, one could postulate that ryanodine and
anthranilamides bind to distinct but allosterically linked sites. Furthermore, this
enhancement may indicate that anthranilamides bind more effectively to
channels in the "partially open" rather than the open or closed states, as would
be the case with ryanodine present.
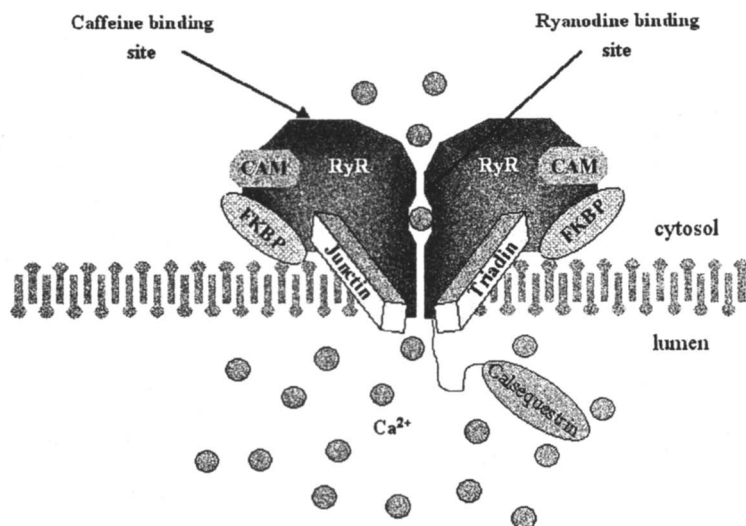
Figure 5. Diagram Depicting the Ryanodine Receptor Complex with its Accessory Proteins. Only Half of the RyR Tetramer is Depicted to Highlight the Ca^{2+} Channel Pore. FKBP = FK506-binding Protein and CAM = Calmodulin.
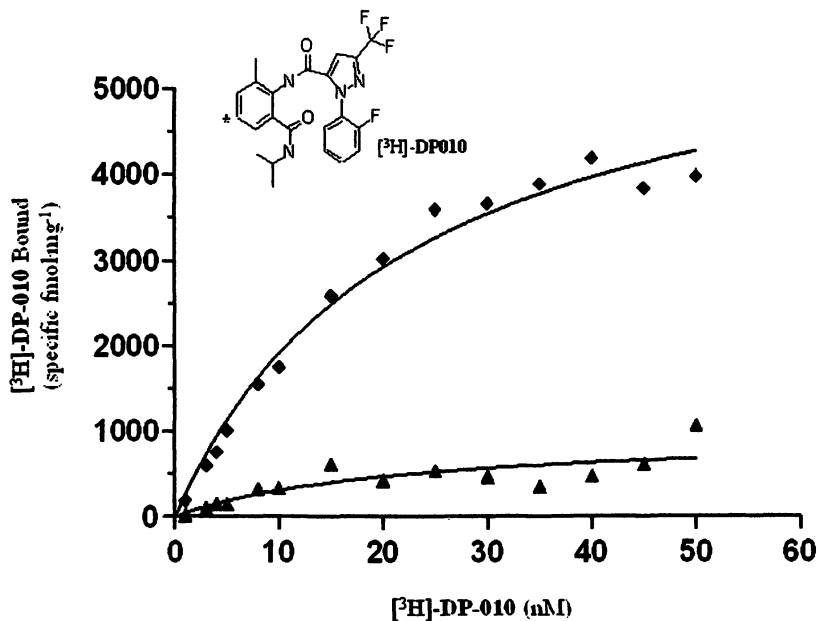
*Figure 6.   Specific Binding of ^{3}H-DP-010 to a Membrane Preparation from
P. americana Legs in the Absence (▲) and Presence (♦) of 10 μM Ryanodine.
(Adapted with permission from Reference 4. Copyright 2005 Elsevier)*

Genetic Validation of Anthranilamide Mode of Action

Cloning and expression of insect RyRs was undertaken to provide genetic validation of the anthranilamide mode of action. As the RyR is a membrane-bound protein encoded by a nucleotide sequence of 15,000 base pairs, cloning and expression of the receptor is particularly challenging. Earlier efforts to establish a cell line that express the full-length RyR from the fruit fly, *Drosophila melanogaster*, have proven problematic *(8)*.   Using various molecular approaches we circumvented toxicity associated with *ryr* gene amplification and have achieved functional expression of full-length insect RyRs in the lepidopteran cell line, Sf9, a cell line devoid of endogenous RyRs. As shown in Figure 7, expression of a *D. melanogaster* RyR confers caffeine and anthranilamide sensitivity in this cell line.
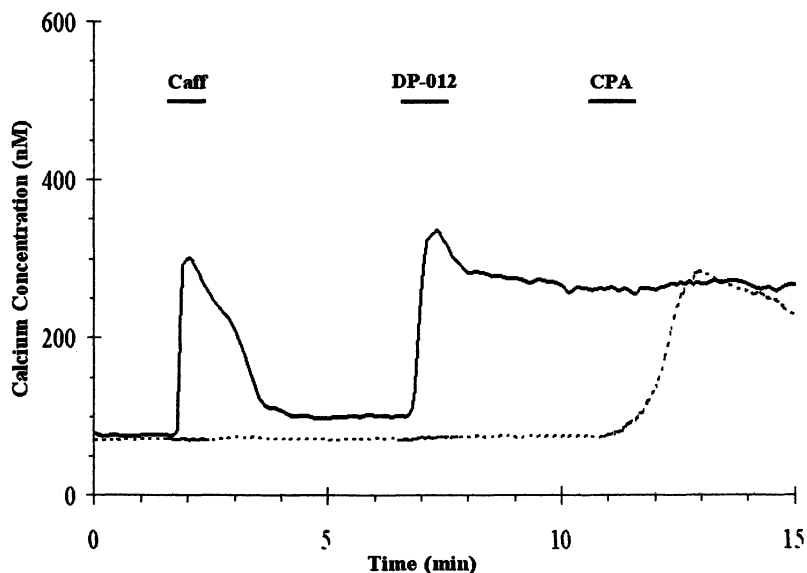
*Figure 7. Caffeine and **DP-012** Response of Sf9 Cells Transiently Expressing
(solid line) and Lacking (dashed line) Full-length D. Melanogaster RyRs.
Cyclopiazonic Acid (CPA), a SERCA Pump Inhibitor Demonstrates the
Presence of Internal Calcium Stores in Cells that are not Expressing
the Drosophila RyR. (Reproduced with permission from Reference 4.
Copyright 2005 Elsevier)*

Functional expression of RyR from lepidopteran and homopteran insects
has also been achieved. Figure 8, shows that recombinant receptors from *H.
virescens* and *D. melanogaster* exhibit similar **DP-012** sensitivity as that
observed with native RyRs from *P. americana*. These findings provide genetic
validation for RyR activation as the mode of action for anthranilamides.
Furthermore, expression of these recombinant receptors offers utility for
discovery of future RyR-active molecules and is the basis of a recently filed
patent application *(9)*.
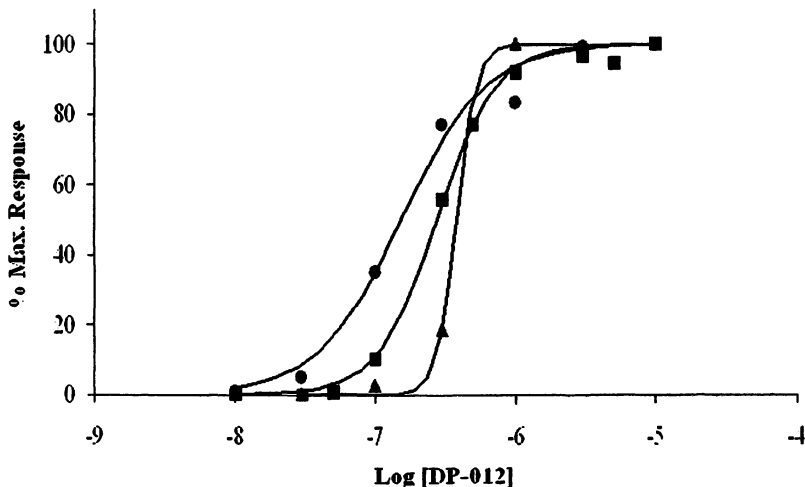
*Figure 8. Comparative **DP-012** Dose Response for Native P. americana
Embryonic Neurons (▲) and Sf9 Cells Stably Expressing Recombinant RyRs
from D. melanogaster (●) and H. virescens (■).*

Insect Selectivity of Anthranilamides

RyRs play a key role in mammalian muscle function with three distinct
types found in mammals. Receptors of Types 1 and 2 are found primarily in
skeletal and cardiac muscle, respectively, whereas receptors of Type 3 are
heterogeneously distributed *(6)*. Unlike mammals, insects possess a single form
of the RyR with only 47% similarity to that of mammalian receptors at the
amino acid level *(10)*. Anthranilamides were tested against two mammalian cell
lines, PCl_2 (rat), which expresses both RyR_1 and RyR_2, and C_2Cl_2 (mouse),
which expresses both RyR_1 and RyR_3 *(11)*. As shown in Figure 9, **DP-012**
stimulates RyR-mediated calcium release in PCl_2 cells with 500-fold lower
potency than that observed with insect receptors; similar selectivity is also
observed with C_2Cl_2 cells. This selectivity extends across anthranilamides as a
class with up to 2000-fold selectivity for insect RyRs over that of mammalian.
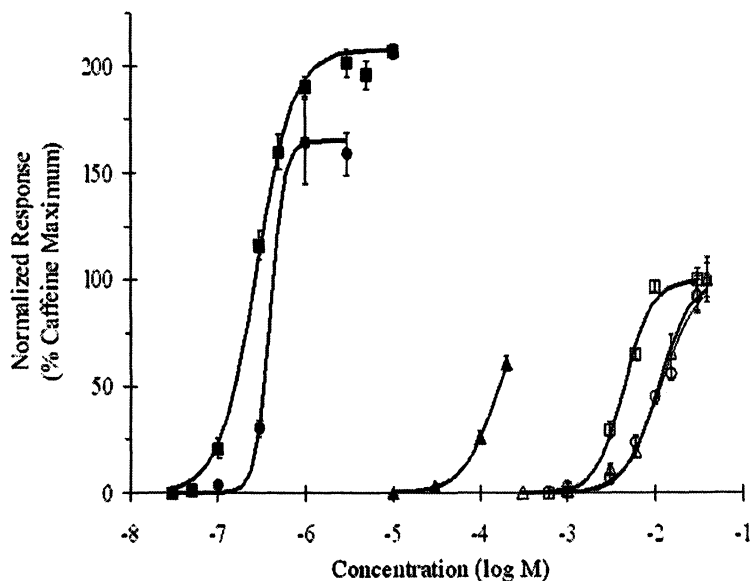
*Figure 9. Comparative Caffeine (open symbols) and **DP-012** (closed symbols) Response for P. americana neurons (●), Sf9 Cells Expressing Recombinant D. melanogaster RyR (■), and the Rat Pheochromocytoma Cell Line, PCl₂ (▲). **DP-012** Concentrations Higher than 200 μM Were Not Investigated Due to Limited Aqueous Solubility. Reproduced with permission from Reference 4. Copyright 2005 Elsevier)*

Conclusion

Here we have presented a new class of highly potent insecticides, the anthranilamides, which control pest insects via a novel mode of action. This chemistry exhibits broad-spectrum insect control with exceptional activity against lepidopteran larvae. RyR activation has clearly been demonstrated as the mode of action for the anthranilamides. Unregulated receptor activation results in depletion of internal calcium stores, muscle paralysis and ultimately insect death. In addition to this chemistry representing one of the first examples of a potent, synthetic RyR-active molecule, anthranilamides exploit a unique binding site on the receptor, distinct from that of ryanodine or caffeine.

234

Equally important to describing the mode of action for anthranilamides, we have successfully cloned and expressed RyRs from multiple insect species. This represents the first known example of a stable insect cell line that expresses a functional full-length insect RyR. Such recombinant cell lines offer a powerful tool for discovery of additional receptor-active molecules and are the basis of a recent patent application.

Anthranilamides exhibit exquisite differential selectivity toward insect, over mammalian receptors. Consequently, this chemistry offers a novel tool for characterization of pharmacological differences between vertebrate and invertebrate RyRs. More importantly, with the combined attributes of insect potency, novel mode of action, and insect selectivity, anthranilamides hold great promise for pest management strategies.

References

1. Nauen, R.; Bretschneider, T. *Pesticide Outlook* **2002**, *6*, 241-245.
2. Melzer, W.; Herrmann-Frank, A.; Luttgau, H.C. *Biochim Biophys. Acta* **1995**, 1241, 59-116.
3. Lahm, G.P.; Selby, T.P; Freudenberger, J.H.; Stevenson, T.M.; Myers, B.J.; Seburyamo, G.; Smith, B.K.; Flexner, L.; Clark, C.E.; Cordova, D. *Bioorg Med Chem Lett* **2005**, 15, 4898-4906.
4. Cordova, D.; Benner, E.A.; Sacher, M.D.; Rauh, J.J.; Sopa, J.S.; Lahm, G.P., Selby, T.P., Stevenson, T.M.; Flexner, L.; Gutteridge, S.; Rhoades, D.F.; Wu, L.; Smith, R.M.; Tao, Y. *Pest Biochem Phys.* **2006**, 84, 196-214.
5. Buck, E.; Zimanyi, I.; Abramson, J.J.; Pessah, I.N. *J. Biol Chem.* **1992**, 267, 23560-23567.
6. Sitsapesan, R. In *The Structure And Function Of Ryanodine Receptors*; Sitsapesan, R.; Williams, A.J., Eds.; Imperial College Press: London, 1998; pp.47-74
7. Bhat, M.B.; Zhao, J.; Zang, W.; Balke, C.W.; Takeshima, H.; Wier, W.G.; Ma, J. *J. Gen. Physiol.* **1997**, 110, 749-762
8. Xu, X.; Bhat, M.B.; Nishi, M.; Takeshima, H.; Ma, J. *Biophys J.* **2000**, 78, 1270-1281.
9. Gutteridge, S.; Caspar, T.; Cordova, D., Rauh, J.J.; Tao, Y.; Wu, L.; and Smith, R.M. US Patent Appl 20040171114, 2004.
10. Takeshima, H.; Nishi, M.; Iwabe, N.; Miyata, T.; Hosoya, T.; Masai, I.; Hotta, Y. *FEBS Lett.* **1994**, 337, 81-87.
11. Bennett, D.L.; Cheek, T.R; Berridge, M.J.; De Smedt, H.; Parys, J.B.; Missiaen, L.; Bootman, M.D. *J. Biol. Chem.* **1996**, 271, 6356-6362.

Chapter 18

Phthalic Acid Diamides Activate Insect Ryanodine Receptors

Peter Lümmen[1], Ulrich Ebbinghaus-Kintscher[1], Christian Funke[1], Rüdiger Fischer[1], Takao Masaki[2], Noriaki Yasokawa[2], and Masanori Tohnishi[2]

[1]Bayer CropScience AG, Alfred-Nobel-Strasse 50,
D–40789 Monheim, Germany
[2]Nihon Nohyaku Company, Ltd., 345, Oyamada-cho, Kawachi-Nagano,
Osaka 586–0094, Japan

Flubendiamide represents the novel chemical family of substituted phthalic acid diamides with potent insecticidal activity. Evidence is presented here that phthalic acid diamides activate ryanodine-sensitive intracellular calcium release channels in insects. Flubendiamide induces cytosolic calcium transients which are independent of extracellular calcium in isolated neurons from the pest insect, *Heliothis virescens*. In addition, phthalic acid diamides increase the ryanodine binding affinity while not changing the number of high-affinity binding sites. Furthermore, flubendiamide interferes with the calcium regulation of ryanodine binding. The flubendiamide binding site has been found to be distinct from the ryanodine binding site. In addition, flubendiamide binding itself is regulated by the calcium concentration. We propose that the phthalic acid diamides stabilize the (sub)conductance conformational state of the ryanodine receptor.

235

Introduction

Ryanodine receptors (RyR) mediate the release of calcium from intracellular stores of the sarcoplasmic/endoplasmic reticulum (SR/ER) following a small calcium influx *via* voltage-gated calcium channels of the cytoplasmic membrane after depolarization. The process, referred to as calcium-induced calcium release, triggers muscle contraction after electrical excitation in mammalian cardiac as well as in insect striated muscles *(1)*. Three RyR isoforms exist in mammals: Type 1, which is predominantly expressed in skeletal muscles; Type 2, which is expressed in cardiac muscle; and the more ubiquitously expressed Type 3 *(2)*.

RyR polypeptides of approximately 560 kDa molecular weight form homotetrameric complexes. The three-dimensional structures of all three mammalian subtypes have been reconstructed from cryoelectron micrographs. The N-terminal part of the receptor accounting for roughly 80% of the protein mass protrudes into the cytoplasm and contains the binding sites for diverse RyR modulators like calmodulin, ATP, the FK506-binding protein FKBP12, and calcium.

The C-terminal domain comprises the transmembrane region including the ion-conducting pore *(3)*. Although the exact number of transmembrane helices remains to be established, a model based on homology with the bacterial KcsA potassium channel structure has been established to define key structural elements important for ion conductance, ion selectivity, and the gating mechanism *(4)*.

Ryanodine receptors undergo extensive conformational changes upon activation and closing, which are regulated at least partly by intramolecular interactions between the cytoplasmic domains, and between cytoplasmic and transmembrane domains, respectively. Known RyR effectors like calcium and caffeine are believed to modulate these interactions. Additionally, evidence is accumulating that calcium release is also controlled by the concerted activation and closing of physically interacting RyR channels arranged in ordered arrays in the endo(sarco)plasmic membranes *(5)*.

The plant alkaloid ryanodine selectively binds with low nanomolar affinity to the ion-conducting conformational state of the ryanodine receptor. This property makes it a useful pharmacological probe to study the regulation of channel activation. The ryanodine binding site has been localized in the pore region of the C- terminal transmembrane domain *(6;7)*.

In insects, much less is known about ryanodine receptors. There seem to be single RyR genes in the *Drosophila melanogaster* and *Heliothis virescens* genomes *(8-10)*. A few insect RyRs have been characterized pharmacologically: single high-affinity ryanodine binding sites have been described in preparations

from houseflies, cockroaches, and *Heliothis*. Similar to their mammalian counterparts, insect RyR are regulated by the intracellular calcium concentration *(11;12)*. Ryanodine and close structural analogues exhibit insecticidal activity. Consequently, ryanodine receptors have been suggested as molecular target sites for novel insecticides *(13)*.

In this communication, we present evidence that the phthalic acid diamides, a novel chemical class of highly potent insecticides discovered by Nihon Nohyaku Co., Ltd. *(14)*, act on ryanodine-sensitive calcium release channels in insects by a mechanism distinct from that of ryanodine.

Materials and Methods

Chemicals and Reagents

The phthalic acid diamides flubendiamide and the corresponding sulfoxide were synthesized by Nihon Nohyaku Co., Ltd., and Bayer CropScience AG. Ryanodine, Fura-2 acetoxymethyl ester (Fura-2 AM) and Fura-2 were obtained from Sigma and stored frozen as aliquots (stock solution 1mM in DMSO).

Fura-2 Fluorescence Measurements on Isolated Neurons from *Heliothis Virescens*

Fura-2 fluorescence measurements were done on isolated neuronal cell bodies obtained from fifth instar *Heliothis virescens* larvae as described previously *(15)*. The fluorescence emission was detected using a Fura filter set (DCLP 410, LP 470).

Equilibrium Binding Assays

Equilibrium binding assays with [^{3}H]ryanodine (Perkin Elmer, spec. activity: 2.072 TBq mmol^{-1}) and [^{3}H]flubendiamide (in-house synthesis, 905.6 GBq mmol^{-1}) were performed on microsomal membrane preparations from *Heliothis virescens* flight muscles as described previously *(16)*.

Results

Phthalic Acid Diamides Elicited Intracellular Calcium Transients in *Heliothis* Neurons

Due to its low water solubility ($\approx$ 0.03 mg/L), the usability of flubendiamide (Figure 1, **I**) in physiological and biochemical experiments was limited, so the

more water-soluble sulfoxide analogue (Figure 1, **II**) was employed in most cell-physiological experiments.
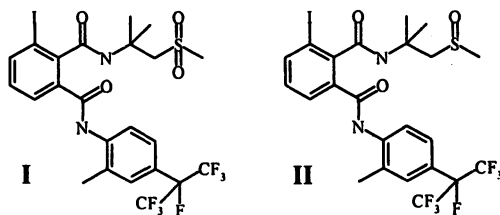
Figure 1. Structures of the Phthalic Acid Diamides Employed in the Current Study: (I, flubendiamide; II, flubendiamide-sulfoxide)
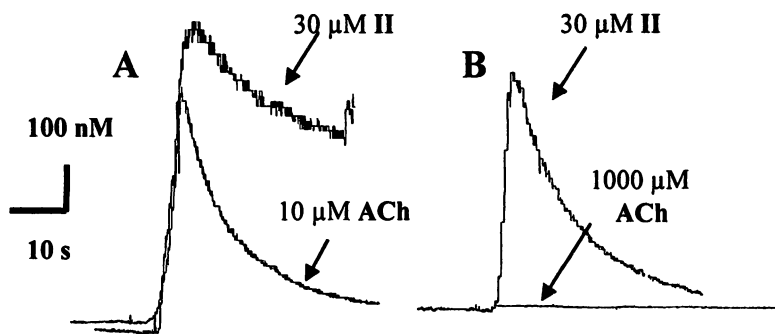
Figure 2. Phthalic diamide-induced Ca^{2+} release in isolated Heliothis neurons. A: Superimposed, representative Ca^{2+} responses induced by 30 µM of flubendiamide-sulfoxide, and by 10 µM ACh. B: The response to 1000 µM acetylcholine was completely prevented when Ca^{2+} was removed from the application solution. In contrast, the $[Ca^{2+}]_c$ transients induced by flubendiamide-sulfoxide were nearly the same as under control conditions.

Application of 30 µM flubendiamide-sulfoxide to isolated *Heliothis* neurons caused an increase in the cytosolic calcium concentration, $[Ca^{2+}]_c$ (Figure 2A), which was independent of the calcium concentration in the extracellular medium.

In the same experimental setup, application of 10 μM acetylcholine evoked Ca^{2+} transients by opening of calcium-permeable ion channels in the plasma membrane, including the nicotinic acetylcholine receptor and voltage-gated calcium channels activated by the depolarization of the membrane. Consequently, when calcium was omitted from the extracellular medium, acetylcholine-induced calcium transients were completely abolished (Figure 2B).
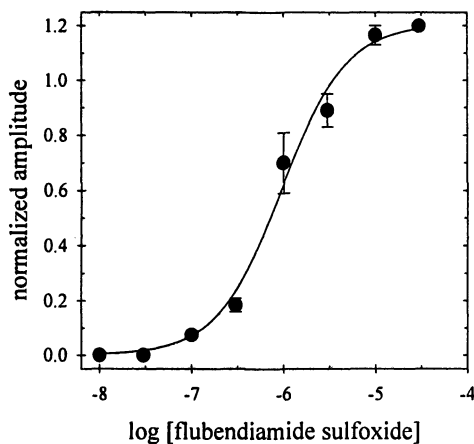
Figure 3. Concentration-dependent intracellular calcium release elicited by flubendiamide sulfoxide (II). Amplitudes of the calcium transients were normalized to the maximum response evoked by 10 mM caffeine (n = 4).

The normalized amplitude heights of the calcium response induced by flubendiamide-sulfoxide were concentration-dependent with an apparent EC_{50} of 0.7 μM (Figure 3). It is noteworthy that calcium transients could be specifically blocked with 50 μM ryanodine, but not with xestospongine, a blocker of IP_3-gated Ca^{2+} release channels *(16)*.

Phthalic Acid Diamides Increased [³H]Ryanodine Affinity

The [³H]ryanodine affinity of the *Heliothis* RyR was found to be calcium-sensitive: ryanodine bound in a cooperative fashion at 100 μM $[Ca^{2+}]$ under equilibrium conditions (Figure 4A). Data were fitted to the modified binding isotherm according to Hill, $B = B_{max} [L]^n/(K_D^n + [L]^n)$, where B_{max} represents the total number of receptors, [L] is the concentration of unbound ligand, and K_D is the dissociation constant of ryanodine. The apparent K_D was 37.7 nM (4 experiments) and the calculated Hill coefficient, n = 1.5, deviated significantly

from unity (t-test: $p<0.002$) indicating positive cooperativity between the ryanodine binding sites. The B_{max} was 1060 fmol/mg membrane protein.
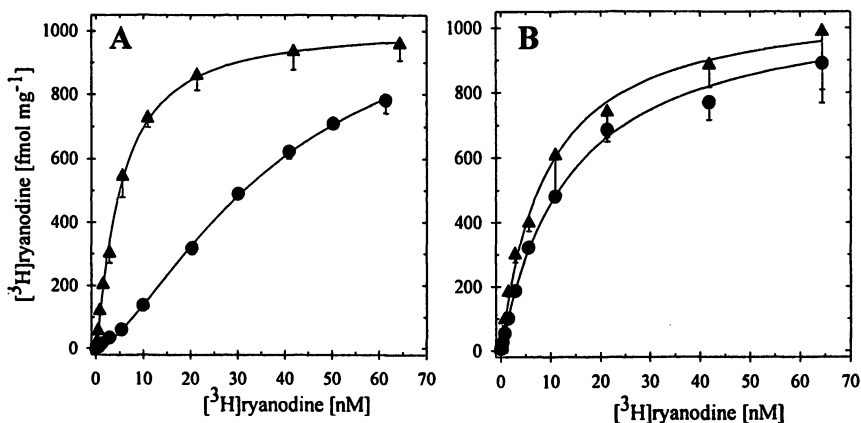
Figure 4. Effect of flubendiamide-sulfoxide on equilibrium saturation binding of [^{3}H]ryanodine at two different calcium concentrations. Saturation binding was performed essentially as described earlier [16] with 100 µM (A) or 800 µM (B) calcium, respectively. Control assays (●) and assays including 1.0 µM of flubendiamide-sulfoxide (▲) were performed in quadruplicate and the data were fitted to the binding equation (Hill).

Remarkably, in the presence of 1.0 µM flubendiamide-sulfoxide, the resulting binding isotherm had a simple hyperbolic character (Hill coefficient, $n = 1.0$), which indicated a homogeneous population of independent sites. Ryanodine affinity was increased with an apparent dissociation constant $K_D = 5.2 +/- 0.8$ nM (4 experiments). However, the number of binding sites, B_{max}, remained essentially unchanged (1072 fmol/mg) as compared to the control.

When increasing the calcium concentration to 800 µM, specific binding of ryanodine could be fitted to the simple hyperbolic equation with $n = 1.0$ (Figure 4B). The K_D of ryanodine was calculated as $13.6 +/- 1.4$ nM (4 experiments) and the receptor density was determined as 1086 fmol/mg. Flubendiamide-sulfoxide (1.0 µM) decreased the apparent K_D slightly, but still significantly, to $7.9 +/- 0.9$ nM (t-test: $p < 0.03$).

Flubendiamide (1.0 µM) had a similar effect on the apparent K_D values at both calcium concentrations tested (data not shown). As in the case of the

sulfoxide, the apparent number of receptor sites (1089 fmol/mg) was not changed.

In summary, phthalic acid diamides increased the ryanodine affinity of the *Heliothis* ryanodine receptor. At low $[Ca^{2+}]$ the compounds offset the cooperativity between the ryanodine sites.

Flubendiamide Increased [^{3}H]Ryanodine Binding in a Concentration-Dependent Fashion

Ryanodine binding to the *Heliothis* RyR was regulated by both the calcium and the flubendiamide concentrations (Figure 5). At 800 µM $[Ca^{2+}]$,
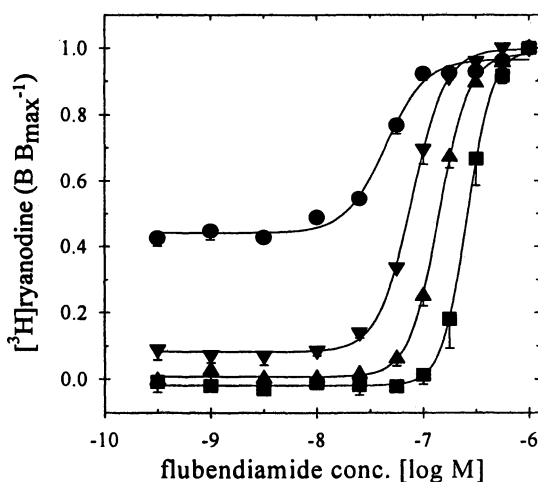
Figure 5. Concentration-dependent effect of flubendiamide on high-affinity [^{3}H]ryanodine binding (4 nM) at different calcium concentrations. Calcium concentrations: (●) 800 µM, (▼) 100 µM, (▲) 50 µM, and (■) 10 µM (n = 4).

flubendiamide increased [^{3}H]ryanodine binding with an EC_{50} of 40 nM. Maximum binding in the presence of flubendiamide was about twice the binding of the controls (no flubendiamide added). With decreasing $[Ca^{2+}]$, higher flubendiamide concentrations were necessary to achieve the same increase in [3H]ryanodine binding (470 +/- 19 fmol/mg). For example, at 100 µM $[Ca^{2+}]$, the EC_{50} was 79 nM, and at 10 µM $[Ca^{2+}]$ the EC_{50} was 251 nM.

Flubendiamide Affected the Calcium Regulation of [³H]Ryanodine Binding

To further investigate the effect of phthalic diamides on the calcium regulation of RyR, ryanodine binding to the *Heliothis* RyR was measured as a function of $[Ca^{2+}]$ (Figure 6).
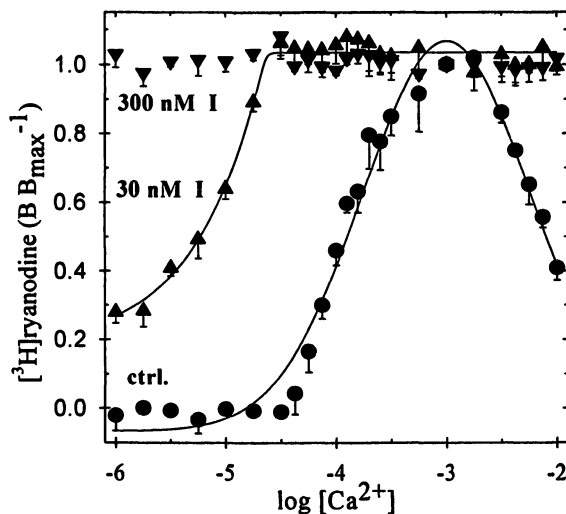
Figure 6. Ryanodine binding as a function of the calcium concentration was affected by flubendiamide (I). The concentration of [³H]ryanodine was 4.4 nM; the B_{max} was 540 +/- 36 fmol/mg protein. Flubendiamide (I) concentrations: control (●), 30 nM (▲), and 300 nM (▼).

At low micromolar $[Ca^{2+}]$ no specific binding was observed. Starting at about 10 µM, binding increased steadily with increasing $[Ca^{2+}]$ up to a maximum around 800 µM $[Ca^{2+}]$. At millimolar calcium concentrations ryanodine binding was incrementally inhibited.

A relatively low concentration of flubendiamide (30 nM) enhanced the high-affinity binding of ryanodine in the micromolar $[Ca^{2+}]$ range so that maximum binding was achieved at 18 µM $[Ca^{2+}]$. Remarkably, the inhibitory effect of millimolar calcium concentrations was completely abolished. In the presence of 300 nM flubendiamide, ryanodine binding became independent of $[Ca^{2+}]$.

Specific Binding of [³H]Flubendiamide

[³H]flubendiamide was used as a radioligand in equilibrium binding experiments to characterize the phthalic diamide binding site pharmacologically.
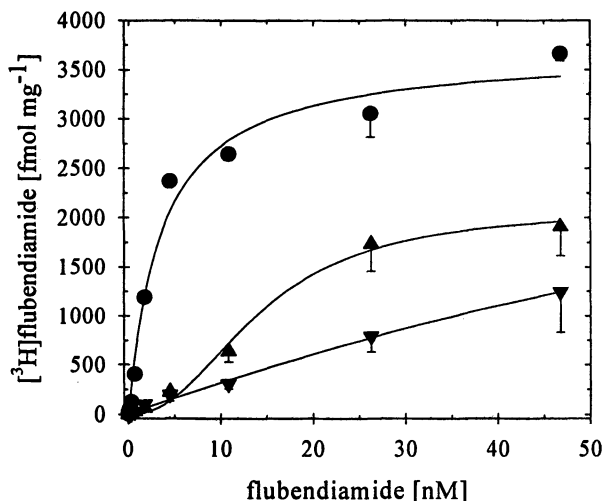
Figure 7. Equilibrium saturation binding of [³H]flubendiamide to Heliothis microsomal membranes. Specific binding was measured at 800 μM (●), at 10 μM (▲), and without added calcium (▼), respectively.

In the presence of 800 μM calcium, [³H]flubendiamide bound with low nanomolar affinity to a homogeneous population of receptor sites (Figure 7) with an apparent K_D = 3.4 +/- 0.3 nM (Hill coefficient = 1.0). Interestingly, the receptor density (B_{max} = 3690 +/- 92 fmol/mg) was much higher than the receptor density for ryanodine.

At 10 μM [Ca^{2+}], flubendiamide binding was clearly cooperative as indicated by the Hill coefficient, n = 2.1. From the sigmoidal fit an apparent K_D = 14 nM was estimated. Additionally, the B_{max} was drastically reduced to 1800 fmol/mg, indicating that a larger fraction of receptor sites was insensitive to the radioligand.

Without any calcium added, specific binding increased with the radioligand concentration, but saturation was not reached and meaningful kinetics could not be calculated. None of the known RyR ligands like ryanodine, calmodulin, methylxanthines, ATP, cADP-ribose, nor dantrolene affected flubendiamide binding.

Discussion

Phthalic Acid Diamides Elicited Calcium Release Mediated by Ryanodine Receptors

It is known that structurally diverse low-molecular weight compounds modulate the calcium conductance of ryanodine-sensitive calcium release channels (RyR) in mammals. For example, methylxanthines such as caffeine induce RyR-mediated Ca^{2+} release from the sarcoplasmic reticulum and decrease the apparent dissociation constant of ryanodine *(17)*.

The current study shows that phthalic acid diamide insecticides, represented by flubendiamide and its sulfoxide analogue, activated ryanodine receptors present in isolated *Heliothis* neurons, as concluded from the following results. Firstly, calcium transients evoked by phthalic acid diamides were independent of the extracellular $[Ca^{2+}]$, in contrast to the signals elicited by acetylcholine. This was interpreted as calcium release from intracellular stores of the endo(sarco)plasmic reticulum, which could in principle be mediated by two different release channels, namely the ryanodine receptor and the IP_3 receptor.

Secondly, the calcium transients were sensitive to inhibition by ryanodine, but they were not affected by the IP_3R blocker xestospongine *(18;19)*. Consequently, it was concluded that the ryanodine receptor was the target site of phthalic acid diamides.

Phthalic Acid Diamides Increased the Ryanodine Affinity of Ryanodine Receptors

To further investigate the molecular mechanism of action of the phthalic acid diamides, saturation binding experiments with [3H]ryanodine were performed. The ryanodine binding site is most likely located in the pore region of the C-terminal domain since mutations affecting ryanodine binding (and channel gating) have been assigned to the proposed inner transmembrane helix, the pore helix, and the putative selectivity filter of mammalian RyR2, respectively *(20)*.

It is generally accepted that [3H]ryanodine binds with low nanomolar affinity to a calcium-conducting conformational state of the RyR channel. Consequently, [3H]ryanodine binding is frequently used to assess the function of ryanodine receptors *(6;21)*. So in the context of this discussion, potentiation or attenuation of ryanodine affinity are consistently interpreted as channel activation or inactivation, respectively. The validity of this assumption has been confirmed by correlating [3H]ryanodine binding results with direct calcium release measurements in isolated *Heliothis* neurons.

Equilibrium binding of [^{3}H]ryanodine to *Heliothis* flight muscle microsomes clearly revealed cooperativity between the binding sites at 100 µM [Ca^{2+}]. Based on the assumption that RyRs are arranged in arrays of calcium release units in insect as well as in mammalian sarcoplasmic reticulum membranes *(22)*, a plausible explanation would be that ryanodine receptors opened by calcium may have activated adjacent RyR channels by intermolecular interactions. Phthalic acid diamides completely converted the receptors to the high-affinity conformation as revealed by the hyperbolic binding isotherm.

Interestingly, even at 800 µM [Ca^{2+}], when the *Heliothis* RyRs were in the ryanodine-binding state, phthalic acid diamides further increased the affinity to [^{3}H]ryanodine slightly but significantly. From these results, it can be concluded that the compounds induced and/or stabilized the activated, calcium-conducting channel state.

Furthermore, the effect of phthalic acid diamides on ryanodine affinity was both concentration-dependent and sensitive to the calcium concentration. At 800 µM [Ca^{2+}], relatively low flubendiamide concentrations increased ryanodine binding; an apparent EC_{50} value of 40 nM was calculated. At decreased calcium concentrations, e.g. 100, 50, or 10 µM, higher flubendiamide concentrations were necessary to achieve maximum [^{3}H]ryanodine binding. One may speculate that phthalic diamides and calcium together potentiated the ryanodine affinity of the RyR: if a certain proportion of channels were activated by higher concentrations of the physiological effector calcium, lower flubendiamide concentrations were sufficient to cause full activation as revealed by maximum [^{3}H]ryanodine binding. At saturating phthalic diamide concentrations, e.g. 1.0 µM, all channels were detected in the high-affinity state independent of the calcium concentration added.

Phthalic Diamides Disrupted the Calcium Regulation of the Ryanodine Receptor

As already mentioned, calcium is the most important physiological effector of RyR activity *(10;11;23)*. High-affinity calcium binding sites have been described in mammalian RyR subtypes *(24;25)*. In addition, calcium regulation of ryanodine binding and channel opening of insect RyR has been reported previously *(11;12;26)*.

Ryanodine binding measured as a function of the calcium concentration exhibited a bimodal behaviour characterized in the first instance by the potentiation of [^{3}H]ryanodine binding at micromolar calcium concentrations. Maximum binding was detected at about 800 µM [Ca^{2+}]. Subsequently, inhibition of [^{3}H]ryanodine binding was observed at millimolar [Ca^{2+}]. Interestingly, addition of 30 nM flubendiamide shifted the activation curve to the left, showing enhanced [^{3}H]ryanodine binding at lower [Ca^{2+}]. This could be

interpreted as the sensitization of the RyR to calcium. High phthalic acid diamide concentrations, e.g. 1.0 μM, induced the open, ryanodine-binding conformation even when calcium was omitted. However, we can not exclude the presence of traces of calcium ions in the preparation which may have contributed to channel activation together with the phthalic diamide.

It is noteworthy that the inactivation of the *Heliothis* RyR at millimolar [Ca^{2+}] was prevented at all flubendiamide concentrations tested. This could plausibly explain the insecticidal mechanism since deactivation of calcium release channels at high [Ca^{2+}] would be essential to terminate the intracellular calcium transient *(27)*. According to this hypothesis, ryanodine receptors would be fixed in the (sub)conductance conformation leading to calcium store depletion and, possibly, to subsequent activation of capacitative calcium entry through plasma membrane channels. This would override compensatory calcium removal mechanisms such as the sarcoplasmic Ca-ATPase (SERCA) activity and the sodium-calcium exchanger (NCX) in the plasma membrane. The sustained high intracellular [Ca^{2+}] would finally lead to muscle contraction paralysis that is consistently observed in flubendiamide-affected lepidopteran larvae.

High-Affinity Binding of [3H]Flubendiamide was Regulated by Calcium

Saturable binding of [3H]flubendiamide to *Heliothis* microsomes was measured at a calcium concentration of 800 μM. Interestingly, the 3.5 to 4 times higher binding site density (B_{max}) compared to [3H]ryanodine may reflect the stoichiometry of one flubendiamide binding site per RyR subunit in contrast to the accepted stoichiometry of one ryanodine site per homotetrameric channel. However, this needs to be explored further.

An intriguing result was the calcium-dependency of flubendiamide binding. By reducing the calcium concentration, the equilibrium binding of [3H]flubendiamide was distinctly cooperative and the apparent dissociation constant was clearly increased. Considering that the ryanodine receptor is a highly allosteric protein that undergoes long-range conformational changes upon activation and closing, we postulate that phthalic acid diamides preferably bind to the open channel conformation which can be induced, for example, by calcium. Given the low nanomolar dissociation constant of the flubendiamide-RyR_{open} complex, the conformational equilibrium would be shifted toward the open state. The hypothesis predicts that pharmacological RyR activators such as caffeine and ryanodine (at low micromolar concentrations) should have similar effects on flubendiamide binding. This is currently under investigation.

Flubendiamide Selectively Activated Insect ryanodine Receptors

As an important feature, phthalic diamides seem to be specific for insect RyR: no calcium release could be measured after application of flubendiamide to the mammalian skeletal muscle subtypes RyR1 (and RyR3) present in differentiated mouse C_2Cl_2 cells *(16)*. In addition, flubendiamide had no effect on [³H]ryanodine binding to the mammalian cardiac muscle subtype RyR2 prepared from pig heart (unpublished results).

Besides their importance as potent insecticides, phthalic acid diamides, a new class of allosteric ryanodine receptor effectors, may be used as novel pharmacological tools in the functional and structural characterization of this fascinating ion channel.

References

1. Takekura, H.; Franzini-Armstrong, C. *Biophys.J.* **2002,** *83*, 2742-53.
2. Williams, A. J.; West, D. J.; Sitsapesan, R. *Quart.Revs.Biophys.* **2001,** *34*, 61-104.
3. Ma, J.; Hayek, S.M.; Bhat, M.B. *Cell Biochem Biophys.* **2004,** *40*, 207-24.
4. Welch, W.; Rheault, S.; West, D.J.; Williams, A.J. *Biophys.J.* **2004,** *87*, 2335-51.
5. Yin, C.C.; Blayney, L.M.; Lai, F.A. *J.Mol.Biol.* **2005,** *349*, 538-46.
6. Du, G.G.; Guo, X.; Khanna, V.K.; MacLennan, D.H. *Proc.Natl.Acad.Sci.USA* **2001,** *98*, 13625-30.
7. Du, G.G.; Sandhu, B.; Khanna, V.K.; Guo, X.H.; MacLennan, D.H. *Proc.Natl.Acad.Sci.USA* **2002,** *99*, 16725-30.
8. Takeshima, H.; Nishi, M.; Iwabe, N.; Miyata, T.; Hosoya, T.; Masai, I.; Hotta, Y. *FEBS Lett.* **1994,** *337*, 81-87.
9. Puente, E.; Suner, M.; Evans, A.D.; McCaffery, A.R.; Windass, J.D. *Insect Biochem.Mol.Biol.* **2000,** *30*, 335-47.
10. Xu, X.; Bhat, M.B.; Nishi, M.; Takeshima, H.; Ma, J. *Biophys.J.* **2000,** *78*, 1270-81.
11. Scott-Ward, T.S.; Dunbar, S.J.; Windass, J.D.; Williams, A.J. *J Membr.Biol* **2001,** *179*, 127-41.
12. Schmitt, M.; Turberg, A.; Londershausen, M.; Dorn, A. *Pestic.Sci.* **1996,** *48*, 375-85.
13. Usherwood, P.N.; Vais, H. *Toxicol.Lett.* **1995,** *82-83*, 247-54.

14. Tohnishi, M.; Nakao, H.; Furuja, T.; Seo, A.; Kodama, H.; Tsubata, K.; Fujioka, S.; Kodama, H.; Hirooka, T.; Nishimatsu, T. *J.Pestic.Sci.* **2005**, *30*, 354-60.
15. Hayashi, J.; Oland, L. A. *J.Exp.Biol* **1992**, *171*, 15-42.
16. Ebbinghaus-Kintscher, U.; Luemmen, P.; Lobitz, N.; Schulte, T.; Funke, C.; Fischer, R.; Masaki, T.; Yasokawa, N.; Tohnishi, M. *Cell Calcium* **2006**, 39, 21-33.
17. Zucchi, R.; Ronca-Testoni, S. *Pharmacol.Rev.* **1997,** *49*, 1-51.
18. Ehrlich, B.E.; Kaftan, E.; Bezprozvannaya, S.; Bezprozvanny, I. *Trends Pharmacol.Sci.* **1994,** *15*, 145-49.
19. Walz, B.; Baumann, O.; Zimmermann, B.; Ciriacy-Wantrup, E.V. *J.Gen.Physiol* **1995,** *105*, 537-67.
20. Zhao, M.; Li, P.; Li, X.; Zhang, L.; Winkfein, R.J.; Chen, S.R. *J.Biol.Chem.* **1999,** *274*, 25971-74.
21. Samso, M.; Wagenknecht, T.; Allen, P.D. *Nat.Struct.Biol.* **2005**, *12*, 539-44.
22. Wang, S.Q.; Stern, M.D.; Rios, E.; Cheng, H. *Proc.Natl.Acad.Sci.USA* **2004,** *101*, 3979-84.
23. Zahradnik, I.; Gyorke, S.; Zahradnikova, A. *J.Gen.Physiol.* **2005,** *126*, 515-27.
24. Fessenden, J.D.; Feng, W.; Pessah, I.N.; Allen, P.D. *J.Biol.Chem.* **2004,** *279*, 53028-35.
25. Du, G.G.; MacLennan, D.H. *J.Biol.Chem.* **1999,** *274*, 26120-26.
26. Lehmberg, E.; Casida, J. E. *Pestic.Biochem.Physiol.* **1994,** *48*, 145-52.
27. Stern, M.D., Cheng, H. *Cell Calcium* **2004,** 35, 591-601.
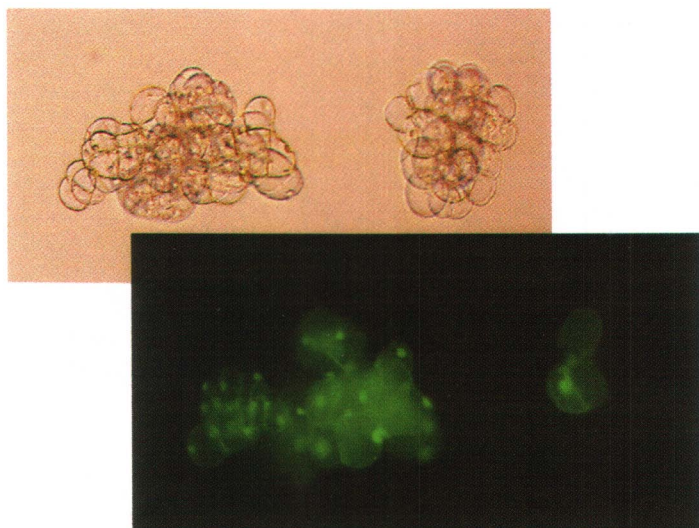
Figure 3.2   Use of Fluorescein Diacetate to Estimate Cell Viability
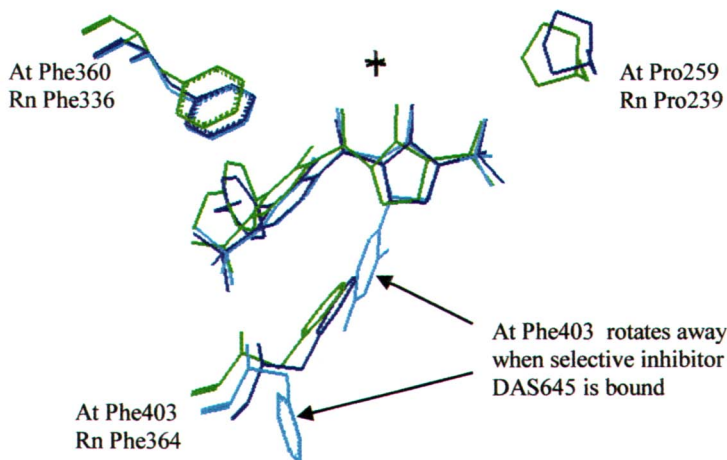
Figure 9.5: π-stacking network. AtPhe403 rotates away when DAS645 binds to the enzyme. AtHPPD-869 in dark blue, AtHPPD-645 in cyan, RnHPPD-869 in green.
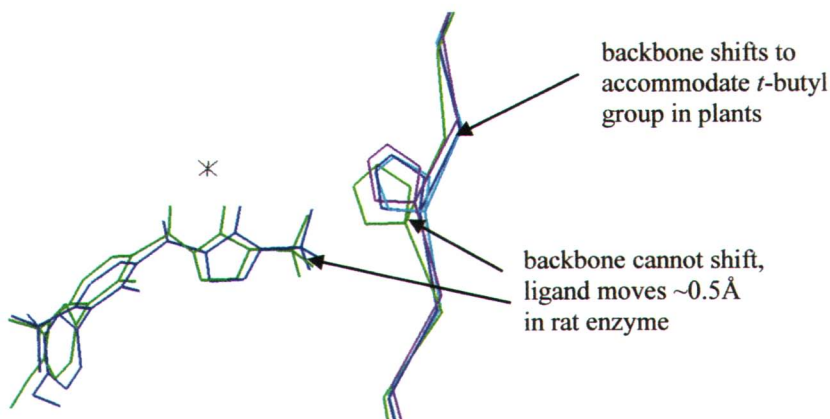
Figure 9.6: Shifting of the ligand towards the middle of the binding site to accommodate the position of RnPro239 resulting in a more crowded binding site. AtHPPD with DAS869 in dark blue; RnHPPD with DAS869 in green; AtHPPD with DAS645 in cyan; At HPPD with no bound ligands in purple.

Strobilurin (5 µg / leaf)   FSA V (10 µg / leaf)
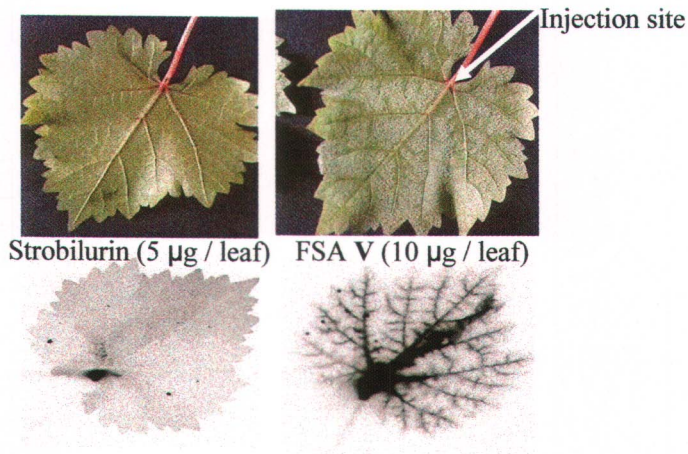
Figure 11.3. Distribution and Efficacy of V after Petiole Injection

(a) Apical Meristem Uncovered

(b) Apical Meristem Covered
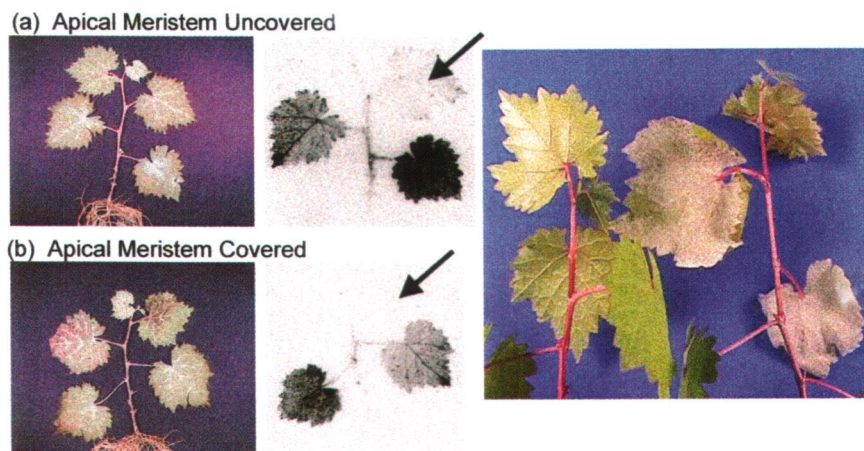
Figure 11.5. Importance of Delivery to Apical Meristems for Control of
P. viticola by V in newly emerged Vine shoots

Author Index

251

Subject Index

A

Acetamiprid
  chemical classification, 69*t*
  overview, 68*t*
Acivicin and derivatives
  Bristol–Myers synthesis of racemic
    acivicin, 123*f*
  C(3) derivatives, 125
  C(5) and C(2') derivatives, 125
  cycloadditions leading to C(5)- and
    C(2')-substituted, 127*t*
  fungicidal activity of acivicin, 122*t*
  fungicidal activity of
    aminotransferase inhibitors,
    131*t*, 132*t*, 133*t*
  fungicidal activity of COOH-
    derivatized compounds, 129*t*
  fungicidal activity of NH$_2$-
    derivatized compounds, 128*t*
  fungicidal activity of racemate,
    threo and homo derivatives, 124*t*
  glutamine transaminase inhibitors,
    134*f*
  isolation, 121
  mimic and antimetabolite of
    glutamine, 130*f*
  mode of action, 130
  NH$_2$ and COOH derivatives, 125,
    128*t*, 129*t*
  purine biosynthesis inhibitors, 121–
    122
  structure-activity relationships,
    127*f*
  structures, 122, 134*f*
  synthesis, 123, 125
  synthesis of 3-substituted, 126*f*
2-Acylimino-3-phenylthiazolines
  cotton field testing, 206

effect of heterocyclic ring on
    relative preemergence activity,
    202*f*
  effect of R^1 and R^2 substituents on
    preemergence activity, 204*f*
  effect of X and Y substituents on
    preemergence activity, 203*f*
  inhibition of cartenoid biosynthesis
    by 2-acylimino-thiazolines, 205*f*
  lead discovery, 199–201
  mode of action, 204–205
  optimization development from
    second lead, 201, 203–204
  optimization strategy for second
    lead, 202*f*
  structural similarity with known
    herbicides and design plan, 201*f*
  synthetic strategy for new lead,
    200*f*
Agrochemical discovery, measure of
    innovation and productivity, 3
Agrochemical industry
  opportunities, 2–3
  See also Physical property
    requirements of agrochemicals
Agrochemical rule of five,
    development, 7–8
Agrochemicals
  discovery of new, 93–94
  drug discovery, 198–199
  molecular target sites, 106
  See also 2-Acylimino-3-
    phenylthiazolines
Agrotis segetum, metabolism of
    thiamethoxam, 60, 61, 62*f*
Alkyl hydroxylation, metabolic
    reaction in plants, 31*f*
Amidotransferase inhibitors
  fungicidal activity, 131*t*

253

activity against, 155, 158
feeding assay using, 167–168
Toxicology, metabolism of
thiamethoxam and, 76–77
Transfer hypothesis, fipronil against
termites, 188
Translaminar systemicity,
agrochemicals, 10
Transpiration stream concentration
factor (TSCF)
equation, 11, 18
hydroponic barley, 12*f*
soybeans, 19*f*
Trifloxystrobin
metabolic degradation, 31*f*
metabolism assay, 28–29
metabolism in wheat, 34
mitochondrial electron transport,
138
penetration into leaf, 9
redistribution properties, 13*t*
See also Strobilurins

U

United States Department of
Agriculture, Forest Service and
termiticides, 181
United States Environmental
Protection Agency (EPA), soil–
applied liquid termiticides, 180

V

Volatility, efficacy of soil insecticides,
19, 20*f*

W

Wheat
metabolism of commercial
standards in, cell culture, 29–
30
metabolism of florasulam in, cell
culture, 32, 33*f*
metabolism of trifloxystrobin, 34
See also Powdery mildew
Wireworm larvae, metabolism of
thiamethoxam, 60, 61, 62*f*
Wood damage rating, termiticides,
184–185

X

Xylem systemicity, agrochemicals,
10–14

Y

Yellow fever mosquito (YFM),
activity against, 155